INTRODUCTION TO THE PHYLUM HEMICHORDATA

JÖRG MALETZ and CHRISTOPHER B. CAMERON

The recognition of fossil Hemichordata is quite difficult as these organisms in general are soft-bodied and rarely leave any trace of their existence (MALETZ, 2020a). Thus, the fossil record is relatively poor. Of the three extant groups of Hemichordata (Enteropneusta, Pterobranchia, and Planctosphaeroidea), only the tube-building Pterobranchia (Fig. 1.2–1.4) are common in the fossil record due to the preservability of their organic housing, the tubarium (Fig. 1.2). The Enteropneusta (Fig. 1.1) possess a fossil record reaching back into the middle Cambrian, but the Planctosphaeroidea (Fig. 1.5) are only known from a few larvae (e.g., SPENGEL 1932; HYMAN, 1959; HART, MILLER, & MADIN, 1994).

All extant Hemichordata share a tripartite body plan of their wormlike soft-bodied organization as a characteristic feature. Modern taxa investigated with DNA analysis indicate a phylogenetic position of the Hemichordata as a sister group to the echinoderms (e.g., HALANYCH, 1996; CANNON & others, 2009; LI & others, 2019) (Fig. 2). The extant Pterobranchia may have evolved from an enteropneust-like ancestor through a reduction in size and morphological complexity, a colonial or pseudocolonial life style, and development of the colony zooids through asexual budding (CAMERON, GAREY, & SWALLA, 2000). Interestingly, a miniaturization also occurs in enteropneusts (e.g., *Meioglossus* WORSAAE & others, 2012).

BATESON (1885a) introduced the term Hemichordata for the Enteropneusta, but it was FOWLER (1892a, p. 132) who revised the Hemichordata to also include the colonial Pterobranchia. The status of the Planctosphaeroidea in the Hemichordata is still uncertain (see p. 189). The Hemichordata are comparable to the Helminthomorpha of GROBBEN (1908, p. 505), who included the Enteropneusta and Pterobranchia. SPENGEL (1932, p. 26) included *Planctosphaera* as a third class in the Helminthomorpha. The Helminthomorpha GROBBEN, 1908 has commonly been used in German literature and may easily be confused with the Helminthomorpha POCOCK, 1887, a clade of millipedes.

The Hemichordata range in length from less than 1 mm (WORSAAE & others, 2012) to more than 2 m. Of the living hemichordates, the Enteropneusta are the most well known members. They are benthic marine worms that are distributed from the shallow intertidal zone to the deep sea and appear not to be limited by temperature barriers. They are usually infaunal elements, but deep-water enteropneusts include epibenthic demersal drifters (OSBORN & others, 2012). The enteropneust *Saxipendium coronatum* WOODWICK & SENSENBAUGH, 1985 is known to congregate on rock surfaces near hydrothermal vents.

Uncertainty about the relationships of the Hemichordata has been present since the first enteropneust was discovered in 1821 and was thought to be an atypical holothurian (ESCHSCHOLTZ, 1825). HYMAN (1959) provided a thorough historical treatment of early hemichordate classifications. KOWALEWSKY (1866) provided the first anatomical study of an acorn worm including the discovery of pharyngeal openings that aligned the Enteropneusta with the Chordata. METSCHNIKOFF (1869) found that the tornaria larva was an enteropneust rather than an asteroid larva, adding weight to the echinoderm and enteropneust relationship. Then, BATESON (1885a) placed a subphylum Hemichordata in the phylum Chordata based on the presence of a notochord, the central nervous system, and the gill slits. This position was protested by SPENGEL (1893) and subsequently abandoned by the German, French, and American treatises
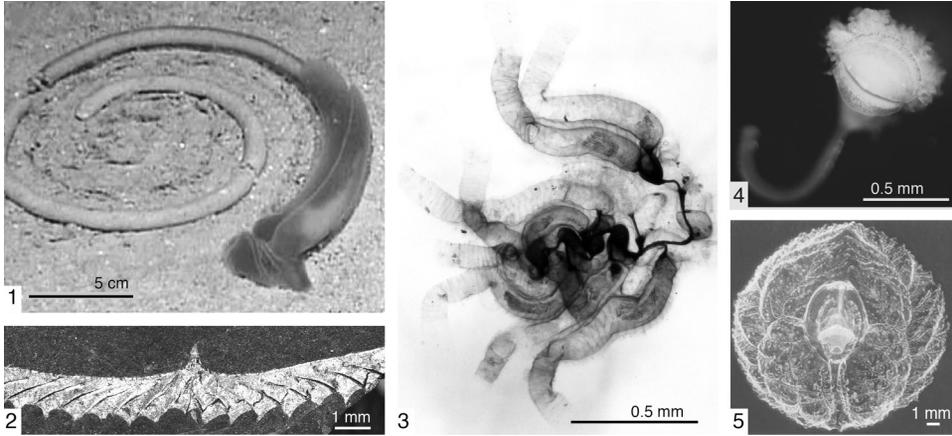
Fig. 1. Examples of the Hemichordata. *1,* Torquaratorid enteropneust with fecal string (Holland & others, 2005, fig. 3E); *2, Expansograptus hirundo* (Salter, 1863a), flattened tubarium, PMO 234.064, Tøyen Shale, Oslo region, Norway (new); *3, Rhabdopleura compacta* Hincks, 1880a, tubarium with zooids (Cavers, 2005, fig. 1.1); *4, Cephalodiscus planitectus* Miyamoto, Nishikawa, & Namikawa, 2020, ventral view of zooid (Miyamoto, Nishikawa, & Namikawa, 2020, fig. 2C); *5, Planctosphaera pelagica* Spengel, 1932 (Hart, Miller, & Madin, 1994, fig. 1B). Color images available, *Treatise Online* 157.

on invertebrates, namely van der Horst (1939), Dawydoff (1948), and Hyman (1959). The similarities and close relationship of the hemichordates to the echinoderms was the predominant view for the latter half of the twentieth century, although the common ancestor remained contentious. On one side, Bather (1900) referred to the dipleurula larva, a name introduced by Semon (1888), as a common ancestor. The larva shared features of the enteropneust tornaria or asteroid auricularia. It was soft, bilaterally symmetric with a ventral mouth, apical organ, ciliated bands, and three pairs of coelomic sacs that were arranged on either side of the gut (Gislén, 1930), referred to as the protocoel, mesocoel, and metacoel. The protocoel opened to the exterior by a ciliated duct and pore. The hypothesis that this dipleurula elongated to become the ancestral chordate animal (Garstang, 1928) gained acceptance.

Grobben (1923) advanced the hypothesis that the echinoderms are derived from the pterobranchs. The ancestor was similar to *Cephalodiscus* M'Intosh, 1882 in that it had five pairs of arms with tentacles. The cephalic shield was comparable in posi-

tion to the attachment pit of the crinoid and asteroid larvae that was drawn out to become a stalk. Most people regarded the pterobranchs as more primitive than enteropneusts because of their simple nervous system. The echinoderms then would have evolved by the extension of the protocoel (echinoderm hydrocoel) into multiple arms. The protocoel opened to the exterior by a pore. The digestive tract was comprised of an esophagus, stomach, and intestine and curved to open into an anus on the anterior ventral side. This ancestor metamorphosed into an echinoderm with the right protocoel and five arms diminished, and the body attained a circular disklike shape. The remaining arms radiated in five directions to form the echinoderm rays. Jeffries (1986) developed a similar calcichordate hypothesis whereby the echinoderms and the chordates evolved from a pterobranch-like ancestor that had fallen over and then elaborated one side. The prevailing hypotheses of the twentieth century was that pterobranchs were either basal deuterostomes (Gee, 1996; Nielsen, Scharf, & Eibye-Jacobsen, 1996) or plesiomorphic hemichordates (Hyman, 1959; Barrington, 1965).
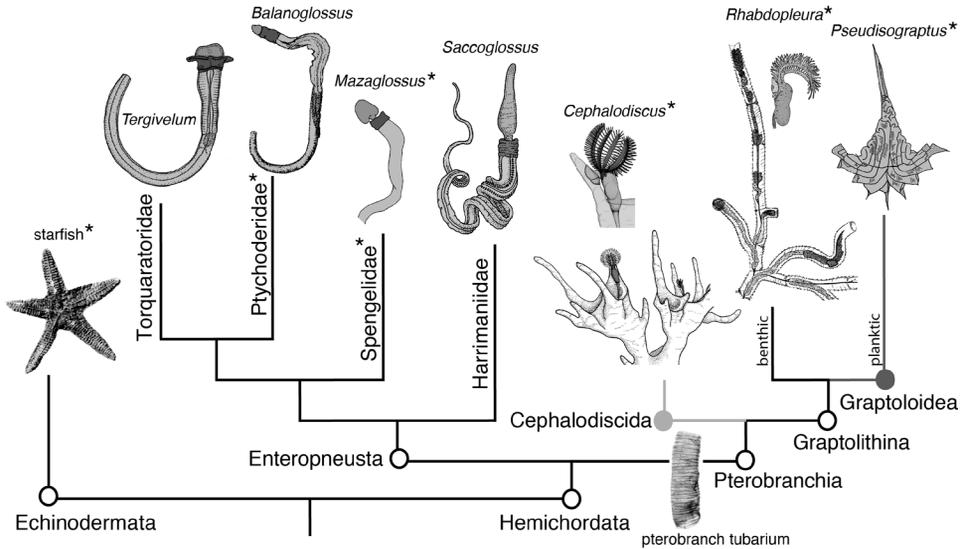
FIG. 2. Phylogenetic understanding of the Hemichordata. Taxon names with * indicate taxa known also from fossils or only from fossil material (new).

The GUTMANN (1981) hypothesis posits that the ancestral deuterostome, based on a functional-mechanical analysis, was a metameric, coelomate wormlike animal with complex body muscles that formed the basis of a hydrostatic skeleton. The sequence of morphological changes leading to the chordate ancestor was, in chronological order, the appearance of a notochord, the dorsal hollow nerve cord, the post-anal tail, and the branchial basket. This primitive chordate would have been most like a lancelet. From here, the enteropneusts lost the notochord, dorsal nerve cord, and segmented condition and developed a muscular burrowing proboscis. The collar originated to prevent water from exiting the mouth. Pterobranchs then arose from this acorn worm by a reduction in the branchial basket and an elaboration of the collar into arms and tentacles, and finally, the appearance of the tubarium. By this hypothesis, echinoderms arose from the pterobranch-like ancestor by specializing for sessile life, developing feeding tentacles and losing the branchial basket.

The twenty-first century saw the dawn of a new hypothesis, that the common ancestor to the deuterostomes was an enteropneust-like worm with chordate-like gills (CAMERON, GAREY, & SWALLA, 2000). This worm hypothesis was further elaborated by CAMERON (2002a, 2005), who stated that the ancestral deuterostome was a benthic vermiform organism with a terminal mouth and anus and a pharynx perforated with gill slits bordered by gill bars of collagen used in filter feeding (CAMERON, 2002a). This organism possessed a simple nerve plexus with little sign of regionalization. The enteropneust collar cord is not a homolog of the chordate dorsal nerve cord. It had a cluster of vacuolated cells with myofilaments, expanded extracellular matrix, and extracellular spaces developed from the middorsal wall of the archenteron that provided the foundation for the independent evolution of the chordate notochord and enteropneust stomochord. Iodotyrosine was produced in cells lining the gut, but these cells had not yet coalesced into an endostyle. It is not known if this animal had trimeric or metameric coeloms, but the ancestor probably had well-developed circular and longitudinal muscles (CAMERON, 2005). On the branch

to the Ambulacraria, the dipleurula larva appeared. The first echinoderm adult was bilaterally symmetric (RAHMAN & others, 2015) and may have possessed echinoderm-like ossicles (CAMERON & BISHOP, 2012) and gill slits (e.g., *Jaekelocarpus* KOLATA, FREST, & MAPES, 1991, see DOMINGUEZ, JACOBSON, & JEFFRIES, 2002). The first pterobranchs, then, similarly evolved from an acorn worm-like ancestor.

The discovery of two Cambrian Burgess Shale enteropneust fossils that are tubicolous (CAMERON, 2018), and another with arms and tentacles (NANGLU, CARON, & CAMERON, 2020) suggest that these traits originated before the pterobranchs. Therefore, the major innovations of pterobranchs are coloniality and a reduction in size that resulted in the loss of the gill skeleton, branchiomeric nephridia, and three pairs of coelomic diverticula—the perihaemal, peripharyngeal, and peribuccal coeloms (CAMERON, 2005). The hypothesis that the ancestor to the deuterostomes was an enteropneust-like worm is supported by morphological and molecular phyloge-netic trees (CAMERON, 2005; CANNON & others, 2009), molecular development (LOWE,

2021), and comparative genomics (SIMAKOV & others, 2015). An important caveat to this hypothesis, which points to fruitful future avenues of research, is the almost total absence of pterobranch molecular develop-mental studies (SATO & others, 2009) and the absence of a pterobranch genome.

The preservation of the Hemichordata as fossils depends strongly on the type of sediments in which they are embedded and the environmental conditions in these sediments (MALETZ, 2020a). In general, indications of the organic soft tissue of organisms is only preserved under very special conditions and can be found in rare Lagerstätten, such as the Burgess Shale of British Columbia, the Chengjiang fauna of China (CAMERON, 2018), and the Mazon Creek fauna of North America (CAMERON, 2016).

The fossil record of the Pterobranchia is extensive, as evidenced by the common occurrence of graptolite tubaria in Paleozoic sediments, but does not include any identifiable organically preserved zooids (MALETZ, 2020a; RAMÍREZ-GUERRERO & CAMERON, 2021).

INTRODUCTION TO THE CLASS ENTEROPNEUSTA

CHRISTOPHER B. CAMERON

MORPHOLOGY

The Enteropneusta are free living, solitary marine worms. Their occurrence ranges from the Cambrian to the present. The acorn worm body is arranged into an anterior proboscis, a collar, and a posterior trunk (Fig. 3). Body length can vary from less than 1 mm (WORSAAE & others, 2012) to 1.5 m (SPENGEL, 1893). The proboscis is muscular, and its epidermis is replete with sensory, ciliated, and glandular cells (BENITO & PARDOS, 1997). Acorn worms deposit-feed by trapping sediment in mucus and transporting it to the mouth with cilia. A pre-oral ciliary organ on the posterior proboscis (BRAMBELL & COLE, 1939) (Fig. 4.1) directs the food-laden mucous thread into the mouth (GONZALEZ & CAMERON, 2009). The proboscis coelom contains a turgid stomochord (Fig. 3, Fig. 4.2a), an anterior projection of the dorsal collar buccal cavity that consists of vacuolated cells arranged around a central ciliated cavity and encapsulated in a collagen sheath (WELSCH & STORCH, 1970). The result is a rigid structure against which the pericardium (heart) compresses the intervening blood sinus so that urine can be forced across the glomerulus (kidney) into the proboscis coelom (BALSER & RUPPERT, 1990). The stomochord is not a homolog of the chordate notochord (SATOH & others, 2014). The right protocoelom is small or absent, and the left coelom is dominant and extends a ciliated duct, which is lined with nephridia (mesothelial, monociliated podocytes and myocytes) to the exterior via a left dorsal lateral urinary proboscis pore (RUPPERT & BALSER, 1986) (Fig. 3). There is extensive inter- and intraspecific variation in the form of this proboscis heart-kidney-coelom complex (DELAND & others, 2010). The stomochord is supported ventrally by a collagenous Y-shaped nuchal skeleton (Fig. 3, Fig. 4.2a–b). The skeleton extends poste-riorly through the neck and bifurcates into paired horns in the collar (SPENGEL, 1893; HORST, 1939; EZHOVA & MALAKHOV, 2009).

The collar lip forms the mouth anteriorly, and its interior is the buccal cavity (Fig. 3). In some species, the anterior lip is muscular and flexible, adept at guiding sediment laden strings of mucus from the proboscis into the mouth or rejecting them over the lip and onto the collar. The collar epidermis is usually differentiated into histologically distinct zones of transverse bands of numerous gland cells and dense bands of cilia (BENITO & PARDOS, 1997; HORST, 1939), with distinct mucin and glycoprotein secretory patterns (SIMAKOV & others, 2015). The acorn worm nervous system is an epidermal plexus with two longitudinal intraepidermal nerve cords in the trunk and a neurulated cord in the collar (BULLOCK, 1940; KNIGHT-JONES, 1953). Sensory cells, ganglion cells, interneuronal junctions, and motor innervation are arranged diffusely (BULLOCK, 1940; BENITO & PARDOS, 1997). The collar cord is intraepithelial even where the epithelium containing the nerves becomes internalized, and most commonly has paired, parallel, and discontinuous lacuna that are lined with cilia. There is no central nervous system. The collar cord is a simple conduction pathway (CAMERON & MACKIE, 1996) and is aligned with the perihaemal muscles, suggesting a role in the rapid contraction of the proboscis (RUPPERT, 2005). This cord is unlike the hollow, neuroepithelium in the rays of echinoderms or the hollow, neural tube of chordates (BULLOCK, 1940; CAMERON & MACKIE, 1996; RUPPERT, 2005). Paired diverticula of the trunk coeloms, called perihaemal and peribuccal coeloms, project anteriorly into the collar (Fig. 3). Paired mesocoel ducts connect the collar coeloms to the first pair of gill pore atria in the anterior trunk (Fig. 3). The acorn worm trunk bears middorsal and midventral longitudinal grooves that
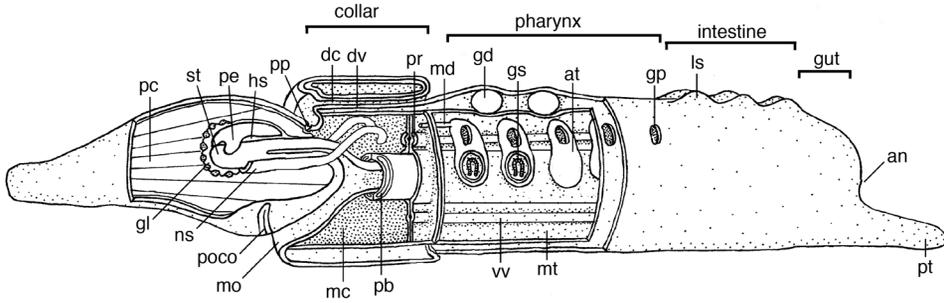
Fig. 3. Illustration of a generalized morphology of an enteropneust. Anus (*an*), atrium (*at*), dorsal nerve cord (*dc*), dorsal blood vessel (*dv*), gonad (*gd*), filtration glomerulus (*gl*), gill pore (*gp*), gill slit (*gs*), heart sinus (*hs*), liver sacs (*ls*), mesocoel (*mc*), paired mesocoel ducts (*md*), mouth (*mo*), metacoels (*mt*), Y-shaped nuchal skeleton (*ns*), peribuccal coeloms (*pb*), protocoel (*pc*), pericardium (*pe*), ventral post-anal tail (*pt*), preoral ciliary organ (*poco*), urinary pore (*pp*), perihaemal coeloms (*pr*), stomochord (*st*), and ventral blood vessel (*vv*) (adapted from Cameron 2005, fig. 1).

correspond to the location of longitudinal nerves and blood vessels (Pardos & Benito, 1990) (Fig. 3). The dorsal and ventral nerve cords are connected anteriorly by a circumpharyngeal ring (Bullock, 1940; Kaul-Strehlow & others, 2015). The ventral cord is the fastest conducting cord due to its proximity to the large ventral longitudinal muscles (Pickens, 1970; Cameron & Mackie, 1996). The trunk is differentiated into regions along its length that correspond to the specializations of the gut. The anterior region bears paired dorsolateral series of gills, followed by an esophagus and an intestine that terminates at an anus (Fig. 3). The gill slits, demarcated by a series of M-shaped collagenous gill bars, are connected to the outside pores by atrial cavities, akin to those of cephalochordates. The ciliated bars pump water through the pharynx, slits, and pores, removing food particles from suspension (Cameron, 2002a; Gonzalez & Cameron, 2009). Support for the hypothesis that gills are a deuterostome plesiomorphy are shared patterns of genes expressed during gill and pharynx development and the organization of these genes in synteny in acorn worms and vertebrates (Gillis, Fritzenwanker, & Lowe, 2012; Simakov & others, 2015). The food and mucus are then transported down the gill bars to the ventral gut, concentrated into a mucous food cord, and then transported posteriorly through the esophagus.

Iodine[125] binding experiments suggest that an endostyle function may reside in the entire pharyngeal lining of Enteropneusta and in *Schizocardium* Spengel, 1893, in which an epibranchial ridge is organized into zones of cells, reminiscent of the chordate endostyle (Ruppert, Cameron, & Frick, 1999; Ruppert, 2005; see also Satoh & others, 2014) (Fig. 4.3). The muscular esophagus functions to eliminate excess water from the food cord as it passes to the intestine. Anteriorly, the intestine is usually darkly pigmented. It is a simple tube except in *Schizocardium* and the family Ptychoderidae, in which it develops dorsally projecting rows of hepatic sacs, presumably to deal with a diet of heavy sediment. Gonads occur along the pharyngeal region, and in the family Ptychoderidae, they develop in external paired longitudinal ridges or wings. A few species have a curious pygochord structure in the posterior ventral trunk that Willey (1899) suggested may be a homolog to the chordate notochord. It is comprised of vacuolated cells positioned between the posterior ventral trunk mesenteries (Willey, 1899; Spengel, 1903; Uribe & Larrain, 1992; Miyamoto & Saito, 2007) or intestine (Horst, 1939). Punnett (1906) suggested that the structure may be a vestigial collateral intestine, which may instead function to support the fragile trunk as it projects from the burrow to eject fecal sediment. Distinct

protuberances characterize the epidermis of the acorn worm trunk. These are formed by secretory and sclerocyte cells that occlude extracellular spaces, where microscopic calcium carbonate ossicles develop. In *Ptychodera* (Fig. 4.4a) and *Saccoglossus* (Fig. 4.4b), the ossicles form a polycrystalline aggregate of laminar layers, with perforations that are comparable to echinoderm stereom (CAMERON & BISHOP, 2012). The functions of the pygochord and the ossicles are unknown.

DEVELOPMENT AND REPRODUCTION

The sexes are separated except for *Yoda purpurata* PRIEDE & others, 2012, which is a hermaphrodite (see PRIEDE & others, 2012). Fertilization is external (BURDON-JONES 1951; LOWE & others 2004) although vivipary is known for *Xenopleura vivipara* GILCHRIST, 1925 and the deep-sea *Coleodesmium karaensis* OSBORN & others, 2013, which broods their embryos in sacs that connect to a gonadal wing by a narrow stock (OSBORN & others, 2013). In most species, eggs are released in a jelly coating that breaks down following fertilization (COLWIN & COLWIN, 1954). All subsequent development occurs in the seawater. Cleavage is holoblastic, radial, and more or less equal. Cell fates and axis specifications are in most respects similar to that of an echinoderm (HENRY, TAGAWA, & MARTINDALE, 2001). A coeloblastula is followed by gastrulation by invagination. The blastopore is located posteriorly but closes before a new anus and mouth are formed (BURDON-JONES, 1952; COLWIN & COLWIN, 1953). The fertilization envelope weakens and ruptures, releasing ciliated, swimming embryos by late gastrula. The organization of the coelomic sacs is comparable to echinoderms. The ambulacrarian coeloms are organized anterior to posterior as paired protocoel, mesocoels, and metacoels (CRAWFORD & CHIA, 1978). They develop as independent pouches from the archenteron by enterocoely (KAUL-STREHLOW & STACH, 2013). Reports of schizocoely have not been substantiated (HADFIELD, 1975). GEMMILL (1914) provided a thorough comparative study of coelomogenesis in the asteroid (starfish), *Asterias rubens* LINNAEUS, 1758 and an enteropneust (summarized in CAMERON, 2005).

Harrimaniid worms (e.g., *Saccoglossus*) develop from a large, yolky egg to a ciliated, non-feeding larva with a telotrochal band and apical tuft that allows for a brief swimming and exploratory period (COLWIN & COLWIN, 1953). Following settlement, the juvenile worm has a ciliated, adhesive, post-anal tail (Fig. 5.3) that allows for rapid forward and reverse locomotion, adhesion, and release (BURDON-JONES, 1952; BURDON-JONES 1956; CAMERON, 2002b; STACH & KAUL, 2011) that may be a homolog to the pterobranch stalk (BURDON-JONES, 1952; HYMAN, 1959; LESTER, 1985; CAMERON, 2005). Ptychoderid worms (e.g., *Ptychodera*) shed small transparent eggs. Development is rapid and indirect via a tornaria larva that resembles an echinoderm auricularia (MORGAN, 1891; GEMMILL, 1914; GISLÉN, 1930; TAGAWA & others, 1998; URATA & YAMAGUCHI, 2004) (Fig. 5.4). These dipleurula larvae are delicate and transparent with a preoral ciliated feeding band (Fig. 5.4) that creates an upstream feeding current using monociliated cells (MORGAN, 1891; STRATHMANN & BONAR, 1976) and a perioral ciliated band that manipulates and conveys food into the esophagus (LACALLI & GILMOUR, 2001). The free-swimming, feeding tornaria are able to turn due to a band of multiciliated cells that comprise the locomotory telotroch (Fig. 5.4), an acorn worm innovation. The tornaria apical plate retractor muscle (and associated coughing behavior) (MORGAN, 1891) is another acorn worm larval apomorphy. Tornaria may persist in the plankton for months before metamorphosis and settlement to a suitable juvenile worm habitat. The larval body elongates differentiating the three body regions and organs. The larval apical tuft, nervous system, and feeding band are lost, followed by the telotroch band. The gills develop as
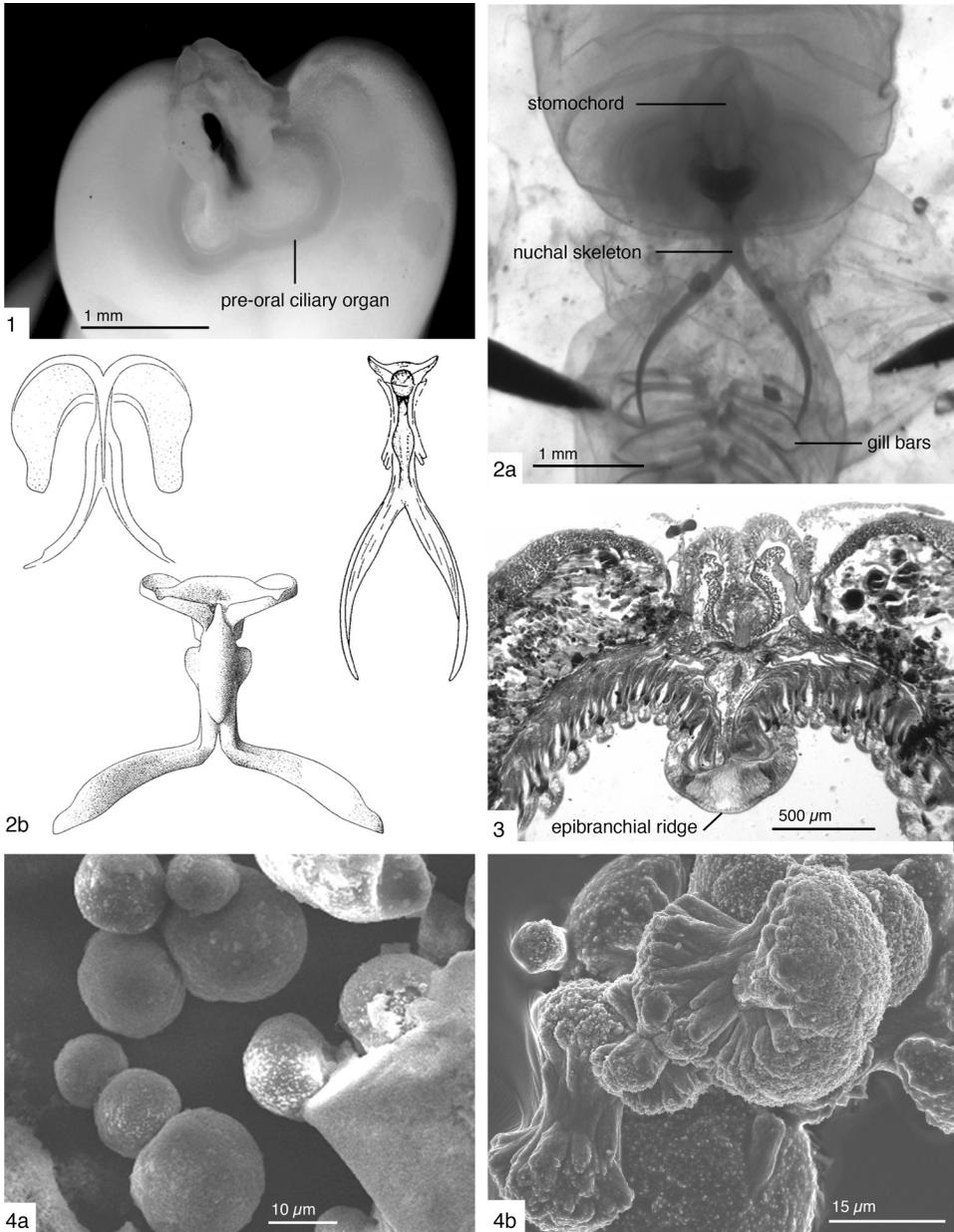
FIG. 4. Acorn worm anatomy. *1,* Pre-oral ciliary organ of *Protoglossus graveolens* GIRAY & KING, 1996; *2a,* stomochord, nuchal skeleton, and gill bars of *P. graveolens; 2b,* illustrations of nuchal skeletons, in clockwise order, *Protoglossus koehleri* (CAULLERY & MESNIL, 1900), *Saccoglossus ruber* TATTERSALL, 1905, and *Balanoglossus hydrocephalus* HORST, 1940; *3,* epibranchial ridge of *Schizocardium peruvianum* SPENGEL, 1893; *4a,* ossicles of *Ptychodera flava* var. ESCHSCHOLTZ, 1825, Galapagos; *4b,* ossicles of *Saccoglossus bromophenolosus* KING, GIRAY, & KORNFIELD, 1994 (all, new).
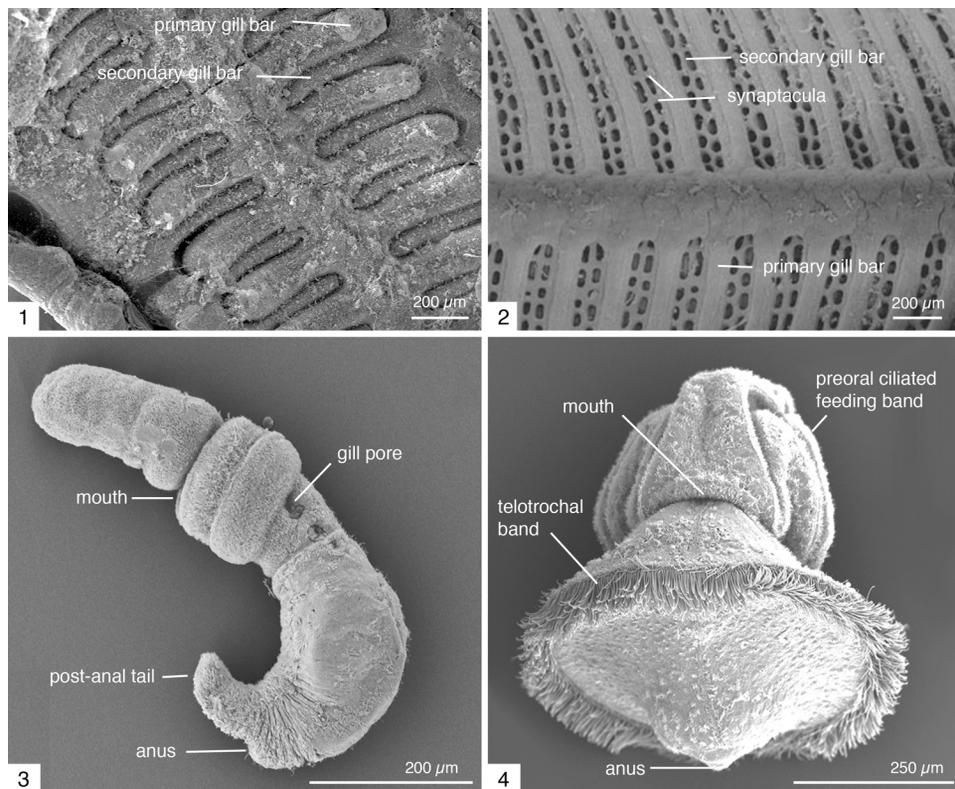
FIG. 5. SEM photos of details. *1,* Gill region of *Harrimania planktophilus* CAMERON, 2002b; *2,* gill region of *Ptychodera* sp.; *3, Saccoglossus kowalevskii* AGASSIZ, 1873 at the three-gill pore stage, showing a typical harrimaniid juvenile post-anal tail; *4,* posteriofrontal view of a tornaria larva of *Schizocardium* sp., showing the swimming telotrochal band (all, new).

out-pockets of the gut that open to the exterior by paired dorsolateral pores. Nothing is known of torquaratorid development, but the exceptionally large egg size (OSBORN & others, 2012; PRIEDE & others, 2012) hints that development is direct, via a loss of a feeding tornaria, parallel to the ontological loss of the larva in the line to modern harrimaniids.

Asexual reproduction by fragmentation is widespread among enteropneusts, including ptychoderids (GILCHRIST, 1923; PACKARD, 1968; MIYAMOTO & SAITO, 2010; HUMPHREYS & others, 2010), a spengelid (URATA, IWASAKI, & OHTSUKA, 2012), and the minute harrimaniid *Meioglossus psammophilus* WORSAAE & others, 2012, which lacks males and repro-

duces by paratomy. Regeneration is particularly well developed in the ptychoderids, a group especially susceptible to breakage due to their larger and fragile bodies. The posterior fragments are particularly good at regeneration, although some experimentally bisected animals can regenerate new individuals from both anterior and posterior fragments (WILLEY, 1899; DAWYDOFF, 1909, 1948; RAO, 1955; TWEEDELL, 1961; PACKARD, 1968; PETERSEN & DITADI, 1971; RYCHEL & SWALLA, 2009; HUMPHREYS & others, 2010; MIYAMOTO & SAITO, 2010). The cells that participate in blastema formation and morphogenesis during regeneration have not been identified (RYCHEL & SWALLA, 2009; MIYAMOTO & SAITO, 2010).

LIFE HABITS

Acorn worms are exclusively marine and usually burrow into the sand or mud or are associated with the underside of rocks, although species have also been found entangled in kelp holdfasts (RITTER, 1900). To burrow, they penetrate the sediment using muscular peristaltic contractions of the proboscis and transport the sediment using the ciliated epidermis of the proboscis and collar.

Burrow structure varies greatly. They may be Y-shaped, with one arm forming a feeding funnel (DUNCAN, 1987), U-shaped (RAO, 1954), coiled (BURDON-JONES, 1950) (Fig. 6.1), sinuous, irregular (BRAMBELL & GOODHART, 1941; KNIGHT-JONES, 1953), poorly defined (BURDON-JONES, 1956), or absent for animals that occupy interstitial spaces (CAMERON, 2002b; WORSAAE & others, 2012). Most acorn worms form mucus-lined burrows (Fig. 6.1) that smell of haloindols or brominated phenols (HIGA, FUJIYAMA, & SCHEUER, 1980; GIRAY & KING, 1997; WOODIN, WALLA, & LINCOLN, 1987). In the absence of a burrow or in response to stress, a mucous tube may be produced (BURDON-JONES, 1952; HALANYCH & others, 2013). The antibiotic properties of the phenols stabilize the sediment around the burrow (CEDHAGEN & HANSSON, 2013) and likely repel predators, such as gastropods on the coasts of Japan and South Carolina that have been known to nip the tail from defecating ptychoderids (K. TAGAWA, E. E. RUPPERT, personal communications). *Saxipendium* WOODWICK & SENSENBAUGH, 1985 cling to rocky outcroppings near hydrothermal vents (WOODWICK & SENSENBAUGH, 1985), and members of the deep-sea family Torquaratoridae reside on the seafloor.

Enteropneusta are mucociliary feeders that collect their food particles on the proboscis with abundant mucin and glycoprotein secretions and transport them to the mouth with cilia (BARRINGTON, 1940; KNIGHT-JONES, 1953; BURDON-JONES, 1962; I. M. THOMAS, 1972). Many are facultative filter feeders that pump water into the mouth, then through the pharynx and gills slits using cilia that line the gill bars (BARRINGTON, 1940; KNIGHT-JONES, 1953; BURDON-JONES, 1962; CAMERON, 2002a; GONZALEZ & CAMERON, 2009). Balanoglossids ingest copious amounts of sand, in some cases forming feeding funnels at the mouth of the burrow system. *Saccoglossus* extend a long proboscis from the burrow to exploit surface sediments and marine snow, sometimes forming feeding rosettes. To defecate, the worm protrudes its posterior from the burrow system and ejects the fecal casting with rapid force. These surface castings are typically the best clue that acorn worms reside below the sediment surface (Fig. 6.2).

Torquaratorids have evolved several unique traits for life in the deep sea. Most notably, they are commonly brightly colored; and, rather than residing in burrows, they are epibenthic deposit feeders (Fig. 6.3). The collar of many species is elongated into lips that are used to collect and transport sediment to the mouth (HOLLAND & others, 2005; OSBORN & others, 2012; PRIEDE & others, 2012). Their castings form tightly wound spiral coils to wandering, switchback loops on the sea floor (BOURNE & HEEZEN 1965; SMITH, HOLLAND, & RUHL, 2005) (Fig. 6.3).

Trace fossils may provide some indirect evidence of acorn worms in the fossil record. See MALETZ (2014a) for a review of trace fossils with possible enteropneust affinities, including ones of a spiral form. Many typical meandering deep-water trace fossils (e.g., graphoglyptid traces, *Nereites* ichnofacies) may be explained as mucus-coated fecal casts produced by enteropneusts. The gut contents act as ballast, and when voided, the worms may drift through the demersal zone (SMITH, HOLLAND, & RUHL, 2005; OSBORN & others, 2012; HOLLAND, KUHNZ, & OSBORN, 2012). This adaptation allows for economical, long-distance movements to a new feeding site in an environment where food is typically heterogeneous and limited (OSBORN & others, 2012; JONES & others, 2013).
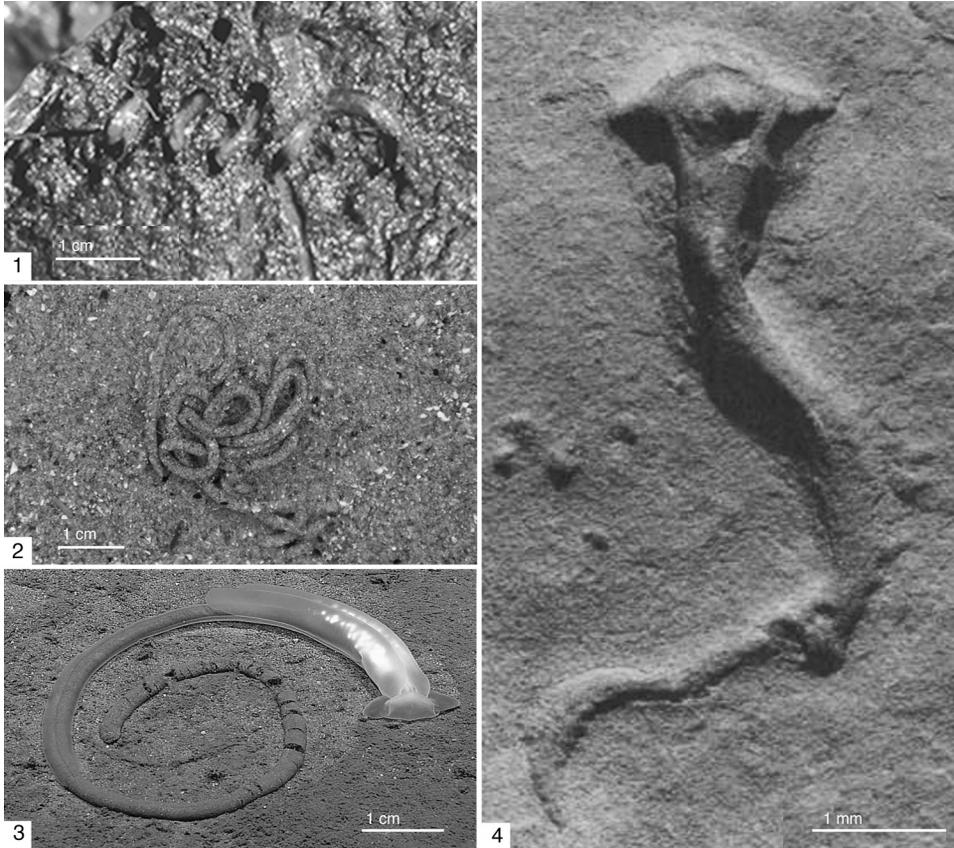
Fig. 6. Enteropneust traces. *1,* Helical-shaped burrow of *Saccoglossus bromophenolosus* King, Giray, & Kornfield, 1994, Willapa Bay, Washington, USA, exposing the brominated lining of the burrow (new, photo, M. K. Gingras); *2,* fecal casting of *Saccoglossus pusillus* Ritter, 1902 (new); *3,* fecal trail of *Tergivelum* sp? (photo courtesy of NOAA Office of Ocean Exploration and Research); *4,* resting trace of torquaratorid enteropneust (Twitchett, 1996, fig. 2.1). Color version of *1–3* in *Treatise Online* 109.

Two species of *Glandicepts* Spengel, 1893 from the west Pacific swim by flattening the trunk in a dorsoventral aspect and then undulate and turn as the worm ascends to the sea surface (Spengel, 1909; Yoshimatu & Nishikawa, 1999; Urata, Iwasaki, & Ohtsuka, 2012). This behavior does not appear to be coordinated with spawning (Urata, Iwasaki, & Ohtsuka, 2012). An unusual feature of some ptychoderids is their ability to produce light when stimulated (Kuwano, 1902; Crozier, 1917; Harvey, 1926; Rao, 1954). This luminescence is neurally mediated and appears to be intracellular, though luminous slime is also produced (Baxter & Pickens, 1964). The role of swimming and bioluminescence in acorn worms is unknown.

EVOLUTION

The embryologist Bateson (1884, 1885a) studied the direct-developing acorn worm *Saccoglossus kowalevskii* Agassiz, 1873 and concluded that the notochord, gill slits, collar nerve cord, and mesoblast development were comparable to amphioxus and therefore regarded enteropneusts as sister to chordates. Earlier, Metschnikoff (1869) studied the development of the genus *Balanoglossus* Delle Chiaje, 1829 and noted

many similarities of the tornaria to echinoderm larvae, so regarded hemichordates as sister taxon to echinoderms, a superphyletic group that he called Ambulacraria. With the advent of modern cladistics and phylogenetic methods, early phylogenies were consistent with these early ideas that envisioned the deuterostome ancestor as either a sessile tentaculate filter-feeding organism similar to a pterobranch (ROMER, 1967) or to a dipleurula larva (GARSTANG, 1928). This dichotomy, and the polyphyletic relationship of enteropneusts (as sister to chordates) and pterobranchs (allied with echinoderms), persisted for nearly a century (GEE, 1996; HOLLAND, HOLLAND, & HOLLAND, 2015; LOWE & others, 2015; SATOH, 2016; PETERSON & EERNISSE, 2016). These hypotheses have fallen out of favor, replaced by the hypothesis that the deuterostome ancestor was a free-living worm with a pharynx perforated with gill slits, used in filter feeding—similar to a modern enteropneust (e.g., CAMERON, GAREY, & SWALLA, 2000; CAMERON, 2002b; LOWE & others, 2015; SATOH, 2016). This hypothesis is consistent with an extensive morphological phylogeny for hemichordates (CAMERON, 2005) and current molecular phylogenies, which regard Enteropneusta and Pterobranchia as sister taxa and the monophyletic Hemichordata as sister to the Echinodermata, together forming the Ambulacraria (Fig. 7) (WINCHELL & others, 2002; PETERSON & others, 2013; CANNON & others, 2014; TELFORD & others, 2014; SIMAKOV & others, 2015).

The class Enteropneusta consists of three major clades, one comprised of the three families Ptychoderidae, Torquaratoridae, and Spengelidae; the monophyletic Harrimaniidae (OSBORN & others, 2012; CANNON & others, 2014); and the stem group Cambrian fossils (Fig. 7). According to a molecular clock estimate based on the genomes of *Ptychodera flava* ESCHSCHOLTZ, 1825 and *Saccoglossus kowalevskii,* the three-family clade and Harrimaniidae clade diverged 373 million years ago (SIMAKOV & others, 2015). Among the larger three-family

clade, Spengelidae is sister to the Ptychoderidae and Torquaratoridae (CAMERON, 2005; OSBORN & others, 2012; CANNON & others, 2014). OSBORN and others (2012), sequenced 25 torquaratorids and found them to be a monophyletic sister group to the Ptychoderidae. Based on two unidentified specimens, CANNON and others (2014) suggested that the Torquaratoridae are nested within the family Ptychoderidae (i.e., ptychoderid paraphyly). Torquaratorids have several unique morphological adaptations to life in the deep sea that are absent from ptychoderids. Interestingly, these adaptations did not evolve by parallelism in the deep-sea acorn worms *Glandiceps abyssicola* SPENGEL, 1893 (Spengelidae) (HOLLAND & others, 2013), *Ritteria* DELAND & others, 2010, nor *Saxipendium* (Harrimaniidae) (DELAND & others, 2010; HOLLAND, OSBORN, & KUHNZ 2012).

The family Harrimaniidae is monophyletic and sister to the three-family clade (Fig. 7). Within the Harrimaniidae there are three clades that differ in the arrangements of their proboscis musculature (DELAND & others, 2010). *Saxipendium*, a genus previously assigned to the monospecific family Saxipendidae, has been reclassified as a harrimaniid based in part on the shared presence of diffusely arranged proboscis musculature with *Mesoglossus* DELAND & others, 2010 and *Ritteria*. The proboscis muscles of *Saccoglossus* are arranged in concentric rings, whereas radially arranged muscles are the ancestral acorn worm state (DELAND & others, 2010).

The three-family clade and Harrimaniidae clade, inclusive of their fossil species, together comprise the crown Enteropneusta and diverged from a common ancestor approximately 373 million years ago (Fig. 7). Neither clade can be regarded as ancestral or derived. Each of the clades (as well as each family and species) exhibits ancestral and derived traits, although in general, the evolution of harrimaniids is characterized by losses of tornaria larval traits, whereas that of ptychoderids is characterized by gains of adult complexity. Harrimaniidae develop via a swimming, non-feeding, ciliated larva that
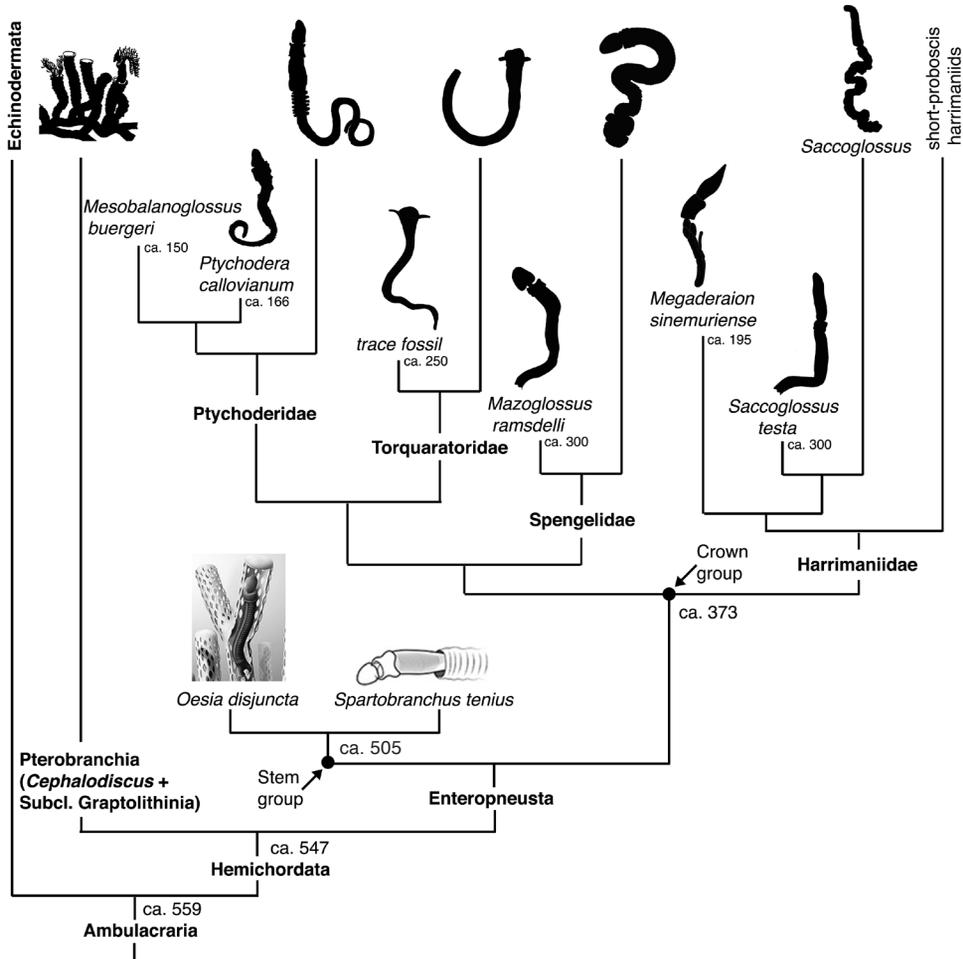
Fig. 7. Phylogenetic tree of acorn worms. The age of each fossil is provided in millions of years, and the stratigraphic details are provided in the text. Neither the tree branch lengths nor the worm silhouettes are to scale. The age of the Ambulacraria, Hemichordata, and crown group are molecular clock estimates from Simakov & others (2015) (adapted from Cameron, 2016).

swims with a telochrochal ciliated band—an acorn worm innovation. The harrimaniid larval telotroch suggests that the tornaria larva was lost in this family.

The modern families are a crown group clade with respect to the Cambrian fossil stem group, which includes *Oesia disjuncta* and *Spartobranchus tenuis* (Fig. 7). These 505 million-year-old fossils are the closest representatives of the ancestral acorn worm condition, and in most respects, they have a harrimaniid-like body plan. The Cambrian fossils lack hepatic sacs, genital wings, and

synaptaculae that bridge the primary and secondary gill bars that characterize ptychoderids and the spengelids *Spengelia* Willey, 1898 and *Schizocardium*. Thus, this trait evolved by parallelism in Cephalochordata (Fig. 5.1–5.2). Tubes are unique to stem enteropneusts. Those of *Oesia disjuncta* are fibrous (Fig. 8.1), and those of *Spartobranchus tenuis* sometimes branch (Fig. 8.2). Dozens of the *O. disjuncta* and approximately one-quarter of the *S. tenuis* specimens are associated with tubes, suggesting a facultative tubicolous habit (Caron, Conway

MORRIS, & CAMERON, 2013; NANGLU & others, 2016). The tubes are interpreted as a homologue to pterobranch tubes, abandoned on the internode branch to the crown enteropneust clade.

PALEONTOLOGY

Fossils of the soft-bodied enteropneusts are rare and typically occur in Konservat-Lagerstätten. The oldest of these are the Cambrian fossils *Oesia disjuncta* WALCOTT, 1911 and *Spartobranchus tenuis* (WALCOTT, 1911) from the Burgess Shales of British Columbia, Canada and date to approximately 505 million years ago. *O. disjuncta* is abundant in the Raymond Quarry and the Marble Canyon Quarry (see p. 191, Fig. 116,*2*). Its body is dominated by a broad and long pharynx that extends to nearly the posterior end of the animal. There is no appreciable intestine. A few of the specimens have what appears to be a posterior grasping appendage. Based on these unusual traits, NANGLU and others (2016) speculated that it may be a basal hemichordate, but here it is allied with *S. tenuis* in the stem Enteropneusta with which it shares tubes and a similar age. *O. disjuncta* occupied tubes that were formerly classified as the algae *Margaretia* WALCOTT, 1931. The tubes are cosmopolitan, comprised of woven fibers that form a sediment anchor basally and project into the water column (Fig. 8.1). The large pharynx, tube-dwelling habit, and the lack of sediment in the gut suggest it was an epibenthic filter feeder. *S. tenuis,* from the Walcott Quarry, has a body plan that resembles that of a modern harrimaniid worm, including an extensive pharynx followed by a vermiform, unembellished intestine (see p. 191, Fig. 116,*1a–b*). It occupied infaunal tubes that could tear, although fibers are not apparent. The discovery of a torquaratorid inside a mucous tube has led to the idea that *S. tenuis* was a member of the family Torquaratoridae (HALANYCH & others, 2013; CANNON & others, 2014). This idea is rejected because *S. tenuis* lacks all diagnostic torquaratorid traits, mucus does not fossilize

(NANGLU, CARON, & CAMERON, 2015), and the Cambrian fossils predate the origin of the crown enteropneusts (SIMAKOV & others, 2015). *S. tenuis* was probably a facultative filter and deposit feeder. The tubes of Cambrian acorn worms provide evidence of a link to the tubarium of pterobranchs, including graptolites (CARON, CONWAY MORRIS, & CAMERON, 2013; NANGLU & others, 2016).

Following the Cambrian, more than 200 million years passed before the next fossil acorn worms appeared during the Carboniferous, and after the divergence of the modern families at approximately 373 million years ago (SIMAKOV & others, 2015). Though a precarious exercise, the Carboniferous, Triassic, and Jurassic acorn worms have been assigned to the four modern families: Harrimaniidae, Spengelidae, Ptychoderidae, and the deep-sea Torquaratoridae (CAMERON, 2016). *Mazoglossus ramsdelli* (see BARDACK, 1985, 1997; MALETZ, 2014a) and *Saccoglossus testa* CAMERON, 2016 are from the Mazon Creek fauna, Illinois, USA (~307–309 million years ago). *M. ramsdelli* BARDACK, 1997 has a wide anterior trunk suggesting a well-developed pharynx (see p. 193, Fig. 117,*3*). Gill pores are reported (BARDACK, 1985), but having viewed all of the specimens to date, this author was unable to detect them. The enlarged gonadal-branchial region and absence of gonadal wings suggest it was a member of the family Spengelidae (CAMERON, 2016). The two *S. testa* specimens, also from Mazon Creek, are located next to each other in a single concretion (see p. 193, Fig. 117,*1*). They possess a long proboscis and therefore likely represent a re-emergence to surface deposit feeding. The proboscis of living saccoglossids are aposomatically colored—usually orange, red, or peach—and chemically defended. The Mazon Creek fauna is replete with predators including horseshoe crabs, sea scorpions, crustaceans, a shark, and the Tully monster (MCCOY & others, 2016; SALLAN & others, 2017), so, while somewhat speculative, chemical defense and

aposomatic colors may have evolved as early as *S. testa* (CAMERON, 2016).

The next evidence of an acorn worm is a resting trace fossil from the Lower Triassic Werfen Formation of northern Italy (TWITCHETT, 1996) (Fig. 6.4). It has collar lips that extend laterally and a pharynx that narrows posteriorly, characteristic of the Torquaratoridae, a family of surface-dwelling, pelagic deep-sea acorn worms (HOLLAND & others, 2005; PRIEDE & others, 2012). *Megaderaion sinemuriense* ARDUINI, PINNA, & TERUZZI, 1981 is from the Sinemurian (Lower Jurassic) strata of Osteno, northern Italy (see p. 193, Fig. 117,2). It is a single, small (2 cm) specimen that lacks gonadal wings, hepatic sacs, and an enlarged branchial region, characteristic of the family Harrimaniidae. It resembles *Mesoglossus,* a harrimaniid worm with a medium-long proboscis (DELAND & others, 2010).

Ptychodera callovianum (ALESSANDRELLO, BRACCHI, & RIOU, 2004) was a ptychoderid (see p. 193, Fig. 117,4) from the lower Callovian (Middle Jurassic) of La Voulte-sur-Rhone, France. The youngest fossil is *Mesobalanoglossus buergeri* BECHLY & FRICKHINGER in FRICKHINGER, 1999 from the lower Tithonian (Upper Jurassic) Solnhofen Limestones, southern Germany (see p. 193, Fig. 117,5). It is assigned to the Ptychoderidae due to its length (68.8 cm) and enlarged genital wings, but the proboscis preservation is poor and the presence of bristles in the pharynx (FRICKHINGER, 1999) suggest that it was not an acorn worm.

See p. 190–194 for Enteropneusta systematic descriptions.

FUTURE RESEARCH

In the intervening years since the most recent edition of the graptolite *Treatise* (BULMAN, 1970) in which only a short note on the Enteropneusta appeared, 22 new, living enteropneust species have been described, and with it, their zoogeographic range is currently better appreciated (see especially, CAMERON, DELAND, & BULLOCK, 2010), particularly with respect to their
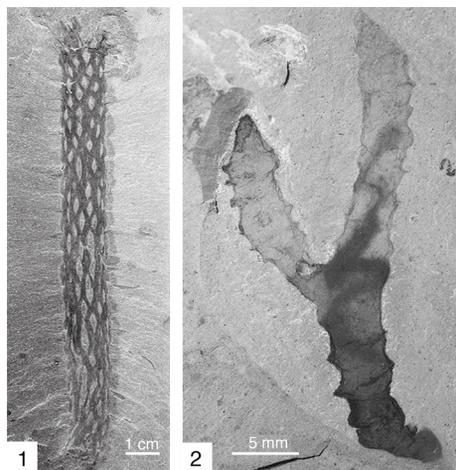

FIG. 8. Tubes of Cambrian fossil acorn worms. *1,* spirally arranged pores perforate the tube of *Oesia disjuncta* WALCOTT, 1911*,* ROM 63716 (Nanglu & others, 2016, fig. 4a); *2,* branching tubes of *Spartobranchus tenuis* (WALCOTT, 1911), ROM 57170 (Caron, Conway Morris, & Cameron, 2013, fig. 2f). Color version, *Treatise Online* 109.

abundance in the deep sea (OSBORN & others, 2012; PRIED & others, 2012; CANNON, SWALLA, & HALANYCH, 2013). Although fossil enteropneusts were unknown to BULMAN (1970), seven fossil acorn worm species are now known to extend from the Jurassic to the Cambrian periods. Fine details of cellular ultrastructure (see especially PARDOS & BENITO, 1990) have been brought to light, contributing to a better appreciation of the functional morphology of the group. Surprising observations have been made on their life habits. Interest in the molecular developmental of the group has revealed body plan patterns conserved with their common ancestor, chordates (LOWE & others, 2003; LOWE & others, 2006). The current phylogeny is robust, with broad taxonomic sampling (CANNON & others, 2014), with the exception of the family Spengelidae. The genomes of *Saccoglossus kowalevskii* and *Ptychodera flava* have been sequenced, providing a tremendous resource for future investigations (TAGAWA, 2016; SIMAKOV & others, 2015). The conserved linkage, or micro-synteny, of transcription

factors involved in gill development have been revealed (Gillis, Fritzenwanker, & Lowe 2012; Simakov & others, 2015). Similar studies on other organ systems will come, and higher levels of conserved linkages, or macro-synteny, may be expected. The genes involved in the biosynthesis and degradation of the sialic acid molecule, a deuterostome synapomorphy (Cameron, 2005), includes nine that arrived as transposons from a prokaryote or protist donor (Simakov & others, 2015). In their review of the development of the group, Kaul-Strehlow and Röttinger (2015) emphasized a need for more investigations on the development of the nervous and muscular systems, and one might add the coelomic, reproductive, and immune systems. There is a single paper on the immunodefense of the group (Tassia, Whelan, & Halanych, 2017). Interest in acorn worm biology has grown—affirmed by the 1st International Hemichordate Meeting, Hopkins Marine Station at Stanford University, December 2016—and the future looks bright.

Future fruitful avenues of research may include: 1) A more extensive sampling of South America, Africa, Asia, as well as deep water worldwide where many species remain to be found. 2) The burrow shape of acorn worms varies tremendously and there seems to be some genus-specific patterns. The fossil record of burrow trace fossils is rich (Bromley, 1996; Seilacher, 2007; Gingras & others, 2008) and may provide some insight on the origin of modern acorn worm genera. Horst (1940) suggested that an enteropneust similar to *Saccoglossus* is responsible for the spiraling trace fossil, *Gyrolithes* Saporta, 1884. This, as well as changes to burrow structure—depending on season or sediment parameters—should be explored. 3) Intensive sampling of many individuals within a species is needed to assess the amount of intraspecific varia-

tion, in the structure of the heart-kidney coelomic process, the collagenous gill bars and nuchal skeleton, the ossicles, as well as developmental genes—because variation is what selection works on. Such studies are rare, the most comprehensive study being that of the many *Ptychodera flava* variants from the Indian Ocean (Punnett, 1906). 4) Do closely related species have similar developmental processes—as might be expected—or is the variation substantive, as in the direct developer *Saccogossus kowalevskii* to the tornaria of *Schizocardium californicum* (see Gonzalez, Uhlinger, & Lowe, 2017)? Experimental molecular developmental approaches that include gene knock-down (Tagawa, 2016), RNAi, CRISPR, and single-cell sequencing (Klein & others, 2015), will provide more robust and nuanced tests of homology. 5) Nearly nothing is known of the post-juvenile development of acorn worms, but the powerful potential of these investigations is that the ontological development can be compared with the paleontological equivalents, particularly with the Cambrian forms that are abundant and preserve exquisite details of extracellular matrix structures, including gill bars and tubes. 6) Nothing is written on the quantitative genetics, the population-based studies of continuously varying characters, nor how these characters respond to selection. 7) Slightly more is known about the neural physiology (Pickens, 1970; Cameron & Mackie, 1996) and respiratory physiology of acorn worms (Azariah, Ismail, & Najib, 1975; Ditadi, Mendes, & Bianconcini, 1997). Is the physiological role of the gill slits respiratory as the name Enteropneusta—Greek for gut-breathing—implies, or is the primary role of the acorn worm gills in ammonia exchange or acid-base regulation? Even less is known of embryonic and larval physiology and behavior. Clearly, much more research awaits.

INTRODUCTION TO THE CLASS PTEROBRANCHIA

JÖRG MALETZ and CHRISTOPHER B. CAMERON

The class Pterobranchia LANKESTER, 1877 is comprised of sedentary to planktic organisms with communal or colonial zooids that first appeared during the Cambrian and includes extant species, such as *Rhabdopleura* ALLMAN in NORMAN, 1869a. They are present worldwide in marine environments. Pterobranchia zooids are divided into three body regions: preoral lobe (cephalic shield), collar, and trunk. The collar extends to form one or more pairs of arms, each bearing double row of ciliated tentacles used in feeding. An elongated trunk serves as an interconnection between zooids in colonial forms. Most species feature external organic housing referred to as the tubarium. Tubaria have been preserved in the fossil record and, thus, their structures form the basis for the classification of the Pterobranchia.

The Pterobranchia can be differentiated into two main groups: the pseudocolonial Cephalodiscida and the entirely colonial Graptolithina. The Cephalodiscida include organisms with separate individuals, but clonal, asexually produced zooids are connected to their mother individuals when immature (Fig. 9.1). After reaching maturity, they may separate from their mother zooid and lead an independent life in their communal housing constructions. There is no apparent difference between sexually and clonally produced mature zooids in the Cephalodiscida.

The truly colonial Graptolithina start their colonies from a sexually produced mother zooid, the sicular zooid, comparable to the ancestrula of the Bryozoa. All subsequently produced clonal zooids are interconnected for life through the stolon system (Fig. 9.2). Apart from extinct benthic and planktic graptolites, which constitute the largest group of taxa, the Graptolithina also includes the small group of extant, benthic rhabdopleurids (MITCHELL & others, 2013), that remain nearly unchanged since the Early Ordovician (e.g., ANDRES, 1980; MIERZEJEWSKI, 1986).

The Pterobranchia possess a number of special developments and features that set them apart from the rest of the phylum Hemichordata—namely, small-sized, individual zooids with a specialized anatomy, a complex cycle of sexual and asexual reproduction, and most importantly, from a fossil point of view, the secretion of a special housing structure, the tubarium (Fig. 9.2). In short, the Pterobranchia can be described as tube-building, communal to colonial, marine organisms with a benthic to planktic lifestyle and a complex sexual and asexual cycle of reproduction.

EVOLUTIONARY ORIGINS

Latest interpretations (e.g., CANNON & others, 2014; NANGLU, CARON, & CAMERON, 2015; SIMAKOV & others, 2015) indicate monophyly of the Pterobranchia relative to the Enteropneusta (Fig. 10). Information on the early evolution of the Pterobranchia is scarce and can only be estimated from the record of a few early to middle Cambrian fossil tubarium fragments. The cladistic analysis of benthic graptolites (MITCHELL & others, 2013) indicates a poor resolution of most groups, but the Cephalodiscida can easily be differentiated by their non-colonial development. The invariably colonial Graptolithina have the highest amount of evolutionary diversification with the planktic Graptoloidea as the geologically most important group. The Enteropneusta differ from the Pterobranchia by the position of the anus at the end of their elongated body; the Pterobranchia have a U-shaped gut with the anus positioned directly below the collar.

If these interpretations are correct, the evolution of the pterobranchs may be based on the miniaturization of the individuals associated with a simplification of their body construction and loss of complex internal
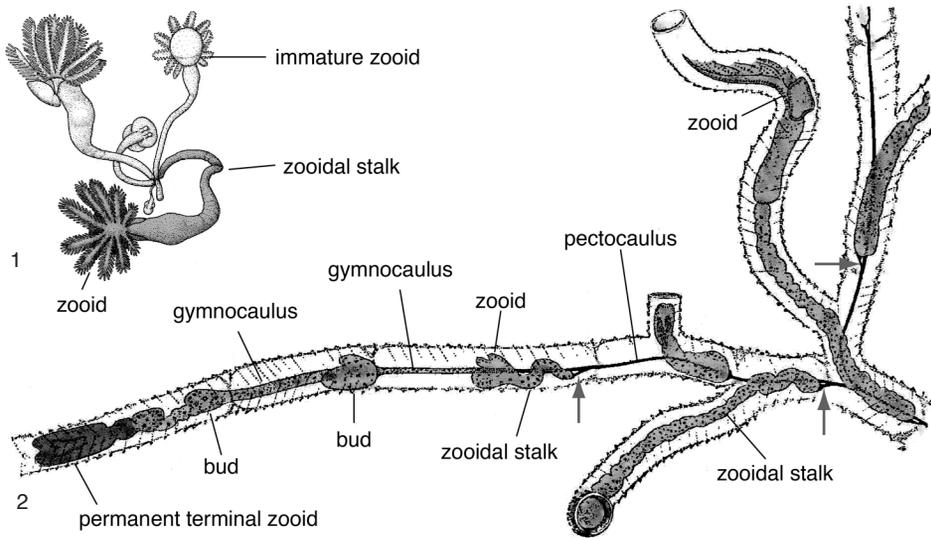
FIG. 9. Pterobranch organization. *1, Cephalodiscus gracilis* M'INTOSH, 1882, zooid with juveniles (adapted from Lester, 1985, fig. 2); *2, Rhabdopleura normani* ALLMAN in NORMAN, 1869a, part of tubarium with permanent terminal zooid, showing terminology of the stolon system (adapted from Ridewood, 1907, fig. 7). *Arrows* point to the short zooidal stolons of the *Rhabdopleura* zooids.

organs and, eventually, the exploration of a colonial lifestyle with the generation of numerous asexually produced members or zooids. The evolution of these characteristics and the origin of the secretion of the typical pterobranch tubarium is not clear. Many of the features of fossil zooids can only be estimated from the characters of extant taxa, as the actual organisms are almost completely unknown from the fossil record.

The miniaturization of the pterobranch zooids can be simply understood by comparing the related enteropneusts, worm-like organisms of up to 2 m in length, with the generally small pterobranch zooids (~0.6–10 mm). However, miniature enteropneusts, measuring less than 1 mm long, have also been discovered (WORSAAE & others, 2012). Cephalodiscid zooids can reach lengths of several mm and, thus, are larger than the 0.6–2 mm long rhabdopleurid zooids. The size of the zooids of the extinct taxa of the Graptolithina is more difficult to estimate (e.g., SUDBURY, 1991; RIGBY & SUDBURY, 1995), but considering the small tubes and apertural openings in most taxa, they would

not have been larger than the zooids of a modern *Rhabdopleura*.

The construction of the pterobranch tubarium can be quite complex, and details are discussed in this volume's sections on taxonomy of individual groups. The general features of both fossil and extant Pterobranchia are described in *Morphology of the Pterobranch Tubarium* (p. 29–80), first published as MALETZ, LENZ, & BATES, *Treatise Online,* 2016. The evolutionary origin of the peculiar housing system of the Pterobranchia is unclear. One possibility, based on the tube-dwelling habitat of the Cambrian acorn worms *Spartobranchus* CARON, CONWAY MORRIS, & CAMERON, 2013 and *Oesia* WALCOTT, 1911 may be that tubes are a hemichodate plesiomorphy. If this is true, these tubes were then elaborated on in the Pterobranchia and lost on the branch to the extant worms (CARON, CONWAY MORRIS, & CAMERON, 2013; NANGLU & others, 2016).

Modern Enteropneusta produce mucus-lined burrows from glands on the proboscis (NØRREVANG, 1965; NANGLU, CARON, & CAMERON, 2015). The composition of this
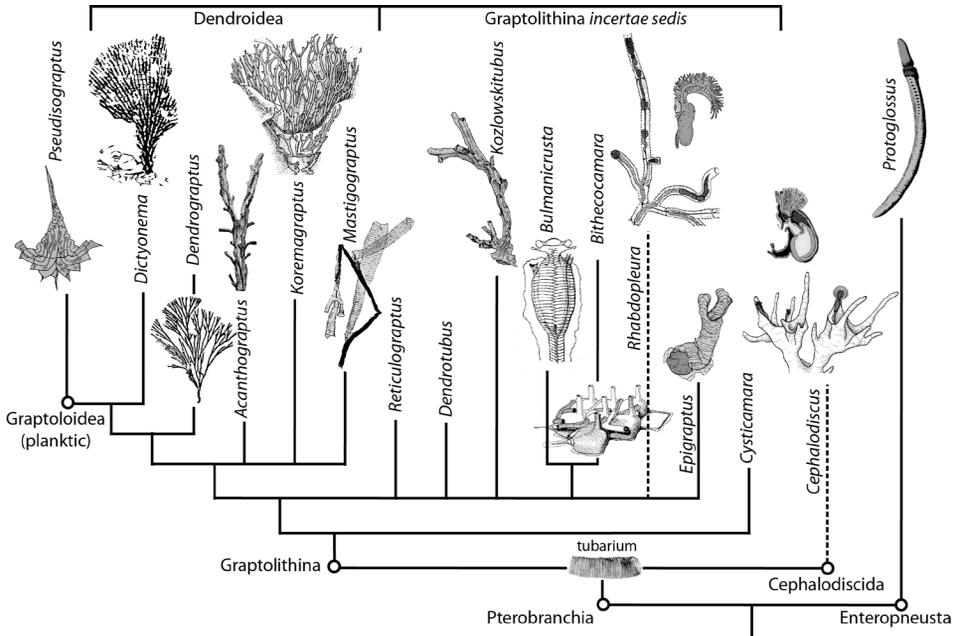
Fig. 10. Relationships of the main groups of the Graptolithina. Diagram based in part on Maletz (2014b). *Dotted lines* in diagram indicate extant members.

mucus and its possible relationship to the secretionary material of the tubaria in the Pterobranchia may be important to study in the future, especially since Nanglu, Caron, and Cameron (2015) suggested that the burrows of *Spartobranchus* from the Cambrian Burgess Shale were unlikely to be based on the secretion of mucus alone, because these fragile burrows would then have easily been destroyed. The tubes of *Oesia,* previously described as the alga *Margaretia,* were fibrous but unlike pterobranch tubes, were permeated with holes (Nanglu & others, 2016).

In the Enteropneusta, the proboscis is completely covered with the mucus secreted from its glandular cells, whereas in the Pterobranchia, the glandular secretion is limited to a special area on the proboscis, the cephalic shield (Dilly, 1986, 1988). In *Rhabdopleura,* secretion of the dome of the colony occurs by secretory cells of the ventral epidermis of the larva, and this site probably becomes the ventral surface of the cephalic shield in the later ontogeny of the zooid (Lester, 1988a, 1988b). There is no information on mucus production in modern

pterobranchs. Interestingly, non-fusellar tissue occurs in some rhabdopleurids (e.g., Kulicki, 1971; Mierzejewski, 1986; Mierzejewski & Kulicki, 2003a) and may be indicative of early development of tubarium secretion.

PTEROBRANCH ZOOIDS

The zooidal anatomy of the Pterobranchia is known from the few extant taxa and has been described in detail. Pterobranch zooids (Fig. 11–12) are divided into three parts: the cephalic shield or proboscis (protosome), the collar bearing the arms (mesosome), and the trunk (metasome). A slender, flexible zooidal stalk is located at the end of the trunk and connects the individual zooids of the colonies to the stolon system, or pectocaulus, in the Graptolithina (Fig. 9.2), and to a common, motile, ciliated disk in most Cephalodiscida (Fig. 9.1). The zooidal anatomy of the Cephalodiscida (*Cephalodiscus* M'Intosh, 1882; *Atubaria* Sato, 1936) and Graptolithina (*Rhabdopleura*) differs in a number of modifications of the body, such as the number and development
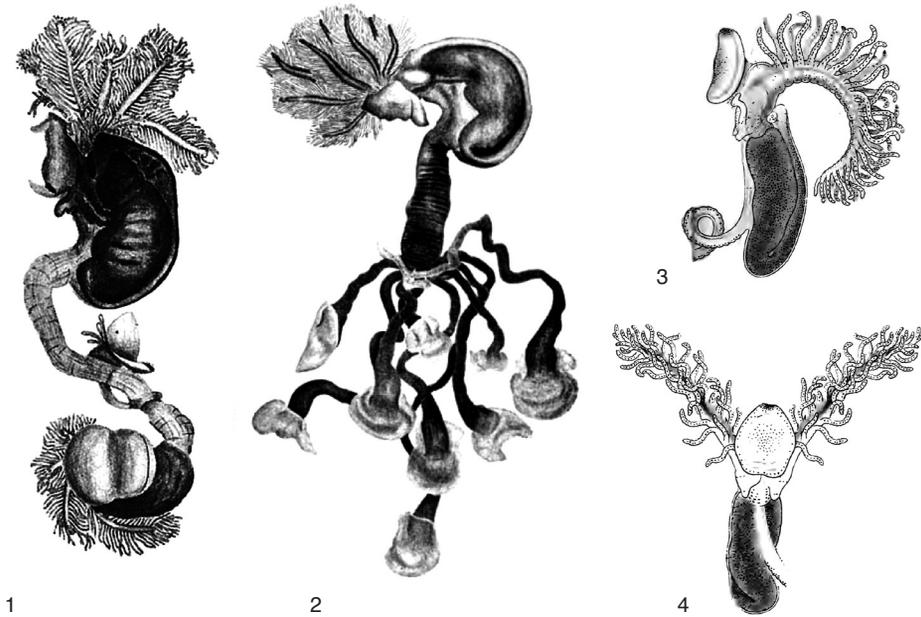
FIG. 11. Pterobranch zooids. *1, Cephalodiscus* (*Acoelothecia*) *kempi* JOHN, 1931, mature zooid with two buds in different stages of development (John, 1931, pl. 35,*2*); *2, Cephalodiscus* (*Cephalodiscus*) *fumosus* JOHN, 1931, mature zooid with at least nine budding individuals (John, 1931, pl. 35,*3*); *3–4, Rhabdopleura normani* ALLMAN in NORMAN, 1869a, lateral (*3*) and ventral (*4*) view of zooids (adapted from Sars, 1874, pl. 1,*1–2*).

of the arms and gonads and the presence or absence of gill pores. Other differences appear in the size of the zooids and their interconnections.

MASTERMAN (1897, 1898a, 1898b, 1900, 1903), HARMER (1905), ANDERSON (1907), SCHEPOTIEFF (1907a, 1908), JOHN (1932), DILLY, WELSCH, and REHKÄMPER (1986a, 1986b, 1986c) and WELSCH, DILLY, and REHKÄMPER (1987) described the anatomy of the zooids of *Cephalodiscus* in some detail. HORST (1939) and HYMAN (1959) provided an overview of the knowledge. STACH, GRUHL, and KAUL-STREHLOW (2012) described the central nervous system. The mature zooids of *Cephalodiscus* (Fig. 11.1– 11.2) are ∼2–14 mm long and bear four to nine pairs of tentaculated arms on the dorsal side of the collar. The cephalic shield is flexible and possesses a characteristic red pigment line parallel to the posterior edge. The arms form two curved rows on the dorsal side of the collar, whereas the ventral side bears the mouth of the zooid. The arms

are extensions of the collar coeloms and have ∼25–50 paired tentacles. A terminal glandular or tentacular knob is present in some species of *Cephalodiscus*. The trunk consists of a wide, saclike, anterior part that culmidates in a slender stalk used for attachment. The U-shaped gut and the gonads are located in the trunk (Fig. 12.2). A single pair of gill pores are behind the posterior border of the collar. The zooidal stalk is hollow and has a ciliated adhesive disk at the end, with which the zooid attaches itself to the tubarium. This is also where the asexually produced buds appear (Fig. 11.1–11.2). The zooids of *Cephalodiscus* grow attached to the adhesive disk until they mature (Fig. 11.2), and then they may separate and live free. After maturation, they are also able to produce new zooids by asexual budding.

The zooids of *Atubaria* (Fig. 12.1) are similar to those of *Cephalodiscus* but differ in the development of the arms. The antero-internal arm pair bears a long, tentacular rod distally, covered with granules similar to the
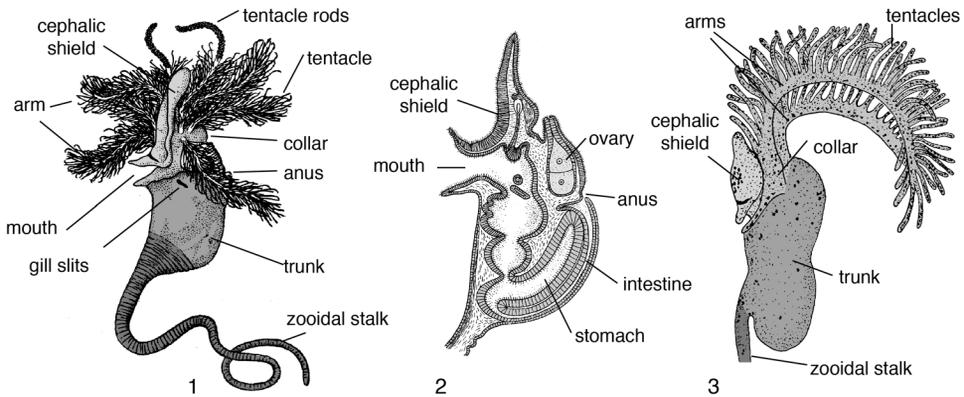
Fig. 12. Zooidal anatomy. *1–2, Atubaria heterolopha* Sato, 1936; *1,* single zooid (adapted from Komai, 1949, fig. 1); *2,* sagittal section of the body of a female zooid (adapted from Komai, 1949, fig. 2); *3, Rhabdopleura normani* Allman in Norman, 1869a, single zooid with part of zooidal stalk (adapted from Hyman, 1959, fig. 67C).

clubs on the arms of certain *Cephalodiscus* species. Another difference is the lack of an adhesive disk at the end of the stalk. All known zooids of *Atubaria* are female (Sato, 1936). Nothing is known on the lifestyle and reproduction of this taxon. According to Sato (1936), the two different zooidal forms can be identified as immature and mature specimens, suggesting that the juveniles separate at an early stage from their mother zooid or do not represent clonally reproduced individuals.

Details of the zooidal anatomy of *Rhabdopleura* (Figs. 11.3–11.4) are provided by Lankester (1884), Schepotieff (1904, 1906, 1907b, 1909), Lester (1988a, 1988b), and Mayer and Bartholomaeus (2003). The mature zooids of *Rhabdopleura* are ~1 mm or less in length. They are organized similarly to *Cephalodiscus* and are differentiated into cephalic shield, collar, and trunk regions (Fig. 12.3). The cephalic shield is oval and has a central glandular region for the secretion of the tubarium. The red pigment strip is sometimes present as in *Cephalodiscus*. The collar of *Rhabdopleura* bears a single pair of arms with paired tentacles, and the mouth is on the shorter ventral side.

The zooids of a *Rhabdopleura* colony are interconnected for life through the stolon system or pectocaulus (Fig. 9). A single zooid,

the sicular zooid, is the founder of the colony and is the only sexually produced zooid. All subsequent zooids develop asexually on the advancing stolon of the colony. Thus, contrary to the situation in *Cephalodiscus,* each zooid of *Rhabdopleura* is only able to produce a single additional zooid through asexual budding.

Hyman (1959) provided an overview on the internal anatomy of the pterobranchs, but details are not discussed herein, as the zooidal anatomy is not known from the fossil record and unlikely to be preserved in fossil specimens. The zooids are either male, female, or neuter, but hermaphroditic ones also exist. The most important difference in the anatomy between enteropneusts and pterobranchs is easily visible in the form of the gut. The small pterobranch zooids have a U-shaped gut and the anus is below the collar on the dorsal side of the body, opposite to the mouth (Fig. 12.2).

The sexes are separate in *Cephalodiscus* but impossible to differentiate externally. Male and female zooids may occupy a single tubarium, but tubaria may also include a single sex. Hermaphroditic zooids, in which one gonad is female and the other is male, are not uncommon. Harmer (1905) described *Cephalodiscus sibogae* Harmer, 1905 with neuter and male zooids, but no females. The neuter zooids appear to

normally have four pairs of tentaculate arms and lack gonads, whereas the males have two arms without tentacles, a vestigial digestive tract, and a trunk filled with two large testes.

The stolon system (Fig. 9) is a defining feature of the colonial Graptolithina and connects the individual zooids. The Cephalodiscida do not possess an equivalent of the soft stolon or gymnocaulus, nor do they have the black stolon or pectocaulus (Schepotieff, 1906) of the Graptolithina. Instead, buds develop from a common point or ciliated disk (Fig. 9.1). Cephalodiscid zooids attach to this point by a flexible, extendable zooidal stalk. In *Rhabdopleura,* the zooidal stalk connects the stolon to a gymnocaulus or pectocaulus. These can bifurcate and have the potential to differentiate and form asexual zooid buds. The stolon develops from the gymnocaulus of the advancing terminal zooid in *Rhabdopleura.*

Lankester (1884) described and illustrated the stolon system of *Rhabdopleura normani* Allman in Norman, 1869a in some detail and differentiated the gymnocaulus and pectocaulus. The gymnocaulus, or soft stolon, is the flexible connection of the zooid to the black stolon or pectocaulus, a hard and inflexible structure. A short zooidal stolon as the direct connection between the zooidal stalk and the main stolon can usually be observed; the zooidal stalk is not a continuation of the main stolon (arrows in Fig. 9.2).

According to Lankester (1884), the pectocaulus develops from the gymnocaulus through the formation of a sclerotized cuticle around the gymnocaulus, which he termed the caulotheca or stalk-pipe. Lankester (1884, p. 634) differentiated between the axial stalk and the contractile stalk of the zooid, but remarked that both are "essentially the same thing." The zooidal stalks differ considerably from the gymnocaulus behind the permanent terminal zooid of the Rhabdopleura colony because they are unable to produce new buds for zooidal growth (Fig. 9.2). Therefore, the zooidal stalk is separated here from the gymnocaulus.

Urbanek and Dilly (2000, p. 201) described the stolon of *Rhabdopleura* as a thread of soft tissue produced by the terminal zooid through an extension of its stalk. The gymnocaulus produces a chain of buds behind the terminal zooid, thus forming the colonial organism. According to Urbanek and Dilly (2000), the stolonal threads have distinct diaphragm complexes from which the zooids develop. The origin and construction of these diaphragm complexes are unclear, but a comparison can be made to the dormant buds. These are encased completely into a thickened, pigmented wall or capsule. The diaphragm complexes are similarly constructed but have an open end. Thus, the diaphragm complex may represent a protective shell for the developing buds (see Stebbing, 1970a, p. 210; Urbanek & Dilly, 2000, p. 216). The walls of the stolon, the dormant buds, and the diaphragm complexes are constructed from crassal fabric (Urbanek & Towe, 1974); thus, they may be secreted similarly from the surface of the organism, and in this respect, differ from the tubarium secretion. Contracted specimens of *Rhabdopleura compacta* Hincks, 1880a have the coiled gymnocaulus within the diaphragm complex (Urbanek & Dilly, 2000, p. 216), clearly indicating that the zooids are moving in and out of their tubes.

The development of the stolon is more complex in dendroid graptolites with diad and triad budding, but details are only known from a few taxa (e.g., Bulman, 1945; Kozłowski, 1949, 1963; Bates & Urbanek, 2002; Saunders & others, 2009). Saunders and others (2009) described the development in *Desmograptus micronematodes* (Spencer, 1884) and presented evidence of a development similar to the diaphragm complex of *Rhabdopleura* in the dendroid graptolites. Due to the durability of the stolon system, it may be preserved in many sediments, as evidenced by numerous fragments previously identified as hydroid remains (e.g., Kozłowski, 1959a; Mierejewski, 1986; Maletz, 2014b; Muscente, Allmon, & Xiao, 2015). Studies of the fossil

record of early planktic graptolites rarely mention the presence of a stolon system (e.g., HUTT, 1974a; LEGRAND, 1974; COOPER & others, 1998), even though it is clear from the tubarium construction that it must have been present. Very likely, the stolon was not strongly sclerotized and, thus, was not preserved in the fossil record.

ONTOGENY AND ASTOGENY

All extant Pterobranchia from which we know any details, may have a life cycle with a double mode of reproduction—sexual reproduction resulting in a single zooid (the sicular zooid), and asexual budding that forms all subsequent zooids in the pterobranch colony (Fig. 13). The ontogeny of the zooids combines with the budding mechanism to form the astogeny of the colony or pseudo-colony. There is no information available on the ontogeny and life cycle in *Atubaria,* even though mature and immature specimens have been discovered. These are all separate individuals, and a clonal origin has not been verified. The evolutionary origin of this asexual, clonal development in the Pterobranchia is not unique in the deuterostomes but can be compared to that of the colonial tunicates. Pterobranchs are unique among animals in that the colonies may be male, female, or contain zooids of both sexes.

Details of the breeding and fertilization are incompletely known for the pseudo-colonial *Cephalodiscus.* It is not known if fertilization is internal and embryos are released from the zooid or if fertilization is external. The embryos develop in the tubarium. Within a short time, they metamorphose into a ciliated larva (ANDERSSON, 1907, fig. 23; HYMAN, 1959, fig. 63D) and hatch from the fertilization membrane. The larva was identified as a planula larva in RAMIREZ-GUERRERO, KOCOT, & CAMERON (2020, p. 847), a lecithotrophic (non-feeding) larva. SCHIAPARELLI, CATTANEO-VIETTI, and MIEREJEWSKI (2004) described a protective larval cocoon in *Cephalodiscus densus* ANDERSON, 1907. The larva may swim freely for a short

time before it settles. At metamorphosis, probably during the free-swimming period (JOHN, 1932, p. 201), it attains the typical zooidal shape with the stalk and the arms in a rudimentary state. When the juvenile *Cephalodiscus* finds a suitable place to establish a new colony, it settles, develops the arms and stalk, and begins to secrete its tubarium. Further development and astogenetic growth of the *Cephalodiscus* pseudo-colony is by asexual budding. This asexual budding of new zooids occurs near the base of the stalk. DILLY (1985) referred to this site as a sucker, but in *Cephalodiscus gracilis* HARMER, 1905 it is a ciliated and motile pad. This common point or pad is the location of cell division and differentiation resulting in new zooidal buds (Fig. 9.1, Fig. 11.2). DILLY (2014) interpreted these *Cephalodiscus* buds as representing a colonial organism and counted up to an estimated 14 individuals, as he was unable to definitively observe individual zooids. When mature, the zooids can detach themselves from the colony, produce new zooids through asexual budding, and secrete a new pseudo-colonial tubarium.

LESTER (1988a, 1988b) described in some detail the life cycle of *Rhabdopleura normani* (Fig. 13), especially the ontogenetic development of the sicular zooid (called ancestrula in LESTER, 1988a) from the early larval stage onward. The uniflagellated spermatozoans are elongated, filiform (LESTER, 1988a), and are probably released into the seawater. The fertilization site is not known, but may occur within the tubarium, where the eggs are kept in special brood chambers by the female zooids. The females of *Rhabdopleura normani* secrete the initial part of their individual tube, which is coiled at least 360° (LANKESTER, 1884; LESTER, 1988a). This structure is used as a brood chamber in which the embryos hatch. The fertilized egg develops into a ciliated larva and escapes from its parental tube by squeezing itself past the female zooid and the younger embryos and then swims for as many as 24 hours before settling (Fig. 13.1). After finding a suitable place to establish a new colony,
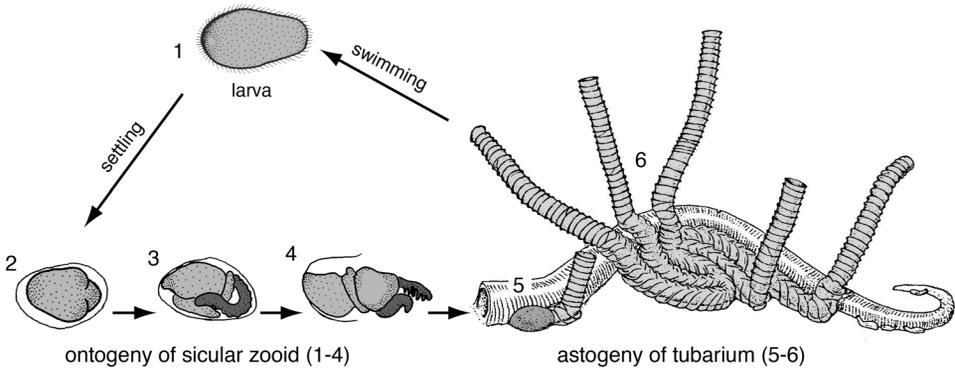
FIG. 13. The ontogeny and astogeny of *Rhabdopleura compacta* HINCKS, 1880a (adapted from Maletz, 2015, fig. 5). *Rhabdopleura* colony is attached to a tube of *Serpula vermicularis* LINNAEUS, 1767 (adapted from Stebbing, 1970b, fig. 3).

the larva secretes the prosicular dome and metamorphoses into a mature zooid (Fig. 13.2–13.4).

The mature sicular zooid attaches with its stalk on one side of the dome and produces a hole in the other side of the dome, through which it emerges to secrete the first tube. The first asexually budded zooid develops from the base of the stalk of this founding sicular zooid (LESTER, 1988a), but further development has not been observed in *Rhabdopleura normani*. A similar development can exist in *Rhabdopleura compacta*. STEBBING (1970a) described the early astogenetic development of the colony of *Rhabdopleura compacta,* and stated that the sicular zooid secretes only a few segments of a creeping tube with the typical dorsal zigzag suture before forming an erect tube with fusellar full rings and the typical collar structures. At this stage, the zooid is fully developed and begins to bud off the asexually produced zooid from the base of the gymnocaulus. This second zooid secretes a septum, separating part of the dome. After this, it breaks down the wall of the dome and secretes its own tube. Further development is not described; thus, it is unclear from what point the next bud originates and which zooid will form the permanent terminal bud.

The sexes are separate in *Rhabdopleura normani* (see LESTER, 1988a), but both may exist in a single colony together with neuter individuals as in *Rhabdopleura compacta* (STEBBING, 1970a). Typically, several sicular zooids are associated and together form intermingling colonies. Thus, it may be difficult to identify and separate individual colonies of *Rhabdopleura*. Zooids that reproduce sexually are apparently morphologically different from other zooids. They generally have reduced arms and tentacles, but also reduced inner organs, suggesting that they do not feed themselves (STEBBING, 1970a).

The life cycle of extinct graptolite taxa (Fig. 14) is expected to be similar to that of the extant *Rhabdopleura,* as all taxa are truly colonial, evidenced by the presence of the common canal connecting the individual thecal tubes (BARRANDE, 1850; MALETZ, 2015). Historically, graptolites have been considered extinct; and no modern relatives have been recognized, even though the graptolites were identified as the group most closely related to the extant *Rhabdopleura*. Therefore, the mystery of the soft-body anatomy of the graptolite zooids remained unresolved, especially because no remains of fossil graptolite zooids that reveal anatomical details have been discovered. The secretion of the graptolite tubarium has been difficult to explain, but problems have also arisen from a lack of information on the secretion of the tubaria in the extant pterobranchs *Rhabdopleura* and *Cephalodiscus*. KIRK (1972a), among others (e.g., BULMAN,
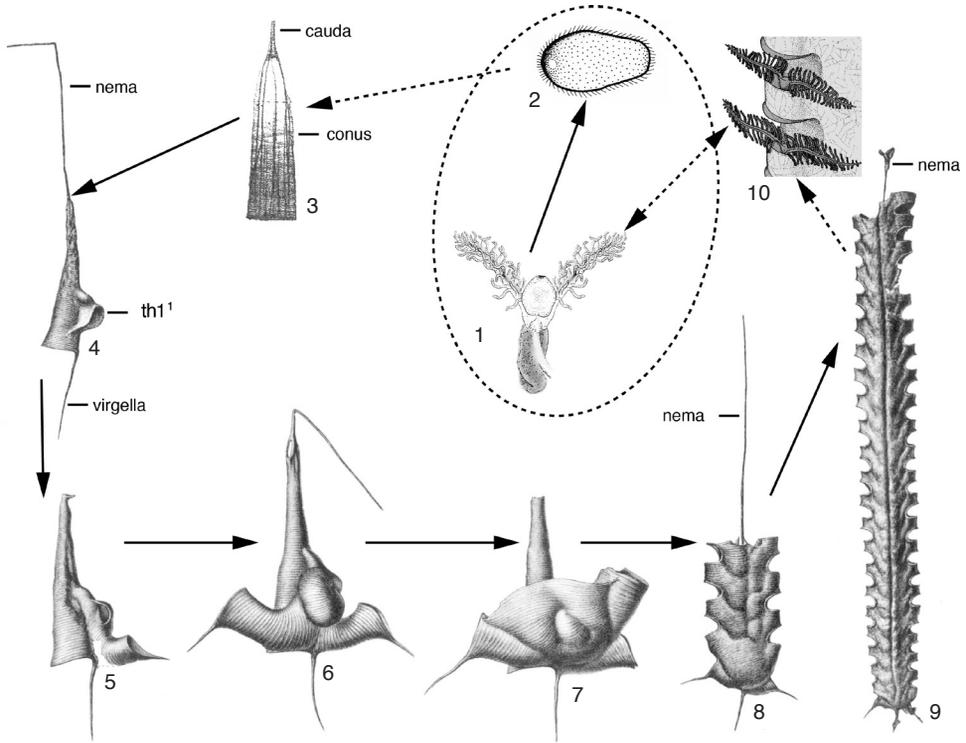
Fig. 14. Ontogeny (*1–3*) and astogeny (*4–10*) of the Graptolithina, based on the astogenetic series of tubaria of *Pseudamplexograptus distichus* (Eichwald, 1840) (Maletz, 2015, fig. 6).

1970; Rickards, 1975; Urbanek, 1976), preferred the explanation that secretion of the graptolite tubarium occurs underneath a peridermal membrane. After a detailed investigation of the construction of the tubaria from fuselli and cortical tissues, Crowther and Rickards (1977), Crowther (1978), and Andres (1977, 1980) suggested a pterobranch-like zooid was responsible for the construction. Bulman (1955, 1970) based his reconstruction of graptolite zooids on a rhabdopleurid type of zooid, and this analog has been used frequently (see Erdtmann, 1982a; Sudbury, 1991; Underwood, 1993; Rigby & Sudbury, 1995). Since the recognition of the extant genus *Rhabdopleura* as a living graptolite (Mitchell & others, 2013), the debate has reached consensus that graptolite zooids are bilaterally symmetrical, small organisms, probably with a single pair of arms comparable to those of *Rhabdopleura*.

Still, a certain variability should be considered likely for the anatomy of the zooids, although it cannot be proven from the fossil record.

LIFESTYLE

A number of researchers have observed and described the lifestyle and development of the extant Pterobranchia since the earlier appearance of works by Sars (1874), Schepotieff (1906), Burdon-Jones (1954), and Gilmour (1979), among others. The zooids of all pterobranchs are able to crawl out of their inhabited tubes and roam on the surface of the tubarium. Whereas the zooids of the unattached *Cephalodiscus* can glide freely inside and outside the tubaria, the zooids of *Rhabdopleura* are more restricted by their attachment to the stolon. However, the stolons can be stretched to allow considerable movement of the zooids. The zooids of *Rhabdopleura* can retract quickly into the

tubes when disturbed, but the subsequent extension is by slow, ciliary gliding. The zooids of *Cephalodiscus* and *Rhabdopleura* secrete external cortical bandages during the zooidal movements outside of the tubaria. The presence of external cortical bandages in extinct graptolite taxa indicates that this was also the case in these organisms.

Very little is known on the ecology of the various pterobranch species, even though living zooids have been observed a number of times (e.g., ANDERSSON, 1907; GILCHRIST, 1915; RIGBY, 1993). Colonies of *Cephalodiscus* have been found at depths ranging from intertidal to ~650 m, attached to various substrates from remains of other organisms to rock surfaces. Species can be found from tropical to Arctic and Antarctic regions, but according to the sparse record (see HYMAN, 1959, p. 177), such discoveries of cephalodiscids may be merely accidental and not indicative of their real biogeographical distribution. The zooids filter feed from the tips of their tubaria (LESTER, 1985), but their dietary needs are unknown.

Rhabdopleura has been found at depths ranging from shore facies to 550 m deep (DILLY & RYLAND, 1985) but appear to be most common at depths between 100–300 m from tropical to Arctic and Antarctic regions. The taxon appears to be worldwide in distribution but has rarely been found due to its small size and, therefore, may easily be overlooked. For example, only in relatively recent times, have rhabdopleurids been discovered in the Mediterranean Sea (LAUBIER, 1964, 1966). Specimens are usually attached to rocks, corals (*Lophelia*), or other living or dead remains of organisms, but they can also hide under empty shells, as is often the case with *Rhabdopleura compacta* (STEBBING, 1970b).

THE FOSSIL RECORD

The fossil record of the Pterobranchia relies completely on the presence of the sclerotized tubaria, as the tiny zooids are not preservable (MALETZ, 2014a; MALETZ & STEINER, 2015). It is known from observing modern pterobranchs that the zooids are unrecogniz-able after only a few days of decay (BRIGGS & others, 1995). The poor fossil record of putative pterobranch zooids indicates some lumps of diagenetic minerals in the regions where zooids may be expected (e.g. BJERRESKOV, 1978; RICKARDS & STAIT, 1984; LOYDELL, ORR, & KEARNS, 2004), but no definite details of the animals' anatomy. However, DURMAN and SENNIKOV (1993, fig. 3,*2*) and SENNIKOV (2016a, 2016b) described the remains of possible zooids from a middle Cambrian (Drumian) rhabdopleurid (*Sphenoecium obuti* DURMAN & SENNIKOV, 1993) as including an indication of arms and tentacles. The photos of the zooids in SENNIKOV (2016a, 2016b) and the interpretative drawings indicate some features, but are not entirely convincing. ZALASIEWICZ and others (2013, p. 143) described the "polymorphic organization in a planktonic graptoloid," based on a strongly tectonized, single tubarium of *Dicranograptus* sp. No evidence of zooidal development was found, and the interpretation of the specimen as most likely representing a stolon-like system is conjectural.

Few early fossil taxa have been compared to the Pterobranchia (Fig. 15). Among these is the genus *Herpetogaster* CARON, CONWAY MORRIS, & SHU, 2010, based on a number of well-preserved specimens from the middle Cambrian Burgess Shale of British Columbia (CARON, CONWAY MORRIS, & SHU, 2010). The suggested relationship of these specimens to the Pterobranchia was supported by the presence of a muscular stalk with an attachment disk and the presence of paired dendritic oral tentacles (Fig. 15.1). However, the presence of the tentacles on the anterior of the head, its dendritic construction, the size of the organism, and the attachment site of the stalk in the middle of the segmented body makes a relationship unlikely and suggests an independent evolution of this stalked organism.

HOU and others (2011) described *Galeaplumosus abilus* HOU & others, 2011, from the lower Cambrian of China, as the oldest, best-preserved, and largest pterobranch of
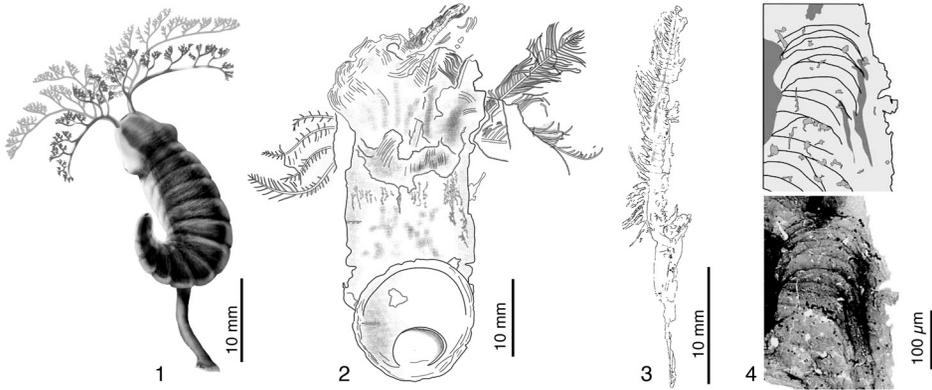
FIG. 15. Putative early pterobranchs. *1, Herpetogaster collinsi*, reconstruction (Caron, Conway Morris, & Shu, 2010); *2, Xianguangia* CHEN & ERDTMANN, 1991 (illustration drawn and used with permission by Qiang Ou, 2015); *3, Galeaplumosus abilus* HOU & others, 2011, holotype (Hou & others, 2011, fig. 2a); *4*, pterobranch fusellum (Harvey & others, 2012, fig. 4).

the fossil record, based on a single specimen (Fig. 15.3). The specimen consisted of arms (probably paired) with rows of paired tentacles, part of a body, and possible indications of a tube with a banding interpreted as fusellar. This specimen is highly fragmentary and a pterobranch relationship cannot be substantiated. OU and others (2017) assembled three Cambrian fossil taxa, including *Galeaplumosus abilus* into a single organism, now identified as the possible cnidarian *Xianguanxia* Chen & Erdtmann, 1991 (Fig. 15.2).

The specimens of *Ectocystis communis* NITECKI and SCHRAM, 1976 from nodules in the Carboniferous Mazon Creek biota of Illinois, are large (several cm long) and possibly represent colonial organisms. Apart from the general outline, details of the anatomy of this organism are not available. The outline vaguely resembles large pterobranch zooids. The arms are not differentiated into tentacles as in pterobranchs, and other characters cannot be compared with the known pterobranch anatomy. Thus, there is no compelling evidence to identify *Ectocystis* as a pterobranch.

HARVEY and others (2012) provided the oldest evidence of true Pterobranchia from a few fragments of fusellar wall material from the middle Cambrian Kaili Formation of China (Fig. 15.4), but it is unclear whether this fragmentary material can be referred to

the Cephalodiscida or the Graptolithina. Early definite pterobranchs include *Sphenoecium mesocambricus* (ÖPIK, 1933) from the middle Cambrian of Sweden and Norway (ÖPIK, 1933; BENGSTON & URBANEK, 1986; MALETZ & STEINER, 2015). A number of specimens from the Wheeler Shale of Utah, USA, have been referred to *Sphenoecium wheelerensis* MALETZ & STEINER, 2015. A poorly illustrated specimen of *Dalyia annularoides* RESSER & HOWELL, 1938, from the Kinzers Formation of Pennsylvania may represent the genus *Sphenoecium;* and, thus, this specimen from the lower Cambrian *Olenellus* Zone would be the oldest recorded pterobranch fossil.

RICKARDS and DURMAN (2006) and MALETZ and STEINER (2015) discussed middle to upper Cambrian Graptolithina and provided a general analysis of the evolutionary relationships of the early taxa. Very little is known on the evolution of upper Cambrian pterobranch taxa until the sudden appearance of planktic graptolites close to the base of the Ordovician system. After the extinction of the planktic graptolites in the Lower Devonian (Emsian), the fossil record of the Graptolithina is very poor. Only a few specimens of rhabdopleurids and cephalodiscids are known from the Lower Ordovician to the Eocene (e.g., RICKARDS, CHAPMAN, & TEMPLE, 1984; MIERZEJEWSKI, 1986).

MORPHOLOGY OF THE PTEROBRANCH TUBARIUM

Jörg Maletz, Alfred C. Lenz, and Denis E. B. Bates

INTRODUCTION

The housing of the Pterobranchia, the tubarium, is a complexly organized organic structure with an extensive fossil record. However, the soft-bodied inhabitants of the tubarium are virtually unknown from the fossil record. Therefore, the anatomy of the Pterobranchia is based on the few extant members (*Atubaria* Sato, 1936; *Cephalodiscus* M'Intosh, 1882; *Rhabdopleura* Allman in Norman, 1869a). The variation and evolutionary changes of the tubarium through time are useful for the biostratigraphy in the planktic graptolites (Graptoloidea). A detailed knowledge of the construction of the tubarium is also important for the understanding of graptolite taxonomy. Basic terminology for the pterobranch tubarium is introduced herein (also see *Glossary of the Hemichordata,* p. 165–180), with special features of individual groups discussed in more detail in the taxonomic chapters.

Nearly all known Pterobranchia produce a housing structure from an organic material (Fig. 16), secreted in modern pterobranchs largely by the cephalic shield of the individual zooids and produced in distinct increments called the fuselli. The poorly known extant cephalodiscid *Atubaria* appears to be the only taxon that does not produce a tubarium. The initial part of some benthic colonies (e.g., *Rhabdopleura; Epigraptus* Eisenack, 1941a), the sicula, was secreted by dermal glands of a larval organism prior to the development of the preoral shield of the mature zooid (see Lester, 1988b). All subsequent housing development is by secretion from the preoral shield of the zooids. This housing was termed a tubarium by Lankester (1884) in the extant *Rhabdopleura,* and Hyman (1959) referred to it as the coenecium in modern Pterobranchia. Törnquist (1890) termed the homologous construction of the fossil groups of the graptolites the rhabdosome. This unique organic development has often been identified as an exoskeleton, but it represents a secreted housing for the pterobranch zooids and, thus, the term skeleton is inappropriate.

The pterobranch tubarium originally may have been highly translucent, as in modern *Rhabdopleura* and *Cephalodiscus,* either colorless or slightly brownish or yellowish in color. Sometimes organic and sediment particles are incorporated in the construction of the tubes and the interconnecting tissue, especially in *Cephalodiscus* tubaria (e.g., *Cephalodiscus agglutinans* Harmer & Ridewood, 1913). The organic material of the tubaria appears to darken with time, and Paleozoic material in general is dark brown to black in color. Sometimes the fossil tubaria are still partly translucent, as, for example, shown by Maletz (1994a) in *Pterograptus* Holm, 1881a, in which most specimens are not artificially bleached. It is not clear, however, whether this translucency is an effect of weathering of the sample.

TUBARIUM CONSTRUCTION

The pterobranch tubarium consists of variably developed independent chambers or communal living compartments for the individual zooids or of interconnected tubes. The two groups of the Pterobranchia, the Cephalodiscida and the Graptolithina, produce similarly developed tubaria, but those of the Cephalodiscida do not have the interconnection and seriality of the tubes in the colonial Graptolithina. The individual zooidal tubes of the tubarium are termed thecae (singular, theca) in fossil graptolites (Fig. 16.1). The term is also used herein for the individual tubes of extant pterobranchs (Fig. 16.2, Fig. 17.6).
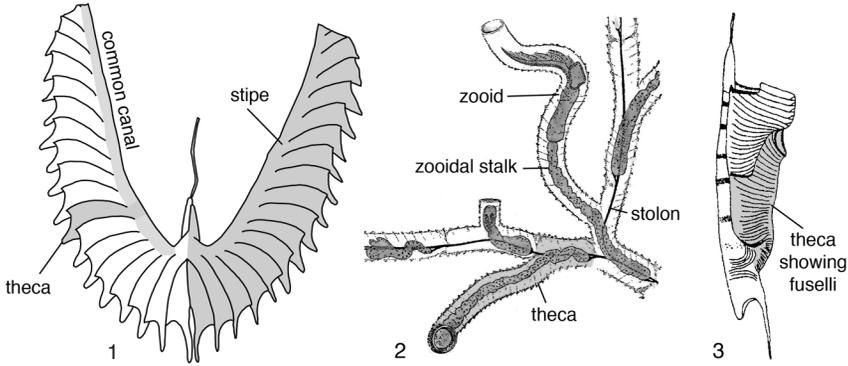
FIG. 16. The structure of the tubarium. *1, Isograptus mobergi* MALETZ, 2011a, tubarium showing two reclined stipes formed from numerous overlapping thecae; common canal indicates colonial organization (adapted from Maletz, Carlucci, & Mitchell, 2009, fig. 5E); *2, Rhabdopleura normani* ALLMAN in NORMAN, 1869a, part of extant tubarium, showing thecal tubes and interconnected zooids, with one thecal tube in *gray* (adapted from Ridewood, 1907, fig. 7a); *3, Heisograptus micropoma* (JAEKEL, 1889), small tubarium showing fusellar construction (adapted from Maletz, 1999a).

The tubaria of the Cephalodiscida (Fig. 17.1–17.2) differ in a number of aspects from those of the derived colonial Ptero-branchia. They are quite variable in development, ranging from completely separate, proximally closed tubes for the individual zooids with their developing buds to an array of interconnected structures with a common internal cavity inhabited by the zooids. In forms with individual tubes, these are usually embedded in a coarse cortical mass or are laterally in contact, at least for part of their length. In one subgenus (*Acoelothecia* JOHN, 1931), the housing consists of a network of branched spines and bars without a common cavity. Because the tubaria of *Cephalodiscus* are formed from social groups of clonally developing organisms, they, unlike the Grapto-lithina, do not possess a recognizably differentiated housing tube for the founder of the colony. A dome or a sicula, as in the derived colonial Pterobranchia, does not exist (MITCHELL & others, 2013).

The thecal tubes of all Graptolithina are interconnected and form a communicating housing system through the common canal (Fig. 16.1). The tubes of *Rhabdopleura,* the only extant genus of the Graptolithina and interpreted as a fairly ancient and primitive taxon, are formed from creeping parts with a dorsal zigzag suture and an erect part with fusellar full rings (Fig. 17.5–17.6). The erect parts of each tube originate through a lateral resorption foramen from the creeping tubes (LANKESTER, 1884); thus, tube building differs considerably from tube growth in more derived graptolithines, in which an initial, primary opening is left for the emergence of the zooids. The development and differentiation of thecae is not well known in most dendroid graptolites, as tips of stipes with growing ends are difficult to obtain. In many benthic graptolites and in the planktic Anisograptidae, the thecae are bundled into triads with lateral origin of new autothecae and bithecae.

COLONY SHAPES

The shapes of pterobranch colonies vary considerably, based on numerous factors (some genetically controlled, others due to ecological interactions of the organisms with their environments). Ecopheno-typic variation most frequently develops in benthic forms in both encrusting and erect taxa. Planktic taxa are less strongly affected by environmental conditions and, thus, generally have a lower amount of ecologically controlled variation. Instead, they possess more highly symmetrical colony shapes, presumably useful for maintaining a stable position in the water column. The main factor determining colony shape is the number of stipes in multiramous colonies.
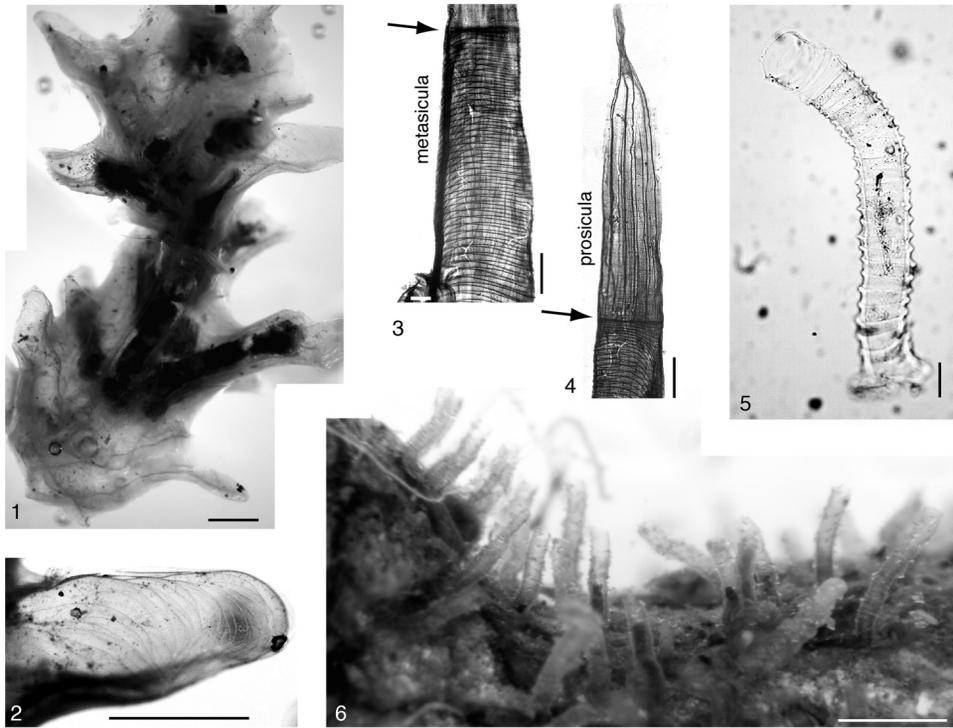
FIG. 17. Colony form and structure in the Pterobranchia. *1–2, Cephalodiscus (Idiothecia) levinseni* HARMER, 1905, origin unknown, extant, SMF 75728; *1,* fragment of a tubarium showing isolated tubes inhabited by zooids (darker matter); *2,* enlarged view of aperture of thecal tube showing irregular fuselli (adapted from Mitchell & others, 2013, fig. 3); *3–4,* isolated and bleached prosicula and metasicula of the Graptoloidea, *arrows* mark boundary between prosicula and metasicula (adapted from Palmer & Rickards, 1991, pl. 13–14); *5–6, Rhabdopleura normani* ALLMAN in NORMAN, 1869a; *5,* individual erect tube showing fuselli, extant (new); *6,* MB.G. 1122, Jaeger collection, Museum für Naturkunde, Berlin; large colony growing on coral, extant, Heltjefjord near Bergen, Norway, ~100 m depth (new). Scale bars, 1 mm (*1–2, 6*); 0.1 mm (*3–5*).

Graptolithines can produce two-dimensional (sheetlike) and three-dimensional (bushy) colonies. Sheetlike colonies can develop secondary three-dimensional shapes, from curved fans to conical colonies, in erect benthic forms and in planktic colonies.

BENTHIC ENCRUSTING COLONIES

Encrusting colonies can form only two-dimensional shapes (Fig. 17.6), but the amount of variation may still be high, depending on the shape of the overgrown surface. Thigmophilic colonies form dense masses of zooidal tubes connected to hardground or other hard surfaces, be it rocks, shells of bivalves and brachiopods, or the corallites of corals. The individual tubes grow in close contact to each other and do not leave any vacant space between them. The extant *Rhabdopleura compacta* HINCKS, 1880a is a good example of this thigmophilic colony shape, but many other benthic pterobranchs possess a similar growth form (see KOZŁOWSKI, 1949). Another common benthic colony form is the runner-type colony of the extant *Rhabdopleura normani* or the Upper Ordovician *Bulmanicrusta*? sp. (MITCHELL, WILSON, & ST. JOHN, 1993), which loosely and quickly covers large areas, though not completely. The individual zooids keep a certain distance from each other and, thus, the stipes never touch. Through their repetitious branching, the colonies can become extremely large.
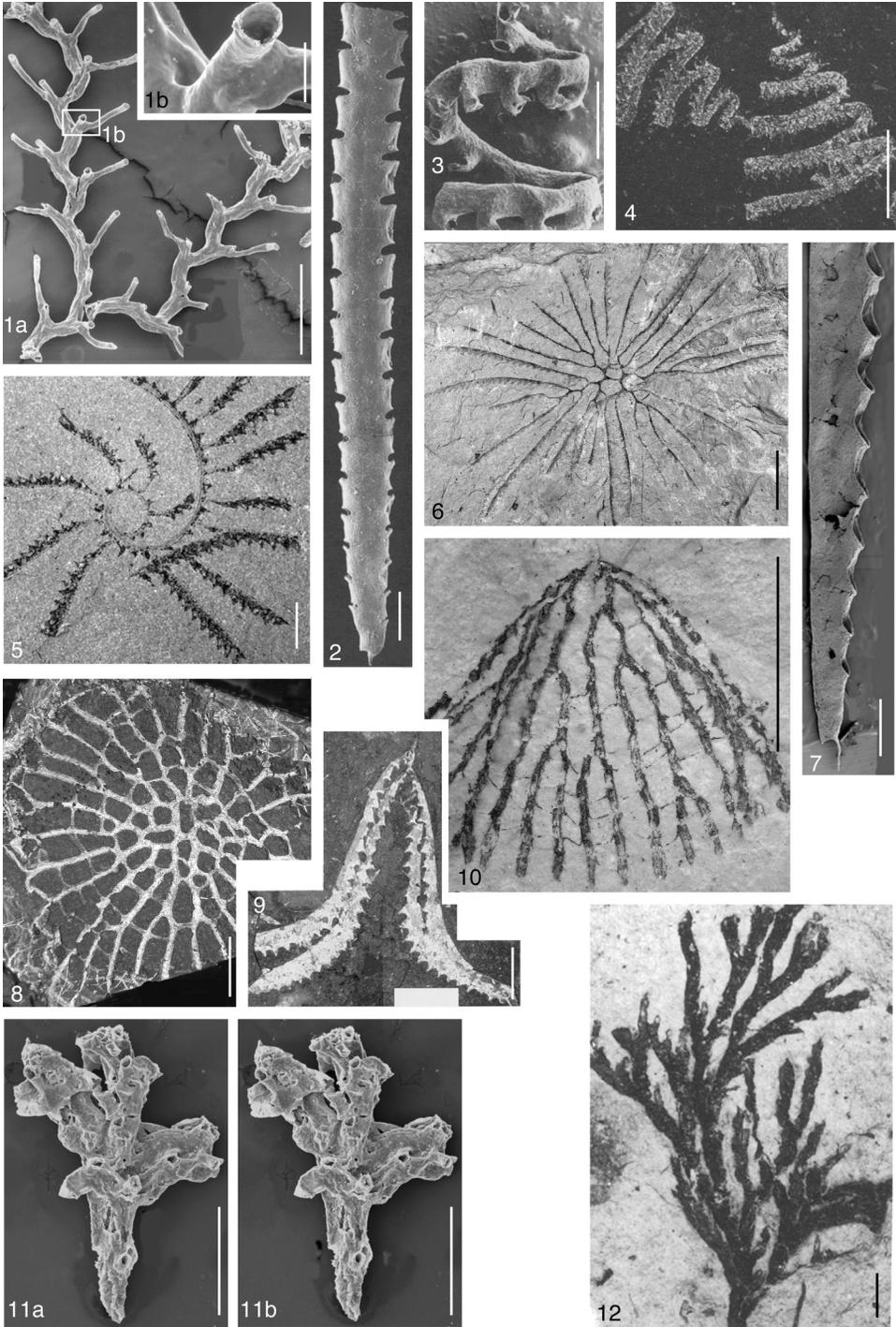
FIG. 18. *For explanation, see facing page.*

BENTHIC ERECT COLONIES

Erect benthic taxa do not develop into thigmophilic shapes, but usually branch at variable distances and form conical, as in planktic *Rhabdinopora* EICHWALD, 1855 (Fig. 18.10), fan-shaped, or bushy (Fig. 18.12) colonies. In conical colonies, the thecae have their openings on the inside of the cone, as evidenced from the few, available, well-preserved specimens (BULMAN, 1933a). In fan-shaped colonies, all openings are oriented in the same direction, whereas in bushy forms, thecal openings can be variably oriented and the colonies are truly three-dimensional. However, in the Dendrograptidae, even in the bushy forms, the thecae appear to be oriented in the same direction on the individual stipes in a serial arrangement. The development of the stipes and the orientation of the thecal openings may be more complex in the Callograptidae, in which individual stipes are formed from a number of overlapping thecal tubes and thecal openings may point in various directions (Fig. 18.1).

PLANKTIC COLONIES

The colony shapes of planktic taxa are generally more symmetrical, due to the need for balance and orientation in the water column. Most multibranched, planktic graptolites grew into an essentially two-dimensional, planar shape (Fig. 18.6). This shape, however, could be transformed either into umbrella-shaped (Fig. 18.8) or strongly conical (Fig. 18.3–18.4, Fig.18.10) colonies. Their three-dimensionality is based on the modification of this original conical arrangement of the stipes in the early planktic genus *Rhabdinopora* (Fig. 18.10). A truly three-dimensional colony growth with highly irregular branching (as, for example, in benthic *Dendrograptus* HALL, 1858 species) has not been recognized in any planktic form. Thus, there are no bushy planktic colonies, as there are in benthic colonies (Fig. 18.11–18.12). Three-dimensional shapes developed in coiled (Fig. 18.3–18.4) and cladial-bearing monograptids (Fig. 18.5) in the Silurian and Lower Devonian, but three-dimensional, spiral colonies were also present in Ordovician dicellograptids and dicranograptids.

THECAL WALL FORMATION

The tubes, or thecae, form housing structures for the individual members of the colony. They have a characteristic and simple construction in the form of fusellar half rings and full rings. The shape of these tubes may vary considerably and is used for taxonomic and phylogenetic interpretations. Isolated, erect tubes may be round in cross section, but creeping tubes are more often flattened on the ventral side. In complex colony structures, they may be shaped irregularly,

FIG. 18. General shapes of graptolite colonies. *1a–b, Acanthograptus* sp. fragment, branching, Silurian (upper Wenlock), Canadian Arctic, scale bar, 1 mm; *1b*, enlarged view of *1a,* showing bitheca and autotheca, scale bar, 0.1 mm (Lenz & Kozłowska-Dawidziuk, 2001, pl. 1,12); *2, Clinoclimacograptus barriei* (ZALASIEWICZ & TUNNICLIFF, 1994), straight, biserial development, Silurian (middle Llandovery), Canadian Arctic, scale bar, 1 mm (Melchin, 1998, pl. 1, fig. 13); *3, Spirograptus guerichi* LOYDELL, ŠTORCH, & MELCHIN, 1993, narrow, conical spiral, Silurian (upper Llandovery), Sweden (Dalarna), scale bar, 1 mm (Loydell, Štorch, & Melchin, 1993, fig. 3B); *4, Spirograptus turriculatus* BARRANDE, 1850, narrow, conical spiral, Silurian (upper Llandovery), Czech Republic, scale bar, 5 mm (Loydell, Štorch, & Melchin, 1993, fig. 3A); *5, Cyrtograptus mehnerti* HUNDT, 1949a, broad, low, conical spiral, Silurian (lower Wenlock, Sheinwoodian), Canadian Arctic, scale bar, 5 mm (Lenz & others, 2012, pl. 22, fig. 1); *6, Praegoniograptus clonograptoides* (HARRIS & THOMAS, 1939), holotype, planar to umbrella shaped, Lower Ordovician, Victoria, Australia, scale bar, 10 mm (new); *7, Pristiograptus dubius* (SUESS, 1851), uniserial, Silurian (middle Wenlock), Canadian Arctic, scale bar, 1 mm (Lenz & others, 2012, pl. 11, fig. 8); *8, Sagenograptus macgillivrayi* (T. S. HALL, 1899), umbrella shaped, Ordovician (Tremadocian), Victoria, Australia, scale bar, 10 mm (new); *9, Tshallograptus fruticosus* (HALL, 1865), pendent, bell shaped, Lower Ordovician (Floian), Canada (northern Yukon), scale bar, 5 mm (Jackson & Lenz, 2006, fig. 6D); *10, Rhabdinopora campanulatum* HARRIS & KEBLE, 1928, cone shaped, Lower Ordovician (Tremadocian), Dayangcha, China, scale bar, 5 mm (new); *11a–b, Thallograptus* sp., bushy, stereopair, Silurian (Ludlow), Canada, scale bars, 1 mm (Lenz & Kozłowska-Dawidziuk, 2004, fig. 2,12); *12, Callograptus huckriedei* RICKARDS, HAMEDI, & WRIGHT, 2001, bushy, Lower Ordovician (Floian), Iran, scale bar, 1 mm (Rickards, Hamedi, & Wright, 2001, fig. 2D).
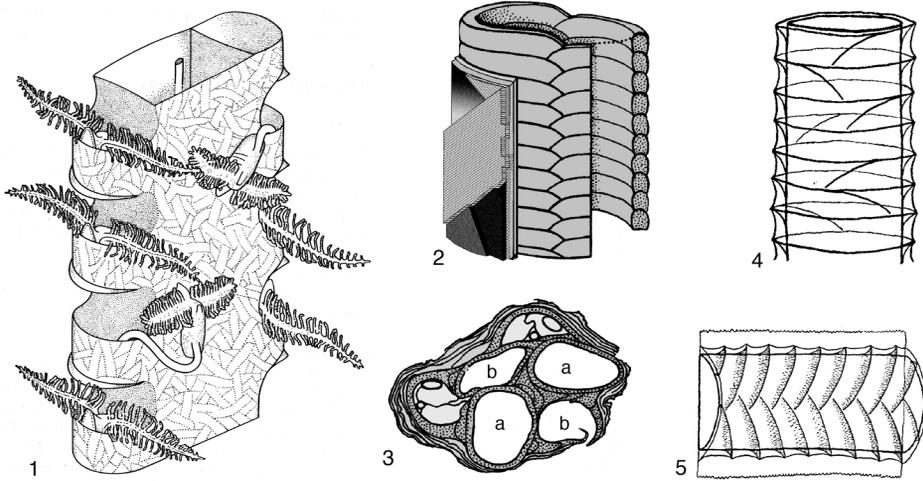
F<small>IG</small>. 19. Thecal construction in the Pterobranchia; illustrations of fusellar and cortical layers. *1,* Part of axonophoran colony with reconstructed zooids and cortical bandaged surface (adapted from Crowther & Rickards, 1977, fig. 3); *2,* zigzag fusellar structure and the outer crisscrossing cortical bandages (adapted from Bulman, 1970, fig. 5,1*,* and Kozłowski, 1938, fig. 2); *3,* cross section through stipe of dendroid showing autothecae (*a*)*,* bithecae (*b*)*,* fusellum and ectocortex (adapted from Bulman, 1955, fig. 6,2); *4–5, Rhabdopleura* sp.; *4,* portion of erect tube with fusellar full rings and irregular sutures; *5,* portion of creeping tube with fusellar half rings and zigzag sutures (Andres, 1977, fig. 4).

depending on the attachment sides and connection between the tubes.

The two, basic constructional features of the thecae are the fusellum (fusellar layer) and the cortex (cortical layer) (K<small>OZŁOWSKI</small>, 1949). These two layers together (Fig. 19.2) have been termed the periderm in the past (W<small>IMAN</small>, 1895), but it is now understood that these layers are formed by a special gland on the cephalic disk of the zooids and are not a dermal layer. As a result, the term periderm is inappropriate.

THE FUSELLUM

Each tube is secreted in individual, narrow increments, the fuselli (singular, fusellus). Numerous fuselli (collectively the fusellum of K<small>ÜHNE</small>, 1955) are stacked one on another with some lateral overlap (Fig. 19.2), forming a distally open tube for the individual housing of each zooid. Each fusellus possesses at least one oblique suture (Fig. 19.4), indicating the method of secretion as a strip of material around the circumference of the tube. The zooid of an extant pterobranch starts at one point and secretes the fusellus while moving its oral disk in a circle around the thecal aperture. In full fusellar rings, a single oblique suture defines the position at which the zooid started and finished the secretion of the individual fusellar ring. In fusellar half rings, two separate fuselli form a full ring of the thecal tube, producing a dorsal and a ventral suture (Fig. 19.2). The fuselli are, thus, growth segments laid down by the zooids in a highly regular and highly symmetrical fashion.

In early members of the Pterobranchia, the fuselli are full rings with irregularly placed sutures (Fig. 17.5, Fig. 19.4); during the evolution of the group, these sutures become more regular and are replaced by fusellar half rings (Fig. 19.5) with a much higher degree of symmetry. Regular fusellar half rings are laid down alternately right and left and produce the dorsal and ventral zigzag sutures of the tubes (Fig. 19.2, Fig. 19.5). Full rings and half rings can, however, occur in the colonies of the extant *Rhabdo-*

pleura. Creeping parts of *Rhabdopleura* colonies possess a distinct zigzag pattern on the dorsal side of the creeping tubes (Fig. 19.5), whereas erect tubes have fusellar full rings with a distinct collar structure (Fig. 19.4). The thickness of the fuselli (and, therefore, the fusellar layer) is usually uniform along the colony, but the height of the individual fuselli may vary considerably, depending on the position in the thecal tube and the ontogeny of the secreting zooid. Early fuselli of a theca are usually of a lesser height than distal or apertural fuselli (WALKER, 1953), but a lesser height may also be present at thecal apertures (BATES, 1987a, pl. 1).

REDUCTION OF FUSELLAR THICKNESS

Fuselli possess an interior part made of fibrils and a thin, denser wall made of the same construction material (see discussion of ultrastructure, p. 36). The amount of material used to form the fuselli varies considerably among groups, and a reduction in wall thickness and density is observable in a number of taxa. The Ordovician genera *Parisograptus* CHEN & ZHANG, 1996, and *Cryptograptus* LAPWORTH, 1880a, possess fairly thin thecal walls, visible often as translucent thecae with clearly observable fusellar structure, whereas associated graptolites on the same sedimentary surface have only thick, dark films of organic material (e.g., WILLIAMS & STEVENS, 1988). In a further reduction of the fusellar wall material, it appears as if the taxa do not possess thecal walls at all, as the wall material is so thin that it rarely survives the fossilization process. For example, the remains of thecal walls may be observable in ragged edges preserved in the cortical bandages of the retiolitids (e.g., BATES & KIRK, 1992, 1997). A considerable reduction may be present only in part of the colonies, but it can also affect the whole colony and may be counteracted by the development of secondary cortical covers. In stratigraphically younger taxa of the genus *Cryptograptus,* for example, the sicula and the first two thecae are so weakly sclerotized

that they have not been found in isolated material. Some authors (e.g., BULMAN, 1945; MALETZ & MITCHELL, 1996) have suggested that because cortical bandages on these structures have not been recognized in isolated material, they were never present.

Thin thecal walls, seldom preserved, and development of lists are traits in all Retiolitidae, most Lasiograptidae, some members of the Abrograptidae (MU, 1958), and as an exception in other taxa. Thecal walls in retiolitids are rarely preserved, even though it exists in isolated material that they were originally present (LENZ, 1994a, fig. 14,*3*, fig.14,*7–9*; LENZ & KOZŁOWSKA-DAWIDZIUK, 2002a, fig. 15) on both the thecal framework and ancora sleeve. Based on very rare preservation of thecal framework walls (LENZ & THORSTEINSSON, 1997) as well as scars and shards in isolated material (BATES, 1987a), it is clear that the thecal framework was comprised of successive layers of fusellar bands. It is not clear, however, in what manner the ancora sleeve layer was constructed, because there appears to be no indication of fusellar laminae (see discussion of the ancora sleeve, p. 75). In other, unrelated groups (e.g., *Retiograptus* HALL, 1865; *Rectograptus* PŘIBYL, 1949), a reduction of the thickness and, ultimately, loss of thecal walls appears to have originated independently.

CORTEX

The cortex, cortical tissue, or cortical bandages are formed in extant pterobranchs in the same way as the fuselli, by the preoral lobe of the zooids. However, the cortical material differs considerably in the way in which it is laid down in the pterobranch colony. It can form thick masses of loose or spongy material around the individual tubes of a *Cephalodiscus* colony or thin layers of material surrounding and covering the surface of thecal tubes in planktic graptolites. In general, a differentiation of ectocortex and endocortex can be made (CROWTHER, 1981; URBANEK & MIERZEJEWSKI, 1984). Endocortex is made of
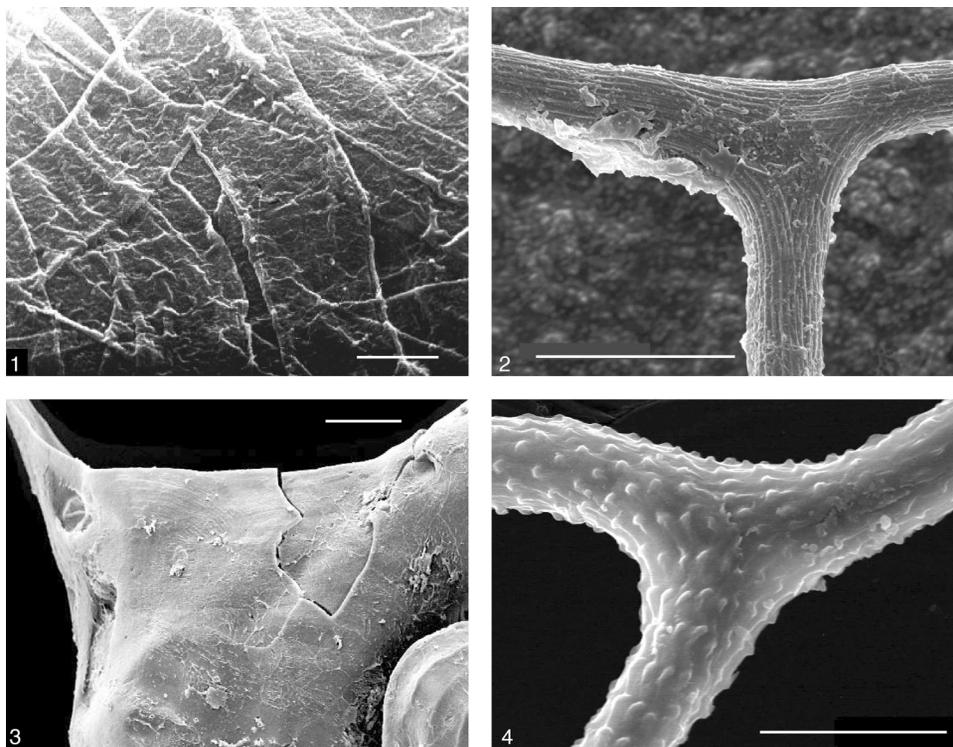
FIG. 20. Cortical bandages. *1, Rectograptus gracilis* (ROEMER, 1861)*,* bandages with distinct raised rims (new, courtesy of Piotr Mierzejewski); *2, Rotaretiolites* sp., showing cortical tissue of strong, parallel, ridgelike bandaging, Silurian (upper Telychian, Llandovery), Canadian Arctic (new); *3, Paramonoclimacis sidjachenkoi* (OBUT & SOBOLEVSKAYA, 1965), Canadian Arctic, showing thin application of cortical material at growing end of colony (new); *4, Plectograptus macilentus* (TÖRNQUIST, 1887), pustulose surface of a plectograptine retiolitid, Silurian (Ludlow), glacial boulder, northern Germany (new). All scale bars, 50 μm.

cortical bandages laid down on the inside of the thecal tubes and is commonly found in some pterobranchs (ANDRES, 1977). It is also present in dendroids (e.g., *Dendrograptus*? sp. in BATES, 1997, pl. 4,*1*). CROWTHER (1981, pl. 16) indicated its presence even in monograptids. Ectocortex (Fig. 19.1–19.4) is much more generally distributed in the Pterobranchia and appears on the outside of colonies.

The cortex is typically secreted in the form of distinct bands or bandages (CROWTHER & RICKARDS, 1977) on the outer surface of planktic graptolite colonies (Fig. 20) and is also present in similar form in benthic colonies (BATES & others, 2011). The precise development of the ectocortex and its distribution in the various groups of Paleozoic graptolites is little understood. Differences in the development are apparent, as some graptolites possess cortical bandages with distinct lateral ridges (Fig. 20.1). Cortical bandages can also be quite indistinct, as in many monograptids, and appear similar to faint brush strokes (Fig. 20.3). In the Silurian retiolitids, there are two kinds of ornamentation on the cortical bandage surfaces: linear striae and pustules (Fig. 20.2, Fig. 20.4).

ULTRASTRUCTURE

DENIS E. B. BATES

The ultrastructure of the fusellar tissue is a complex secretion of the wall material. It can be differentiated into sheet fabric and fusellar fabric (Fig. 21). The details of this construction are visible only under the Scanning Electron Microscope (SEM) and Transmission Electron Microscope (TEM).
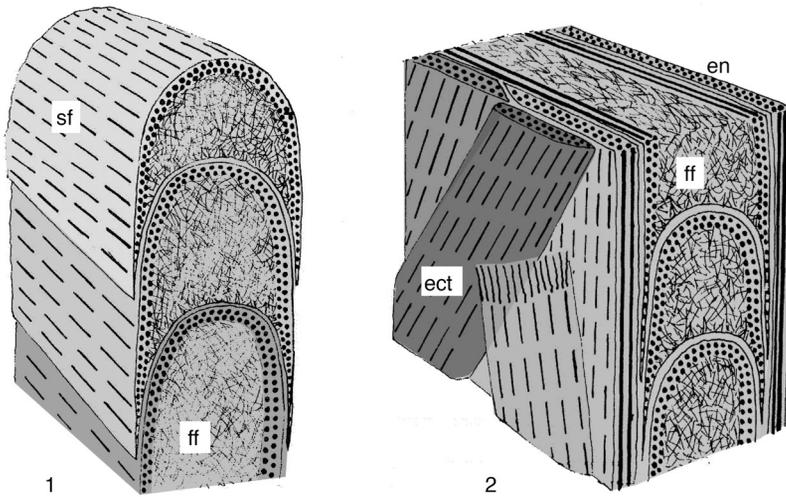
Fig. 21. Ultrastructure of the tubarium wall. *1,* Three stacked fuselli, showing sheet fabric (*sf*) and fusellar fabric (*ff*); *2,* tubarium wall structure with fuselli (*ff*), ectocortex (*ect*), and endocortex (*en*); ectocortex formed as separate bandages (adapted from Bates & Kirk, 1986, fig. 1).

FUSELLI

Each fusellus begins with the deposition of a sheet of granular fabric on the head of the previous fusellus (BATES & KIRK, 1986; BATES & others, 1988). This is succeeded by a three-dimensional meshwork of fibrils, the fusellar fabric (Fig. 21.1–21.2). Generally, these have a random orientation, but variations may be noted. They may start with clumps of fibrils springing up from the base of the fusellus, rather like the roots of mangrove trees or trabeculae. They also tend to become denser toward the arch of the increment. Fibril diameter ranges from 20 nm to 70 nm, with a tendency to increase in diameter toward the bounding sheet of a fusellus. Clockwise spiral striae appear to be present in some taxa (Fig. 22.5, Fig. 22.10).

Each arch is bounded by a sheet, which appears to be finely granular in form. This sheet may contain larger pustules, giving it a knobby surface (Fig. 22.6), the granular sheet fabric *sensu* CROWTHER and RICKARDS (1977). Oval vesicles are also characteristic of this bounding layer; they may be roofed over to give slight swellings, suggesting that there may be two layers to this bounding sheet, or they may appear as unroofed depressions (Fig. 22.6). Beneath the bounding sheet,

there are usually fibrils intermingled with the fusellar fabric, parallel to one another and to the head of the incremental arch (Fig. 22.4).

CORTICAL BANDAGES

Cortical bandages vary in dimensions and ornament and also in the number of fabrics comprising them. In a typical bandage, the lowest layer is a thin sheet, again formed of a finely granular fabric. Occasionally, this is succeeded by random fibrils, especially where a bandage is laid down over an uneven surface (e.g., where it crosses the edge of a previous bandage). The bulk of the bandage is made of closely packed, parallel fibrils, the unit being from one to several fibrils thick, and varying in diameter from 80 nm to 400 nm (Fig. 22.4, Fig. 23.1). Most taxa have an ornament of striae that spirals clockwise (Fig. 22.5).

Interconnecting rods are smaller fibrils, which run perpendicular to the cortical fibrils of the cortex, observed in some genera. They are best developed in *Dictyonema,* in which they are ~27 nm in diameter and are regularly spaced at intervals of ~80 nm (Fig. 22.4–22.5).

The sheet layer covering the bandages is identical to that described for the fuselli (Fig. 22.6). In some taxa, the edges of the bandages are thickened (CROWTHER, 1981);
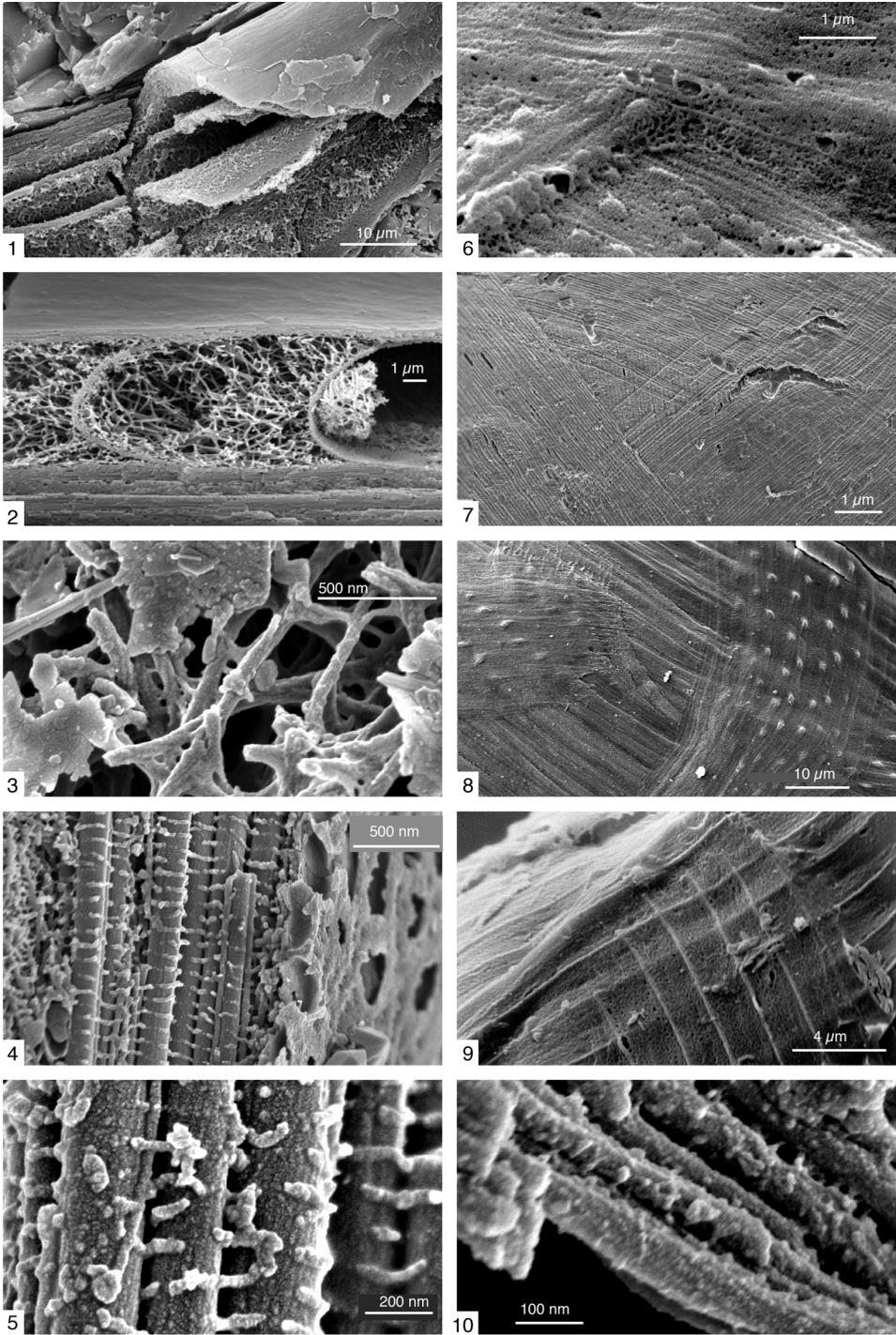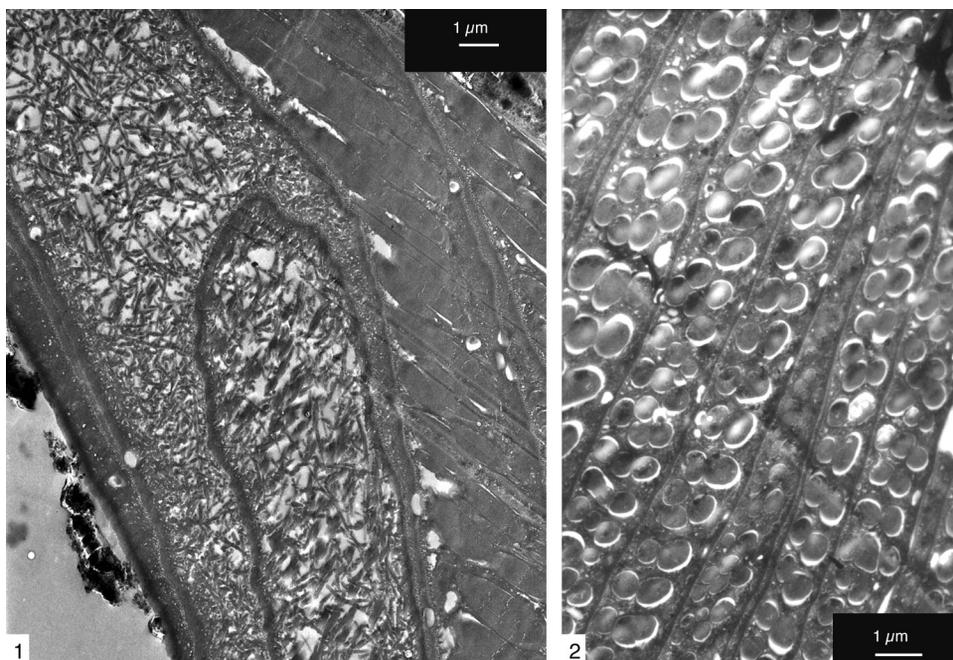
FIG. 22. *For explanation, see facing page.*

FIG. 23. TEM sections of tubarium wall construction. *1, Dendrograptus*? sp., two fuselli and bandages of the ecto-cortex, Gotland, Sweden; *2, Dendrograptus*? sp., cortical bandages, Gotland, Sweden (Bates, 1997, pl. 5).

in others, the bandage is covered by a series of prominent, equally spaced ridges across the bandage (Fig. 22.9). To date, it has not been possible to determine whether these ridges are formed from parallel fibrils or from thickenings of the covering sheet layer. Some Silurian retiolitids have another type of bandage ornament that bears a pattern of blunt tubercles or spines (Fig. 22.8). Internal bandaging (inner cortex) is much more rare. Commonly, internal bandages are much thinner (usually only one fibril thick)

than external ones, and they lack the sheet covering (Fig. 22.7).

CHEMICAL COMPOSITION OF THE TUBARIUM

Pterobranch tubaria consist of organic material, as can easily be recognized from their brownish to black color and their reaction to tectonism within a rock, resulting in the surrounding pressure-shadow minerals (UNDERWOOD, 1992). Specimens weather out as dark films of material that may be

Fig. 22. SEM photographs. *1,6, Geniculograptus typicalis* (HALL, 1865), Viola Springs Limestone, Upper Ordovician (Katian), Oklahoma, USA; *1,* fractured fuselli (new); *2, Desmograptus micronematodes* (SPENCER, 1884), fuselli, with thicker ectocortex below and thinner endocortex above, Racine Dolomite, Silurian (Wenlock), Illinois, USA (new); *3,10, Acanthograptus*? sp., erratic boulder, Middle Ordovician, Mochty, Poland; *3,* fusellar fibrils with spiral striae (new); *4–5, Dictyonema* sp., erratic boulder, Upper Ordovician, Orłowo, Poland; *4,* section through cortical unit with cortical fibrils and interconnecting rods, base of unit on the left, sheet fabric of surface with vesicles on the right (new); *5,* cortical fibrils with spiral striae (new); *6,* bandages with sheet fabric forming their surfaces, both roofed and unroofed vesicles are shown (new); *7, Cyrtograptus lundgreni* (TULLBERG, 1883), internal bandages, one fibril thick and without any sheet fabric, Kolka Borehole, Silurian (Wenlock), Latvia (new); *8, Gothograptus nassa* (HOLM, 1890), bandages on genicular hood with pustules, Mulde Marl, Silurian (Wenlock) Gotland, Sweden (new); *9, Reteograptus geinitzianus* (HALL, 1865), bandages with regularly spaced ridges, Athens Shale, Upper Ordovician (Sandbian), Alabama, USA (new); *10,* cortical fibrils with transverse ridges superimposed on spiraling striae (new).

attacked by bacteria and fungi in the laboratory. Early investigation suggested a material similar to chitin, but neither chitin nor cellulose was proven to be present (FOUCART & others, 1965; FLORKIN, 1969). Instead, the presence of amino acids in three samples of Ordovician and Silurian age showed that they were comprised of proteinaceous substances (e.g., KOZŁOWSKI, 1966a). TOWE and URBANEK (1972), CROWTHER and RICKARDS (1977), and RUNNEGAR (1986), among others, interpreted the graptolite tubaria to be collagenous in composition, based largely on the observation of the banded fibrils in the cortical and fusellar material. The material of the fossil graptolite tubarium consists of an aliphatic polymer and does not contain any protein, even though the structure and analysis of the housing material of modern *Rhabdopleura* (ARMSTRONG, DILLY, & URBANEK, 1984; BUSTIN, LINK, & GOODARZI, 1989; GUPTA, BRIGGS, & PANCOST, 2006) indicated that the building material in fossil graptolites was originally collagen. Even the most recent investigation was unable to define the composition of the building material more precisely (SEWERA, 2011).

ONTOGENY AND ASTOGENY

The Graptolithina have a complex pattern of sexual and asexual reproduction, the most conspicuous aspect of which is the asexual budding of the clonal, colonial zooids. Thus, the ontogenetic development of the individual zooids and their tubes needs to be differentiated from the astogenetic growth of the colony as a whole. The sexually produced founder zooid of the colony is usually easily differentiated from the later zooids. It inhabits (and produces) the sicula, the first theca of the colony.

A new benthic colony starts with the settling of a sexually produced larva and the secretion of the initial part of the sicula. In the extant *Rhabdopleura,* this is accomplished by a ciliated larva. The larva settles on a suitable surface and forms a cocoon or dome (Fig. 24.1–24.3), in which it morphs into

the first zooid (LESTER, 1988b). In derived benthic graptolites (e.g., *Dendrograptus*), the larval stage included a prosicula as the housing for the sicular zooid (KOZŁOWSKI, 1971). The shape of the prosicula of benthic taxa varies considerably but is known from only a very few species. In planktic graptolites, the prosicula always possesses a nema, inferred to indicate a planktic development and life mode.

SICULAR ONTOGENY

A sicula is present in all Graptolithina but not in the Cephalodiscida. It represents the housing of the sexually produced founder zooid of the colony, comparable to the ancestrula of the Bryozoa. Its construction and the construction of the early thecal tubes can be regarded as the most important characters for a specific determination of graptolite taxa.

ATTACHMENT DISK AND NEMA

The attachment of the prosicula to the substrate in benthic encrusting and bushy dendroid forms is poorly known, as mostly only fragments are available and specimens in life orientation often possess considerable cortical overgrowth covering the initial attachment site. Erect, bushy taxa may possess a dendritic holdfast structure to anchor them to a substrate (e.g., *Dictyonema cavernosum* WIMAN, 1896a). There is no credible evidence of any so-called root system in benthic graptolites extending into the sediment, and it has to be assumed that the attachment is invariably produced as cortical tissue by the zooids of the colony fixing the colony to a hard substrate. One extant species of *Rhabdopleura* is known to live in sandy areas and does not depend on attachment to a hard surface (e.g., bivalve shell, coral, or other organism) or hardground.

INITIAL PART OF THE COLONY

The initial part of the colony, represented by the prosicula or dome, has a number of characters that help to identify its development and the phylogenetic relationships of taxa. The dome in extant *Rhabdopleura* (Fig.
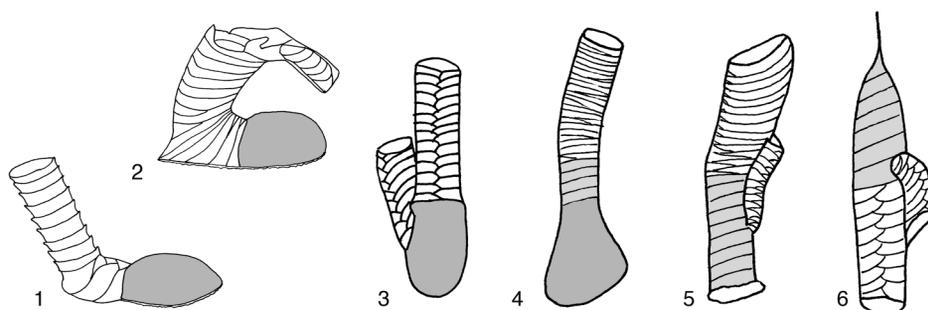
Fig. 24. Prosicular development and comparison with rhabdopleurid dome. *1, Rhabdopleura compacta* Hincks, 1880*a*, lateral view of juvenile with dome and initial (sicular) tube (adapted from Stebbing, 1970b, fig. 3); *2, Epigraptus* sp., juvenile with dome and initial tube (adapted from Kozłowski, 1971, fig. 1); *3, Rhabdopleura* sp., dorsal view of tubarium with initial part of first post-sicular tube (new); *4, Dendrotubus* sp., with distal helical line in the prosicula (adapted from Kozłowski, 1971, fig. 5); *5, Dendrograptus communis* Kozłowski, 1971, tubelike prosicula with helical line (adapted from Kozłowski, 1949, fig. 1); *6,* nematophorous sicula with helical line (adapted from Maletz, Steiner, & Fatka, 2005, fig. 2). *Darker gray,* dome and possible equivalents; *lighter gray,* prosicula with helical line.

24.1, Fig. 24.3) is the only form of initial development known from modern pterobranchs, and it differs considerably from the prosicula of most graptolites. Kozłowski (1971) differentiated the discophorous sicula (Fig. 24.5) of the benthic taxa from the nematophorous sicula of the planktic forms (Fig. 24.6), based on the presence or absence of a free nema.

DOME AND PROSICULA

The prosiculae in *Rhabdopleura normani* and in *Rhabdopleura compacta* are known as a dome (Fig. 24.1, Fig. 24.3). They are formed as a featureless membrane encasing the developing or metamorphosing sicular zooid and are constructed by glands in the ventral epidermis of the larva (Lester, 1988b). In *Cephalodiscus* (*Orthoecus*) *densus* Andersson, 1907, a possibly comparable structure, a cocoon, is formed around developing larvae and is protected on the outside with sand grains (Schiaparelli, Cattaneo-Vietti, & Mierzejewski, 2004). The details of the construction of the dome or the cocoon are unclear. In *Rhabdopleura,* the sicular zooid produces a resorption foramen to hatch from the cocoon and starts to form the initial thecal tube (Lester, 1988b). The development of a dome in place of a prosicula has been documented for the Ordovician genus *Epigraptus* (Kozłowski, 1971; Andres,

1977) but is otherwise unknown in the Graptolithina (Fig. 24.2).

Kozłowski (1971) described the prosicula of the benthic *Dendrotubus* Kozłowski, 1949 (Fig. 24.4) as bottle-shaped, erect, with a helical line in the distal part, homologous to the helical line in the prosicula of planktic graptolites (Fig. 24.6). In contrast to the dome of the rhabdopleurids, the prosicula of *Dendrotubus* is provided with a primary opening, an aperture through which the sicular zooid emerged and started to secrete the metasicular fuselli. This record represents the only evidence of a transition from the dome of the rhabdopleurids to the conical erect or nematophorous prosicula of derived taxa. *Dendrograptus communis* Kozłowski, 1971 (Fig. 24.5) is the only benthic dendroid known to have a tubelike sicula with an attachment and typical helical line in the prosicula.

The nematophorous prosicula of the planktic Graptoloidea is known from many species, and its detailed development was described first by Kraft (1926) for *Rectograptus gracilis* (Roemer, 1861), even though Wiman (1893a, 1893b, 1895) already described and illustrated many of the features from his isolated material. The prosicula is a conical structure with a distinct helical line (Fig. 25.1–25.3), indicating its secretion as a continuous band of fusellar tissue, as is shown by unwound specimens
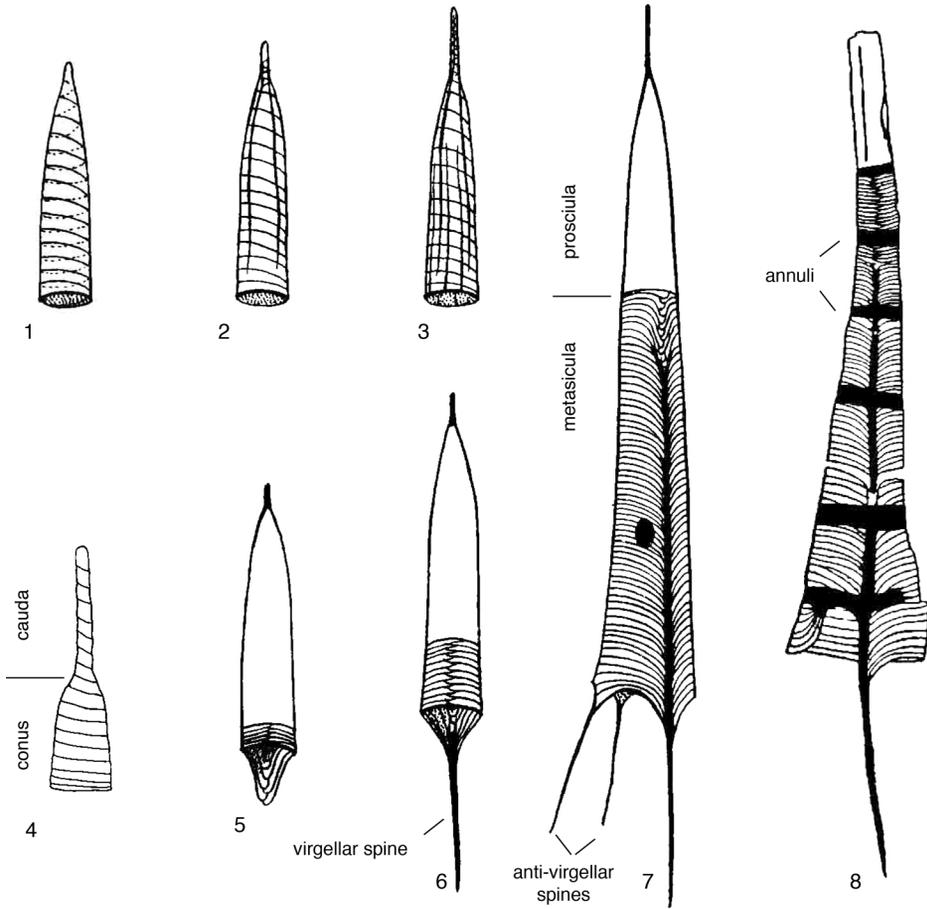
FIG. 25. Sicular development. *1,* Early prosicula with spiral line, cauda incomplete; *2,* prosicula with few longitudinal rods; *3,* mature prosicula with many longitudinal rods (*1–3* adapted from Bulman, 1955, fig. 36); *4,* conus and cauda differentiation in Anisograptidae (Hutt, 1974a, fig. 1); *5,* early metasicula with few fusellar half rings and rutellum; *6,* development of virgellar spine in axonophorans; *7,* complete axonophoran sicula with paired antivirgellar spines and resorption foramen for th1¹ in metasicula (*5–7* adapted from Bulman, 1955, fig. 36); *8,* monograptid sicula with sinus stage and sicular annuli (adapted from Walker, 1953, fig. 1H).

(Kozłowski, 1971). Hutt (1974a) differentiated the prosicula into the conus and cauda (Fig. 25.4), based on the strong constriction at the tip of the conus. The cauda merges into the nema, but it still preserves traces of the helical line, which is not present in the nema. The presence of the helical line can be interpreted to indicate that the conus and cauda were formed together from a juvenile zooid or larval stage. The helical line of the prosicula may be right- or left-handed, but there is no information on quantities

and distribution of right- and left-handed specimens and the development in relation to right- and left-handed growth of the remainder of the colonies. A diaphragm (Fig. 26) has been recognized in the upper part of the conus of many species (Kraft, 1926; Hutt, 1974a; Bates, 1996; Williams & Clarke, 1999).

In a second stage of development, in many species, the prosicula may add a number of longitudinal rods on the outside (Fig. 25.2–25.3). The longitudinal rods do not,
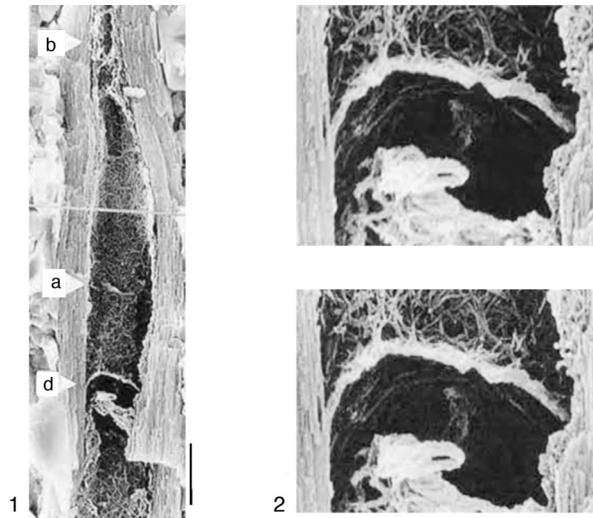
Fig. 26. SEM photograph of prosicular structure. *1*, Top of cauda, below diaphragm (*d*), proximal part of nema (*a*), wider part of nema, and beginning of narrow part of nema (*b*); *2,* stereopair (rotated vertically) showing diaphragm (adapted from Bates, 1996). Scale bars, 1 μm.

in general, encroach onto the metasicula. Thus, they were formed at some later stage during the ontogenetic growth of the prosicula before the metasicular fuselli were added (Kraft, 1926). In *Diplacanthograptus spiniferus* (Ruedemann, 1912) and a number of related Upper Ordovician taxa, one or two thickened strengthening rods remain of the prosicular construction, as the complete prosicula is not recognizable (or perhaps not preserved) in the fossil specimens. This is also occasionally observable in a number of Silurian (Llandovery) retiolitinids. The reason for the presence of the longitudinal rods is uncertain, but it may be noted that a number of early planktic forms lacked the longitudinal rods, whereas they were consistently present in later Ordovician taxa (Williams & Clarke, 1999) and were still present in Silurian to Lower Devonian monograptids (Jaeger, 1991; Urbanek, 1997a).

METASICULA

The metasicula is invariably formed as a distally open tube from fusellar half rings that have a dorsal and ventral zigzag suture, but fuselli may be irregular in dendroid siculae (Fig. 24.4–24.5). It differs consider-

ably from the prosicula in its development and is usually easily differentiated (Fig. 25). The fuselli may be more densely spaced in the proximal part and more widely spaced close to the aperture. In early planktic forms, the differentiation was less prominent, as the helical line may be difficult to separate from the fuselli of the metasicula. Kozłowski (1954) stated that the zigzag sutures in a species of *Didymograptus* M'Coy in Sedg-wick & M'Coy, 1851–1855, s. str. (*Didymograptus artus* group) start only at some distance from the origin of the metasicula, and earlier fuselli were regularly developed.

Maletz (1992, 2010a) used the origin of the first theca to define the ventral side of the sicula. The sicula is often adorned with a rutellum on this side, or with a spine, the ventral virgella (in most axonophorans). The rutellum is a rounded lip on the sicular aperture, formed by a downward extension and broadening of the fuselli at the ventral zigzag suture (Fig. 25.5). Its shape can be quite variable, and stongly elongated rutelli exist. The rutellum is usually broad and short, but it can develop into a distinct spoonlike feature as in *Kinnegraptus* (Skoglund, 1961). A dorsal rutellum is present in some genera and
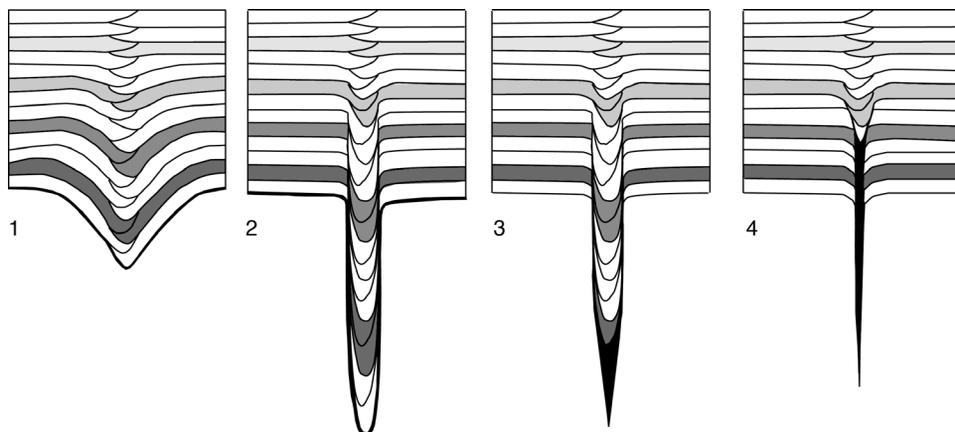
Fig. 27. The stages of development of the virgella. *1,* Rutellum; *2,* lamelliform rutellum; *3,* lanceolate virgella; *4,* virgella (adapted from Maletz, 2010a, fig. 2).

species, especially in the monograptids (e.g., Jaeger, 1978a, fig. 3; Lenz, 2013, fig. 9).

Beginning at the junction of the prosicula and metasicula in graptoloids, distinct, internal, thickened parallel rings, known as sicular annuli (Kozłowski, 1949) (Fig. 25.8), are present in many graptoloids. In many younger graptoloids, and commonly in the monograptids, such as those from the middle and upper Silurian (Lenz & Kozłowska-Dawidziuk, 1998), one or more annuli were formed on the inside walls of the metasicula (Walker, 1953). Unlike the fusellar bands, the annuli are distinct, electron-dense, ringlike structures lying parallel to each other but typically at an oblique angle to the fusellar half rings on the dorsal and ventral sides of the sicula. The number and position of sicular annuli may be fixed in many upper Silurian taxa (Urbanek, 1997a). The function of annuli remains unknown, as does why they generally occur more frequently higher up the stratigraphic column. (Urbanek & others, 2012).

THE VIRGELLA

The metasicula may have a virgella or virgellar spine (Fig. 25.6–25.8, Fig. 27), developing from a prominent rutellum on either the dorsal or ventral side (Maletz, 2010a). Its development can be differentiated into four stages (Fig. 27), often recognizable even in derived virgellate graptoloids. It starts with a rounded process, the rutellum, formed from the distal extension and widening of alternating fuselli on the ventral or dorsal side of the sicula. In a second stage, the rutellum is laterally restricted, and a thickened rim forms around it. At this stage, it is called a lamelliform rutellum (Fig. 27.2). In a third stage, a spine is added at the tip of the lamelliform rutellum, forming the lanceolate virgella (Fig. 27.3). A reduction of the lamelliform rutellum stage in the ontogeny of the virgella forms the true virgella (Fig. 27.4) in the last stage.

The virgella is now known to have originated independently in a number of Early to Middle Ordovician graptoloids (Maletz, 2010a), as was suggested by Bulman (1963a). A dorsal and a ventral virgella are differentiated, based on the position on the sicula (Maletz, 2010a). The ventral virgella is positioned on the side of the origin of the first post-sicular theca with a dorsal virgella on the opposite side of the origin of the first theca.

The sicular aperture can bear a number of additional apertural modifications, other than the rutellum or the virgella (e.g., Mitchell, 1987). A dorsal notch is present in many axonophorans, often associated with

paired antivirgellar spines (e.g., in the Lasiograptidae). The Dicranograptidae possess lateral lobes and paired notches on the sides of the virgellar spine. The Monograptidae bear various apertural modifications; and, whereas there are moderate variations within each pattern, many are species specific, for example, the tonguelike, ventrally curved, dorsal rutellum was a very common development among many single-stipe monograptids of the Lower Devonian (e.g., JAEGER, 1979; LENZ, 2013).

THE NEMA

The nema is a thin rod of material growing from the prosicula (cauda) in planktic graptolites, and the presence of a nema is, accordingly, regarded as evidence of a planktic life style (KOZŁOWSKI, 1971; RICKARDS, 1996). The nema of the Monograptidae has long been named the virgula, but it is now recognized to represent a modified type of nema, forming a leading rod on the dorsal side of the stipes of all monograptids (except those with a pseudovirgula), to which the thecae adhere (BULMAN, 1970; URBANEK & TOWE, 1975). Many biserial graptolites include the nema in the center of the colony, and this is often attached to an interthecal septum. However, the nema may also be off-center or even embedded in the obverse wall of the tubarium (see discussion of the median septum on p. 61). The distal end of the nema always grew in advance of the thecae in the development of the axonophoran colony.

The Monograptidae incorporate the nema as a dorsal rod of their stipes, where it also extends beyond the growing end of the branches. The importance of the nema in monograptids can be inferred from the fact that colonies with cladial branching produce a secondary nema, or pseudovirgula, as 1) the leading rod for the cladial stipe from one of the lateral apertural spines in *Cyrtograptus* CARRUTHERS in MURCHISON, 1867a (see THORSTEINSSON, 1955) and 2) as a separate new structure in the genus *Linograptus* (URBANEK, 1963) and possibly in others. A small number of strongly coiled

Silurian monograptids over time abandoned the original nema, which was free at the isolated tip of the prosicula, and fabricated a pseudovirgula (Fig. 28) along which the stipe grew. This development was first recognized in *Cochlograptus veles* (RICHTER, 1871) by LOYDELL and CAVE (1994) and MALETZ (2001a) and was later also found in the late Wenlock *Testograptus testis* (BARRANDE, 1850) by LENZ and MELCHIN (2008).

In retiolitid taxa without a fully preserved prosicula, the nema is connected to the virgella by the virga (BATES, KOZŁOWSKA, & LENZ, 2005), a list secreted on the surface of the prosicula. It has a flat or grooved inner surface and a convex outer one. In the absence of a preserved prosicula, the length of the virgal groove serves as a proxy for the site and length of the prosicula. Toward (or at) the apex of the prosicula, the virga changes into a full concentric construction, marking the beginning of the nema.

THE INITIAL FORAMEN

The genus *Rhabdopleura* has a resorption foramen, an opening for the emergence of the sicular zooid from the dome, and a second resorption foramen for the origin of the first post-sicular zooid (STEBBING, 1970a). All subsequent zooids resorb a foramen into their compartment of the tube of the growing branch. The presence of a continual terminal zooid indicates a monopodial growth of the colony (URBANEK & DILLY, 2000). The derived taxa of the Graptolithina are an example of a sympodial growth in which each new zooid represents the temporary terminal zooid (URBANEK, 1986).

The origin of the first post-sicular zooid is through a foramen in the sicula. The position and type of this foramen have considerable implications for the higher-level taxonomy of the graptoloids. Initially, it was a resorption foramen, known from a few benthic specimens and most early planktic taxa. It is positioned in the middle to upper (distal) part of the erect tubular prosicula in *Dendrograptus communis* (KOZŁOWSKI,
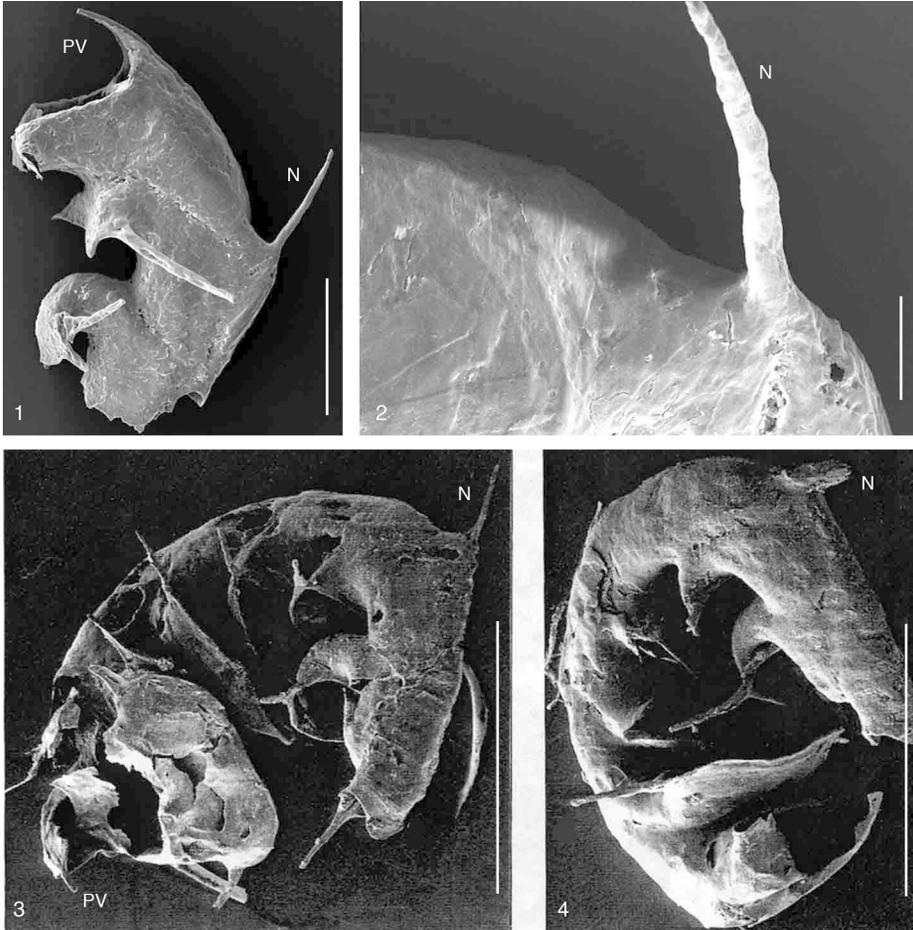
FIG. 28. SEM photographs of pseudovirgula. *1–2, Testograptus testis* (Barrande, 1850), Silurian (upper Wenlock), Canadian Arctic; *1,* tubarium fragment, scale bar, 0.5 mm; *2,* enlargement of pseudovirgula, scale bar, 0.2 mm (Lenz & Melchin, 2008, fig. 4A1–4A2); *3–4, Cochlograptus veles* (Richter, 1871), Silurian (upper Llandovery), Dalarna, Sweden, complete specimen with well-developed pseudovirgula, scale bars, 1 mm (Maletz, 2001a, fig. 3). *N,* nema, *PV,* pseudovirgula.

1971). Legrand (1964a) and Hutt (1974a) described the resorption foramen in the middle part of the conus in the upper Tremadocian *Adelograptus* Bulman, 1941, but it is unknown whether this position was typical of all Anisograptidae. A similar position occurred in the basal Tremadocian *Rhabdinopora* (Legrand, 1974). The foramen was located in the middle part of the conical prosicula in species of the upper Floian *Didymograptellus* Cooper & Fortey, 1982, but it was in the lowermost (distal) part of the prosicula in the closely related *Yutagraptus* Riva, 1994 and *Xiphograptus* Cooper & Fortey, 1982 (Maletz, 2010a). In most dichograptids, the origin of the first theca was in the lowermost part of the prosicula (Williams & Stevens, 1988; Williams & Clarke, 1999). The resorption foramen appeared in the metasicula in the axonophorans (Mitchell, 1987), mostly lying on the right side of the virgellar axis (Fig. 29.1), although sometimes the foramen developed precisely along the virgellar axis, before the origin of the virgellar spine (Loxton & others, 2011).
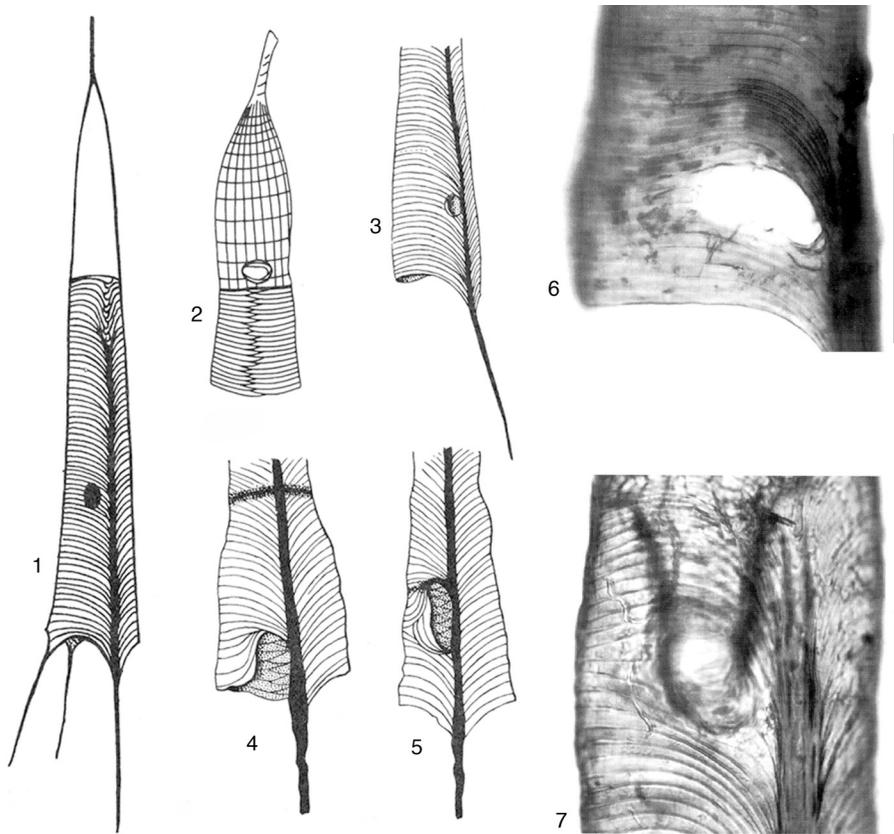
FIG. 29. Foramen development. *1, 3,* Resorption foramen in metasicula, typical of biserial graptolites; *2,* resorption foramen in lower part of prosicula as found in early dichograptids; *4–5,* sinus (*4*) and lacuna (*5*) stages, forming the primary opening for the first theca and developed only in monograptines; *6–7,* lenticular foramen in *Monograptus* sp. cf. *M. arciformis* CHEN & LIN, 1978, Silurian (lower Llandovery), scale bars, 0.1 mm (Dawson & Melchin, 2007, pl. 1).

At some point, a change occurred in the Monograptidae (Fig. 29.4–29.7). Previously, the foramen in the monograptids was considered to be a primary foramen left as an initial opening during the growth of the sicula through the sinus and lacuna stages (EISENACK, 1942). Isolated material indicates that early monograptids (e.g., *Atavograptus* RICKARDS, 1974; *Pribylograptus* OBUT & SOBOLEVSKAYA, 1966; *Coronograptus* OBUT & SOBOLEVSKAYA in OBUT, SOBOLEVSKAYA, & MERKUREVA, 1968; and *Lagarograptus* OBUT & SOBOLEVSKAYA in OBUT, SOBOLEVSKAYA, & MERKUREVA, 1968) possessed a resorption foramen (LUKASIK & MELCHIN, 1994, 1997). A modified resorption foramen with additional fusellar deflection developed in a number of *Monograptus* s.l. species (MELCHIN & KOREN', 2001). DAWSON and MELCHIN (2007) recognized the lenticular foramen (Fig. 29.6–29.7) as the first primary type of foramen, in which an opening for the emergence of the first post-sicular zooid is left in the metasicula. The originally described primary foramen of the younger monograptids with its typical sinus and lacuna stages (Fig. 29.4–29.5) was widely distributed in the greater portion of the Silurian and Devonian monograptids.

THECAL ONTOGENIES

The thecae of the Graptolithina are simple tubes, formed by repetitive clonal constructions, either with identical constructional mode or following a gradual change along
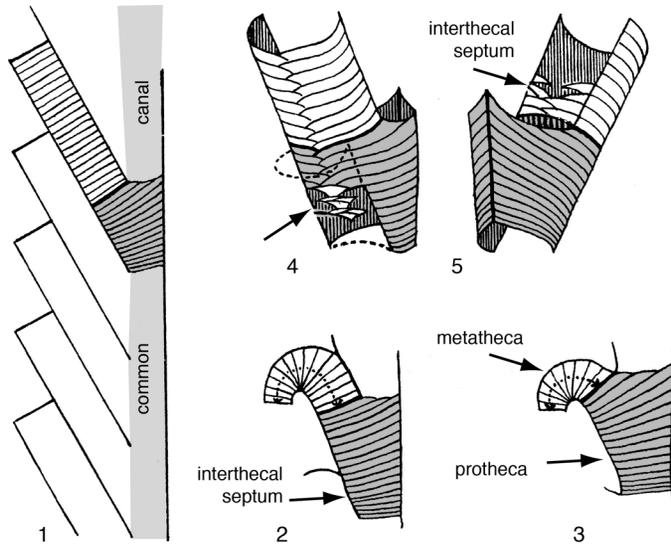
FIG. 30. Generalized shape and terminology of thecae. *1*, Lateral view of simple dichograptid (or pristiograptid) stipe with serially arranged thecae; *2–3*, lateral views of hooked thecae; *4*, oblique dorsal view showing development of interthecal septum; *5*, oblique ventral view showing development of interthecal septum (adapted from Bulman, 1955, fig. 30). *Light gray,* common canal; *dark gray,* prothecae.

the stipes (URBANEK, 1973). Fairly abrupt changes in the morphology of the thecae along a stipe occur in some species. The tubes in the Cephalodiscida, however, are formed as independent, not interconnected assemblages and are simple, round tubes when possessing an isolated aperture, sometimes provided with a distinct, perhaps ventral, rutellum, as in *Cephalodiscus (Idiothecia) nigrescens* HARMER, 1905. Even though modern pterobranchs, such as the extant *Rhabdopleura,* may possess separate male and female zooids, this differentiation is not expressed in the secretion of the housing tubes and interpretation is impossible from the fossil record.

The thecae, the housing structures for individual zooids, are the main building blocks of the graptolite colonies and define their construction and shapes. Individual thecae are interconnected through an opening in the Graptolithina, through which the next bud emerged to form its own thecal tube. The combined initial parts of the thecal tubes of a stipe are generally referred to as the common canal (Fig. 30.1)

to emphasize the interconnection of the clonal, colonial development of the colonies; its existence, in fact, provides the evidence for a truly colonial organism. The common canal can be quite variable in size, depending on the geometry of the tubes and the shape of the prothecal parts of the thecae.

The thecae generally have a distinct thecal overlap, with the wall common to two overlapping thecae called an interthecal septum or internal septum (Fig. 30.5). The interthecal septum was secreted either by the first-formed thecal zooid or, in case of concurrent growth, as a combined effort of both thecal individuals (WALKER, 1953; URBANEK, 1958).

The degree of thecal overlap is quite variable and can reach high values (FORTEY, 1983). It is generally measured as a percentage of thecal length. Among the monograptids, a number of genera (e.g., *Campograptus* OBUT, 1949; *Rastrites* BARRANDE, 1850; and *Streptograptus* YIN, 1937) have little or no thecal overlap. Distally increasing thecal overlap is typical in many groups (e.g., *Didymograptellus* COOPER & FORTEY, 1982; *Expansograptus* BOUČEK & PŘIBYL, 1952a; *Nichol-*

sonograptus Bouček & Přibyl, 1952a; and certain monograptids including *Monograptus* s. str.) and commonly leads to extremely wide and robust distal stipes. Differences in the amount of thecal overlap can be used for taxonomic purposes, as in *Didymograptellus bifidus* (Hall,1865) by Williams and Stevens (1988). (See discussion of thecal gradients on p. 54.)

The free ventral wall is the portion of the ventral theca margin that extends beyond the aperture of the preceding theca. The length of the free ventral thecal wall depends on the growth patterns of the thecae and is used for taxonomic differentiation in certain groups. It tends to be greater in thecae with low inclination.

The differentiation of the protheca and metatheca (Fig. 30) can be problematic, as a distinct break in the fusellar growth is not present in most thecae. The protheca may be recognized as the part of a theca before the insertion of an interthecal septum, but this varies from species to species. In taxa without an interthecal septum, the point at which the theca becomes a complete tube (for example, when the foramen of the daughter theca is closed) can be defined as the start of the metatheca (Fig. 30.3). This definition follows the distinction advocated in Bulman (1955, 1970). Münch (1938) discussed the common canal in monograptid thecae in some detail and suggested the terms semitubus, metatubus (protheca), and thecatubus (metatheca) to differentiate parts of the thecae, although these differ little from protheca and metatheca.

AUTOTHECAE AND BITHECAE

Two main thecal types can be differentiated: the autothecae and the bithecae (Cooper & Fortey, 1983). Many benthic graptoloids, and even a few early planktic forms, possessed this distinct differentiation of their thecal tubes, with larger tubes identified as autothecae and smaller ones as bithecae. The reason for this differentiation is unknown, although a sexual differentiation has been
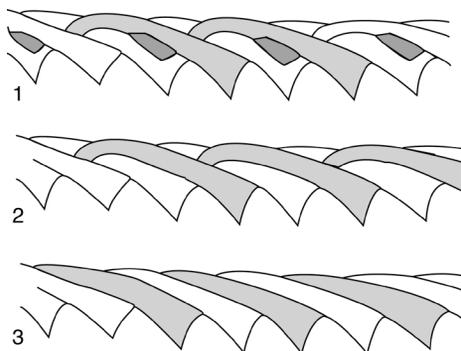

Fig. 31. Triad budding and plaited thecal overlap. *1*, Bithecate stipe in lateral view with lateral originating, alternating autothecae (*light gray*) and bithecae (*dark gray*), same construction would be seen on the other side of the stipe; *2*, non-bithecate stipe with plaited thecal overlap and lateral thecal origination; *3*, non-bithecate stipe with dorsal origins of autothecae (adapted from Lindholm, 1991, fig. 4).

suggested (e.g., Hutt in Palmer & Rickards, 1991). Alternatively, Kirk (1973) suggested that the smaller bithecae may have housed cleaning individuals.

Autothecae and bithecae (Fig. 31) are arranged in a consistent and highly geometrical pattern in most bithecate colonies. Each autotheca is connected to a bitheca, except at branching points, where the bitheca is replaced by a second autotheca. Normally, the bithecae occur alternately on both sides of the stipes, but irregularities are common in some taxa. Several successive bithecae on one side of a stipe are present in *Kiaerograptus kiaeri* (Monsen, 1925), for example (Spjeldnaes, 1963; Lindholm, 1991). Complex growth patterns of bithecae occur in many dendroid graptolites (e.g., Bulman, 1955; Rickards & others, 2003).

A number of other thecal types have been described in the various benthic taxa. Conothecae, microthecae, and umbellate thecae occur in the Cyclograptidae Bulman, 1938, while autothecae are modified into highly inflated camerae and erect columns in the Cysticamaridae Bulman, 1955. The details are discussed in the various taxonomic sections.

THECAL MORPHOLOGY AND MODIFICATIONS

The thecae of the Graptolithina are highly variable (Fig. 32), and the simple tubes of early benthic taxa are considerably modified in later forms. Structural modifications are here differentiated by their position on the thecae and their development. In the past, thecal types have been differentiated and named after their characteristic genera. Thus, dichograptid (Fig. 32.9), climacograptid (Fig. 32.11, Fig. 32.15), diplograptid (Fig. 32.10), glyptograptid (Fig. 32.13), nemagraptid, leptograptid (Fig. 32.17), and other thecal types are commonly used in the descriptive terminology of graptoloid thecae (BULMAN, 1970). Initially, differences in the thecal shapes originate from the variation of widening of the thecae, which may be gradual and persistent (e.g., simple dichograptid), or in increments, producing bulges or cupulae (e.g., in *Pseudostreptograptus* LOYDELL, 1991a, and *Streptograptus* YIN, 1937) on the dorsal sides of thecae (Fig. 32.4, Fig. 32.8). In others, the thecae widen considerably from an initial width and then continue parallel sided (e.g., in climacograptids) or even decrease in width distally (e.g., *Dicranograptus* HALL, 1865, and some climacograptids).

The geniculum (Fig. 32.11, Fig. 32.15) is a distinct angular feature on the ventral side of the theca and quite common in the biserial groups as well as in some monograptids. It is often enhanced by hoodlike genicular flanges (Fig. 32.6, Fig. 32.2); but spines, lobed additions, and other enhancements may be present. The geniculum can also be rounded, but it invariably involves an abrupt change in inclination of the ventral thecal wall. Geniculate thecae are common in graptolites of all groups, from the dichograptids (*Aulograptus* SKEVINGTON, 1965) to axonophorans (*Climacograptus* HALL, 1865; *Archiclimacograptus* MITCHELL, 1987; *Dicellograptus* HOPKINSON, 1871; Fig. 32.17), to monograptids (*Monoclimacis* FRECH, 1897), and retiolitinids (Fig. 32.7). The geniculum in all these graptolites is structurally homologous, but evolutionarily analogous, as is evidenced by its independent origination in many groups.

Thecae with a distinct recurved thecal aperture are called hooked thecae. The thecal hook is formed from an isolated metatheca with continuous fuselli. A typical example is *Monograptus priodon* BRONN, 1849 (Fig. 32.5), in which the distal metathecae form an open hook. A lateral or transverse widening of the thecal apertures

FIG. 32. Thecal morphologies. *1, Proteograptus opimus* (LENZ & MELCHIN, 1991), Silurian (Wenlock, upper Sheinwoodian), Canadian Arctic, scale bar, 1 mm (Lenz & others, 2012, pl. 13); *2, Demirastrites triangulatus* (HARKNESS, 1851) Silurian (Llandovery), central Wales, scale bar, 1 mm (Palmer & Rickards, 1991, pl. 74); *3, Crinitograptus operculatus* (MÜNCH, 1938), Silurian (lower Ludlow), Canadian Arctic, scale bar, 0.1 mm (Lenz & Kozłowska-Dawidziuk, 2004, pl. 30); *4, Pseudostreptograptus williamsi* LOYDELL, 1991a, Silurian (Llandovery, lower Telychian), Sweden, scale bar, 1 mm (Palmer & Rickards, 1991, pl. 76); *5, Monograptus priodon* (BRONN, 1849), Silurian (middle Wenlock), Canadian Arctic, scale bar, 1 mm (Lenz & others, 2012, pl. 8); *6, Okavites spiralis* (GEINITZ, 1842), Silurian (Llandovery, upper Telychian), Canadian Arctic, scale bar, 1 mm (new); *7, Papiliograptus papilio* LENZ & KOZŁOWSKA-DAWIDZIUK, 2002a, Silurian (Wenlock, upper Homerian), Canadian Arctic, showing thecal geniculae with large, supragenicular hoods, scale bar, 1 mm (Lenz & Kozłowska-Dawidziuk, 2002a, fig. 11); *8, Streptograptus galeus* LENZ & KOZŁOWSKA, 2006, Silurian (Wenlock, lower Homerian), Canadian Arctic, scale bar, 0.5 mm (Lenz & Kozłowska, 2006, fig. 12); *9, Expansograptus abditus* WILLIAMS & STEVENS, 1988, Lower Ordovician (Floian), Newfoundland, Canada, with simple, tubelike thecae, cleared to show fusellar half rings, scale bar, 1 mm (Williams & Stevens, 1988, pl. 14); *10, Neodiplograptus sinuatus sinuatus* (NICHOLSON, 1869), Silurian (middle Llandovery), Canadian Arctic, with biform thecae, scale bar, 1 mm (Melchin, 1998, pl. 3); *11, Clinoclimacograptus barriei* (ZALASIEWICZ & TUNNICLIFF, 1994), Silurian (middle Llandovery), Canadian Arctic, with strong geniculae, scale bar, 1 mm (Melchin, 1998, pl. 1); *12, Chigraptus supinus* JACKSON & LENZ, 2003, Lower Ordovician (Tremadocian), Canada (northern Yukon), scale bar, 1 mm (Jackson & Lenz, 2003, fig. 6a); *13, Glyptograptus elegans* ssp., Arctic Canada, scale bar, 1 mm (Melchin, 1998, pl. 3.13); *14, Lobograptus scanicus* (TULLBERG, 1883), Silurian (lower Ludlow), Canadian Arctic, with large, lobelike thecal lappets, scale bar, 1 mm (Lenz & Kozłowska-Dawidziuk, 2004, pl. 32); *15, Glyptograptus elegans* (s.l.) PACKHAM, 1962, Silurian (Llandovery), Canadian Arctic, scale bar, 1 mm (Melchin, 1998, pl. 5); *16*, Lignigraptus *kinnegraptoides* (ERDTMANN, MALETZ, & GUTIÉRREZ-MARCO, 1987), Lower Ordovician (Floian), Canada (Yukon), scale bar, 1 mm (Jackson & Lenz, 2006, fig. 7n); *17, Jiangxigraptus vagus* (HADDING, 1913), Middle Ordovician (upper Darriwilian), Scania, Sweden, scale bar, 1 mm (new).
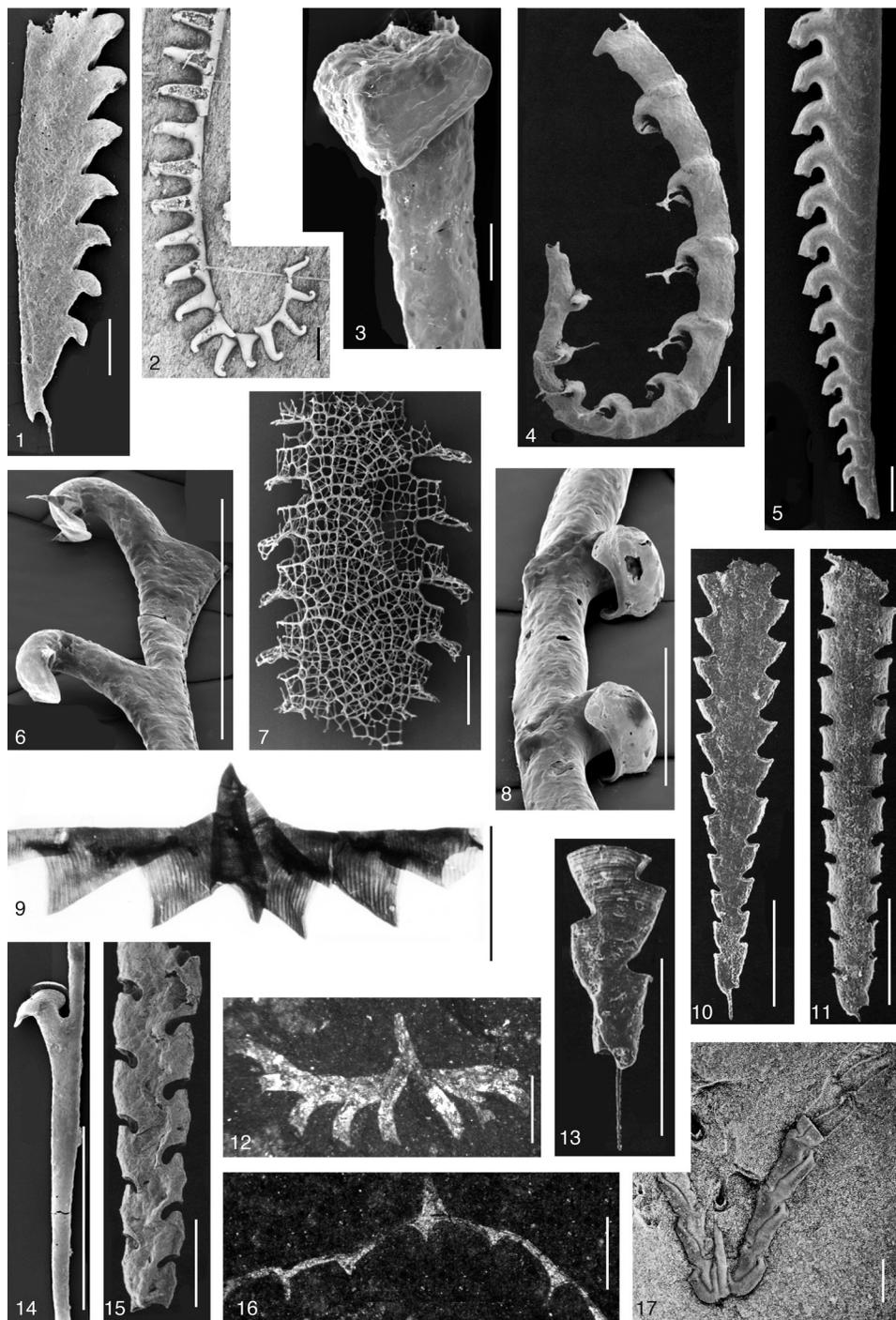
Fig 32. *For explanation, see facing page.*

may be associated with this thecal development, but restricted apertures may also be present. Hooked thecae may or may not have thecal overlap or even astogenetic variation in this character (e.g., *Stimulograptus* PŘIBYL & ŠTORCH, 1983 and *Monograptus*). A special case of the hooked thecal aperture is identified as lobate (BULMAN, 1970), in which the metatheca grows back on itself, e.g., *Campograptus lobiferus* (M'COY, 1850) and *Lapworthograptus* BOUČEK & PŘIBYL, 1952b). Hooked thecae are most common in the Monograptidae, and more numerous and varying elaborations are present in these forms than in any other group.

A thecal development that may appear very similar to the hooked thecae has been identified as hooded thecae (BULMAN, 1970). In this form, a thecal hood covers the thecal aperture (Fig. 32.3). The thecal hood is formed either as an extension of the dorsal wall of the theca or as a secondary, sometimes genicular addition to the thecal aperture. It is not comparable in development to the hooked theca, in which the development is completely formed by the dorsal and ventral thecal walls. Hooded and hooked thecae are very difficult to differentiate in flattened material. Isolated specimens possessing fusellar structure may be needed to recognize the precise development.

The thecae of the monograptids have the greatest variety—simple tubes, smoothly hooked (Fig. 32.5), tall, scarcely overlapping, elongated, distally hooked (Fig. 32.2, Fig. 32.4), bi- or multiform, or complex proximally to simpler distally (Fig. 32.1). They may have large thecal hoods that obscure the thecal aperture (Fig. 32.3), strongly hooked theca (sometimes with torsion), and/or various kinds of spines (Fig. 32.6), or have lobate and asymmetrical lappets (Fig. 32.14). On the other hand, thecae with fairly complex or unusual features were already present in a few Tremadocian and Floian taxa, such as *Paradelograptus* ERDTMANN, MALETZ, & GUTIÉRREZ-MARCO, 1987; *Psigraptus* JACKSON, 1967; and *Chigraptus* JACKSON & LENZ, 1999 (Fig. 32.12).

Thecal isolation is common in many graptolites. In the benthic Callograptidae and Acanthograptidae, the typical thecal tubes possess isolated apertures, but thecal overlap is present on the stipes. An isolation of thecal apertures occurs in many planktic graptoloids. The metathecae can be completely or only partially isolated. In taxa with complete metathecal isolation, there is no thecal overlap and, accordingly, no interthecal septum is present (Fig. 32.2).

Partial isolation is present in benthic taxa and also in many planktic forms. Partial isolation of the metatheca has been described in the Tremadocian genera *Chigraptus* (Fig. 32.12) and *Kiaerograptus* and is common in Silurian monograptids with thecal hooks (e.g., *Monograptus*, *Streptograptus*). Completely isolated metathecae are present in *Rastrites* BARRANDE, 1850; *Demirastrites* EISEL, 1912; *Lituigraptus* NI, 1978; and a number of other monograptid genera, in which a gradual change in thecal shape is typically also present. The term triangulate has been used frequently for the thecal shapes in this group (SUDBURY, 1958) (Fig. 32.2).

The orientation of the thecal aperture ranges from introverted through perpendicular to everted, unless hooks modify the apertural orientation. This orientation can also be affected by apertural modifications, which are common in graptolites and often used for identification of both species and genera. Apertural modifications are highly variable and can be difficult to interpret in flattened material. Even the number and orientation of spines and flanges cannot be identified correctly without isolated, three-dimensionally preserved specimens. Apertural modifications are defined independent of the orientation of the aperture and may include a wide variety of spines (Fig. 32.4, Fig. 32.6), lobes, shelves, and selvages. These can be defined by their position on the theca as dorsal, ventral, or lateral.

Prothecal folds and intrathecal folds, termed recumbent folds by COOPER and NI (1986), are features related to the origin of

the thecae in some Sinograptina and in the axonophorans and have not been recognized in benthic graptolites. Thecal folding is indicated through a change in growth direction of a thecal tube. The theca generally grows back on itself, forming a conspicuous bending of the tube. The growth direction is taken to differentiate prothecal and intrathecal folds (Fig. 33). The development of a prothecal fold forms around the base of an interthecal septum (Fig. 33.1), whereas in intrathecal folds, a secondary bar or septum forms from the dorsal side of the stipe (Fig. 33.2). The details of the development of prothecal and intrathecal folds are not known from isolated material.

Prothecal folds have been used to define the Sinograptidae (MU, 1957) but are now known to be present in a number of independent groups of planktic graptoloids. The earliest example includes the dichograptid *Cymatograptus undulatus* (TÖRNQUIST, 1901) from the lower Floian of Scandinavia (JAANUSSON, 1965), but bithecate taxa with apparent prothecal folding have also been described. Prothecal folds in the upper Tremadocian *Cymatograptus lauzonensis* ERDTMANN, 1966, now *Kiaerograptus lauzonensis* (see MALETZ & EGENHOFF, 2001), are enhanced by the presence of bithecae with lateral thecal origins, the plaited thecal overlap of LINDHOLM (1991).

SERIALITY OF THECAE

The zooids of *Rhabdopleura* bud from each other in a sequential manner, forming a serial succession. However, the secreted tubes of the individual zooids branch irregularly from this succession to both sides of the main axis (Fig. 16.2). The erect tubes in *Rhabdopleura normani,* for example, may originate on the left and right side of the central axis (Fig. 16.2), with no apparent regular organization (LANKESTER, 1884). Due to the clonal development of the colonies and the constructional mode of new tubes, a distinct regularity evolved and occurs in most derived graptolites. Irregularities are most pronounced in benthic
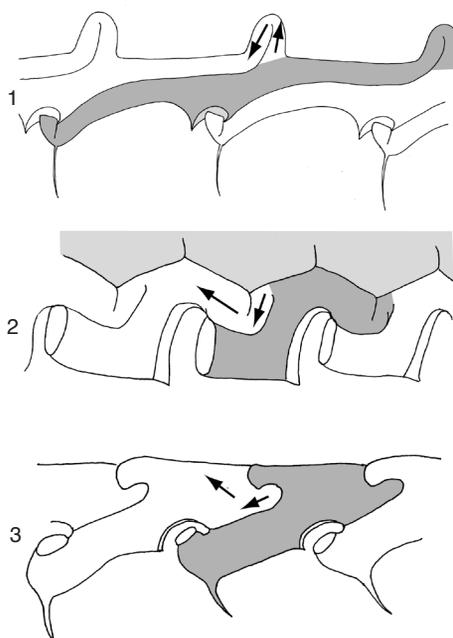

FIG. 33. Diagrams of prothecal and intrathecal folds. *1, Holmograptus* sp., with pronounced prothecal fold; *2, Haddingograptus* sp., intrathecal folds with bar originating from median septum, second thecal series in *light gray; 3, Dicellograptus* sp., intrathecal fold in relief specimen without fusellar structure; all reconstructions adapted from relief material, one theca indicated in *darker gray* in each illustration, arrows indicate growth direction (new).

encrusting colonies, probably recalling the original unordered development of the *Rhabdopleura* colonies. The Cyclograptidae retain some of the disorganization of their thecal tubes but develop a distinct internal regularity, fostered by their underlying budding system. The thecal tubes in these forms are round, with isolated apertures. A differentiation into a dorsal and ventral side is visible only through the presence of the zigzag sutures of the regularly organized fusellar half rings of the tubes.

Most dendroids and graptoloids developed a highly precise seriality of their thecal arrangements in which all thecal apertures on the stipe are precisely oriented in the same direction (Fig. 16.1, Fig. 30.1, Fig. 31). This arrangement has been retained by all planktic taxa, including the Silurian to

Lower Devonian monograptids (Fig. 32). The ventral rutellum and the development of thecae without complete apertural isolation were already present in such dendroid graptolites as *Dendrograptus* and *Dictyonema* (WIMAN, 1896; BULMAN, 1933a). This differentiation of the dorsal and ventral sides of the thecal tubes developed in all derived pterobranchs with serially arranged thecae.

THECAL GRADIENTS

Thecal gradients or astogenetic variation of thecae is an aspect of many planktic graptolites and has been studied in some detail (e.g., BULMAN, 1963; URBANEK, 1973). Minor gradual change in size of thecae is most commonly observed in graptolites, especially in the dichograptids, typically associated with a distally increasing thecal overlap (see COOPER & FORTEY, 1982; WILLIAMS & STEVENS, 1988). Biform or multiform colonies are common in many axonophorans (biserials and monograptids), with different thecal styles at the proximal and distal ends (Fig. 34). Changes can be fairly gradual and include minor structural modifications of the apertures, but taxa with dramatic changes along the stipes are not uncommon, such as in *Paramonoclimacis sidjachenkoi* (OBUT & SOBOLEVSKAYA, 1965) and *Monograptus limatulus* TÖRNQUIST, 1892. These changes may be dramatic enough that the stipe fragments could easily be referred to different genera. The modifications may be precisely located, and a distinct change may occur at a certain theca along the length of the colony (Fig. 34), but they can also be more variable.

THE WIMAN RULE AND TRIAD BUDDING MODEL

The Wiman rule originally described the interconnection of three thecal types and the branching of the thecal tubes, which is the external expression of the internal stolon system (KOZŁOWSKI, 1949). Initially, triad budding was understood as a branching in triads from a stolotheca, in which the stolotheca does not possess an apertural opening but is accompanied by a new autotheca and a bitheca. KIRK and BATES (in KIRK 1969) and BULMAN (1970, p. 26) recognized the stolotheca as the "immature basal portion of the succeding autotheca." Thus, a separate stolothecal zooid does not exist, and the stolotheca and succeeding autotheca are now regarded as a single unit, the autotheca (COOPER & FORTEY, 1983).

In a typical triad, each autotheca produces a new autotheca and a new bitheca (Fig. 35.1), effectively eliminating the need of the term stolotheca. The Wiman rule, in its revised meaning, essentially states that at each branching point a new autotheca is formed on one side of the stipe, while on the other side, a bitheca is developed at the same point. This development produces bithecae and autothecae, alternately, on the left and right side of the stipes (Fig. 31.1, Fig. 35). All thecal origins are lateral in these taxa, forming a structure that was termed plaited thecal overlap (Fig. 31.1) by LINDHOLM (1991), including taxa in which bithecae are absent (Fig. 31.2).

The number of bithecae of the planktic graptoloids became fewer over time, apparently in all lineages. By the end of the Tremadocian, they were scarce and were completely absent during the Floian. The details of these changes are still unclear, but a number of separately evolving lineages may have lost their bithecae and the plaited thecal overlap independently (FORTEY & COOPER, 1986; LINDHOLM, 1991). In derived graptoloids, the thecal origins are on the dorsal side of the stipes, even though lateral thecal origins from a dicalycal theca may still occur at branching points.

THE DICALYCAL THECA

The structural details of the branching in graptolite colonies is known from specimens preserved in full relief and from isolated specimens. Dichotomous branching is invariably related to the presence of a dicalycal theca (Fig. 35), a theca that produces two autothecae instead of an autotheca and a bitheca (MALETZ, 1992). In forms with triad budding, branching is achieved through
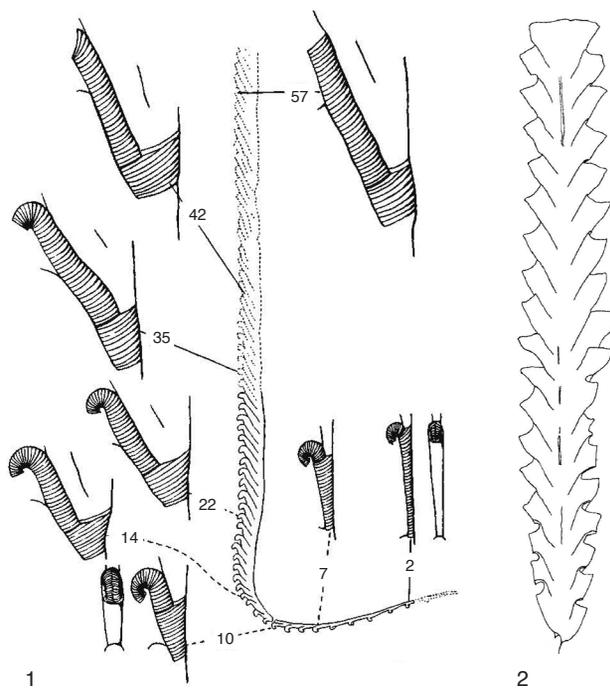
FIG. 34. Thecal gradients. *1, Pernerograptus argenteus* (NICHOLSON, 1869), thecal modifications along the stipes of a specimen; *numbers* indicate position of thecae along stipe (Bulman, 1955, fig. 29); *2, Neodiplograptus apographon* (ŠTORCH, 1983), thecal gradient (Loydell, 2007, fig. 10D).

the replacement of a bitheca with an autotheca at one of the triads. A bitheca, therefore, is missing at the branching point (Fig. 35.1–35.2). The previous autotheca curves distinctly in the direction of one of the new stipes, and the first new autotheca of this stipe grows along its back. The second theca produced by the dicalycal theca bends directly away to form the second stipe (Fig. 35.2).

Successive dicalycal thecae are present in early planktic graptolites (e.g., *Staurograptus* EMMONS, 1855; *Rhabdinopora* EICHWALD, 1855), but apparently a dicalycal theca can produce only one additonal dicalycal theca and one normal autotheca (MALETZ, 1992). In younger graptoloids, dicalycal thecae were separated by at least one normal monocalycal theca and, thus, were not successive.

In graptolithines without triad budding, the development differs slightly, but follows the same general rules described by MALETZ (1992). The main difference is that in non-bithecate taxa, autothecae can produce only a single new theca (an autotheca), whereas a dicalycal theca retains the ability to produce two new autothecae (Fig. *35.3).* Another difference occurs in the origination of daughter thecae, which are no longer paired, but originate at different levels on the mother theca (Fig. 35.3).

THECAL NOTATION

Thecal notation was introduced by ELLES (1897) for biserial colonies and was adopted and modified by BULMAN (1970). Its modern use is discussed by COOPER and FORTEY (1982) and is followed herein. It is easy for two-stiped colonies, in which the thecae of thecal series 1 (the primordial series of ELLES, 1897) are labeled th1^1, th2^1, th3^1, etc., and the thecae of thecal series 2 are labeled th1^2, th2^2, th3^2, etc. (Fig. 36). The thecal notation is a bit more complicated in taxa with a
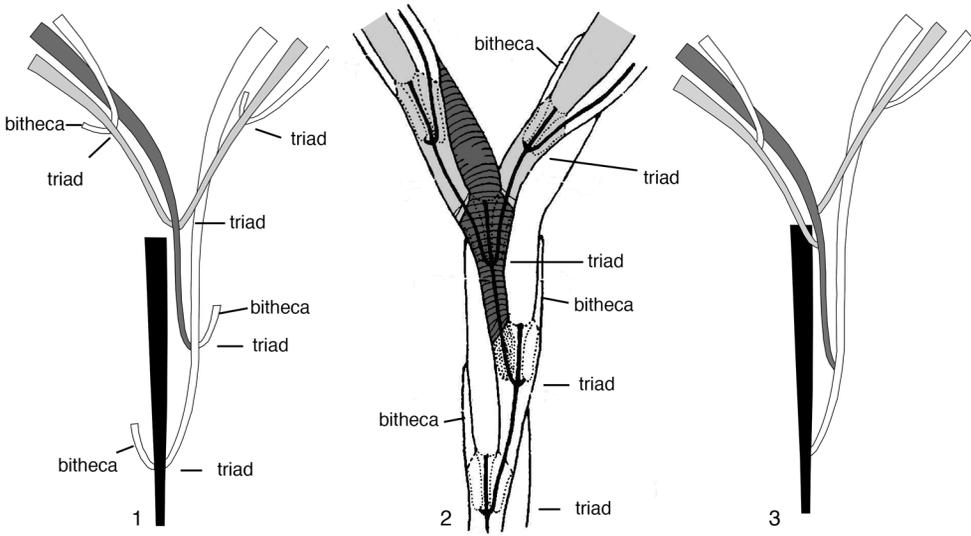
FIG. 35. Triad budding and dicalycal theca. *1,* Diagram of bithecate taxon showing the triad budding system (adapted from Cooper & Fortey, 1983, fig. 7); *2,* branching division of *Rhabdinopora flabelliformis* (EICHWALD, 1855), also showing the internal stolon system (adapted from Bulman, 1970, fig. 13.1); *3,* thecal diagram of non-bithecate form; note that the two daughter thecae originate at different levels on the dicalycal theca (adapted from Cooper & Fortey, 1983, fig. 7). *Dark gray,* dicalycal thecae; *light gray,* derived autothecae.
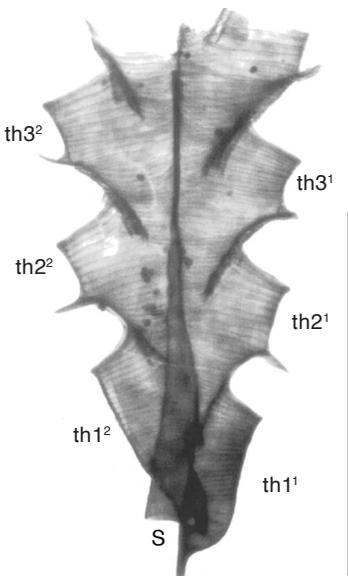

FIG. 36. Thecae labeling procedure on the scandent biserial *Paraclimacograptus exquisitus* RICKARDS, 1970; *S,* sicula; scale bar, 1 mm (adapted from Russell, Melchin, & Koren', 2000).

higher number of stipes, but it is rarely used. COOPER and FORTEY (1982, 1983) provided a useful system for such taxa and compared it with the system of BULMAN (1970). The system used by LEGRAND (1964a) is not supported here.

THE STOLON SYSTEM

An important aspect of the Grapto-lithina is the stolon system (Fig. 35.2, Fig. 37.1), which connects the individual zooids in the extant *Rhabdopleura* (URBANEK & DILLY, 2000), and is also known from fossil graptolites (e.g., KOZLOWSKI, 1949; HUTT, 1974a; BATES & URBANEK, 2002; SAUNDERS & others, 2009). The stolon system, which is not secreted by the cephalic shield, may represent the only preservable part of the actual organisms, the zooids. In the Cepha-lodiscida, the new zooids originate from the base of the zooidal stalk (originally called the peduncle or contractile stalk) and separate when mature. In the Graptolithina, a stolon system develops connecting the individual zooids for life as a true colony (LANKESTER,
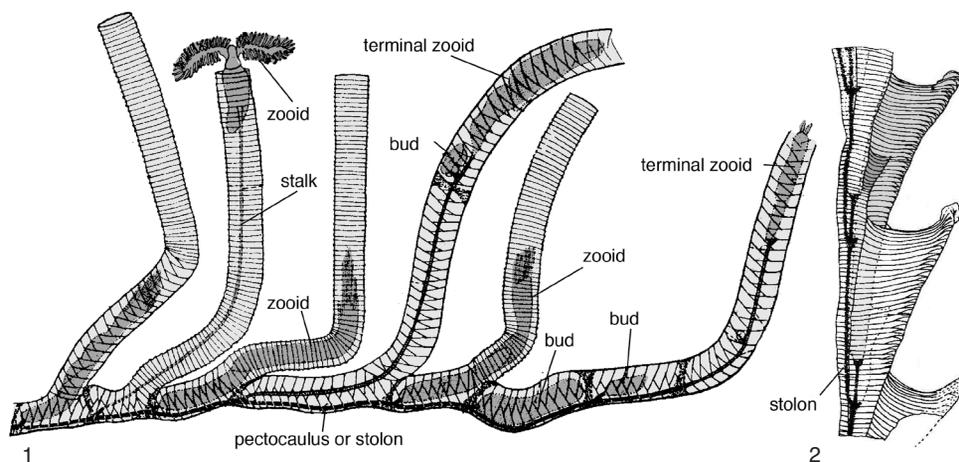
FIG. 37. The stolon system. *1,* Pectocaulus (stolon) in *Rhabdopleura* (adapted from Kozłowski, 1949, fig. 11, and Schepotieff, 1907b, pl. 22); *2,* stolon system (*black*) in stipe fragment of *Adelograptus tenellus* (LINNARSSON, 1871) (adapted from HUTT, 1974a, fig. 8).

1884; SCHEPOTIEFF, 1906). The zooidal stalk attaches the zooid to the stolon, the sclerotized and inflexible strand of organic matter connecting all zooids with each other (Fig. 37). Details of the stolon system are difficult to obtain and are unknown from most planktic graptoloids.

COLONIAL ASTOGENY
OBVERSE AND REVERSE SIDE

The two sides of the graptolite colonies may differ considerably in their appearance, especially when the proximal development on the reverse side of the tubarium is complex. This is clearly present in all Graptoloidea, except for the single-stiped Monograptidae. The initial portions of the first few thecae, the crossing canals, grow across the sicula and cover it in part on one side of the tubarium. This side is generally identified as the reverse side. The only part of the sicula visible on the reverse side of a biserial colony is the aperture and the virgella (Fig. 38.5), but on the obverse side, at least part of the sicula is visible (Fig. 38.6). In nonbiserial taxa, the complete sicula is visible on the obverse side (Fig. 38.2). The genera *Pseudisograptus* (Fig. 38.1) and *Arienigraptus* cover a larger part of the sicula on the reverse side of the

colony, where the complex construction of the manubrium takes place.

DEXTRAL AND SINISTRAL DEVELOPMENT

The proximal geometry, structure, and development types of the major groups of the Graptoloidea were redefined by COOPER and FORTEY (1982, 1983), and dextral and sinistral developments were differentiated (Fig 39). Dextral and sinistral growth types have been illustrated from various anisograptid and dichograptid specimens, but the frequency of the dextral and sinistral development types is unknown, due to the very limited number of specimens available (MALETZ, 2021). The dextral and sinistral development of the proximal end may not be connected to the dextral and sinistral development of the helical line of the prosicula. Most authors (e.g., BULMAN, 1936a; LEGRAND, 1964a; HUTT, 1974a) agree that the proximal development in anisograptids can be either dextral or sinistral. SPJELDNAES (1963) discussed the dextral and sinistral development of the late Tremadocian genera *Bryograptus* LAPWORTH, 1880a; *Kiaerograptus* SPJELDNAES, 1963; and *Ancoragraptus* JACKSON & LENZ, 2003 in some detail and provided illustrations of both types
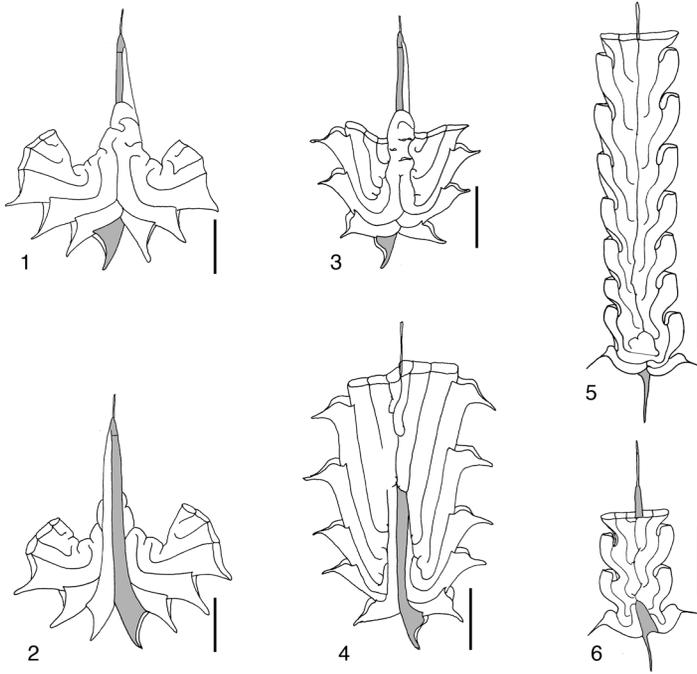
FIG. 38. Obverse and reverse sides of colonies. *1–2, Pseudisograptus bellulus* COOPER & NI, 1986, in reverse (*1*) and obverse (*2*) views; *3–4, Exigraptus uniformis* MU in MU & others, 1979, reverse (*3*) and obverse (*4*) views; *5–6, Levisograptus austrodentatus* (HARRIS & KEBLE, 1932) reverse (*5*) and obverse (*6*) views; sicula shaded to highlight the differences of obverse and reverse sides, scale bars, 1 mm (new).
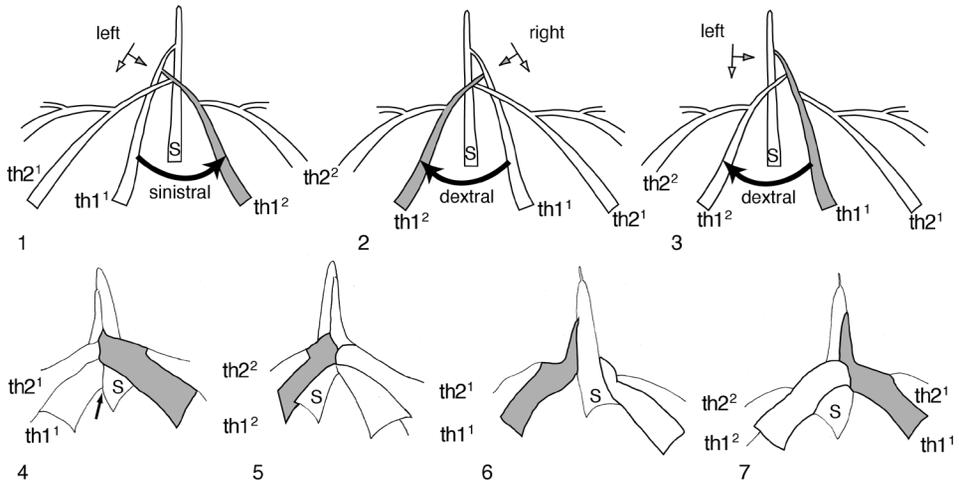
FIG. 39. Dextral and sinistral development and the proximal development types in Dichograptacea (with thecal notation). *1–3,* Thecal diagrams; *1,* isograptid-type, sinistral development; *2,* isograptid-type development, dextral; *3,* artus-type development, dextral; *4–7,* reconstructions of proximal developments; *4–5,* isograptid-type development in *Cymatograptus* sp., sinistral (*4*) and dextral (*5*) style; *6–7,* dextral, artus-type development in *Cymatograptus bidextro* TORO & MALETZ, 2008, obverse (*6*) and reverse (*7*) views (Toro & Maletz, 2008, fig. 6).

in his relief specimens from the uppermost Alum Shale Formation of Norway. Toro and Maletz (2008) described dextral and sinistral specimens of *Cymatograptus bidextro* Toro & Maletz, 2008 from the middle Floian of Argentina, the youngest- known taxon in which dextral and sinistral development is present. The dextral development is the standard in younger graptoloids and a sinistral development is extremely rare (Cooper & Fortey, 1983).

THE PROXIMAL DEVELOPMENT

Stebbing (1970a) described the early astogeny of extant *Rhabdopleura compacta* zooids and the tubarium structure. The sicular zooid buds a new zooid from the base of the zooidal stalk, then forms a septum to separate a part of the dome as an initial housing for the first zooid. The first zooid subsequently resorbs a foramen into its part of the dome and starts secreting fuselli and a new tube alongside the tube produced by the founder zooid.

The development is similar in species with an erect or planktic prosicula. However, the zooids construct a tube much smaller than the initial tube of the first post-sicular zooid of *Rhabdopleura*. Growth is initially in the direction of the sicular aperture, and is related to a considerable widening of the tubes and an increasingly regular development of the fuselli. This initial growth pattern occurs in all graptoloids, including normalograptids, except the monograptids in which the first theca emerged and always grew in a direction opposite to that of the sicular aperture.

The most important aspect of the next step in the astogeny of the graptolite colony (other than uniserial taxa) is branching, and especially the branching of Early Ordovician forms, as it defined the shape of the emerging colony. Branching was accomplished by the development of a branching division, expressed as a dicalycal theca in the tubarium.

The proximal development has been the focus of numerous investigations, which provided the basis for the main taxonomic interpretations and classification of the graptoloids. Elles (1922) differentiated four types of proximal development: the dichograptid, leptograptid, diplograptid, and monograptid types. This early concept was elaborated on by a number of people, and more than 30 different proximal development types and subtypes are now differentiated (e.g., Mitchell, 1987, 1994; Melchin, 1998; Melchin & others, 2011).

The earliest proximal development type is called the isograptid type (Cooper & Fortey, 1983), with a first dicalycal theca at th1^2 (Fig. 40.1). The artus-type development (Fig. 40.2) differs mainly in the change to a first dicalycal theca at th1^1. It is interesting, however, to mention that almost all nonaxonophoran graptoloids have the isograptid-type development no matter what thecal style or stipe orientation the colonies possess. The only difference from the artus-type development is the position of the dicalycal theca (Cooper & Fortey, 1983). A finer differentiation of the proximal development types of the Dichograptina could otherwise easily lead to another plethora of proximal development types.

The majority of the described proximal development types are from the axonophorans with their complex, proximal-end structure. These types basically define the position of the initial dicalycal theca and the development of the crossing canals, but commonly include numerous independent characters of the sicula and thecae (Fig. 41). Cooper and Fortey (1983) differentiated the proximal-end construction into the proximal development type and the proximal structure, but this distinction was not adopted by axonophoran taxonomists.

Following Mitchell (1987), Melchin and Mitchell (1991), Melchin (1998), and Melchin and others (2011) defined a number of proximal development types in the axonophorans. These were based on increasingly smaller differences in the construction of the graptolite colonies. The main characters of these proximal developent patterns include the position of the dicalycal
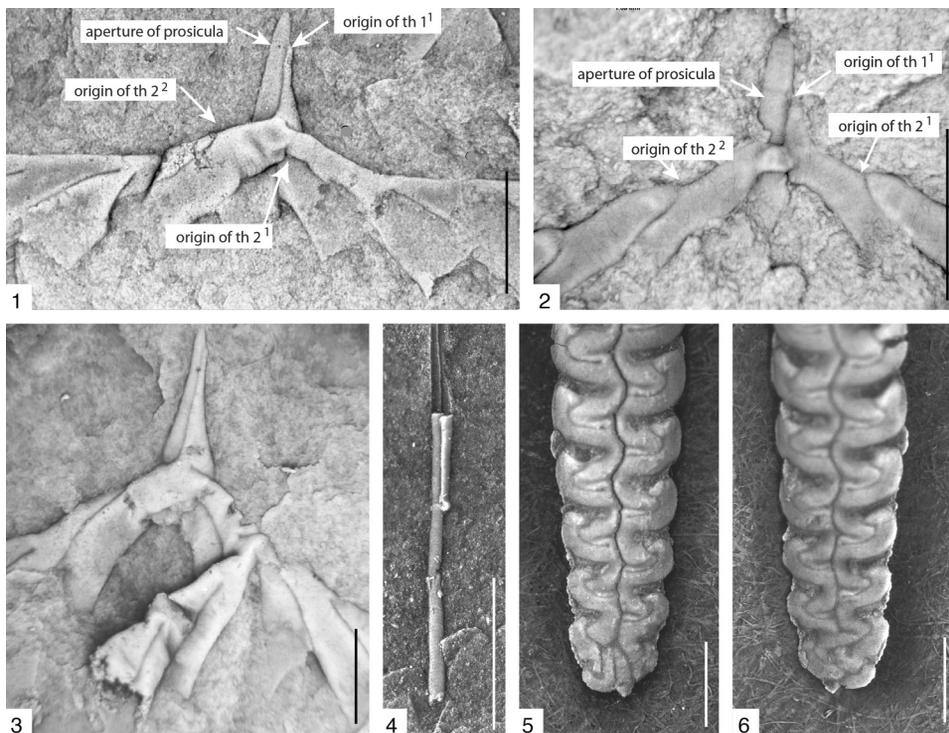
FIG. 40. Proximal development types. *1, Expansograptus holmi* (TÖRNQUIST, 1901), reverse side, isograptid-type development, latex cast (adapted from Toro & Maletz, 2008, fig. 5); *2, Cymatograptus bidextro* TORO & MALETZ, 2008, reverse side, artus-type development (adapted from Toro & Maletz, 2008, fig. 5); *3, Tetragraptus amii* ELLES & WOOD, 1902, reverse side, isograptid-type development, latex cast; *4, Huttagraptus* sp., pattern M astogeny, early monograptid development with long sicula, LO 11856t, (Maletz, Ahlberg, & others, 2014, fig. 1F); *5, Archiclimacograptus* sp., obverse side; *6, Archiclimacograptus* sp., reverse side, pattern C astogeny, LO 2413t (see Hadding, 1913, pl. 3.20); (*5–6*, new). All scale bars, 1 mm.

theca, the origin and growth direction of the primordial thecae, and the placement of the insertion of the median septum. Some of these patterns originated independently several times during the evolution of the axonophorans (MALETZ, 2011b).

The proximal development patterns are not known for many graptolites. Chemically isolated or, at least, relief specimens and growth series of juveniles are needed to establish the development. The interpretation of the proximal development types is difficult or impossible for flattened material (see also discussion in MITCHELL, 1987).

CONTINUED THECAL GROWTH

The number of thecae simultaneously growing at the tip of a stipe depends consid-erably on the length, overlap, and inclination of the thecae and is difficult to estimate. In slender sigmagraptines, a single theca may be growing at any time. However, in wide-stiped dichograptids, as well as in biserial colonies, a variable number of thecae may simultaneously grow at the tip of the stipe. WILLIAMS and STEVENS (1988) demon-strated the continued thecal growth in the growth series of *Didymograptellus bifidus* (HALL, 1865); *Expansograptus nitidus* (HALL, 1865); and *Expansograptus pennatulus* (HALL, 1865) from western Newfoundland. They concluded that, especially in *E. pennatulus,* numerous thecae continued growing inter-mittently during the astogeny of the colony, leading to a continuous widening of the stipes for quite some time and a consider-
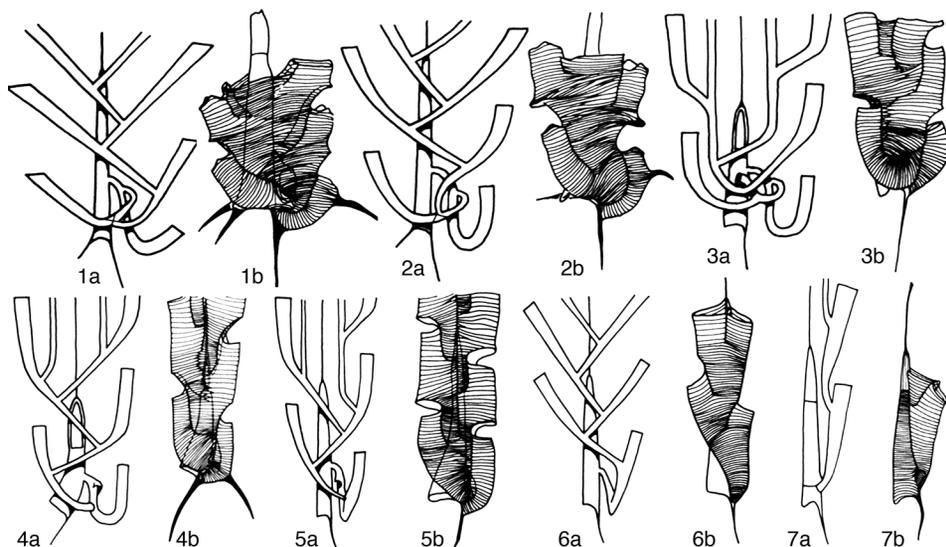
FIG. 41. Proximal development and proximal structure in axonophorans. *1a–b, Amplexograptus maxwelli* (DECKER, 1935a), pattern G; *2a–b, Anticostia lata* (ELLES & WOOD, 1906), pattern K; *3a–b, Styracograptus tubuliferus* (LAPWORTH, 1876a), pattern D; *4a–b, Diplacanthograptus spiniferus* (RUEDEMANN, 1912), pattern E; *5a–b, Normalograptus kuckersianus* (WIMAN, 1895), pattern H; *6a–b, Glyptograptus tamariscus* (NICHOLSON, 1868a), pattern I; *7a–b, Pristiograptus* sp., pattern M (all adapted from Melchin & Mitchell, 1991, fig. 1–2).

able changing of the tubarium shape during late-stage astogeny into the gerontomorph colony (Fig. 42).

THE MEDIAN SEPTUM

The development of the median septum in biserial axonophoran graptolites varies depending on the taxonomic group. The median septum is essentially the shared wall separating the two thecal series and is visible as the line separating the two thecal series in relief material (Fig. 43.1–43.2). There is little information on the detailed construction of the median septum in most graptolites, but some general information is available. BULMAN (1970) commented on the fact that there is no evidence that the median septum comprises more than a single layer of fuselli, following the description of URBANEK (1959) of the median septum of *Urbanekograptus retioloides* WIMAN, 1895, as a single-layered feature with numerous intercalating fuselli. Rare specimens of biserial graptolites can separate and rejoin the two thecal series temporarily as in *Cardiograptus amplus* HSÜ, 1947 (HAN & CHEN, 1994), suggesting that the median septum may be formed from two separate fusellar layers. The median septum can be complete (Fig. 43.1) or incomplete, and may begin at some distance from the proximal end (Fig. 43.3). URBANEK (1959) introduced the term cryptoseptate for *Gymnograptus linnarssoni* (MOBERG, 1896), in which the nema is attached to the tubarium walls by rods (adapertural ring) but lack a fusellar sheet.
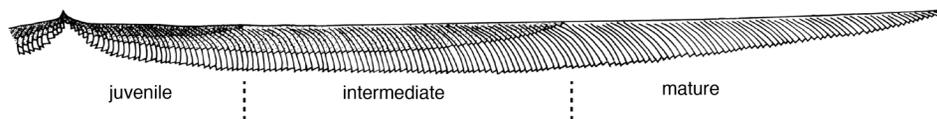

juvenile ┆ intermediate ┆ mature

FIG. 42. Astogeny and thecal growth in *Expansograptus pennatulus* (HALL, 1865) showing continuing, but periodic, lengthening of early-formed thecae as the tubarium lengthens and matures (Williams & Stevens, 1988, fig. 44).
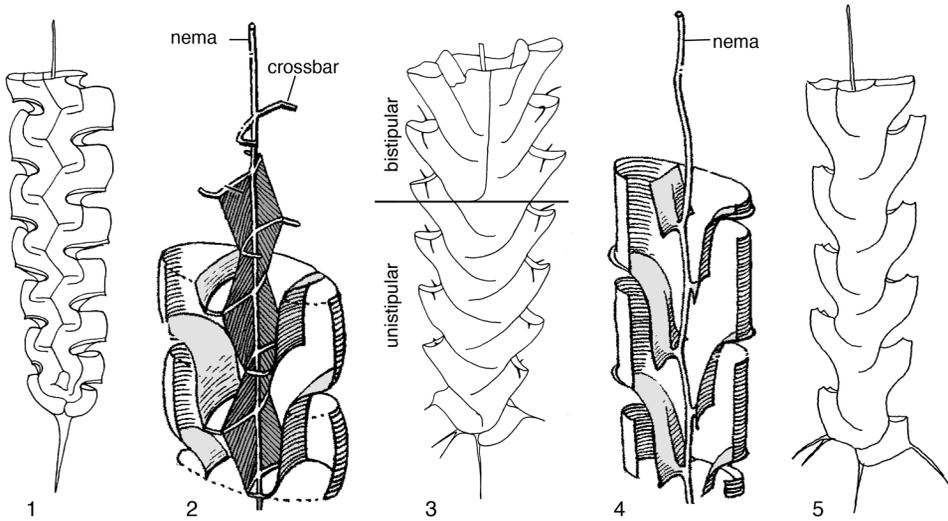
Fig. 43. Median septum. *1, Haddingograptus oliveri* (Bouček, 1973), bistipular colony with complete, strongly zigzag median septum, reverse view; *2,* the complete median septum (adapted from Bulman, 1955, fig. 34); *3, Orthograptus quadrimucronatus* (Hall, 1865), reverse view, showing unistipular and bistipular parts of colony; *4,* tubarium without median septum, nema connected centrally to interthecal septa (adapted from Bulman, 1955, fig. 34); *5, Anticostia macgregorae* (Stewart & Mitchell, 1997), reverse view, unistipular colony with alternating thecae (reconstructions in *1, 3,* and *5,* from Maletz, 2014b). *Dark gray,* median septum; *light gray,* interthecal septa.

The median septum may be present on one side of the tubarium only, usually the obverse side, but not on the reverse side in many Silurian taxa, e.g., *Cephalograptus* Hopkinson, 1869; *Petalolithus* Suess, 1851 (Bates & Kirk, 1992, fig. 41). The embedded nema and base of the partial median septum always appear to be attached to the obverse wall in axonophorans (see examples in Melchin, 1998).

A median septum may be lacking completely (Fig. 43.5) in unistipular taxa in which the thecal origins develop alternately (e.g., *Amplexograptus* Elles & Wood, 1907; *Gymnograptus* Bulman, 1953; and *Anticostia* Stewart & Mitchell, 1997), or they could develop intermittently, as in *Skanegraptus* Maletz, 2011b. A number of taxa delay the dicalycal theca and produce a unistipular proximal part without a median septum and a bistipular distal part of the colony with a delayed insertion of the median septum (Fig. 43.3).

A median septum is also present in tri- and quadriserial taxa (*Phyllograptus* Hall, 1858; *Pseudophyllograptus* Cooper & Fortey, 1982;

Pseudotrigonograptus Mu & Lee, 1958), in which it is formed in a complex way through the dorsal sides of three or four connected thecal rows. In *Phyllograptus,* the dorsal thecal walls are largely lacking and the structure is represented only by the columnella supported by a complex network of struts and horizontal perforated plates (Cooper & Fortey, 1982).

The monopleural taxa of the Glossograptidae do not possess a median septum. The two thecal series are attached laterally to each other and appear to have a double layer of fusellum, which is visible in relief specimens.

BRANCHING

Benthic and many planktic graptolites are able to produce multiramous colonies due to the branching of stipes in a number of different ways (Fig. 44). Theoretically, the number of stipes in pterobranch colonies is unlimited, and some benthic colonies are more than 50 cm in diameter and contain thousands of zooids on numerous branches. Planktic species (e.g., *Paratemnograptus magnificus* Pritchard, 1892), may have
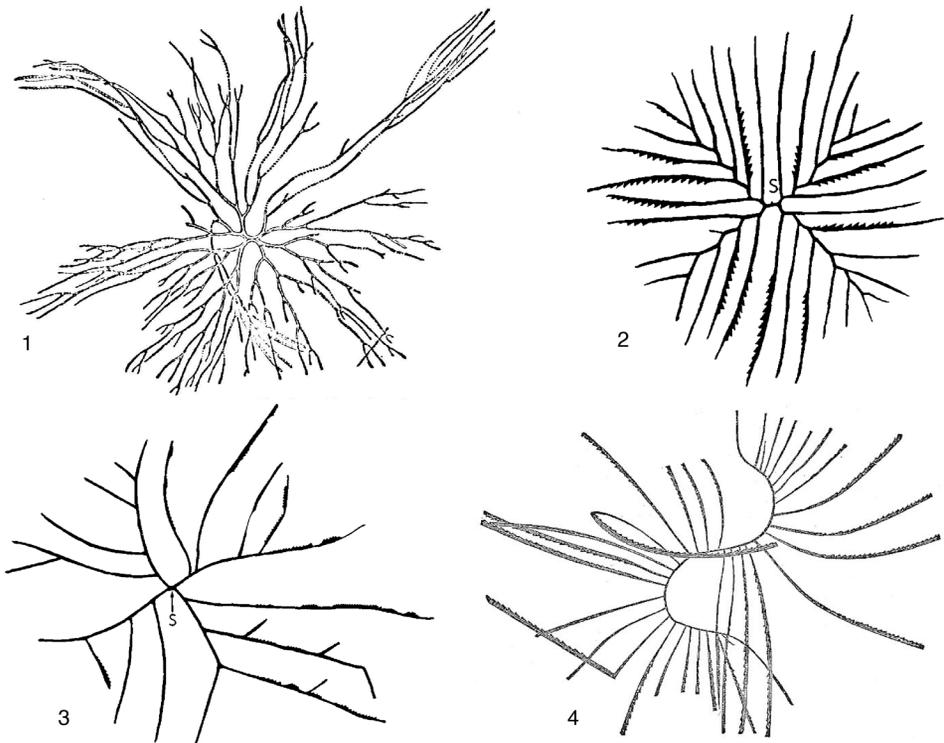
FIG. 44. Branching styles in multiramous colonies. *1, Clonograptus flexilis* (HALL, 1858), showing progressive dichotomous branching (Hall, 1865, fig. 8); *2, Goniograptus* sp., monoprogressive branching with four main stipes forming a zigzag line, *S*, sicula (Bulman 1970, fig. 77.1); *3, Schizograptus* sp., dichotomous lateral branching from four second-order stipes, *S*, sicula (Bulman, 1970, fig. 80.1); *4, Nemagraptus gracilis* (HALL, 1847), reconstruction, cladial branching at regular intervals on one side of the two main stipes (Hall, 1859a, fig. 10).

diameters as large as 100 cm. The longest monograptid has been measured at 1.45 m long and is still incompletely preserved (LOYDELL & LOVERIDGE, 2001). The exact development and differentiation of the stipes is often impossible to recognize, especially in flattened material, but the main features have been identified from chemically isolated specimens and can be referred to two structural types, dichotomous and cladial branching.

DICHOTOMOUS BRANCHING

Branching in earlier pterobranchs developed entirely and invariably at the tips of the stipes, the growing end, where new thecae are added to the colony (Fig. 44.1). This type of branching is identified as dichotomous branching, even though in some taxa, branching appears to be based on a lateral

origination of the new stipes (Fig. 44.3). A secondary, later branching from an older part of the stipes cannot be produced by these colonies. The details of the branching structure are only recognizable in well-preserved, isolated material or in relief specimens.

In dichotomus branching, the two resulting stipes diverge at identical angles from the path of the previous branching division (Fig. 44.1, Fig. 45); thus, the original direction of the prebranching stipe is not continued (e.g., in *Adelograptus* BULMAN, 1941; *Clonograptus* NICHOLSON, 1873). In some species, one of the resulting stipes follows the original direction, whereas the second stipe grows at a distinct angle (e.g., *Schizograptus* NICHOLSON, 1876; *Trichograptus* NICHOLSON, 1876). In this development, it appears as if the second stipe is produced differently
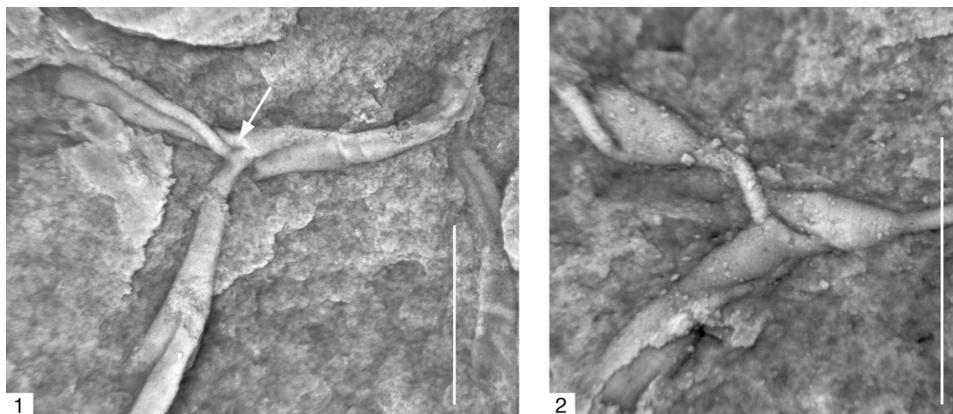
FIG. 45. Dichotomous branching. *1, Trichograptus dilaceratus* (HERRMANN, 1885), Lower Ordovician (lower Floian), DI 858, slightly curved main stipe with lateral branch growing downward in photo, note lateral origin of theca at branching point (*arrow*), latex cast; *2,* indeterminate dichograptid on slab with GSC 123228 (Jackson & Lenz, 2003, fig. 9m), Lower Ordovician (upper Tremadocian), showing thin prothecae and strongly widening metathecae, all thecae originate laterally, latex cast, scale bars, 1 mm (new).

and has a lateral origin (Fig. 44.3). Relief specimens indicate that this lateral branching is only an apparent difference: the construction of both the lateral and the dichotomous branching divisions is structurally identical. It is, however, observable that lateral branches often start growing later after the main stipe has already achieved a certain length. (Fig. 44.3).

The distances between branching divisions can be quite variable and increase distally along the colony in most species (Fig. 44.1). This progressive branching includes a highly variable number of thecae of each stipe division, and irregularities are common. A more regular type of branching appears in the monoprogressive branching of *Goniograptus* M'COY, 1876 (Fig. 44.2) and a few other genera, in which branching regularly develops after one or two thecae. The main stipe in these genera displays a distinct zigzag shape, with branches originating alternately on both sides, resulting in fewer distal branches. This type of branching is also present in a few benthic graptolites (e.g., *Ptilograptus* HALL, 1865).

CLADIAL BRANCHING

Cladial branching (Fig. 46) represents a special type of branching, which is quite different from the normal dichotomous branching at the tip of the colonies, but its precise construction is often impossible to recognize in flattened specimens (see *Nemagraptus,* Fig. 44.4). Cladial branching is secondarily produced by mature zooids, and branches originate from the aperture of its mother theca, not from the dorsal side of the stipe as in dichotomous branching.

Cladial branching is recognized when a thecal tube develops at the apertural opening of a previously formed theca and at some distance proximally from the growing end of the main stipe. At first, small flanges of fusellar material attached to the thecal aperture are produced by the daughter zooid of the mother thecae and subsequently develop into a thecal tube. The thecal shape may be identical to that of its mother theca, but can also be quite different. Cladial branching is best known from *Cyrtograptus* (see THORSTEINSSON, 1955) (Fig. 46.1, Fig. 46.4) but is also known in taxa such as *Linograptus* FRECH, 1897; *Diversograptus* MANCK, 1923; and *Neodiversograptus* URBANEK, 1963 (Fig. 46.2–46.3).

Theoretically, cladial branching may be present at any place in the colony, but it is usually restricted to certain positions in most genera and species. In the
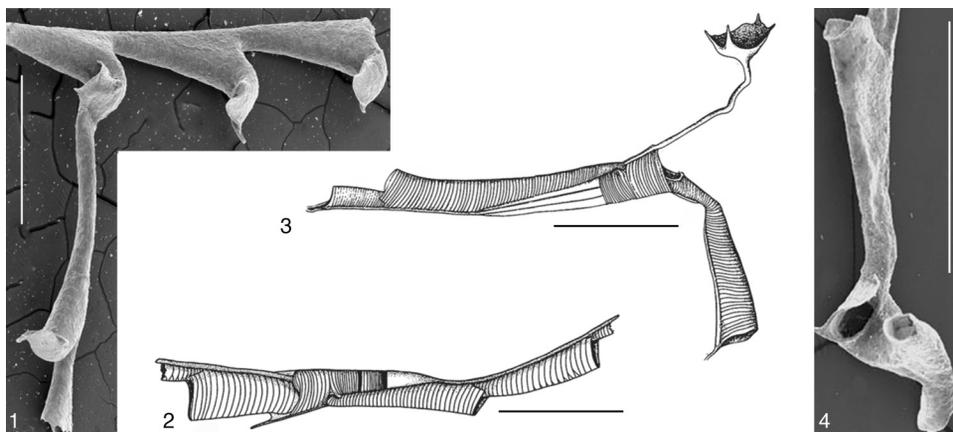
Fig. 46. Cladial branching in *Cyrtograptus, Linograptus, and Neodiversograptus. 1, Cyrtograptus perneri* Bouček, 1933, fragment with thecal cladium, Silurian (Wenlock, upper Sheinwoodian), Canadian Arctic (new); *2, Neodiversograptus nilssoni* (Barrande, 1850), specimen with wide, sicular cladium, Silurian (Ludlow, lower Gorstian) (Urbanek, 1997b, fig. 2B); *3, Linograptus posthumus* (Richter, 1875), reconstruction showing sicular cladium and idealized virgellarium attached to virgella, upper Silurian (Urbanek, 1997b, fig. 5D); *4, Cyrtograptus radians* Bouček, 1933, fragment with thecal cladium, Silurian (Wenlock, lower Homerian), Canadian Arctic (Lenz & Kozłowska, 2006, fig. 16.2). All scale bars, 1 mm.

genus *Cyrtograptus,* thecae produce cladial branching at regular distances, and the position of cladia can be important for the taxonomic identification of various species. Paired cladial branches and multiple cladial branches occurred in a small number of Ordovician to Lower Devonian genera and species (e.g., *Amphigraptus* Lapworth, 1873b; *Tangyagraptus* Mu, 1963a; *Abiesgraptus* Hundt, 1935a; *Linograptus* Frech, 1897). Single and multiple cladial branches also appeared at the sicular aperture in upper Silurian and Lower Devonian monograptids (Fig. 46.2–46.3). Numerous cladia may have developed at the sicular aperture in *Linograptus* (Urbanek, 1963).

The oldest known cladial branching is documented from the Middle Ordovician (Darriwilian) genus *Pterograptus* (Skwarko, 1974; Maletz, 1994a). Cladial branching occurred in *Nemagraptus* and other dicranograptids (*Amphigraptus*, *Tangyagraptus*) but was most commonly developed in the Silurian to Lower Devonian monograptids (*Abiesgraptus, Cyrtograptus*, *Diversograptus*, *Linograptus*, *Sinodiversograptus* Mu & Chen, 1962a). The cladial branching appears to have originated independently numerous times throughout the evolution of the graptolites. Cladial branching in the monograptid genera invariably involved the development of a secondary nema along which the cladial branches grew. Such a structure is not present in the cladia of Ordovician dichograptid and dicranograptid specimens. Thus, Ordovician and Silurian taxa adopted a fundamentally different approach to the construction of cladia.

STIPE ORIENTATION

The colony shapes in planktic graptolites are quite variable, based on the development of the stipes. Generally, the orientation of the stipes is considered in relation to the sicula, although Elles (1922, fig. 42) proposed the nema as the main defining character for the orientation of the colonies. In the standard orientation of the sicula with the aperture downward and the free nema directed upward, the stipe orientation is defined as pendent to scandent and all variations between (Fig. 47). This orientation may not represent the orientation of the living graptolite colonies, because very little can be known for certain about the orientation of graptolite colonies in the
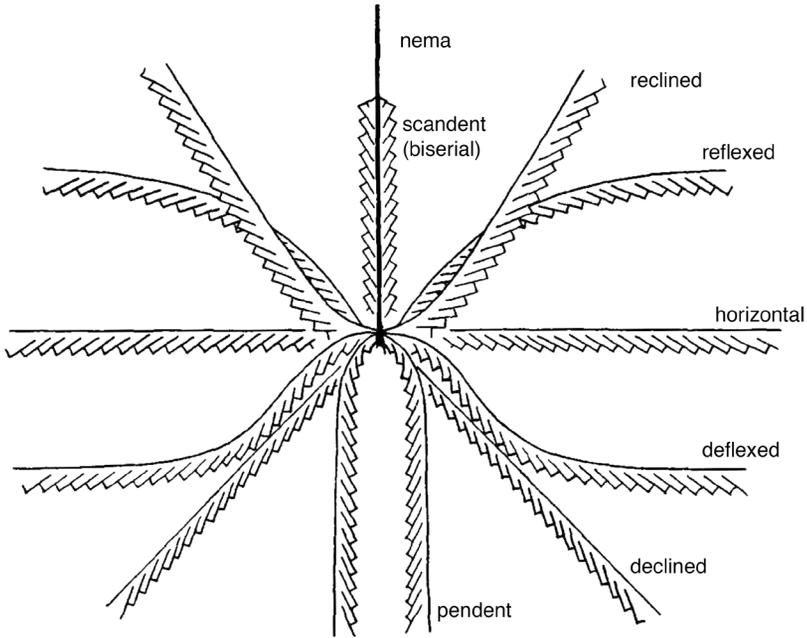
FIG. 47. Diagram illustrating the orientation of graptolite stipes to the nema and the terminology (Bulman, 1970, fig. 38).

water column. The colony shapes of many graptolite species vary considerably, but the general stipe orientation usually can easily be recognized. During the burial process, the highly flexible tubarium was commonly distorted, especially the longer, more mature stipes.

Scandent graptoloids can be constructed in two fundamentally different ways (JAANUSSON, 1960). These colonies usually have two or four stipes connected to each other. In biserial axonophoran colonies, the two stipes are connected back-to-back, a condition identified as scandent (Fig. 47) and dipleural (Fig. 48.4). Four-stiped scandent taxa include the Lower to Middle Ordovician genera *Phyllograptus, Pseudophyllograptus,* and *Pseudotrigonograptus,* in which the colony has a cross-shaped cross section (Fig. 48.5–48.6). Three-stiped scandent taxa are extremely rare. The only example known from well-preserved material is *Pseudotrigonograptus minor* MU & LEE, 1958 (FORTEY, 1971), a phyllograptid graptoloid.

The stipes are connected along their lateral margins in the glossograptids (e.g.,

Glossograptus, Cryptograptus), enclosing the sicula and the initial growth of the proximal thecae. This development is identified as a monopleural arrangement (Fig. 48.1–48.2). In monopleural colonies, the proximal structure is difficult to ascertain, because the details are only visible in juvenile specimens. Mature specimens encase the proximal structure by the later growth of the stipes and completely cover them. Partially monopleural development is present in a few taxa, most notably in *Kalpinograptus* JIAO, 1977 (Fig. 48.3). In *Kalpinograptus,* the proximal end is monopleural, but distally the stipes separate from each other; the outline of the genus is very similar to a typical reclined isograptid. The tubarium structure in taxa with a monopleural development appears to be identical on both sides, whereas in dipleural taxa the structure is different on the obverse and reverse sides.

STIPE CONNECTIONS

Pterobranch colonies are formed from a highly flexible material, and the interference of individual stipes might be common when
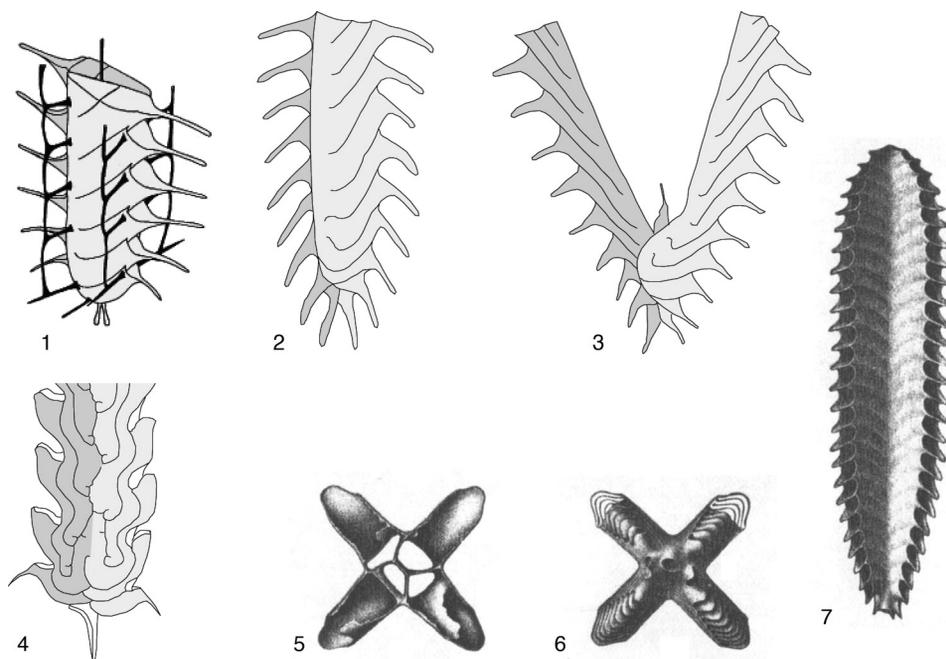
FIG. 48. Monopleural and dipleural development. *1, Paraglossograptus* sp., reconstruction of colony showing monopleural arrangement and development of lacinia from lateral apertural spines (new); *2, Glossograptus* sp., monopleural; *3, Kalpinograptus* sp., with initially monopleural and distally two-stiped colony; *4, Levisograptus austrodentatus* (HARRIS & KEBLE, 1932) dipleural, reverse view, (*1–4*) left and right sides in different *gray* shades (*2–4* adapted from Maletz, Carlucci, & Mitchell, 2009, fig. 5); *5–7, Pseudophyllograptus* sp., quadriserial colony, cross sections (*5–6*) and lateral view (*7*) (Holm, 1895, pl. 13).

overlapping. However, the stipes in multiramous erect and planktic colonies tend to keep a precisely defined, minimum distance between them. This distance might be a function of avoiding unintended interaction and competition during feeding and, thus, be defined by the size of the zooids and the feeding range of their arms (STARCHER & MCGHEE, Jr., 2003). Computer modeling by FORTEY and BELL (1987) added support to the proposal that the various stipe configurations in multiramous forms were designed for maximum feeding efficiency of stipes and minimum interference with their neighbors.

Dissepiments are the easiest, although uncommon, way of giving rigidity to the tubarium and keeping stipes from overlapping or interfering with each other. Dissepiments are thin bands of fusellar and cortical tissue connecting adjacent stipes (URBANEK & MIERZEJEWSKI, 2009). Dissepiments are developed in erect, benthic dendroid colonies (*Dictyonema* HALL, 1851; *Ptiograptus* RUEDEMANN, 1908) and are present in a few early planktic forms (*Rhabdinopora* EICHWALD, 1855; *Staurograptus* EMMONS, 1855; and *Sagenograptus* OBUT & SOBOLEVSKAYA, 1962) (Fig. 49.1). They appear to grow from two adjacent stipes, perhaps as a joint work of zooids from each stipe, and meet in the middle, where they are thinner. Dissepiments can be distributed irregularly along the stipes, depending on the need for separation. In many dissepimentous species, however, they form a highly regular mesh of stipe connections and the density of dissepiments has been used to identify taxa, especially within the genus *Rhabdinopora* (COOPER & others, 1998). This highly regular meshwork is reminiscent of colony development in some bryozoans (e.g., *Fenestella*), and these taxa may easily be confused if the construction material is not considered in fossil specimens. The bryozoans do not produce an organic
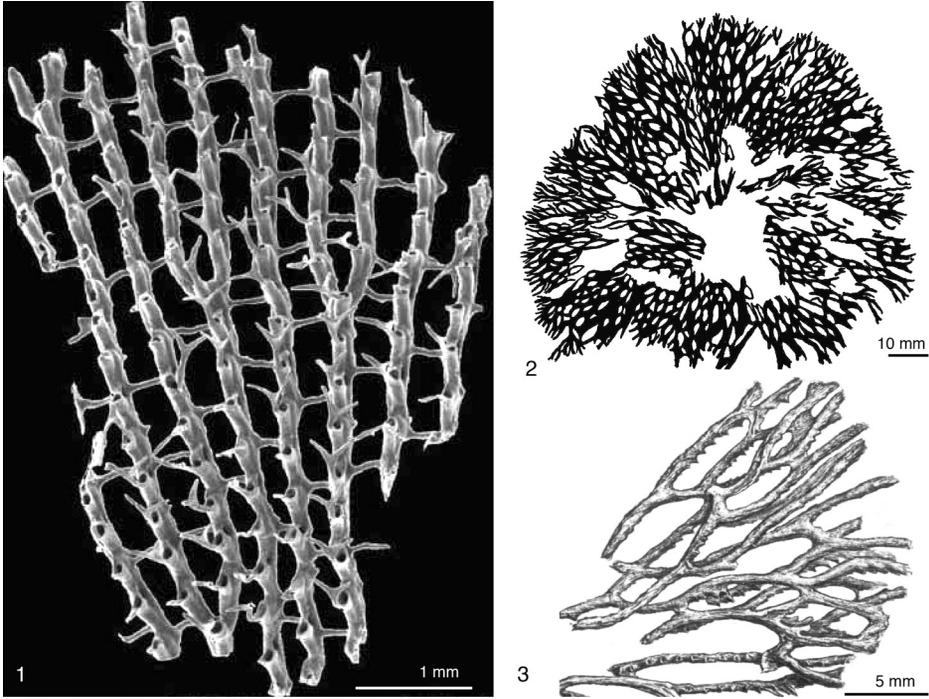
FIG. 49. Dissepiments and anastomosis. *1, Dictyonema* sp. cf. *Dictyonema cervicorne* HOLM, 1890, colony fragment showing well-developed dissepiments, Ordovician, glacial boulder, Poland (Urbanek & Mierzejewski, 2009, fig. 3); *2, Palaeodictyota anastomotica* (RINGUEBERG, 1888), showing anastomozing stipes, upper Silurian (Bulman, 1970, fig. 21,*3*); *3, Desmograptus idoneus* BULMAN, 1933a, fragment showing anastomosis with thecal transfer (Bulman, 1933a, pl. 4,*18*).

housing; instead, they form their housing structures, the zooecium, as a calcified cuticle (LANKESTER, 1884).

HARMER (1905) discussed numerous bridges connecting adjacent branches in *Cephalodiscus dodecalophus* M'INTOSH, 1887. These bridges are structurally homologous to the dissepiments of benthic and planktic graptolites. *Cephalodiscus dodecalophus*, even though not a colonial pterobranch, forms branched, erect structures in a way similar to that of an erect colonial pterobranch.

ZALASIEWICZ (1993) described a rare occurrence of structures resembling dissepiments in *Spirograptus turriculatus* (BARRANDE, 1850), which formed as outgrowths from apertural thecal spines that connected to the dorsal side of the underlying stipe. These developments should not be designated dissepiments because their construction is based on previously secreted and subsequently elongated spines and are not independently developed features. However, they served the same (presumed) purpose of keeping the stipes separate and not overlapping.

Anastomosis includes the transfer of individual thecae or groups of thecae from one stipe to another or the temporary connection of two adjacent stipes (Fig. 49.2–49.3). It exists in the tubarium of a few, erect, benthic pterobranch genera, such as *Desmograptus* (Fig. 49.3); *Koremagraptus* BULMAN, 1927a; or *Palaeodictyota* WHITFIELD, 1902 (Fig. 49.2). This feature is not well understood. BULMAN (1945) described anastomosis in *Koremagraptus kozlowskii* BULMAN, 1945, from the Upper Ordovician of Britain, based on isolated, bleached material. RICKARDS and LANE (1997) differentiated pseudanastomosis as anastomosis with transfer of thecae, from anastomosis as a temporary connection of stipes without thecal transfer.

EXTRATHECAL DEVELOPMENTS

Many different extracolonial features can be recognized in the graptolites, especially in the planktic forms. They are differentiated herein, based upon their position in the colony and precise development.

NEMATULARIA

A short nema is present in most early (Tremadocian) planktic graptoloids, including the branched nemal tufts of some early *Rhabdinopora* specimens (LIN, 1988) (Fig. 50.7). Although the nema is typically short, a long nema and a considerable development of nematularia (Fig. 50) occurred in Lower Ordovician (Floian) species (e.g., *Pendeograptus* BOUČEK & PŘIBYL, 1952a; *Kinnegraptus* SKOGLUND, 1961; *Isograptus* MOBERG, 1892a; and *Pseudisograptus* BEAVIS, 1972).

The nema is incorporated into the colonies of the axonophorans and evolved into the long, slender nemata typical of these taxa, commonly bearing nematularia at the tip (Fig. 50.10). The nema is either incorporated into the ventral thecal walls of the biserial colonies and connected to the thickened lists around the thecal origins or may be free inside unistipular tubaria with their alternating thecal origins. It generally extends far beyond the distal end of many axonophoran colonies (Fig. 50).

A number of extracolonial features are connected to the nema at the distal end of the colonies. These features have been called Schwimmblase (DACQUÉ, 1923; MÜNCH 1938), floating device or Schwebeapparat (MÜLLER & SCHAUER, 1969), or buoyancy mechanism (BULMAN, 1970) and were termed—more neutrally—the nematularium by MÜLLER (1975). Nematularia have been suggested to be gas-filled chambers used as flotation devices (e.g., HUNDT, 1939; BOUČEK & PŘIBYL, 1941). However, recent studies have convincingly demonstrated that nematularia are solid, planar structures formed of successive layers of fusellar tissue (URBANEK, KOREN', & MIERZEJEWSKI, 1982; MITCHELL & CARLE, 1986). Examples include two isolated, three-dimensional nematularia associated with *Normalograptus brevis* (ELLES & WOOD, 1906) in which one of the nematularia is clearly a solid, three-vaned structure (BULMAN, 1947, pl. 9,*14–15*). In addition, a few three-dimensionally preserved, two-vaned, paddle-shaped, and three-vaned nematularia—all retaining original shapes and all solid—have been discovered in Silurian retiolitids from the Canadian Arctic (LENZ & KOZŁOWSKA-DAWIDZIUK, 2001) (see Fig. 50.1–50.2).

STØRMER (1933) described a proximal organ in *Rhabdinopora flabelliformis* (EICHWALD, 1840) and interpreted it as a possible disklike floating device. HARRIS and KEBLE (1928) described a similar structure in *R. campanulatum,* although the nematularium appears to be a bundle of fibers (Fig. 50.7). Possible small nematularia are present in the Lower Ordovician species—upper Tremadocian anisograptids (e.g., *Kiaerograptus*? *peelensis* JACKSON, 1974) and the Floian dichograptid *Tshallograptus fruticosus* (HALL, 1858) (see JACKSON & LENZ, 2006) (Fig. 50.6). However, nematularia are more common in Middle Ordovician to Silurian axonophorans. Slender, long, and slightly spiraled nematularia are present in the Dapingian isograptids (MOBERG, 1892a) and appear to be typical for the Middle Ordovician glossograptid *Cryptograptus,* identified as *Tonograptus* by WILLIAMS (1992).

In many taxa, the nema broadens distally, gradually or abruptly, into a prominent nematularium that ranges from a slim to broad band that may be flat (Fig. 50.9), helically spiraled (Fig. 50.10–50.11), or three vaned, disklike, or heart shaped (Fig. 50.8), or it may develop as multipronged structures distal to the growing end of the tubarium (Fig. 50.3–50.4). The nema may be recognizable in the center of the structure or reach only to the base of the nematularium.

Generally, nematularia are partially or completely external to the main body of the tubarium, but some band-shaped, paddle-
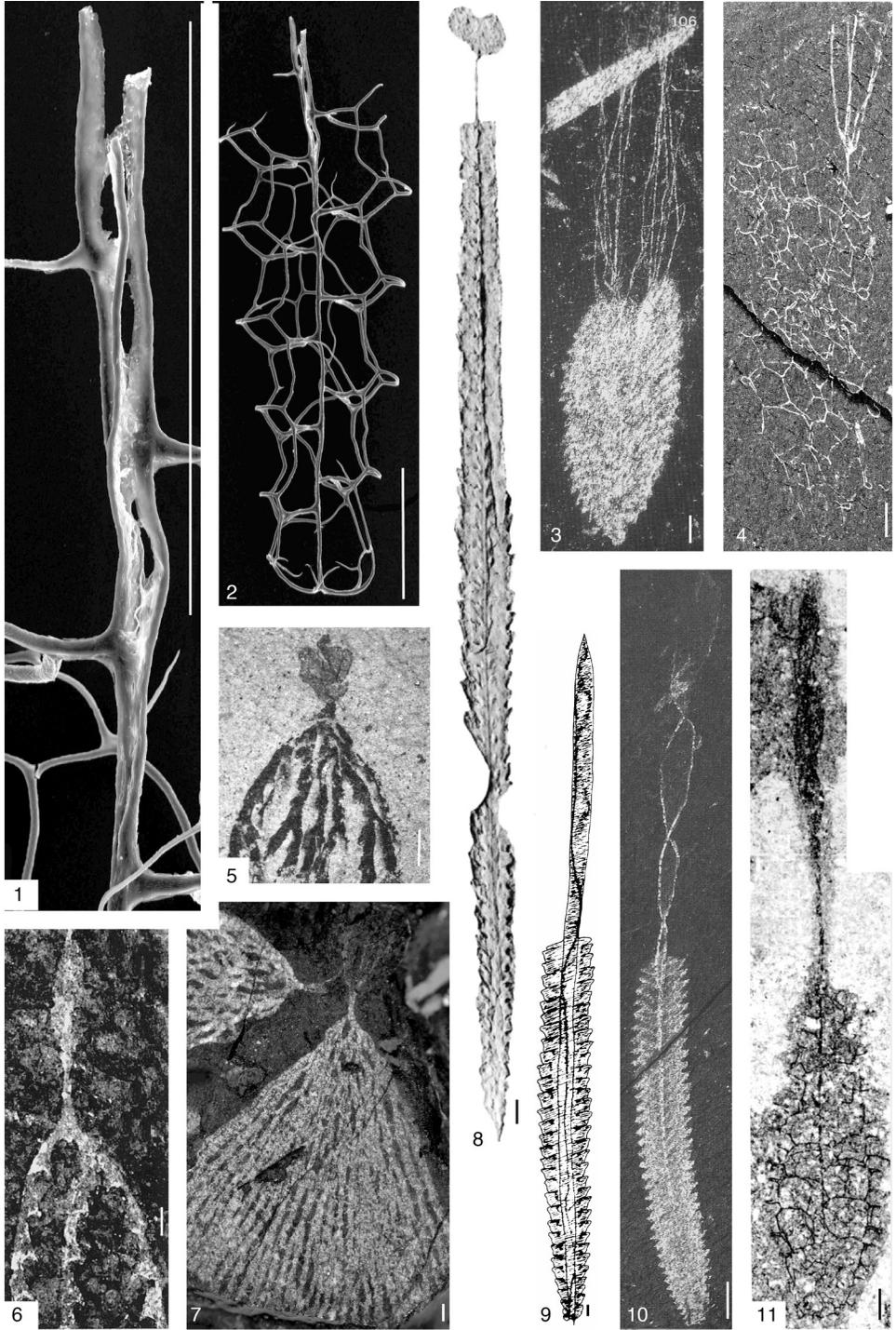
FIG 50. *For explanation, see facing page.*

shaped, two- or three-vaned nematularia, or multifurcating, thickened rods originate well within the (mature) tubarium and continue distal of the main tubarium (e.g., *Cystograptus* Hundt, 1942) (Jones & Rickards, 1967) (see Fig. 50.9). This is particularly evident among the retiolitids, though also present in a number of other biserial graptoloids. As is well known in *Cystograptus vesiculosus* (Nicholson, 1868a) and *Archiclimacograptus decoratus* (Harris & Thomas, 1935), the nematularia may have been constructed at the growing tip of the nema, far beyond the advancing zooidal tubes and overgrown during the later astogeny of the colonies (Fig. 50.8–50.9).

Finney (1985a) summarized the evidence for small, hollow spheres that are attached to the siculae or nemata of some planktonic dendroids and graptoloids, particularly during the very early life stage of the colony. From the relatively poor preservation, however, it is unclear whether these features are a normal feature of juvenile graptolite colonies or an artifact of preservation. They may, perhaps, even be acritarchs or other palynomorphs accidentally attached to the colonies.

PROXIMAL WEBS

Web structures are common in certain groups of graptolites, especially in multiramous Lower to Middle Ordovician dichograptids (Fig. 51). Ruedemann (1947) illustrated numerous dichograptids with web structures. They have been described from shale material, but are unknown from isolated specimens. Therefore, their construction is poorly understood. In a number of genera (e.g., *Dichograptus* Salter, 1863a; *Loganograptus* Hall, 1868; and *Tetragraptus* Salter, 1863a), these webs appear to be formed from fusellar material, considering that growth lines are sometimes recognizable (Fig. 51.2). They connect adjacent stipes and appear to start at the proximal end and grow outward as thin membranes. Jaanusson (1960) described the pendent didymograptid *Didymograptus pakrianus* Jaanusson, 1960, as having a considerable overgrowth of the proximal end, forming a large communal cavity for the proximal thecae.

A distinct, apparent, lateral thickening of the proximal stipes of the colonies is present in numerous multiramous Lower to Middle Ordovican dichograptids, such as *Adelograptus* Bulman, 1941 (Fig. 51.3); *Clonograptus* Nicholson, 1873; and *Stellatograptus* Erdtmann, 1967). Details of this development are uncertain, as isolated material is not available and specimens are flattened. In juvenile specimens of the same species, the stipes are much more slender and thecal apertures can be recognized. These stipe modifications could be interpreted as lateral web structures, similar to the proximal webs of other forms, but alternatively they could represent actual thickening of the stipes, which appears to be common in many dendroid graptolites as a gerontic feature.

Fig. 50. Nematularia and other extraneous structures. *1–2, Paraplectograptus* sp.*, Silurian (upper Wenlock), glacial boulder, Germany; *1,* enlargement showing triradiate cross section of nematularium; *2,* showing internal nematularium (new); *3, Dischidograptus regius* (Hundt, 1957a), showing branched structures distally, Silurian (Llandovery), Germany (Palmer & Rickards, 1991, fig. 106, as *Petalograptus ovatoscopularus* Schauer, 1971); *4, Eiseligraptus eisenacki* (Hundt, 1951a), with multifurcated nematularium, Silurian (upper Llandovery), Hohenleuben, Germany, (new); *5, Rhabdinopora proparabola* (Lin, 1986)*, showing lobate nematularium, Dayangcha, China (new); *6, Tshallograptus fruticosus* (Hall, 1858), showing ovate nema structure, Lower Ordovician (Floian), Canada (northern Yukon) (Jackson & Lenz, 2006); *7, Rhabdinopora campanulatum* (Harris & Keble, 1928), showing proximal end with tuft-like bundle of fibers, Lower Ordovician (Tremadocian), Victoria, Australia (new); *8, Archiclimacograptus decoratus* (Harris & Thomas, 1935), with heart-shaped nematularium, Upper Ordovician, Nevada, USA (Ross & Berry, 1963); *9, Cystograptus vesiculosus* (Nicholson, 1868a), with long nematularium, Silurian (Llandovery), Germany (Schauer, 1971); *10, Parapetalolithus* sp., with a strongly spiraled nematularium, Silurian (Llandovery), Germany (Palmer & Rickards, 1991, fig. 38); *11, Hoffmanigraptus karlsteinensis* (Kozłowska-Dawidziuk, Lenz, & Štorch, 2001), with spiraled nematularium, upper Silurian (Wenlock, upper Homerian), Czech Republic (Kozłowska-Dawidziuk, Lenz, & Štorch, 2001, fig. 6.1). All scale bars, 1 mm.
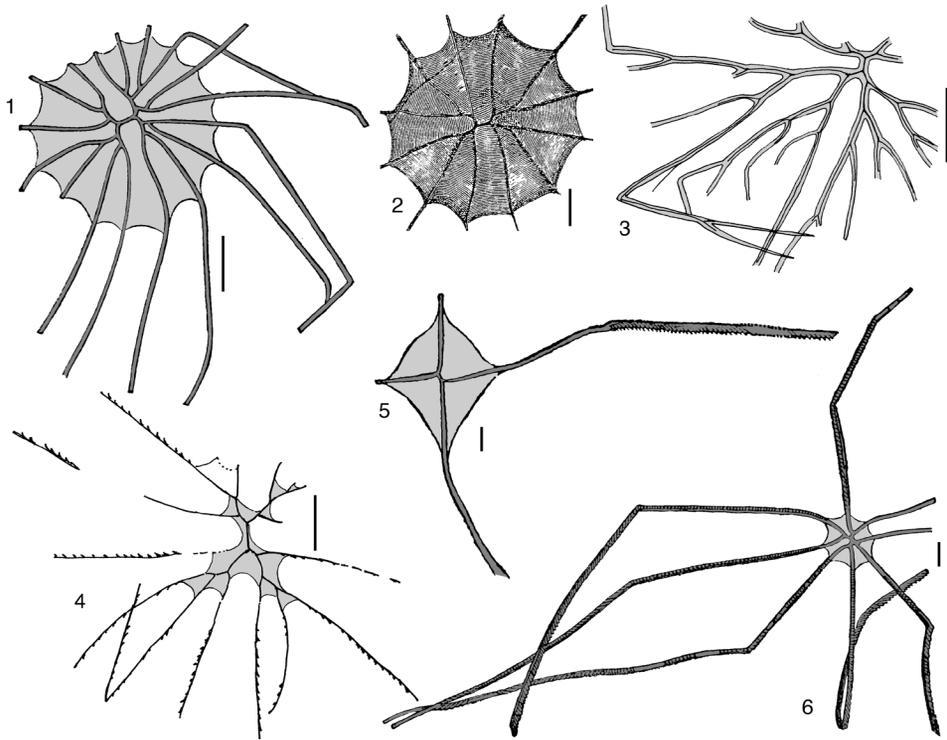
FIG. 51. Proximal webs or membranes. *1, Loganograptus logani* (HALL, 1865)*, extensive membrane development (adapted from Hall, 1865, fig. 6); *2, Loganograptus kjerulfi* (HERRMANN, 1885), proximal membrane (Herrmann, 1885, fig. 10); *3, Adelograptus tenellus* (LINNARSSON, 1871) showing extreme thickening of stipes, particularly in proximal regions (adapted from WESTERGÅRD, 1909, pl. 4,8); *4, Goniograptus palmatus* HARRIS & KEBLE, 1932, membranes between some of the branching divisions (adapted from Harris & Keble, 1932, pl. 6, fig. 5); *5, Tetragraptus headi* HALL, 1865, proximal membrane (adapted from Hall, 1865, fig. 4); *6, Dichograptus octobrachiatus* (HALL, 1858) (adapted from Hall, 1865, fig. 4). All scale bars, 10 mm.

Proximal webs may be present in the axils of Upper Ordovician *Dicellograptus*, where they cover and obscure the sicula (Fig. 52.2–52.3). In outline, these specimens may more closely resemble specimens of *Dicranograptus* HALL, 1865, with a short, wide, biserial proximal end, as, for example, in *Dicellograptus moffatensis* (CARRUTHERS, 1858); and *Dicellograptus ornatus* ELLES & WOOD, 1904 (WILLIAMS, 1982a).

Proximal webs and membrane-like features are extremely rare in monograptids. MOBERG (1893) described *Monograptus pala* MOBERG, 1893, with an apparent large, rounded proximal membrane. As MOBERG's illustrated specimens show the thecae in scalariform view (Fig. 53.8), a more precise identi-

fication is impossible and details of the membrane are not available.

A single *Cyrtograptus* specimen with an extensive proximal membrane has been discovered in the Canadian Arctic (LENZ, 1974). In this specimen, the membrane partly covers the thecal apertures of the proximal end of the specimen. It is, in part, a double membrane that extends along the initial spiral part of the colony. UNDERWOOD (1995) illustrated a similar and more completely preserved membrane in a flattened specimen of *Cyrtograptus murchisoni* CARRUTHERS in MURCHISON, 1867a (Fig. 52.1).

Bladderlike structures, or sacs, developed in a few Ordovician axonophorans, most typically apparent in *Archiclimacograptus*
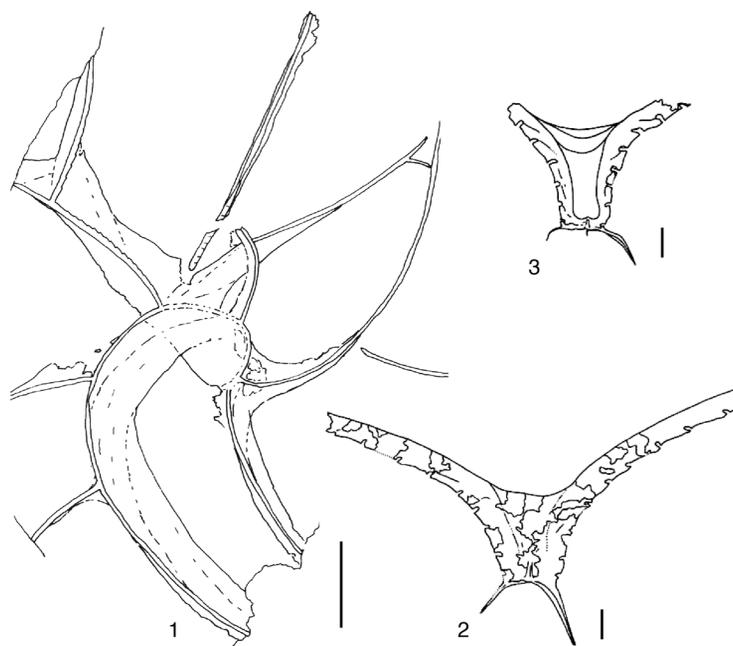
FIG. 52. Proximal membranes. *1, Cyrtograptus murchisoni* CARRUTHERS in MURCHISON, 1867a, with remnants of thin, multilayered membranes, mostly in the proximal region, Silurian (lowermost Wenlock), UK, scale bar 10 mm (adapted from Underwood, 1995, fig. 2c); *2–3, Dicellograptus turgidus* MU, 1963b, showing proximal membrane closing reclined stipes of proximal end, Upper Ordovician, Vinini Formation, Nevada, USA, scale bars, 1 mm (Štorch & others, 2011, fig. 10).

bursifer (ELLES & WOOD, 1906) (ELLES & WOOD, 1906, pl. 27,*6*). A possibly similar development is known from the Llandovery *Glyptograptus auritus* (BJERRESKOV, 1975). It is unclear whether they represent membranes or three-dimensional features. Proximal webs are also constructed in mature specimens of a number of climacograptids, where they grow upward from the dorsal side of the proximal spines in *Climacograptus bicornis* (HALL, 1847) (Fig. 53.2) and may reach the fourth or fifth thecal pair (RIVA, 1976, fig. 6). *Climacograptus*? *papilio* MU, 1963b (Fig. 53.5) may also construct considerable webs based on the proximal spines, but they are not attached to the sides of the colony.

SCOPULAE AND OTHER LATERAL AND PROXIMAL NEMAL DEVELOPMENTS

Scopulae are special developments on the sides of axonophoran colonies and form paddle-like structures (Fig. 53.4). They may originate from the nema, but the development is unclear for most taxa. Scopulae are usually bladelike with a thickened rim around a thin fusellar membrane (BATES, 1987a; BATES & KIRK, 1991). They are most common in the Upper Ordovician Lasiograptidae, but analogous features may be present in a few Silurian normalograptids (e.g., *Dittograptus* OBUT, SOBOLEVSKAYA, & MERKUREVA, 1968; see KOREN' & RICKARDS, 1996).

The paired lateral spines of *Alulagraptus uncinatus* (KEBLE & HARRIS, 1934) (Fig. 53.9), are based on the nema and form during an early stage in the development of the colony (CARTER, 1972). After only a few millimeters of growth of the colony, the nema splits into two rods that grow subhorizontally outward. The nema stops growing, and the colony grows across this point unchallenged and without the production of a new nema. MU (1963b) described a similar development
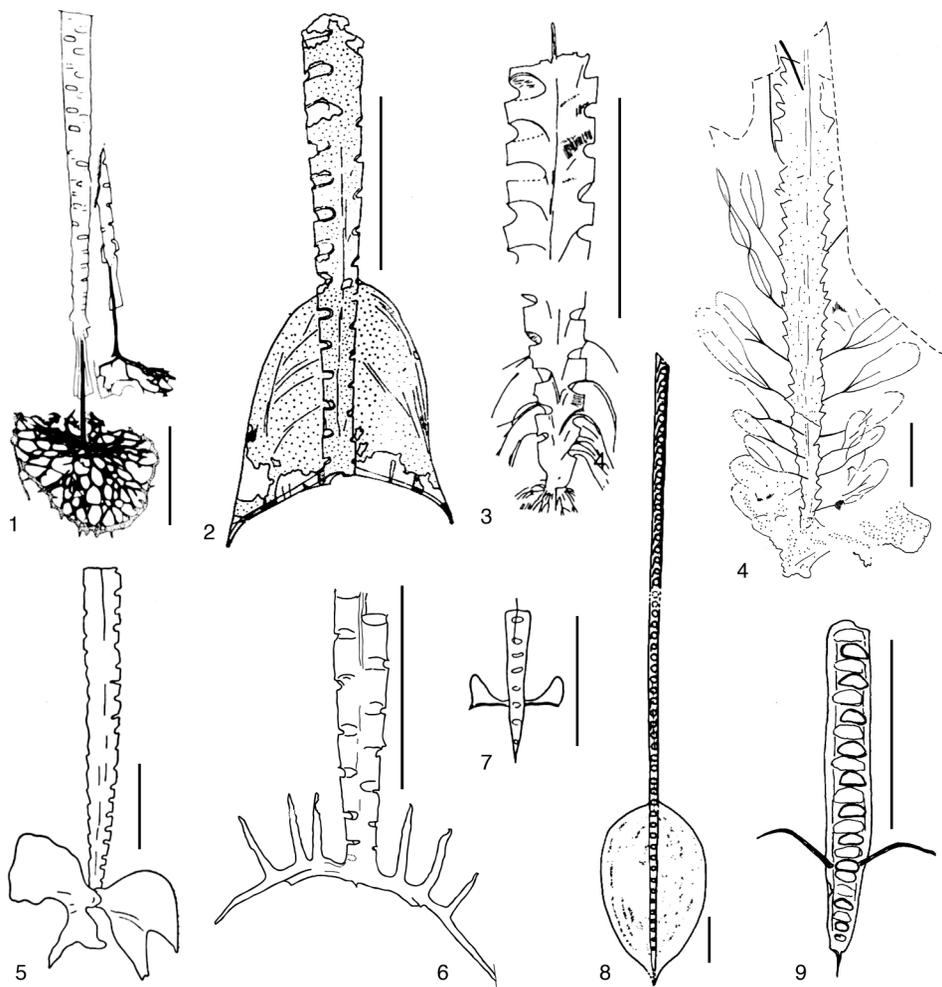
FIG. 53. Scopulae and other extraneous proximal structures. *1, Climacograptus*? *baragwanathi* HALL, 1906, Upper Ordovician (Katian), Australia (VandenBerg & Cooper, 1992, fig. 9D); *2, Climacograptus bicornis* (HALL, 1847), with large proximal membranes, Upper Ordovician (Sandbian), New York, USA (Riva, 1976, fig. 6N); *3, Comograptus comatus* OBUT & SOBOLEVEKAYA in OBUT, SOBOLEVSKAYA, & MERKUREVA, 1968, Silurian (Llandovery), Norilsk region, Siberia, Russia (Koren' & Rickards, 1996, fig. 6G); *4, Dittograptus* sp., specimen with numerous scopulae, Silurian, Thuringia, Germany (Müller, 1977, fig. 11); *5, Climacograptus*? *papilio* MU, 1963b, with proximal membranes, Upper Ordovician, China (Mu, 1963b, fig. 11); *6, Appendispinograptus venustus* (HSÜ, 1959a) showing development of complex parathecae, Wufeng Formation, southwestern China (Mitchell, Chen, & Finney, 2007, fig. 1.4); *7, Alulagraptus ensiformis* (MU & ZHANG in MU & others, 1963), Upper Ordovician, China (Mu, 1963b, fig. 12); *8, Monograptus pala* MOBERG, 1893, with large proximal membranes (Bulman, 1970, fig. 70.15); *9, Alulagraptus uncinatus* (KEBLE & HARRIS, 1934), Upper Ordovician, Vinini Formation, Nevada, USA (Carter, 1972, fig. 2l). All scale bars, 5 mm.

from the poorly known *Alulagraptus ensiformis* (Fig. 53.7), but in this material a nema apparently continues through the colony.

VIRGELLARIA

In *Linograptus posthumus* (RICHTER, 1875), the virgellarium, a construction formed from the tip of the virgella, may represent the typical development of a virgella-related feature. Unfortunately, the details of its development are uncertain, as the isolated specimens do not preserve the remains of the fusellar structure. The virgellarium is formed from a membrane with four

petals, ending in fingerlike or umbrella-like outgrowths (URBANEK, 1963, 1997b) (Fig. 46.3). MÜLLER (1977) illustrated a number of virgellar features as virgellaria and suggested a detailed terminology of these features, but details are extremely rare. Virgellar extensions are limited to the extremely long virgellar spines in a number of biserial taxa (e.g., *Archiclimacograptus* MITCHELL, 1987; *Orthograptus* LAPWORTH, 1873b). Bifurcation of the virgella, as in *Normalograptus bifurcatus* LOYDELL, 2007, appears to be extremely rare (LOYDELL, 2007) and has not been found in other taxa. The development of the ancora umbrella and ancora sleeve in the Retiolitidae also belongs to the modifications of the virgella.

ANCORA SLEEVE

The ancora sleeve is a special development in the Retiolitidae. It consists of a secondary membrane surrounding the tubarium and its original thecal construction. Usually, the ancora sleeve is preserved as a more or less regularly developed system of lists, the reticulum, which developed from the distal extension and development of the virgellar structure, the ancora umbrella. It is comprised of seamed lists made up of cortical tissue and enlarged by concentric layering. This combination of the ancora sleeve forming the outer wall and the thecal framework forming the inner wall is unique among the graptolites. It is clear that the thecal framework was formed by the laying down of a succession of thin fusellar sheets, but the origin of the sheets in the ancora sleeve is unclear (e.g., BATES, 1987; BATES & KIRK, 1992). In the vast majority of specimens, the fusellar layer is too thin to be preserved in the fossil record. It is most commonly recognized through the presence of fusellar shards (Fig. 54.6) in the seams of the list structures (BATES & KIRK, 1992) and, especially the very rare, complete preservation of fusellar sheet layers (LENZ, 1994a; LENZ & THORSTEINSSON, 1997).

Because the lacinia in the Lasiograptidae develops quite differently from the clathrium and reticulum (ancora sleeve) of the Retiolitidae, they may be treated as analogs rather than homologs. Whereas the lacinia lists of the lasiograptids and glossograptids are without list seams, both the clathrial lists (generally the equivalent of the thecal framework; Fig. 54, *white arrows*) and the reticulum (the finer meshwork, mainly related to the ancora sleeve; Fig. 54, *gray arrows*) invariably bear seams that were probably occupied by very thin fusellar bands. Fusellar shards appear only in the seams of the thecal framework lists (Fig. 54.6), whereas the seams of the ancora sleeve are apparently devoid of fusellar shards.

LACINIA

The lacinia is typically a development of a meshwork of rods originating as thecal spines with a concentric core. It produces a complex, three-dimensional, meshwork structure around the entire colony in some Lasiograptidae (Fig. 55.1–55.2). The spines and bars are formed from fusellar material, typically covered and thickened by cortical overgrowth (BATES & KIRK, 1991). At the same time, the fusellar structure of the archiretiolitid colonies is reduced, and generally only thin bars remain outlining the thecal framework (Fig. 55.1). These lists have distinct seams, indicating their origination on the fusellar surfaces of the thecae (BATES & KIRK, 1991). In early lasiograptids, the fusellum is more complete, and the difference from the encasing lacinia is easily recognizable (Fig. 55.2).

A small amount of lacinia appears to develop in the Glossograptidae. Species of the genus *Paraglossograptus* MU in MU & others, 1962, possess lateral thecal spines that are interconnected with vertical bars. Four ladderlike structures are formed in *P. proteus* (HARRIS & THOMAS, 1935) (WHITTINGTON & RICKARDS, 1969), but a more complex meshwork is present in *P. tentaculatus* (HALL, 1865) (Fig. 55.3–55.4). This type of a lacinia is not homologous to the lacinia in the Lasiograptidae. Details of its construction are not available.
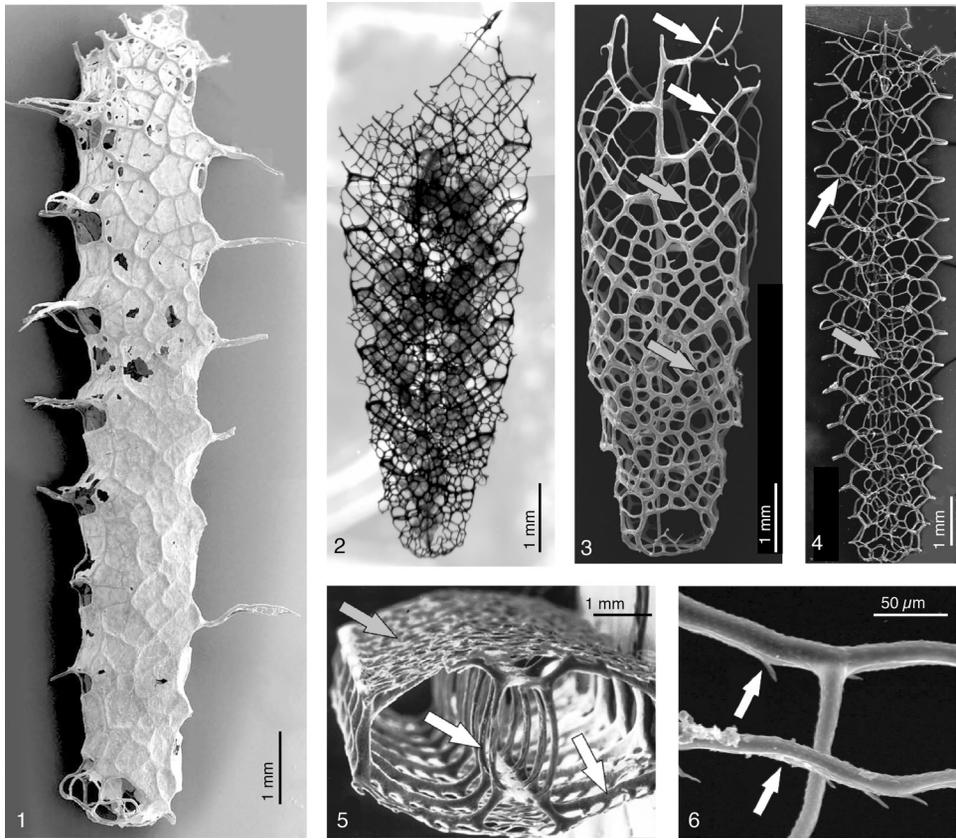
FIG. 54. Clathrium and reticulum. *1, Spinograptus clathrospinosus* (EISENACK, 1951), with preserved ancora sleeve membranes (Lenz & Kozłowska-Dawidziuk, 2002a, fig. 14,*7*); *2, Retiolites geinitzianus* BARRANDE, 1850, showing partial preservation of thecae (Maletz, 2008, fig. 1a); *3, Retiolites* sp., longitudinal view, SEM photograph (new); *4, Paraplectograptus simplex* (KOZŁOWSKA-DAWIDZIUK, 1995), (Lenz & others, 2012, pl. 2); *5, Retiolites* sp., cross section (new); *6, Paraplectograptus eiseli* (MANCK, 1918), enlarged view, showing seams and remains of fuselli in the thecal framework lists (new). *White arrows,* clathrium (*3–4*); *gray arrows,* reticulum (*3–5*); *arrows,* remains of fuselli (*6*).

LATE-STAGE AND GERONTIC MODIFICATIONS

A number of late-stage and gerontic modifications observable in the colonies can considerably change the colony shape and easily lead to misidentifications. They appear in large, supposedly mature tubaria and have never been found in juveniles. These features include the excessive development of cortical tissues in many benthic and a few planktic graptolites and also the resorption of structural details in mature colonies. The parasicula and parathecae or the strongly elongated proximal thecal spines of certain biserial graptolites may also be examples of gerontic development. The elongation of proximal spines and the virgella, although common in many biserial graptolites, does not add any new features to the tubaria and, thus, is not considered herein.

PARASICULA AND PARATHECAE

A colony feature first introduced in some early biserials is the parasicula (VANDEN-BERG, 1990), an apertural elongation of the sicula that forms a tube of various lengths, as illustrated by BULMAN (1947) in *Pseudoclimacograptus scharenbergi* (ELLES & WOOD, 1906). Based on the observations by LOXTON and others (2011) of an isolated specimen of *Appendispinograptus supernus* (ELLES &

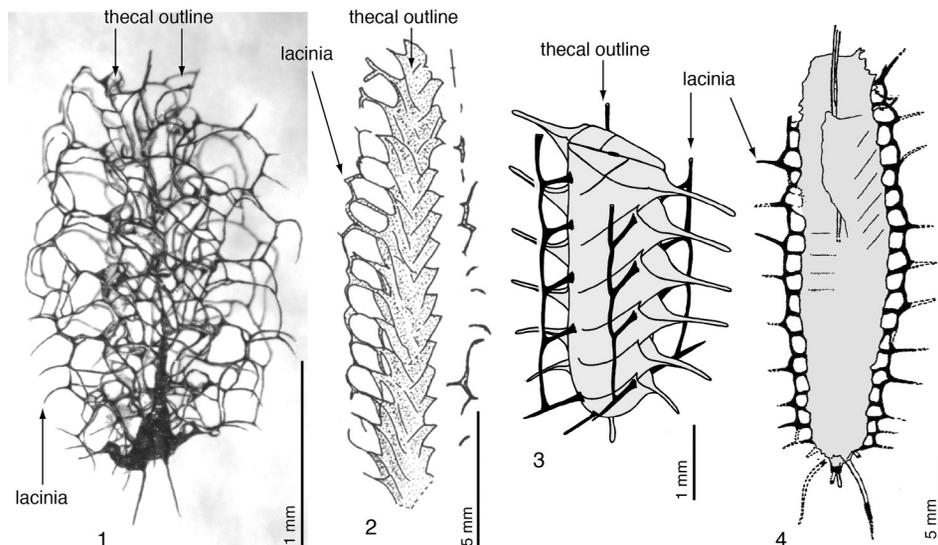FIG. 55. The lacinia. *1, Pipiograptus* sp., specimen showing a vague thecal outline and the extensive lacinia, sicula, and first theca completely sclerotized, Viola Limestone, Oklahoma, USA (new, photograph provided by Daniel Goldman); *2, Neurograptus margaritatus* (LAPWORTH, 1876a), specimen with sclerotized tubarium and lacinia (Williams & Bruton, 1983, fig. 24a); *3, Paraglossograptus* sp., reconstruction showing lacinia (new); *4, Paraglossograptus tentaculatus* (HALL, 1865), GSC 950b, syntype showing lacinia development and connection to lateral apertural thecal spines (adapted from Rickards, 1972, fig. 1a).

WOOD, 1906), the parasicula is comprised of narrow fuselli. The parasicular tube grows along the elongating virgella and may twist around it. A number of climacograptid species develop the parasicula as a species-specific character. MITCHELL, CHEN, and FINNEY (2007) recognized similar tubular extensions of the proximal thecal pairs and termed them parathecae (Fig. 53.6, Fig. 56). MITCHELL, CHEN, and FINNEY (2007) and, more extensively, VANDENBERG (1990) described the development of parasiculae and parathecae in a number of species of *Appendispinograptus* LI & LI, 1985 (Fig. 56.1–56.2, Fig. 56.4). The parasiculae and parathecae originated as tubular outgrowths along the virgella and the proximal thecae, respectively. In some species, these structures progressively grew into very long and robust spinelike structures as the colony matured. The earliest parasicula known is from the lower Darriwilian in the genus *Archiclimacograptus* MITCHELL, 1987 (MALETZ, 1997a).

A number of Lower Ordovician anisograptids (especially the Tremadocian genera *Ancor-*

agraptus and *Chigraptus*), certain Middle Ordovician sigmagraptines (*Perissograptus* WILLIAMS & STEVENS, 1988; *Maeandrograptus* MOBERG, 1892a), and Middle to Upper Ordovician nemagraptids, such as *Nemagraptus gracilis* (HALL, 1847), possess a long, free portion of the apertural part of the sicula that extends well below the lowest level of the thecae (Fig. 56.3). These bear some resemblance to the parasiculae of Ordovician biserials. However, in these taxa, the siculae are completely formed before the development of the stipes; and the free, projecting parts are not a late-stage addition to the colonies. These are not homologous constructions so should not be identified as parasiculae.

Other basal structures, which were probably progressively enlarged as the tubarium matured, include the large meshwork in *Climacograptus*? *baragwanathi* T. S. HALL, 1906 (Fig. 53.1); this is apparently an extension of the virgella and, thus, may be constructionally comparable to the ancora sleeve of the retiolitids. Another example of progressive proximal development is the
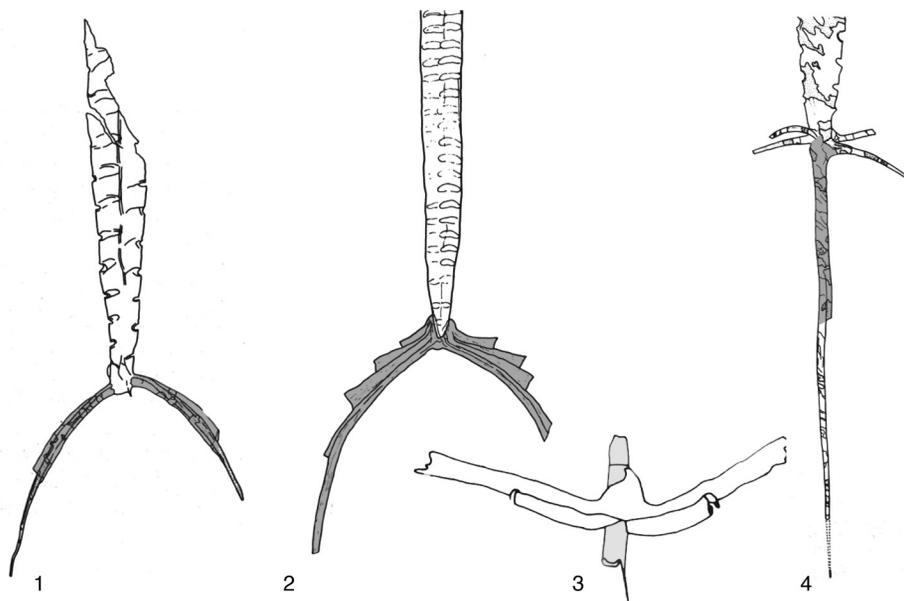
Fig. 56. Parasicula and parathecae. *1–2, Appendispinograptus longispinus* (Hall, 1902); *1,* with at least one pair of parathecae; *2,* mature tubarium with multiples of parathecae and long spine pairs (adapted from Riva, 1974a, fig. 4d); *3, Nemagraptus gracilis* (Hall, 1847), with sicula proximal region extending well below thecal level, and moderately long virgella (adapted from Finney, 1985a, fig. 12–11); *4, Climacograptus hastatus* (Hall, 1902) with multiples of spines, a very long virgella, and long parasicula (Riva & Ketner, 1989, fig. 9b). *Dark gray,* parasiculae and parathecae; *light gray,* sicula in *Nemagraptus.*

numerous spines at the sicula and the early thecae in *Comograptus comatus* Obut & Sobolevskaya in Obut, Sobolevskaya, & Merkureva, 1968 (Fig. 53.3). The development of the bulbous construction at the proximal end of *Climacograptus wilsoni* Lapworth, 1876a (Williams, 1994) appears to start from a short parasicula, but details are unknown. The round shape in most specimens suggests a vesicle of some kind.

CORTICAL OVERGROWTH

A thick cover of cortical tissue (Fig. 57) may cover important structural details in dendroid graptolites and is occasionally present in planktic taxa (Bates & others, 2011). Cortical overgrowth can be excessive in certain taxa and can completely occlude thecal apertures. In general, the cortical overgrowth is more pronounced in the proximal regions of the colonies and, thus, can be regarded as a late-stage or geronto-morph addition, but its secretion may start

early during the astogeny of the graptolite colony. The thecal development and form are completely obliterated in extreme cases, and only a vague outline of the colony shape remains. Therefore, the cortical overgrowth may influence considerably the appearance of the graptolites and provide problems for taxonomic identifications.

RESORPTION

Large parts of the siculae are lacking in mature stages of the colonies of a few species of planktic graptolites. This has been interpreted as a resorption of part or even all of the sicula or other parts of the colonies. One of the most impressive examples was represented by the lack of a visible sicula in the genus *Janograptus* Tullberg, 1880a. However, Albani and others (2001) argued that isolated specimens from the Table Head Group of western Newfoundland are actually regenerated stipes of extensiform dichograptids, and the genus *Janograptus* is
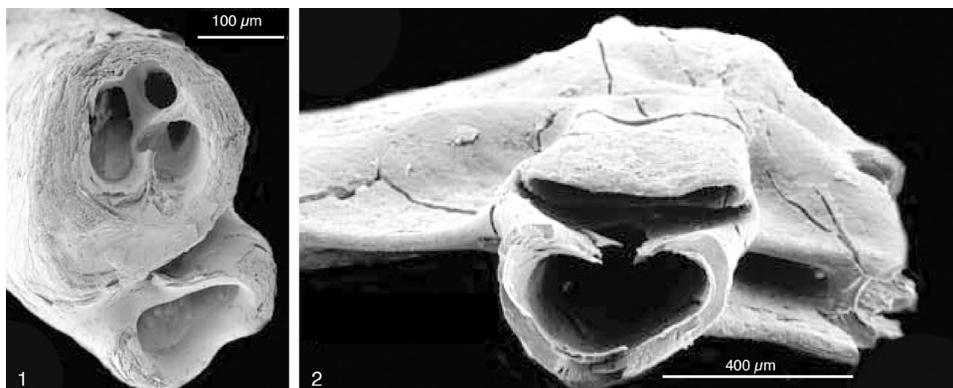
Fig. 57. Cortical overgrowth. *1, Dendrograptus* sp., broken end of stipe showing thecal cavities and excessive cortex development; *2, Amphigraptus* sp., view into thecal opening with thick cortical cover (Bates & others, 2011).

based on regeneration of stipes, a feature that becomes common only in slender Silurian monograptids (see discussion of regeneration and pseudocladia to follow).

A clear effect of resorption is the lack of a visible supradorsal part of the sicula in *Dicellograptus jonstrupi* HADDING, 1915a and related Upper Ordovician taxa (WILLIAMS, 1982a). Juveniles invariably had a complete sicula prominently exposed in the axil of the colony (Fig. 58.1), but the sicula is no longer visible in mature specimens (Fig. 58.2); moreover, the axil may show a slight bump in the horizontal, proximal part of the stipes only. Resorption of the apex of the sicula has also occurred in *Pleurograptus lui* MU, 1950a, from the Upper Ordovician of Nevada (ŠTORCH & others, 2011).

REGENERATION

Graptolite colonies, as all colonial organisms, possess a considerable capacity for regeneration of their damaged tissues and secreted housing structures (Fig. 59). Even though the regeneration of the soft tissue in fossil specimens is not preserved, the tubaria may convey considerable evidence of this capacity (KRAFT, 1926; BULMAN, 1932a; EISENACK, 1941b; URBANEK, 1958; RIGBY, 1994a). In isolated material, damage and repair is evident from unconformities of fusellar structures. Repair is common in juvenile siculae. Many have experienced damage; regeneration of nemata and partly missing prosiculae are common. Where damage occurred at a growing end of a colony (e.g., through breakage of part of the stipe), the zooids were able to regenerate and begin secreting new fuselli without changing the design of the colony. If the damage occurred in older parts of the colonies, cortical tissue was used to repair the tubarium, but normal fusellar tissue no longer developed. The repaired section was instead formed of a structureless film of material (BULMAN, 1970).

Malformation is also visible in graptolites. Biserials can lack the second stipe, as demonstrated from a specimen of *Dicaulograptus hystrix* (BULMAN, 1932a) in which the second stipe is abandoned after a single theca, whereas the first stipe continued to grow a number of thecae (BULMAN, 1932a, pl. 9,*9*). Others develop a third stipe, as described in *Orthoretiolites hami* WHITTINGTON, 1954 (BATES & KIRK, 1991). MALETZ (2003) described an isolated specimen of *Normalograptus scalaris* (HISINGER, 1837) with a typical biserial proximal end and a distal portion lacking a second stipe. In this specimen, a thick covering of cortical material covers the ventral and lateral sides of the uniserial part. The dorsal part does not have a cortical cover and is broken, suggesting a genetically determined control of the deposition of cortical material. Malformation is also apparent in the accidental development
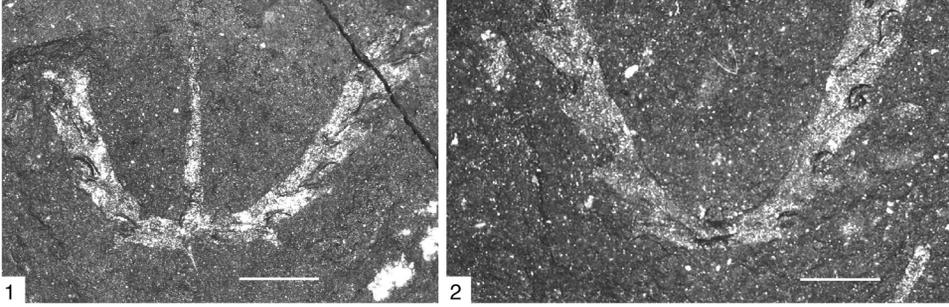
FIG. 58. Resorption in *Dicellograptus jonstrupi* HADDING, 1915a, Risebaeck, Bornholm, Denmark. *1,* LO 2689t, juvenile; *2,* LO 2690t, mature specimen, scale bars, 1 mm (new).

of a partly biserial monograptid that was described by URBANEK (1997a) from isolated material (Fig. 59.1).

A special case of regeneration is the development of pseudocladia (URBANEK, 1963) seen in some species of *Diversograptus* and *Linograptus*. Broken stipe fragments of many monograptids are able to regenerate a complete second stipe as a pseudocladium, producing a bipolar colony without a sicula. RICKARDS (1973a) illustrated a number of Silurian monograptid taxa from shale material, with bipolar colonies that lacked the presence of a sicula, but isolated specimens with evidence of regeneration are extemely rare and usually fragmentary.
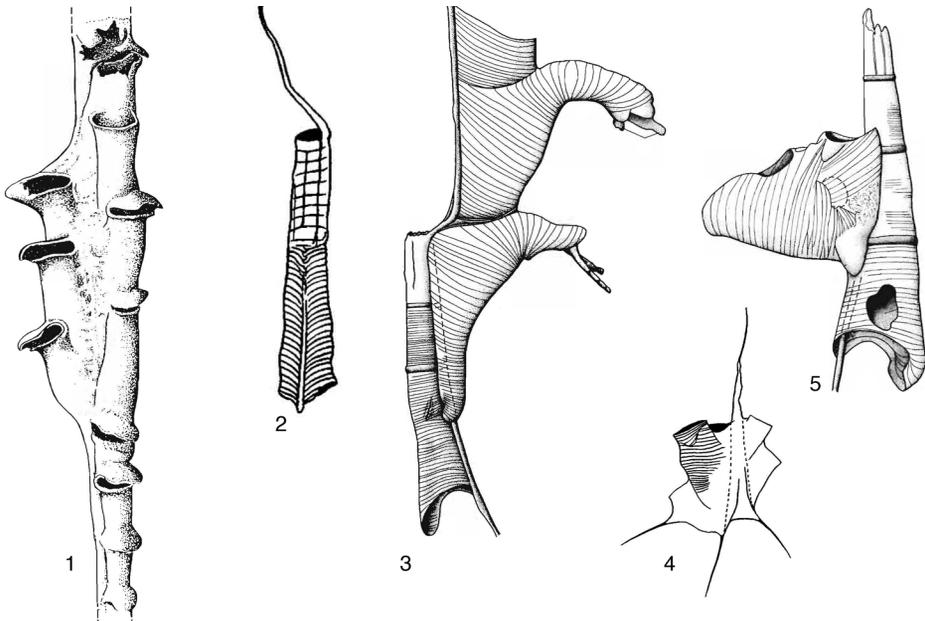
FIG. 59. Malformation and regeneration. *1, Slovinograptus balticus* (TELLER, 1966), abnormal development from uniserial to biserial, upper Silurian, Poland (Urbanek, 1997a, fig. 10); *2, Rectograptus gracilis* (ROEMER, 1861)*,* most proximal portion of prosicula missing (Bulman, 1970, fig. 47); *3, Uncinatograptus spineus* (TSEGELNIUK, 1976), damage to proximal part of sicula and subsequent offset regeneration, upper Silurian, Poland (Urbanek, 1997a, fig. 12); *4, Rectograptus gracilis* (ROEMER, 1861), regeneration of th2[1] (Bulman, 1970, fig. 47; based on Kraft, 1926, pl. 20); *5, Neocolonograptus lochkovensis* (PŘIBYL, 1940a), regeneration of th1 (Urbanek, 1997a, fig. 11).

HEMICHORDATE TAPHONOMY

Jörg Maletz

The investigation of taphonomy has long been neglected in the study of fossil Hemichordata, and the results of taphonomic processes are frequently underestimated. Therefore, misidentifications of pterobranch or graptolite specimens are common, as taphonomic features are repeatedly regarded as genuine taxonomic characters. The extremely poor fossil record of the Enteropneusta (see Maletz, 2014a) indicates that preservation is even more difficult in soft-bodied organisms. The taphonomical changes of a specimen start with the death of the organism and the beginning of the decay of its body. Nanglu, Caron, and Cameron (2015) investigated the decay of extant enteropneusts to understand the morphology and early evolution of this group and found some consistent patterns. Cameron (2016) used this information to interpret the early evolution of enteropneusts and to identify characters previously not recognized in fossil taxa (also see Cameron, 2018). Preservational aspects of the few fossil enteropneusts are largely unknown and details have not been investigated. The Burgess Shale species *Spartobranchus tenuis* (Walcott, 1911), as described by Caron, Conway Morris, and Cameron (2013) which represents the oldest known enteropneust taxon, is based on flattened carbonaceous compressions. It represents an extraordinary preservation, with a number of anatomical details not recognized in other fossil enteropneusts, in which only vague outlines were visible. The taphonomy of the closely related but commonly much smaller pterobranchs has been barely investigated, and little is known on the modifications introduced to the fossils during fossilization and weathering processes. Many features found in fossil graptolites can be shown to represent postmortem effects and the interaction of sedimentary, diagenetic, and metamorphic processes affecting the organic material. In the end, it may be impossible to identify a certain fossil as a pterobranch, as all characteristic features may have been lost.

Benthic graptolites may have been preserved *in situ* in the sediments of the environment in which they grew, but planktic graptolites lived in the water column. Thus, they invariably need to be interpreted as transported and deposited in environments other than the ones in which they lived and therefore represent death assemblages. This fact has considerable implication for the interpretation of graptolite taphonomy, as the formative first changes happened to the colonies even before burial in the sediment.

PRESERVATION POTENTIAL

The differences in the preservation potential of the various tissues of the graptolites leads to considerable influence on the decay processes and the degree of preserved anatomical details. Pterobranchs consist of three different parts: 1) the tubaria, the housing constructions secreted by the zooids from organic material; 2) the zooids made from soft organic tissues; and 3) the stolon system of the graptolites (except for the Cephalodiscida), a highly durable strand of organic material connecting the zooids. Within a few days, the graptolite zooids decay into unrecognizable remains (Briggs & others, 1995), and their fossil record is negligible. The presence of fossil zooids was claimed by Durman and Sennikov (1993) and Sennikov (2016) for the Middle Cambrian *Sphenoecium obuti* (Durman & Sennikov, 1993), preserving evidence of anatomical details, such as the soft and hard stolon and the body with the arms associated with the preserved tubarium, showing fuselli (Fig. 60.8–60.9). Surprisingly, the stolon system is largely lacking in this material, even though it should have been more durable (Beli, Piraino, & Cameron, 2017). Specimens of *Psigraptus* Jackson, 1967
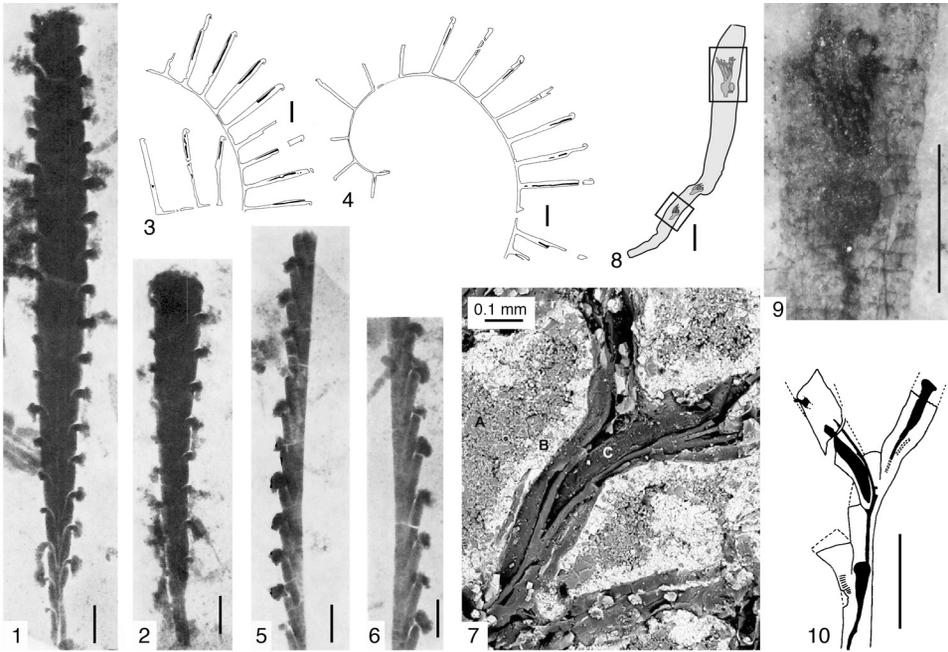
FIG. 60. Remains of fossil zooids and stolons. *1–2, Rhaphidograptus toernquisti* (ELLES & WOOD, 1906) showing pyritic clouds protruding from the thecal apertures (Bjerreskov, 1978, pl. 21); *3–4, Rastrites geinitzii* TÖRNQUIST, 1907, possible remains of the contractile stalk of the zooids in black (Loydell, Orr, & Kearns, 2004, fig. 3); *5–6, Pernerograptus revolutus* (KURCK, 1882), pyritic casts with pyritic clouds at the apertures (Bjerreskov, 1978, pl. 20); *7, Desmograptus micronematodes* SPENCER, 1884, relief specimen showing stolon system (Saunders & others, 2009, fig. 3); *8–9, Sphenoecium obuti* (DURMAN & SENNIKOV, 1993); *8,* drawing of thecal tube with possible remains of three zooids (Sennikov, 2016, fig. 3); *9,* possible zooidal remains (Sennikov, 2016, pl. 2); *10, Psigraptus jacksoni* RICKARDS & STAIT, 1984, fragment showing remains of zooids (Rickards & Stait, 1984, fig. 4i). Scale bars, 1 mm unless stated otherwise.

(RICKARDS & STAIT, 1984; RICKARDS, PARTRIDGE, & BANKS, 1991) (Fig. 60.10) and some Silurian monograptids (BJERRESKOV, 1978, 1994) may provide evidence of decayed zooids through the presence of mineral accumulations inside the tubaria and as cloudy patches in front of the thecal apertures (Fig. 60.1–60.2, Fig. 60.5–60.6). Anatomical details are not present in this material. Otherwise, pterobranch zooids are known exclusively from extant species, and their anatomy is well known (see *Introduction to the Class Pterobranchia,* p. 19–28).

The only parts of the original zooids that have a higher resistance to decay are the stolons of the graptolites, as decay experiments of *Rhabdopleura* ALLMAN in NORMAN, 1869a specimens indicate (BRIGGS & others, 1995; BELI, PIRAINO, & CAMERON,

2017). The preservation of the resistant stolon system is known to be common in benthic graptolites, and details are available for the Dendrograptoidea, as shown in *Desmograptus micronematodes* SPENCER, 1884 (SAUNDERS & others, 2009) (Fig. 60.7) and the Mastigograptidae (BATES & URBANEK, 2002). Isolated material of the stolon system of benthic taxa has been described as hydroid remains (see MIERZEJEWSKI, 1986; MALETZ, 2014b), and their identification still remains difficult. Stolons in planktic taxa have not been described in detail, but JACKSON (1967) and RICKARDS and STAIT (1984) illustrated pyritized stolonal remains in *Psigraptus* (Fig. 60.10), and HUTT (1974a) indicated the presence of a stolon system in *Adelograptus tenellus* (LINNARSSON, 1871). ZALASIEWICZ and others (2013) discussed a

stolon-like system in the planktic graptoloid *Dicranograptus* Hall, 1865 as an abnormal recalcitrant pectocaulus, but the material appears to represent remains of pressure shadow minerals in a poorly preserved and strongly tectonized graptolite. The described structures do not have any organic material and, thus, may not represent a stolon system. Loydell, Orr, and Kearns (2004) discussed the possible preservation of the contractile stalks (zooidal stalk of Maletz & Cameron, see Fig. 9, p. 18) in *Rastrites geinitzii* Törnquist, 1907 (Fig. 60.3–60.4) and *Neolagarograptus*? Štorch, 1998a from Latvia. The stolon system, however, is not preserved nor are the zooids. The remains are preserved as a two-dimensional film of organic carbon residues surrounded by an early diagenetic pyrite fill of the thecal tubes.The fusellum of the graptolite tubaria is comprised of an organic compound, probably collagen (Towe & Urbanek, 1972; Crowther & Rickards, 1977; Runnegar, 1986), but details on the biochemical composition are not available (Foucart & others, 1965; Florkin, 1969; Sewera, 2011). The tubaria of extant pterobranchs are light brown to completely translucent. In some cephalodiscid taxa, foreign material may be incorporated in the tubarium formation (Harmer, 1905; Harmer & Ridewood, 1913). Fossil graptolites are usually dark brown to black (Fig. 61.1–61.5), indicating some compositional modification through the fossilization processes. Sometimes, specimens are lighter brown and partly translucent, indicating their fusellar composition in shale material (Fig. 61.5), but this preservation may, in part, be due to subsequent weathering.

DECAY

The tubes of extant *Rhabdopleura* begin to show signs of decay after four days in oxic environments, as actuo-paleontological data demonstrate (Beli, Piraino, & Cameron, 2017), but the tubaria remained largely unchanged within the sediments for hundreds of millions of years, as observed in chemically isolatable specimens. These were originally regarded as representing the animals themselves, but are now understood to be the housing constructions (Mitchell & others, 2013; Maletz, 2014b) formed from individual fuselli (e.g., Crowther, 1981; Andres, 1961, 1977, 1980). It is clear that the preservation of graptolite tubaria under oxic conditions is quite limited, and most fossil graptolites are preserved in dysoxic or anoxic sediments or have been entombed in the sediments and protected from the damaging effects of oxigenated organic decay.

Graptolites may be part of the marine snow and the clingfilm preservation (Jones, Zalasiewicz, & Rickards, 2002) described for *Spirograptus turriculatus* (Barrande, 1850) and may be more widely distributed, even though difficult to demonstrate. Even though organic material may be eaten by predators, this has rarely been confirmed for graptolites (Underwood, 1993; Loydell, Zalasiewicz & Cave, 1998). The sinking of planktic graptolite colonies may have been retarded through the decay of the zooids, leading to uplift from decay gases. Eventually, however, they started settling through the water column, and the tiny zooids would have likely disappeared by the time their tubaria reached the seafloor. Once there, the tubaria would have been exposed to microbial attacks and damage by burrowers and grazers. Fine hash consisting of graptolite fragments is common worldwide, indicating considerable destruction and fragmentation of the tubaria prior to final burial. This process may be interpreted as bioturbation and/or scavenging within unlithified sediments containing abundant graptolite specimens. Present day microbial destruction may even occur in organically preserved, chemically isolated material in fossil collections (see example in Fig. 62.3). Radzevičius, Schopf, and Kudryavtsev (2013) described possible fossil bacteria on the tubarium surface of Silurian monograptids, forming spherical and spirally coiled structures.
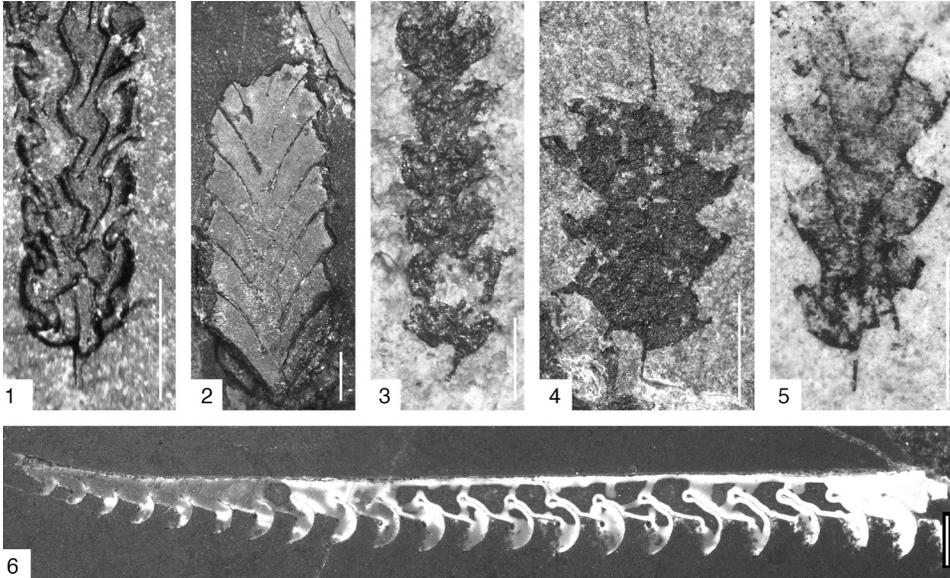
FIG. 61. Graptolite preservation. *1, Archiclimacograptus* MITCHELL, 1987 sp., full relief, Darriwilian, western New-foundland, Canada (new); *2, Petalolithus palmeus* (BARRANDE, 1850), LO 1116t, full relief, pyrite fill, polished section, Tomarp, Sweden (new); *3, Levisograptus sinicus* (MU & LEE, 1958), SMF XXIV 424, partial relief, Karga Village, southern Urals, Russia (new); *4, Orthograptus quadrimucronatus* (HALL, 1865), GSC 139251, flattened, L'Egaré Motel, Quebec, Canada (new); *5, Rectograptus gracilis* (ROEMER, 1861), SMF 75826, flattened, showing fuselli, Maquokea Group, Graf, Iowa, USA (new); *6, Monograptus priodon* (BRONN, 1835), SMF XXIV 401, silica coating in chert, Schnebes, Frankonian Forest, northern Bavaria, Germany (new). All scale bars, 1 mm. Color images available, *Treatise Online* 110.

There are several ways in which the decay of a graptolite tubarium can be stopped or at least slowed down. Retardation of decay may occur through early lithification of the host rock. Paleozoic limestones commonly bear well-preserved graptolites, which are supposedly entombed in the rock through early lithification of the lime mud, sheltered from a destructive oxic environment. Preservation in a dysoxic to anoxic environment is another way of delaying the decay of organic material. This is how most graptolites were preserved, and the often-used term, graptolite black shale, reflects this preservation. However, the common occurrence of graptolites in black shales does not indicate an environment in which graptolites flourished (COOPER & others, 2017).

DEPOSITION AND BURIAL

A number of processes that modify graptolites before they are entombed in the sediments indicate that their behavior should be regarded as similar to that of sediment particles. Post-mortem transport is commonly demonstrated in graptolite tubaria. Depending on the water current pattern, tubaria of planktic graptolites may either sink vertically down onto the sediment surface or experience a variable lateral displacement. Transport from shallow water regions into deep-water basinal regions appears to be common, exhibited exemplarily by the toe-of–slope environment in which the Lower to Middle Ordovician graptolites of the Cow Head Group in Newfoundland were preserved (WILLIAMS & STEVENS, 1988, 1991) and in which fragmented specimens of benthic graptolites are also common.

Graptolites can be randomly distributed in a sediment pile or current aligned (HUNDT, 1935b; MOORS, 1970; COOPER & others, 2017), showing postmortem transport. It is not clear whether premortem

transport in the water column can also lead to alignment on the sediment surface, but it is unlikely in the case of planktic taxa. Current transport may, however, be a reason for the death of the colonies, in which case the alignment is only the final result of transport into unsuitable environments and subsequent death and settlement of the dead colonies. Graptolites are found in turbidites and tempestites (HILLS & THOMAS, 1953; SCHLEIGER, 1968; MOORS, 1969, 1970) and even in bentonite beds (MITCHELL, BRUSSA, & ASTINI, 1998), indicating a possible transport as living organisms caught in water turbulences and, on occasion, trapped in volcanic ash.

Time averaging (KIDWELL & BOSENCE, 1991) may be common in areas of low sediment accumulation rates, causing high concentrations of taxa that were not living in the same environment or at the same time in suitable environments (COOPER & others, 2017). Time-averaged faunas may also indicate a quite variable preservation, because specimens deposited earlier on the sediment surface may already have partly decayed before the latest specimens arrived on the seafloor and before the specimens were covered by a new layer of sediment. Time averaging is most prominent in regions with very low sediment input, commonly in pelagic and hemipelagic sediments, but may also be present in shelf regions with low sediment input.

Benthic graptolites may be covered by layers of sediment and preserved *in situ* (e.g., BOUČEK, 1957; ERDTMAN, 1976), but in most cases their fossil remains represent fragments transported from shallow shelf regions into deeper water environments (MALETZ, 2006), where they may be found in association with numerous planktic taxa (e.g., HALL, 1865). However, quite a number of well-known planktic graptolite faunas are not associated with benthic taxa. There are barely any benthic graptolites associated with the famous Ordovician graptolite faunas of the Tøyen Shale and Elnes formations of Scandinavia (MONSEN, 1937;

MALETZ, 1997a; MALETZ & EGENHOFF, 2005) or the Silurian faunas of Thuringia, Germany (SCHAUER, 1971).

Reworking is expected to have been rare or even impossible in graptolites, as the tubaria may easily break into pieces when exhumed from a sediment. Transport, thus, was restricted to recently deceased colonies and likely records a secondary depositional site. However, transport of graptolites in clasts of resistant rock types is more common. The best examples are from the glacial erratic boulders of Scandinavian origin in northern Germany and Poland (ROEMER, 1861; HEIDENHAIN, 1869; KRAFT, 1926; EISENACK, 1951; URBANEK, 1958; MALETZ, 2008, 2010a; RADZEVIČIUS & others, 2010; MALETZ & SCHÖNING, 2017). Here, Ordovician and Silurian graptolites occur in sediments deposited during the Pleistocene glaciations. A Paleozoic example of transport of graptolites in clasts appears in the Daniel's Harbour conglomerate of western Newfoundland (WHITTINGTON & RICKARDS, 1969; STENZEL, KNIGHT, & JAMES, 1990). Reworked clasts of the Table Cove Formation occur in this conglomerate bed, bearing a graptolite fauna that is out of place and older than the conglomerate and the surrounding sediments of the American Tickle Formation. A good example of larger scale transport is the olistostromes of the allochthonous Dauphin Formation of the Hamburg succession of Pennsylvania, USA, which have been tectonically moved twice. Boulder to kilometer-sized masses containing an Early Ordovician graptolite fauna of slope origin were first transported to a Middle Ordovician trench and encased within a clastic matrix containing a Darriwilian fauna. Tectonic slices of the trench sequence were then structurally transported to the Martinsburg foreland basin during the Taconic orogeny in the Sandbian (GANIS, WILLIAMS, & REPETSKI, 2001; GANIS, 2005).

During transport, the graptolite tubaria may have experienced bending and breakage, especially in long and robust taxa, but slender forms remained more flexible. EISEL (1908) and HUNDT (1910, 1951b)

already described the influence of tectonic deformation in kinked monograptid taxa, thus, indicating the possibility of bending of tubaria without breakage. Bent specimens were, however, rarely illustrated or mentioned (for an exception, see HABER-FELNER, 1931, pl. 1,*19b*). Fragmentation may be more common, but astonishingly large, thought to be complete specimens have been described, such as *Paratemnograptus magnificus* (PRITCHARD, 1892) with an estimated diameter reaching nearly one meter and an incompletely preserved specimen of the straight monograptid *Stimulograptus halli* (BARRANDE, 1850), with a length of 1.45 m (LOYDELL & LOVERIDGE, 2001).

POST-BURIAL MODIFICATIONS

Graptolite tubaria need to be covered within the sediment before stabilization and protection from decay can be established, because they are quite vulnerable to organic decay and destruction when exposed on the sediment surface. After they are covered by a layer of sediment, other factors begin to play a role in the preservation of these seemingly very delicate fossil remains.

Graptolites can be preserved in sediment in full relief (Fig. 61.1) or partly flattened (Fig. 61.3) through infilling with sediment or diagenetic mineral growth before the compaction, leaving the three-dimensional construction still recognizable. Specimens fully preserved in relief may have little outward detail, but slight compaction can reveal the median septum and thecal septae in axonophorans (Fig. 61.1). Early formation of carbonate concretions prevented the compaction of graptolite colonies in many places. Most notably are the beautifully preserved Llandovery, Silurian graptolites in the Kallholn Shale of Dalarna, Sweden (HUTT, RICKARDS, & SKEVINGTON, 1970; LOYDELL, 1991b; LOYDELL & MALETZ, 2004, 2009); Arctic Canada (e.g., LENZ & KOZŁOWSKA, 2006; LENZ & MELCHIN, 1987; MELCHIN, 1998); and the glacial erratic boulders of Scandinavian origin mentioned earlier, all of which represent carbonate concretions.

The first post-burial diagenetic effects on the graptolite tubaria are related to the compaction and dewatering of the surrounding sediment, leading to flattening of the specimens. Because the graptolite tubaria are made from flexible organic material, flattening within the sediment usually does not cause noticeable effects such as breakage and fractures, but certain other effects of deformation, such as shape distortion, may be noticeable (BRIGGS & WILLIAMS, 1981; WILLIAMS & others, 1982). Flattened graptolites are preserved as thin films of organic material in which only the outlines of the colonies are apparent (Fig. 61.4). Thus, several layers of organic material of the originally three-dimensional fossil (Fig. 61.1) can be superimposed so that thecal outlines, sicular shape, and other features become compressed into a relatively thin, difficult to untangle, layer. Even with IR photography or through chemical bleaching of the specimens, most details cannot be recovered (BATES, MALETZ, & ZALASIEWICZ, 2015). Flattened specimens chemically isolated from shales may preserve their fusellar structure (Fig. 62.1), but also have considerable crumbling of the fusellum without breakage (Fig. 62.2).

Although evidence of chemical alteration of the organic material of the tubaria is problematic, it is to be expected. The dark color of most fossil material reveals an incipient alteration, at the very least. GUPTA, BRIGGS, and PANCOST (2006) indicated the presence of aliphatic polymers and lack of proteins in fossil graptolites. Various authors have supposed that the material was originally collagen (TOWE & URBANEK, 1972; BUSTIN, LINK, & GOODARZI, 1989), modified by *in situ* polymerization.

Graptolite tubaria preserved in three dimensions can be filled with various mineral material. Pyrite (Fig. 61.2) is the most common mineral infilling graptolites and can lead to beautiful golden shimmering casts when the covering fusellum is lost. WILLIAMS (1990b) described winnowed beds of three-dimensional pyritic graptolites originally formed as internal casts from the Young-
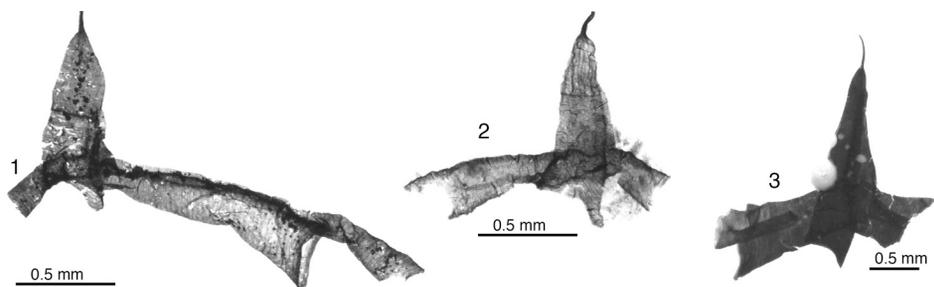
FIG. 62. Flattened graptolites from shales. *1,* Sigmagraptine indet., GSC 140110, showing fusellar construction and prosicula with longitudinal rods, Table Head Group, western Newfoundland; *2,* Sigmagraptine indet., GSC 140111, showing fusellar construction and considerable crumpling, Western Brook Pond, Cow Head Group, western Newfoundland, Canada; *3, Tetragraptus* SALTER, 1863a sp., SGU 9621, specimen showing contemporary fungus growth, Skattungbyn, Dalarna, Sweden. All specimens flattened, chemically isolated from shales, bleached (new). Color images available in *Treatise Online* 110.

sters Gulch Member of the Powers Steps Formation from Bell Island, Newfoundland, Canada. The presumed origin of the pyrite was early diagenetic, sulphide-rich conditions in a prodelta environment that also replaced associated oolites; BJERRESKOV (1991) recognized incomplete infilling with geopetal orientation and pyritic stalagmites and stalactites in Silurian monograptids. The pyrite fill may be weathered to oxides of various colors and the spectacular pink to white examples of *Cymatograptus bidextro* TORO & MALETZ, 2008 are a good example. Phosphatic casts are rare, but have been described for *Climacograptus putillus* (HALL, 1865) from the Elgin Member of the Maquoketa Formation at Graf, Iowa (WERNER & ECHOLS, 1958; GOLDMAN & BERGSTRÖM, 1997). MALETZ and STEINER (2015) discussed the preservation of the Middle Cambrian *Sphenoecium wheelerensis* MALETZ & STEINER, 2015 and noted a lack of organic material. Thus, they interpreted the remains as a replacement of the fusellum with clay minerals, which could be a secondary development due to weathering processes and not a replacement within the sediment.

A replacement of the graptolite tubaria has repeatedly been noted, but appears to be a misinterpretation in most cases. A closer look at the material usually shows a mineral infill or coating of the tubarial walls. A number of papers described silicified graptolites from Silurian chert pebbles

of Germany found in various secondary deposits of glacial or glacio-fluvial origin (HUNDT, 1934, 1946, 1957b; RICHTER, 1948, 1951; MÜNCH, 1951; HORSTIG, 1952). These graptolites actually have internal and external coatings of silica (Fig. 61.6) forming a thin crust around the tubarium (GREILING, 1958). MALETZ (2009) described another instance of silica-coated graptolites from the Middle Ordovician of Quebec, Canada. The specimens possess an irregular mass of silica around the tubaria, keeping the colonies intact when the graptolites were chemically isolated from the limestones. They were, apparently, already somewhat distorted tectonically, before the silica was formed around them. It is not known whether the specimens are also filled with silica. Silica also replaced the biomineralized shells of ostracods in the samples.

The thermal alteration of the graptolite fusellum is known in some detail as a result of the investigation of coalification of organic material to understand the potential for oil and gas generation of graptolite-bearing rocks. This alteration can be regarded as essentially similar in its geological behavior to cuticles of arthropods or to plant tissues. The effect of the thermal alteration is, therefore, similar to the coalification of plant material and can even be compared and correlated with the Color Alteration Index for conodonts (EPSTEIN, EPSTEIN, & HARRIS, 1977; HARTKOPF-FRÖDER & others, 2015).

The material changes considerably in its optical properties (Teichmüller, 1978; Goodarzi, 1990; Hoffknecht, 1991; Inan & others, 2016; Schmidt Mumm, & Inan, 2016). Unaltered fossil graptolite material has a dark brown to black color (Fig. 61.1, Fig. 61.3–61.5) that changes with increasing maturation to an intense silvery shine (Fig. 63.1) that may have been mistaken as a pyritization in the past. This is typical of many graptolite faunas of Scandinavia that were affected by regional or local contact metamorphism. The organic material of the graptolite tubaria disappears completely at a moderate to high metamorphic rank but casts may still be recognizable, such as in schists. In these cases, flattened graptolites would have been destroyed without a trace. Graptolite remains may be able to survive considerable alteration; Dieni and others (2005) described identifiable graptolites from boudins in a greenschist unit in the eastern Alps of northern Italy. The material does not have any discernible tectonic deformation. Greenschist-grade metamorphism can also occur in the sediments yielding early Darriwilian graptolites at Bratland in the Gausdal region of Norway (Lapworth, 1906; Williams, 1984).

DEFORMATION AND RETRODEFORMATION

The morphology of most fossil groups is susceptible to shape distortion from structural deformation in the rock body in which they are found. This, of course, can affect graptolites, sometimes dramatically, and was recognized early. Ironically, the distortion of fossils can assist the structural geologist in kinematic analysis if the undeformed shape of the fossil is known for comparison. Graptolites have been frequently used in this endeavor. Conversely, kinematic analysis can assist the paleontologist in retrodeformation of deformed fossils. Techniques for these procedures have advanced from relatively simple to highly technical. Eisel (1908, p. 219) discussed the deformation of graptolites and the influence on the taxonomic

identification of the material. He used a black rubber layer on which he drew the specimens and then imitated the distortion by pulling the material in various directions. Various methods have subsequently been used to understand graptolite deformation (Hills & Thomas, 1944; Jenkins, 1987; Cooper, 1970, 1990; Williams, 1990a).

A closer look at graptolite deformation shows that the effects are more severe and do not just concern the taxonomic identification of the material. The graptolite specimens are distorted with the tectonic deformation of the encasing sediments. This deformation may be dramatic as demonstrated by the changes in dimensions described by Maletz and others (1998) from Albania and is known from the classic locality of the Wenlock graptolites at Goni, Sardinia, Italy (Gortani, 1922). The direction of deformation can have considerable influence on the appearance of the graptolite specimens as the example of *Spirograptus turriculatus* indicates (Fig. 64.2). Specimens with a wide and low cone are associated with ones having narrow and high cones. On closer examination, the graptolite fusellum shows parallel lines of fractures (Fig. 64.1,Fig. 64.5), indicating the tectonic deformation if the organic material is still preserved and recognizable (Mitchell, Brussa, & Maletz, 2008). Characteristic and easily recognizable tectonically deformed graptolites are preserved as pale mineral films on black shale (Fig. 64.4). In these cases, the graptolites are clearly outlined and provide strong contrast to the surrounding dark sediment. These mineral films can be identified as phyllosilicate minerals growing as pressure shadow minerals around the organic remains of the graptolites (Underwood, 1992). Typically, the organic material of the graptolites is preserved in unweathered specimens. The mineral films can be of various colors, from whitish to yellow and orange, and light green to blue, depending of the composition of the minerals and the amount of weathering. The minerals are often loosely termed chlorite-group minerals and were
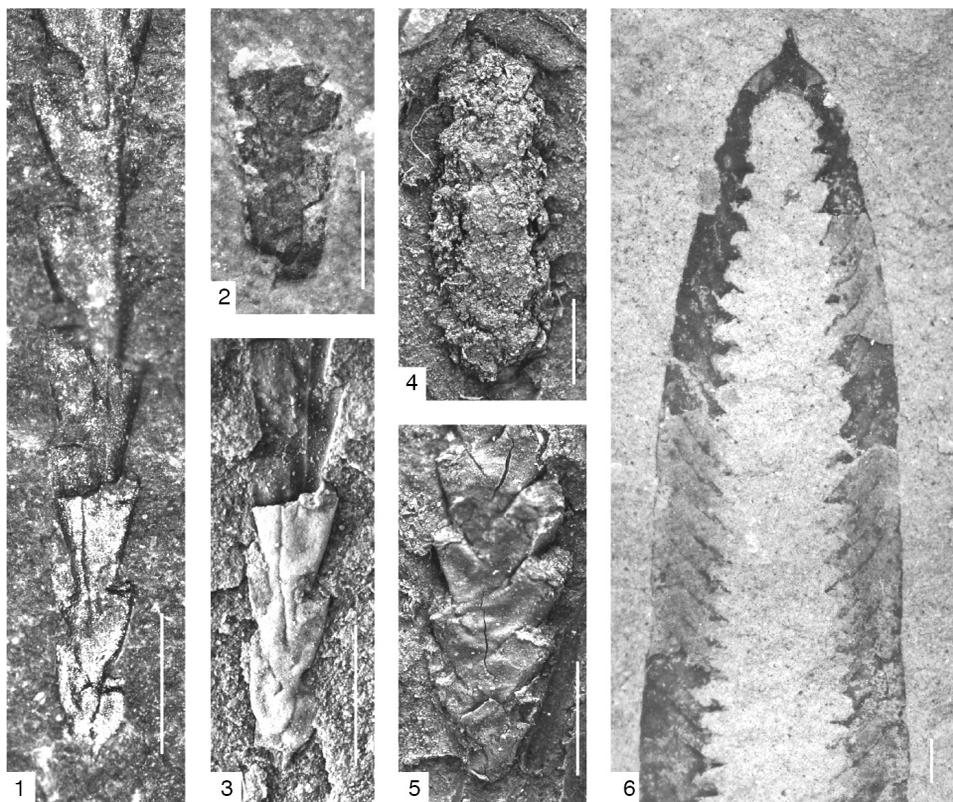
Fig. 63. Weathering. *1, 3, Pronormalograptus antiquus* (Ge in Ge, Zheng, & Li, 1990), PMO 234.061, preserved in relief, Elnes Formation, Slemmestad, Norway; *1,* showing highly coalified, silvery shining fusellum; *3,* same specimen coated with ammonium chloride to highlight structure; *2, Normalograptus mohawkensis* (Ruedemann, 1912), GSC 139252, low relief, weathered pyritic cast with preserved dark fusellum, L'Egaré Motel, Quebec, Canada; *4–5, Pseudorthograptus cyperoides* (Törnquist, 1897), Tomarp, Scania, Sweden; *4,* LO 1294T, strongly weathered pyritic cast; *5,* LO 1296t, weathered pyritic cast, surrounding fractured fusellum; *6, Didymograptus murchisoni* (Beck in Murchison, 1839), SMF 75827, flattened, weathered, Darriwilian, Jordan, exact locality unknown; all scale bars, 1 mm (new).

regarded as replacement of the graptolites in earlier literature. Richter (1853) originally described them as fibrous, silvery white to greenish minerals from the Silurian of Thuringia, but Geinitz (1852) had already termed the material talcum. Gümbel (1868) described the mineral as a pyrophyllite and compared it with the minerals surrounding many Carboniferous plant fossils. Kobell (1870) described the mineral as gümbelite, but this name has rarely been used in the scientific literature.

The scanning electron microscope backscatter method (BSEM) can easily differen-tiate the films of pressure shadow minerals from the organic material of the graptolite fusellum (Fig. 64.5), which is difficult to see with the unaided eye (Fig. 64.6). Even in deeply weathered material, the tectonic lineation or foliation may provide clear evidence of deformation of a graptolite (Fig. 64.3). In this specimen, the fusellum is not preserved and the reddish material represents iron-stained pressure shadow minerals.

WEATHERING

Weathering effects (Fig. 63, Fig. 64) have rarely attracted attention in graptolite
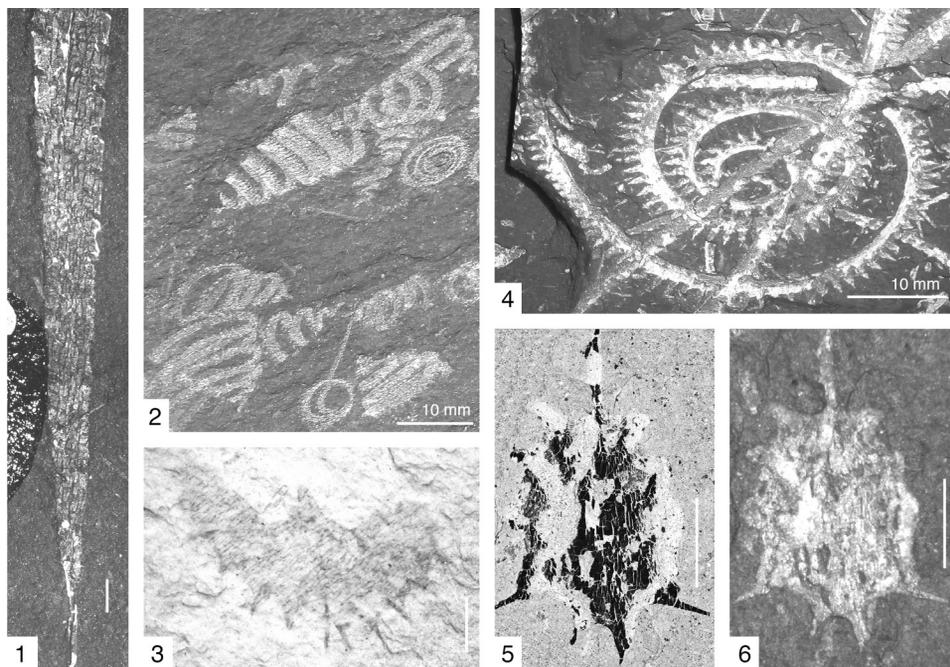
FIG. 64. Deformation and weathering. *1, Normalograptus rectangularis* (M'COY, 1850), SMF XXIV 350, flattened, strongly tectonically distorted, showing parallel fractures in fusellum, Ölsnitz, Voigtland, Germany; *2, Spirograptus turriculatus* (BARRANDE, 1850), SMF XXIV 328 (acquired through exchange from Hemmann), flattened, tectonically distorted, zone 15, locality unknown, Hemmann collection; *3, Arienigraptus angulatus* (MU, GEH & YIN, in MU & others, 1962), SMF 75825, flattened, tectonically distorted and weathered, Wellsford Riffle Range, east of Bendigo, Victoria, Australia; *4, Oktavites spiralis* (GEINITZ, 1842), SMF PK 767, flattened, showing high amount of pressure shadow minerals (white), Grobsdorf, Thuringia, Germany; *5–6, Nanograptus phylloides* (ELLES & WOOD, 1908), paratype, GSE 5495; *5,* BSEM photo showing preserved fusellum in black; *6,* normal light photo, showing light color of fusellum and pressure shadow minerals in contrast to dark sediment; all scale bars, 1 mm, unless stated otherwise (new). Color images (*1, 3*) available in *Treatise Online* 110.

research, even though it is obvious in many graptolite specimens. Black shale may weather to a light grey, yellow, or even whitish color, and the organic material of the graptolites in these cases show a strong contrast, whereas in fresh material they are barely visible. Red iron staining may also be common in specimens and on pressure shadow minerals (Fig. 63.6). Surface weathering of strata or the mineral infilling of the tubaria can degrade or destroy graptolite specimens.

Pyrite weathering (Fig. 63.2) may destroy beautiful relief specimens in short time and even affect material in collections as pyrite disease (BIRKER & KAYLOR, 1986; NEWMAN, 1998) (Fig. 63.4–63.5). Weathering of pyritic casts may lead to the formation of reddish to yellow iron minerals or staining of the sediment surface (Fig. 63.2). Weathering is independent of tectonic deformation and both factors may be difficult to separate in seemingly well-preserved material.

PALEOECOLOGY OF THE PTEROBRANCHIA (CEPHALODISCIDA AND GRAPTOLITHINA)

Roger A. Cooper, Sue Rigby, Denis E. B. Bates, and Jörg Maletz

INTRODUCTION

The Pterobranchia is a widely distributed group of marine colonial organisms with its acme during the early Paleozoic and a few surviving, extant members. The modern taxa are all benthic and live in waters ranging from shallow-coast to deep-marine environments. Consequently, they are of limited use for interpreting the ecology of the extinct planktic Graptoloidea. Nevertheless, the living pterobranchs provide us with important information on the soft-body anatomy of the Pterobranchia that is not available from fossil taxa. The comparison with the modern pterobranchs enables us to reconstruct graptolites as living entities and better understand their biology, including their feeding and tubarium secretion.

Most of the work on graptolite ecology has been directed toward the planktic faunas, and little is known about benthic graptolite ecology. This imbalance sources from a primary focus on the planktic taxa because of their exceptional biostratigraphic utility and the fact that benthic faunas are rarely preserved in their original environments. The following account is based largely on Cooper and others (2012).

LIFE MODE

The Pterobranchia can easily be differentiated into benthic (sessile) and planktic taxa, and interpretation of their lifestyles is based on this knowledge. Benthic taxa have an elongated dome as the initial part of the colony, as in *Rhabdopleura* Allman in Norman, 1869a or *Epigraptus* Eisenack, 1941a (Fig. 65.1–65.2) or a tubular sicula with a flat base for attachment, as in *Dendrograptus* Hall, 1858 and related taxa (Fig. 65.3, Fig. 65.5). In encrusting taxa, the ventral parts of the tubarium adhere to the substrate, whereas the erect, bushy, or tree-like colonies have a specialized structure—a holdfast of varied shape. However, the attachment mode is known from relatively few taxa. In erect-growing Graptolithina, the attachment structure may be rootlike or disk-shaped, but it is invariably a surface attachment feature (Fig. 65.4) and does not extend into the sediment as a root system. All nematophorous graptoloids can be interpreted as planktic (Bulman, 1970; Fortey & Cooper, 1986). They possess a free nema and do not show any indication of attachment (Fig.65.6).

Since benthic graptolites are rarely found *in situ* with their attachment intact, the attachment mechanism is little understood. The erect *Mastigograptus* aff. *tenuiramosus* (Walcott, 1883) is known to have overgrown calcitic shells, as indicated by the features of an attachment disk (Bates & Urbanek, 2002), which indicates the need for a solid surface for attachment. Also, the benthic *Rhabdotubus johanssoni* Bengtson & Urbanek, 1986, may be attached to shell, adhering to the phosphatic shells of the small brachiopods *Acrothele* Linnarsson, 1876 and *Dictyonina* Cooper, 1942, and, more rarely, to trilobite fragments. Rarely, benthic encrusting taxa have been found *in situ* (e.g., Mitchell, Wilson, & St. John, 1993). Most examples of encrusting material have been obtained from chemically isolated material (e.g., Kozłowski, 1949). Erdtmann (1976) described dendroid faunas supposedly preserved *in situ* in the Mississinewa Shale of Huntington, Indiana, USA, as occurring under low-oxygen, low-energy conditions within the photic zone (less than 60 m deep). Some of the specimens appear to be in growth position, but others clearly indicate at least minor transport because of their lateral orientation on the shale surfaces.
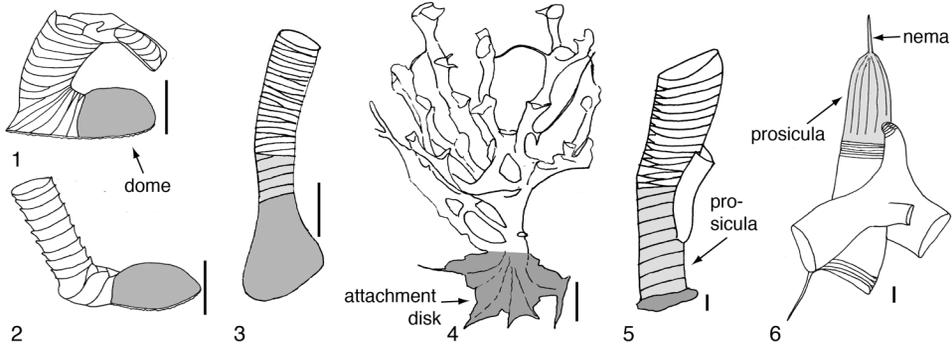
Fig. 65. Sicular development and attachment. *1, Epigraptus* sp. (adapted from Kozłowski, 1971, fig. 1); *2, Rhabdopleura compacta* Hincks, 1880b (adapted from Stebbing, 1970a, fig. 3); *3, Kozlowskitubus erraticus* (Kozłowski, 1963) (adapted from Kozłowski, 1971, fig. 5); *4, Dictyonema cavernosum* Wiman, 1896a with attachment disk (adapted from Wiman, 1896a, pl. 1, fig. 1); *5, Dendrograptus communis* Kozłowski, 1949, tubular prosicula (adapted from Kozłowski, 1949, fig. 1); *6, Xiphograptus* sp., showing prosicula with free nema (new). Scale bars, 0.1 mm in *1–3, 5–6;* 1 mm in *4.*

The Graptoloidea, as a planktic group of the Graptolithina, have long been recognized as an important component of the Paleozoic plankton (e.g., Lapworth in Walther, 1897; Bulman, 1964, 1970; and many others). However, interpretation of the graptoloid habitat within the Paleozoic oceans has proved difficult, and a variety of habitat models have been proposed (see Cooper & others, 2012). Fundamental to all models is the observed distribution of graptoloids in a range of bio- and lithofacies representing all depositional depth zones, from shallow shelf (inshore) to open ocean. Evidence from morphology, inferred feeding mode, and facies preference suggests that graptoloids were able to control the depth at which they lived in the water column, either actively or passively by buoyancy adjustment (Rigby & Rickards, 1989). In other respects, however, graptoloids were largely passive occupants of the water mass in which they lived, and drifted with the ocean currents, both seasonally and as part of the ocean circulatory system. Thus, new species were able to disperse widely and rapidly around the world and establish themselves in new regions.

LOCOMOTION

Benthic graptolites obviously were not actively moving, but their dispersal by means of planktic larvae in extant taxa (e.g.,

Rhabdopleura, Cephalodiscus M'Intosh, 1882) provides a mechanism for their wider geographical distribution. In graptoloids, tubarium structures such as spines, vesicles, or nematularia, and a disk-shaped or netlike colony form have been interpreted as hydrodynamic drag structures and evidence for a passive mode of life (Rickards, 1975; Finney, 1985b; Finney & Jacobson, 1985). However, ecological models for the planktic graptoloids now generally assume that they were able to move relative to the water mass in which they lived, particularly for feeding efficiency. Among the movement mechanisms suggested are turbulence, buoyancy control, and active swimming. Wind turbulence was no doubt significant for graptoloids living in the surface waters of the ocean (Rickards, 1975), but it is unlikely that all species lived in this zone. Models of movement by buoyancy control through gas buildup require extrathecal soft tissue (Bulman, 1964; Rickards, 1975; Finney, 1979), which is incompatible with the pterobranch zooid model (Crowther & Rickards, 1977). Automobility of the tubarium by ciliary propulsion was suggested by Kirk (1969, 1972a, 1972b) and Bates and Kirk (1986). Bates (1987b) also suggested that the negative buoyancy of the tubarium could have been at least partly offset by low density fats within the fibrous fusellar tissue.
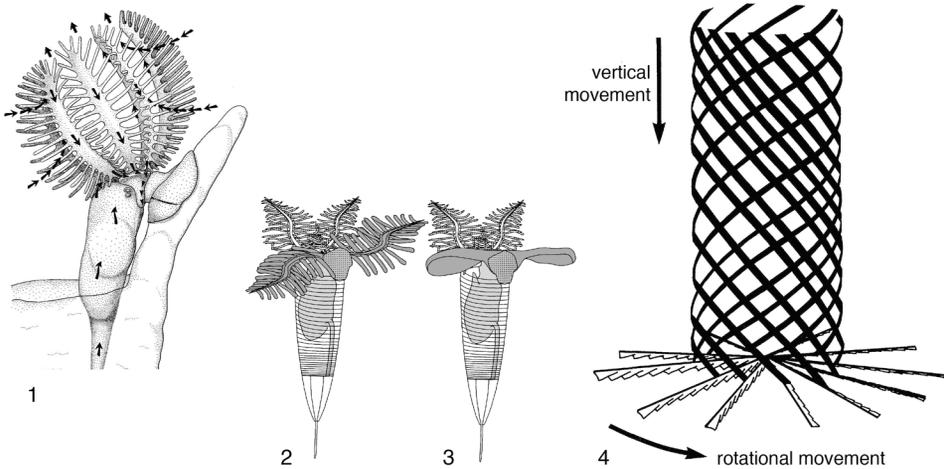
FIG. 66. Feeding and locomotion of graptolites. *1, Cephalodiscus* sp., *arrows* indicate movement of food particles along the arms of a cephalodiscid zooid (Lester, 1985, fig. 3); *2–3,* zooidal reconstruction of MELCHIN and DEMONT, showing enlarged arms (*2*) and possible wing-like muscular extensions of the cephalic shield (*3*) for locomotion (Melchin & Demont, 1995, p. 117, fig. 1); *4,* diagram showing rotational movement of multiramous colony (adapted from Rigby & Rickards, 1989, fig. 4).

MELCHIN and DEMONT (1995) suggested a new model of automobility of the colonies using putative winglike extensions of the cephalic shield for rowing (Fig. 66.2–66.3), as they considered passive buoyancy control unlikely due to the size, architecture, and phylogenetic history of the graptolites. RIGBY and RICKARDS (1989) and RIGBY (1991, 1992) modeled graptoloids in relation to rotation and feeding efficiency during passive sinking.

All considered, however, there are significant problems with all locomotory mechanisms proposed for the graptoloids (COOPER & others, 2012). The topic remains one of the major questions in graptoloid ecology.

FEEDING

The example of the living pterobranchs can be used to infer the feeding mechanisms of fossil benthic graptolites. The extant *Cephalodiscus* and *Rhabdopleura* use their ciliated arms to extract food from the water column. The cilia on the tentacles move water into the center of the basket formed by the arms of the zooid (Fig. 66.1). Food particles are separated and collected in the median canal of each arm. The food is then transported into the mouth (LESTER, 1985).

It is generally agreed that the zooids of fossil benthic graptolites fed by sampling water that passed through the colonies (as seen in extant taxa), but just how the feeding mechanism might have worked is mostly conjecture. KIRK (1969, 1990, 1991) suggested that in conical forms, afferent flows entered through the central opening, and efferent flows passed out through the mesh. This is in conflict with the observations of similarly organized organisms such as modern sponges and bryozoans. Modeling by MELCHIN and DOUCET (1996) showed that afferent flows through the sides and efferent flows through the top of the colonies were more likely. Different colonial morphologies may also be related to the paleoenvironmental conditions under which the graptolites lived (RICKARDS, BAILLIE, & JAGO, 1990; MELCHIN & DOUCET, 1996).

Modeling of planktic graptoloid colonies and water tank experiments (RIGBY & RICKARDS, 1989; RIGBY, 1991, 1992) suggested that flat, horizontal colonies as well as conical to umbrella-shaped colonies may have maintained a stable horizontal orientation in the water and were able to rotate during ascent and descent to improve water sampling and feeding efficiency (Fig. 66.4). Straight

axonophorans are sometimes found on bedding planes with their long axes aligned; this is interpreted to indicate the direction of bottom currents (Moors, 1970; Rantell & Rigby, 2002). Modern analogs may help to infer details of the feeding strategies. Some filter-feeding euphausiids in the Humboldt Current of the eastern Pacific migrate from the surface to the oxygen-minimum zone at 300–400 m deep in the daytime to harvest microplankton and avoid predators (Antezana, 2009).

The fluid-dynamic models of Rigby and Tabor (2006) suggested that water flowed toward the thecal apertures in taxa with simple thecae; however, the complex development of the thecal apertures in many taxa and the development of the external lacinia and ancora sleeve in axonophorans suggest that this model has limited applicability.

PARASITES, EPIBIONTS, AND PREDATORS

Examples of parasites in modern pterobranchs are extremely rare despite the fact that records go back more than a hundred years. However, a few parasites have been found in the following extant species. Calman (1908) described the parasitic copepod *Zanclopus cephalodisci* Calman, 1908 (Fig. 67.1–67.5) from the stomach of *Cephalodiscus gilchristi* Ridewood, 1906. Calman (1908) referred *Z. cephalodisci* to the family Ascidicolidae (now Enterognathidae; Boxshall & Halsey, 2004; Ohtsuka, Kitazawa, & Boxshall, 2010, p. 689). Calman recognized *Enterognathus comatulae* Giesbrecht, 1900, a species infesting the echinoderm *Antedon* de Freminville, 1811, as possibly the closest relative of *Zanclopus* Calman, 1908. A second species of the genus *Zanclopus*, *Z. antarcticus* Gravier, 1912b, was found in the stomach of *Cephalodiscus anderssoni* Gravier, 1912a. Also, Ridewood and Fantham (1907) described the protozoan *Neurosporidium cephalidisci* Ridewood & Fantham, 1907 from the nervous system of *Cephalodiscus nigrescens* Lankester, 1905 as a parasite.

Parasitism has been recognized in well-preserved, chemically isolated material of the fossil record of various benthic graptolite groups and in the graptoloids but is limited to instances in which it resulted in a response by the zooids to the parasite. The parasites themselves have not been preserved. For example, anomalous outgrowths formed from fusellar and cortical tissue are thought to indicate response to infestations by parasites (Kozłowski, 1970a; Maletz, 1997a). The best examples of these infestations include the tubothecae described by Kozłowski (1970a) (Fig. 67.8), tubular growths from cortical material attached to the tubaria in a number of benthic graptolites (e.g., Wiman, 1901; Skevington, 1963a; Urbanek & Mierzejwski, 1982). These tubes do not indicate any internal communication with the tubaria to which they are attached. Kozłowksi (1970a) and Conway Morris (1981) concluded that tubothecae resulted from graptozooids secreting cortical tissue over the parasites (perhaps annelids) living on the graptolite colonies.

In describing possible parasitism in Graptoloidea, Bates and Loydell (2000) differentiated between open-ended tubes and closed blisters of various shapes (Fig. 68). The structures include mostly round or oval blisterlike protuberances (Jackson, 1971; Bates, 1994) on the obverse and reverse side of the colonies (Fig. 68.3–68.4, Fig. 68.7). The most spectacular features are eight tubular outgrowths on a proximal end of *Geniculograptus typicalis* (Bates & Loydell, 2000) that might have considerably changed the hydrodynamic behavior of the colony, but were apparently non-lethal (Fig. 68.1–68.2). Abnormalities in Silurian monograptids were extremely rare. Urbanek and Teller (1974) and Teller (1998, 1999) described a few unusual features in monograptids, but none of these were similar to the blisters and tubes found in Ordovician taxa.

Although called parasites, these outgrowths could alternatively be interpreted as indications of epibionts, organisms growing on
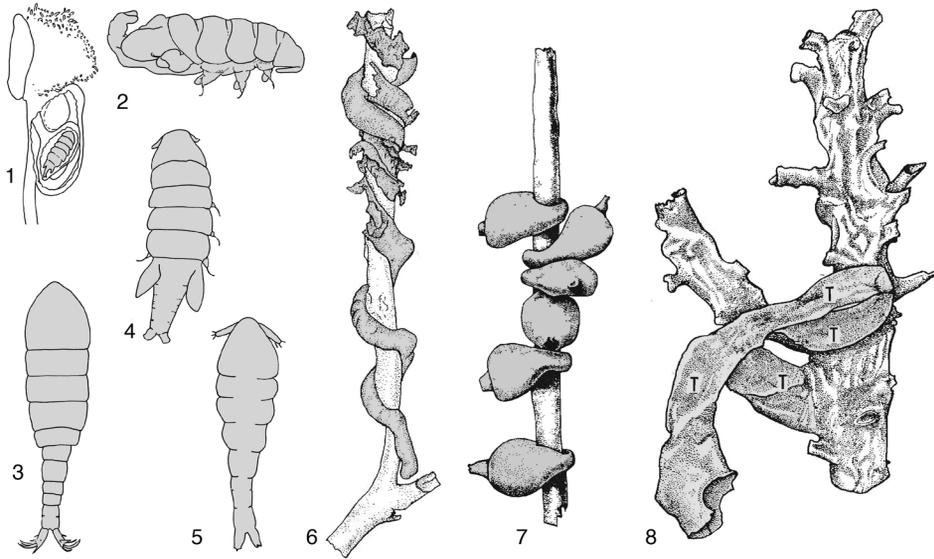
Fig. 67. Pterobranch epibionts and parasites: *1–5,* extant, *6–8,* Middle Ordovician, upper Darriwilian. *1, Cephalodiscus gilchristi* Ridewood, 1906, showing the position of the parasite *Zanclopus gilchristi* Calman, 1908 in its stomach; *2–5, Z. gilchristi, 2, 4,* female in two views; *3,* male in 5th copepodid stage, appendages omitted; *5,* earliest known larval stage (*1–5* adapted from Calman, 1908, pl. 18–19); *6, Helicotubulus dextrogyra* (Kozłowski, 1967), holotype on fragment of *Mastigograptus* sp. (adapted from Kozłowski, 1967, fig. 7); *7, Clistrocystis graptolithophilius* Kozłowski, 1959b (adapted from Kozłowski, 1965, fig. 1); *8,* tubotheca (*T*) on *Acanthograptus* sp. (adapted from Kozłowski, 1970a, fig. 5).

the graptolite tubaria without harming the colony. Other possible epibionts include *Clistrocystis graptolithophilius* Kozłowski, 1959b, an organic-walled microfossil, invariably attached to the stipes of *Mastigograptus* Ruedemann, 1908 (Fig. 67.7). Kozłowski (1965) interpreted this fossil as possible eggs of cephalopods. Another enigmatic fossil is *Helicotubulus dextrogyra* (Kozłowski, 1967) (see Mierzejewski & Kulicki, 2003b), originally referred to the Phoronida (Fig. 67.6). Markham (1971, fig. 5) illustrated a number of possible folliculinid ciliates on an empty tube of the extant *Cephalodiscus* (*Orthoecus*) *densus* Anderson, 1907. Small phosphatic brachiopods are known as epibionts (Wang & others, 2012) on the possible pterobranch *Malongitubus quangshanensis* Hu, 2005, an erect, multibranched fossil identified as an alga in the past.

Graptoloids may represent primary consumers (Underwood, 1998) and have been placed close to the base of the Paleozoic food web. It is possible that they also formed an important food source for other marine organisms, but there is very little evidence of predation on graptolites (Underwood, 1993; Loydell, Zalasiewicz & Cave, 1998). However, Underwood (1993) described possible fecal packages of Silurian monograptids and interpreted accumulations of biserial colonies as fecal accumulations, which could support predation. On the other hand, Bates and Kirk (1986) have suggested that the fusellum of the graptolites might have been too tough for ingestion and that the soft tissues might have been poisonous.

LIFE HISTORY STRATEGIES

Graptolite colonies grew by the distal addition of new thecae. Controls on colony size in benthic graptolites are not clear, because most taxa are found only as fragmented remains and their original growth pattern and size cannot be reliably determined. Diverse benthic graptolite faunas indicate that colonies were able to reach dimensions of more than 50 cm in diameter
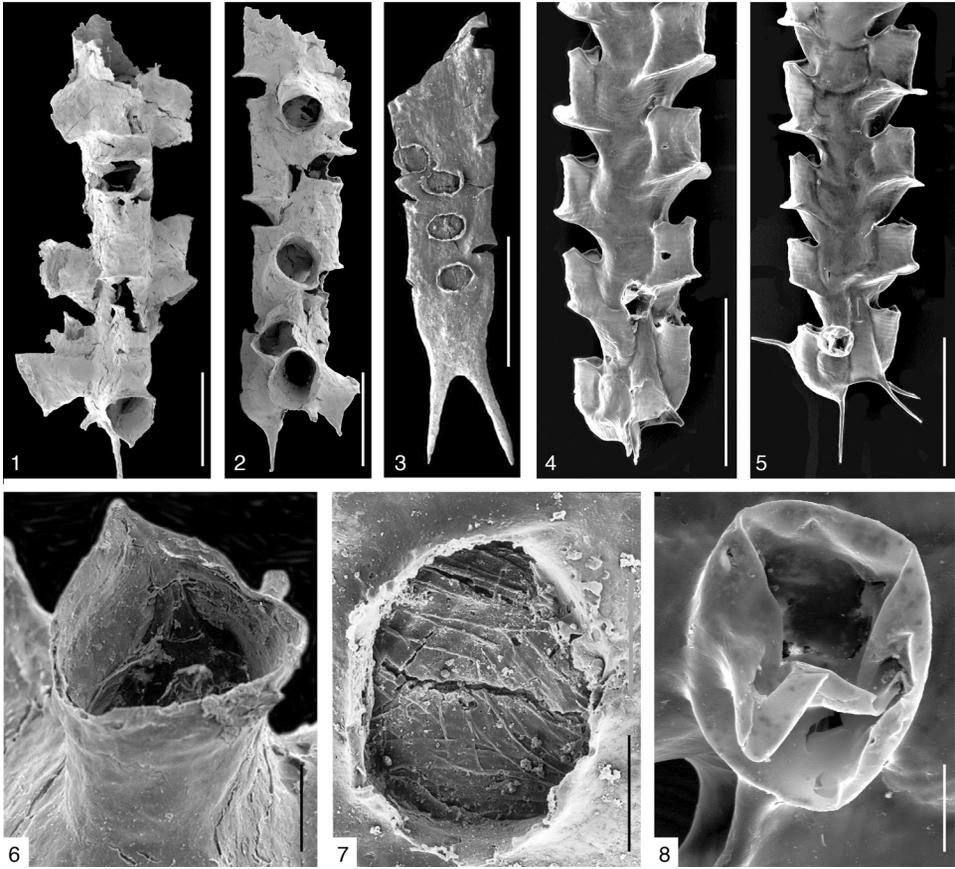
FIG. 68. Possible parasitic developments on Graptoloidea. *1–2, Geniculograptus typicalis* (HALL, 1865) specimen in different views (new; photos provided by David Loydell); *3, Diplacanthograptus spiniferus* (RUEDEMANN, 1912) (Bates, 1994, pl. 1); *4–5, Anticostia lata* (ELLES & WOOD, 1906), from type block of *Climacograptus inuiti* COX, 1933, SMF 75822, 75817 (new); *6,* detail of *1; 7,* detail of *3; 8,* detail of *5;* scale bars, 1 mm in *1–5,* 0.1 mm in *6–8.*

containing thousands of zooids (BOUČEK, 1957; BULL, 1987). Modern *Rhabdopleura* colonies, on the other hand, are relatively small but still may contain dozens of zooids (see LANKESTER, 1884, pl. 37). Growth and final size appears to be restricted mainly by their ecology.

In multiramous planktic graptolites, colonies grew by the distal addition of thecae simultaneously on all stipes in the colony. Their maximum size appears to be unconstrained by their colony design, with some colonies reaching as large as a meter in diameter (see PRITCHARD, 1892). Some Silurian monograptids were also of considerable length (LOYDELL & LOVERIDGE, 2001).

In a few axonophoran species, maximum length appears to have been constrained by the development of an appendix (as in the Retiolitidae) or by the presence of distal vanes (nematularia) at the extremity of the nema, which usually were not overgrown by the developing stipes (e.g., *Archiclimacograptus decoratus* [HARRIS & THOMAS, 1935]). In many graptolites, there were no obvious constraints on stipe development, yet colonies never exceeded a few centimeters in length or, in extreme cases (e.g., *Brevigraptus* MITCHELL, 1988; *Corynoides* NICHOLSON, 1867a; *Peiragraptus* STRACHAN, 1954), a few thecae in total.

RIGBY and DILLY (1993) estimated the life span of individual graptolite colonies.

They used the rate of fusellar ring accretion in *Rhabdopleura* to calculate that a graptoloid zooid takes an average of 6.6 days to secrete a theca. According to these estimations, the life span of a 3 cm long biserial graptoloid was 1.6–2.4 years, and a 75 cm long *Monograptus flemmingii* (Salter, 1852) approximately 13 years. Damage and repair and possible re-colonization of tubes by successive generations of zooids (Rigby, 1994b) may even increase this estimate.

Population structure and dynamics of graptoloids in bedding-plane assemblages have been investigated by Rigby (1993), and in chemically isolated material from limestone nodules by Underwood (1998). The survivorship analyses by Rigby indicated increasing mortality rates with age, but analyses by Underwood indicated constant to decreasing mortality rates with age. Clearly, further such studies are needed before reliable conclusions can be drawn about their ecological implications.

Synrhabdosomes are monospecific assemblages of radially arrayed tubaria attached by the distal extremities of their nemata and occur in various groups of graptolites, from the Dichograptina to biserial and uniserial axonophorans. They have been interpreted as: 1) reproductive adaptations (e.g., Ruedemann, 1895; Kozłowski, 1949; Zalasiewicz, 1984; Underwood, 1993; Ge & Chen, 1995); 2) as chance entanglements (Rigby, 1993; Goldman & Mitchell, 1994); and 3) as adaptations for a variety of other purposes (Kirk, 1969; Gutiérrez-Marco & Lenz, 1998). Synrhabdosomes are rare and known only in a few species; they were clearly not obligate associations that formed part of the life history and ecology of most graptoloids (Maletz, 2015).

SPECIES ASSOCIATIONS AND LOCAL POPULATIONS

Within most graptolitic black shale formations, occasional bedding planes are crowded with colonies, sometimes dominantly of one species. Sometimes all tubaria are at about the same stage of astogenetic growth, suggesting mass mortality (Fig. 69). On the other hand, recurring species associations are common. On some layers, juveniles are associated with mature specimens of the same species, whereas on others either only juveniles or only mature specimens are present (Moors, 1968; Pannell, Clarkson, & Zalasiewicz, 2006). Recurring species associations and monospecific assemblages suggest some segregation of species within water masses.

Multiple species on single bedding planes are common. Highly diverse bedding plane assemblages are less common but not rare in black shale settings (Fig. 70). Although time averaging probably enhanced this diversity, a range of species is likely to have lived in the overlying waters. A diverse Middle Ordovician fauna preserved within a volcanic ash fall was interpreted by Mitchell, Brussa, and Astini (1998) as an instantaneous "catastrophic kill" of the entire suite of depth-stratified populations that lived in the overlying water column. Current evidence, therefore, suggests that many graptolite species lived in swarms, spatially differentiated from neighboring swarms (Cooper & others, 2012). These same species and others, however, are also found in low abundance at widely scattered localities, so swarming was not obligatory. However, quantitative evidence is sparse, and the effects of current sorting and transport need to be considered, particularly in turbidites (Moors, 1970).

PATTERNS OF FACIES OCCURRENCE

Graptolite tubaria are made of an organic scleroproteic material that can be destroyed under oxic conditions. Thus, they are best preserved in organic-rich sediments in the typical graptolitic black shales (see Ruedemann, 1911), where the decay of organic material is hindered by the anoxic conditions under which the sediments were formed.

Graptolites occur in a wide range of marine sediments, from shales of various colors to silt- and sandstones, carbonates,
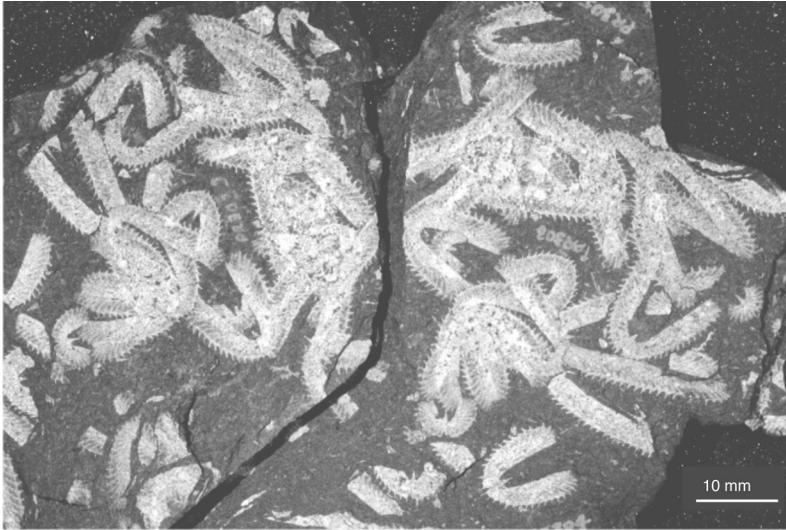
FIG. 69. A monospecific death assemblage of *Isograptus victoriae maximus* (counterparts) from the Dapingian (Castlemainian), Middle Ordovician, Aorangi Mine, New Zealand (Cooper & others, 2012, fig. 7). Color version available in *Treatise Online* 86.

FIG. 70. A diverse bedding plane assemblage from the Dapingian (Yapeenian), Middle Ordovician, Aorangi Mine, New Zealand (Cooper & others, 2012, fig. 9). Color version available in *Treatise Online* 86.

and cherts (Fig. 71). They are most common, however, in fine-grained clastics in black or dark shales, where the flattened remains are present on numerous bedding surfaces. This sedimentary facies is characteristic of the outer shelf to deep-water regions or basinal regions of the oceans, but graptolites can be found in most sediments representing inner cratonic to deep, marine-basin settings. They are associated with various fossil groups, but in shale sequences they are commonly the only fossil group present. Rarely, groups such
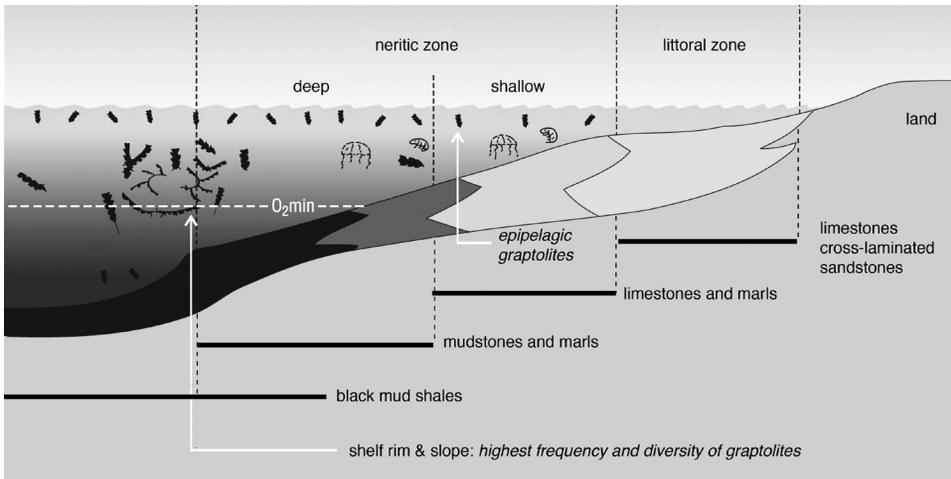
FIG. 71. Schematic distribution of the lithofacies and graptolite biofacies (adapted from Podhalańska, 2013, fig. 3).

as conodonts, scolecodonts, and phosphatic brachiopods are also present on the same bedding planes. However, organic-walled microfossils (acritarchs, chitinozoans) may be common in these sediments.

In turbidite successions, graptolites are mainly preserved in the fine-grained E horizon of the Bouma sequence or in intercalated, pelagic black shales (HILLS & THOMAS, 1953; MOORS, 1969, 1970; COOPER, 1979). More rarely, they are preserved in the A or C horizon as transported fragments (FINNEY & BERRY, 1997; COOPER & others, 2012). Alignment of tubaria on the bedding plane is common and indicates bottom currents and possible transportation (e.g., RUEDEMANN, 1897; MOORS, 1968).

GRAPTOLOID BIOFACIES AND BIOTOPES

The abundance and diversity of graptoloids in sedimentary rocks bordering the Ordovician continents (FORTEY & COCKS, 1986; CHEN, ZHANG, & MITCHELL, 2001; FINNEY & BERRY, 2003) suggest that a favorable life zone existed in the region of the outer shelf and slope. FINNEY and BERRY (1997) interpreted the favorable habitat to be associated with upwelling zones providing nutrients and enhancing bioproductivity.

Although graptoloids are preserved in sedimentary rocks representing depositional environments ranging from inner shelf and craton to the open ocean, many workers have recognized the preferred association of some species with a particular depth facies or offshore facies belt. Both lateral partitioning and depth partitioning of the graptoloid biotope have been proposed and many models have been advanced (Fig. 73). Many researchers have recognized a depth zonation of graptoloids in the water column (ROSS, 1961; BERRY, 1962a, 1974; BERRY & BOUCOT, 1972; ERDTMANN, 1976, 1984; KALJO, 1978; KIRK, 1978; MU & others, 1979, 1986; CISNE & CHANDLEE, 1982; BATES & KIRK, 1984; LENZ & CHEN, 1985; CHEN, 1990; COOPER, FORTEY, & LINDHOLM, 1991; LENZ & others, 1993; GOLDMAN, BERGSTRÖM, & MITCHELL, 1995; GOLDMAN, MITCHELL, & JOY, 1999; CHEN, ZHANG, & MITCHELL, 2001; COOPER & SADLER, 2010), and most models incorporate a depth component. Some models proposed lateral partitioning as the dominant differentiating mechanism of species groups.

Although quantitative data are sparse and the biofacies preference of most species is unknown, a consensus model employing both lateral and vertical partitioning was formed (CHEN, 1990; CHEN, MELCHIN, &
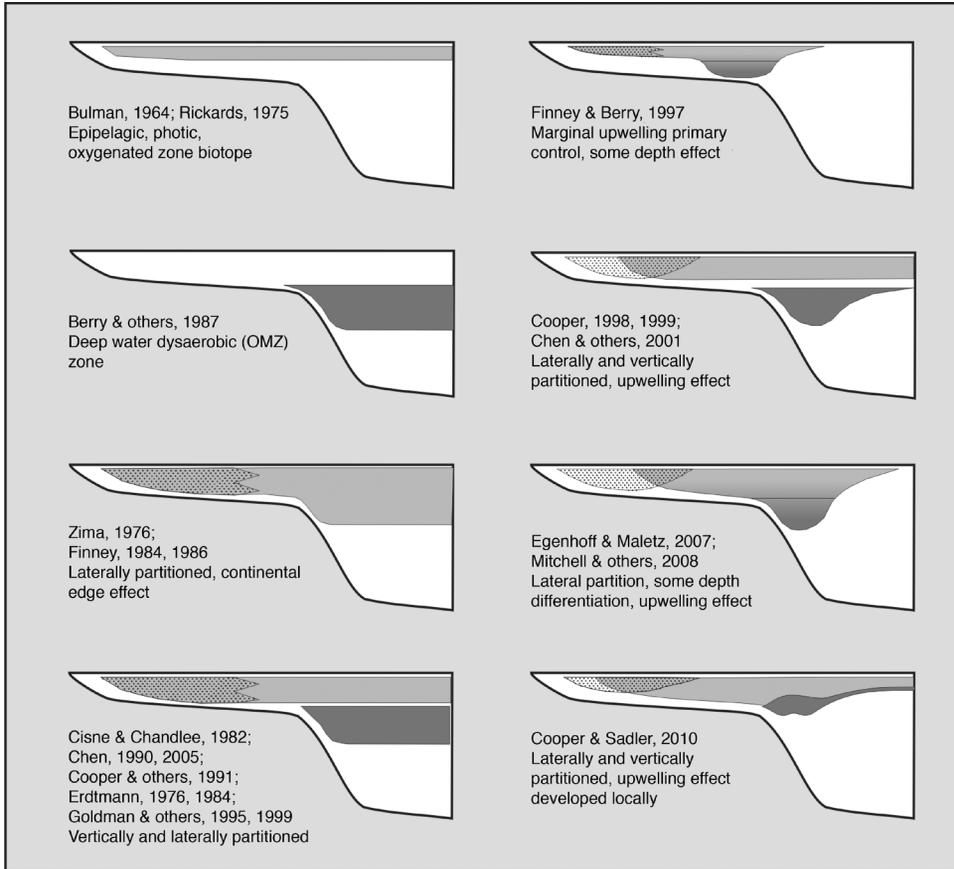
FIG. 72. Some previous models of the graptoloid habitat (adapted from Cooper & others, 2012, fig. 18).

others, 2005; COOPER, FORTEY, & LIND-HOLM, 1991; COOPER & others, 2012). This model was based mainly on species of the Early to Middle Ordovician age, the time period in which most ecological analysis has been done. Three species groups were recognized: 1) taxa restricted to the deep-water facies; 2) taxa present in both the neritic and deep-water facies; and 3) taxa found only in the neritic facies. Group 1 species were inferred to have lived in a deep water biotope and group 2 species in a shallow, epipelagic biotope (Fig. 72, Fig. 73); these two groups were thus separated primarily by depth zonation, which, in modern oceans, is caused by such factors as vertical gradients in water temperature, chemistry, aeration, light intensity, and nutrient supply. The distinctness of the two groups is confirmed by their species extinction probabilities; extinction risk is significantly higher for group 1 species than for group 2 species (COOPER & SADLER, 2010; see also BOYLE & others, 2014). Group 3 species, which are restricted to inner- and mid-shelf waters (neritic biotope), were constrained by lateral partitioning of the water mass, perhaps comparable with the modern continental edge effect. Groups 1 and 2 contained many pandemic species, whereas group 3 species were largely endemic in their distribution. The model was applied to Late Ordovician graptoloid species (GOLDMAN & others, 2013) and, more loosely, to Silurian species (BERRY & BOUCOT, 1972; MU & others, 1986; LENZ & others, 1993; BOUCOT & CHEN, 2009).
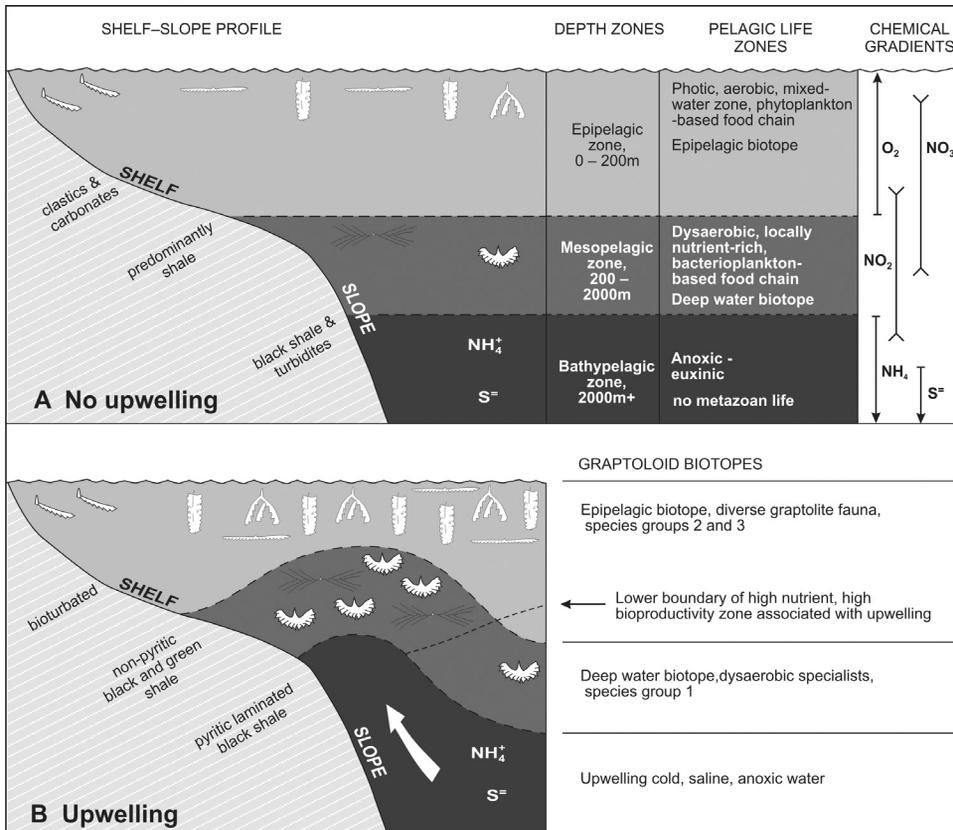
FIG. 73. *A,* Inferred graptoloid life zones in a density-stratified ocean with no upwelling. Epipelagic and deep water graptoloid biotopes are indicated, neritic (inshore) biotope not shown; *B,* in marginal upwelling zone, tongues of dense, oxygen-depleted but nutrient-rich water are brought up into the epipelagic zone (the nutrient pump) generating a nutrient-rich, high-bioproductivity environment (adapted from Cooper & others, 2012, fig. 19 and references cited therein).

In an alternative approach, lateral partitioning is assumed to be the dominant discriminating mechanism (ZIMA, 1976; FINNEY, 1984, 1986). The model proposed by EGENHOFF and MALETZ (2007) and MALETZ and others (2011) does not recognize a discrete habitat for group 2 species or the distinction between species groups 1 and 2.

In modern oceans, the epipelagic life zone extends from the water surface to a depth of ~200 m, where the light level is only at ~1% of that at the surface. Nearly 90% of all marine life exists in this zone, and it is where nearly all primary productivity takes place, mainly by the phytoplankton. This is the obvious biotope of group 2 and group

3 species and was most likely the zone in which most planktic (and benthic) graptolites thrived. In the mesopelagic zone, below 200 m depth to ~2000 m, the ocean waters are depleted of oxygen and there is no light. Bacterioplankton are the basis of the food web, and bioproductivity is generally lower than in the epipelagic zone, although locally, highly productive subzones are present (BRINTON, 1979; LONGHURST & HARRISON, 1989).

In marginal upwelling areas, nutrient-rich waters enrich the epipelagic zone and greatly increase bioproductivity. This in turn enhances the development of a high-nutrient dysaerobic zone at depths where

specialized mesopelagic-zone species thrive (Longhurst, 1967; Judkins, 1980; Longhurst & Harrison, 1989; Brasier, 1995). This deep-water biotope is thought to be the analog of the group 1 species habitat (Berry, Wilde, & Quinby-Hunt, 1987, 1989; Cooper & others, 2012) and ancient upwelling zones to be the sites of abundant and diverse graptolite assemblages (Finney & Berry, 1997).

BIOSTRATIGRAPHY

Jörg Maletz

THE FOSSIL RECORD OF THE HEMICHORDATA

It is now accepted that the Hemichordata are likely to have originated during the late Precambrian to early Cambrian (Fig. 74), given that the fossil record indicates a presence of pterobranchs as early as the Fortunian (basal Cambrian), with the possible rhabdopleurid *Sokoloviina costata* (Kirjanov, 1968) discovered in the Ukraine (Maletz, 2019a). However, early Cambrian records of Pterobranchia are rare, and it isn't until the upper Cambrian (Series 2, Stage 4) and the Miaolingian (Wuliuan) (Fig. 74) that a better fossil record became available, following the discovery of the first Enteropneusta fossils in the Burgess Shale in Canada (Caron, Conway Morris, & Cameron, 2013).

The fossil record of the Enteropneusta is limited to very few specimens and few localities in the Palaeozoic to Mesozoic. The described fossil taxa have been incorporated into the taxonomic scheme and, in part, are referred to extant groups (Cameron, 2018). The early genera *Oesia* Walcott, 1911 and *Spartobranchus* Caron, Conway Morris, & Cameron, 2013 are included in a stem group.

The Cambrian record of the Pterobranchia is of interest largely for taxonomy and evolutionary studies, but the planktic Graptolithina represent one of the most important fossil groups of the Paleozoic for biostratigraphical dating of rock sequences. Their origin close to the base of the Ordovician System (Cooper, Nowlan, & Williams, 2001; X.-F. Wang & others, 2019) can be regarded as one of the major evolutionary events in the history of life on planet Earth and marks the onset of the evolution of planktic macro-organisms. The extinction of the planktic graptoloids during the Early Devonian was a slow process. The reason for

this remains unexplored but may be related to the emergence of plankton feeders in the world's oceans (Maletz, 2017a). This chapter focuses on the interval of biostratigraphical use of the Graptolithina and does not discuss the sparse younger fossil record of the Hemichordata.

GRAPTOLITE BIOSTRATIGRAPHY

As early as 1850, Hall estimated that graptolites, although at that time poorly known, were valuable for identifying certain geological periods. Thus, Hall's 1850 study might be regarded as the starting point of graptolite biostratigraphy, even though at the time few graptolite species had been described. Furthermore, a precise biostratigraphical use was not yet possible. In the same year, Barrande (1850) indicated the practical biostratigraphic use of the Silurian graptolite faunas in the Barrandean region. Nicholson (1868b) provided the first chart showing the distribution in time (biostratigraphic distribution, in modern terms) of graptolite faunas in Britain. It was, however, the impact of Lapworth's (1878) influential study on the Moffat Series that established graptolites as a prime fossil group for biostratigraphy and relative dating of rock sequences of the Paleozoic (Fortey, 1993).

Inevitably, mistakes are made in science, and it has occurred in the interpretation of graptolite biostratigraphy. One of the most glaring examples may be the record of supposed Ordovician graptolites on a small island in the South Orkney Island complex of Antarctica (Dalziel, 1979). Fossil material from the island, now called Graptolite Island, was initially identified as Ordovician graptolites by Gertrude Elles and published by Pirie (1905), leading to considerable problems for the interpretation of the geology of the region. The fossils were
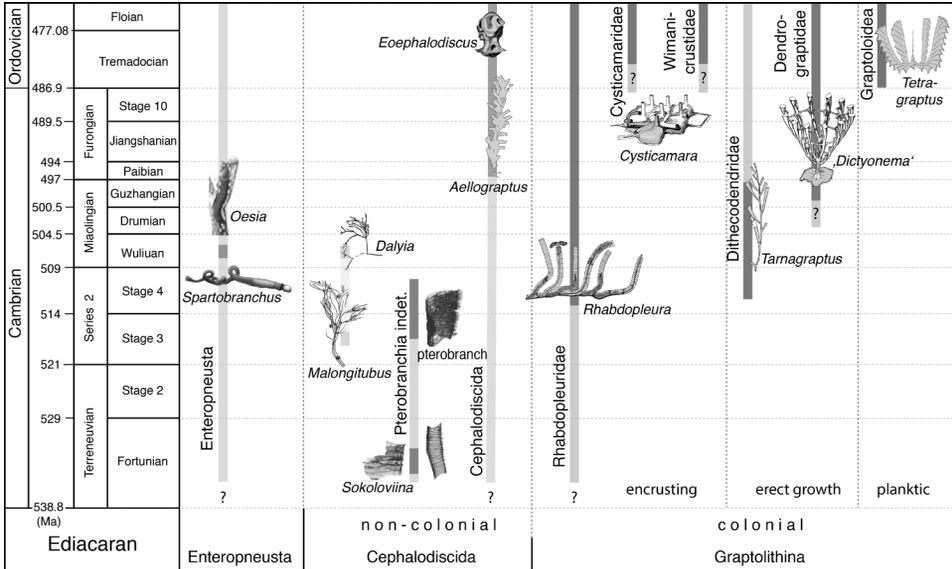
F<small>IG.</small> 74. The Cambrian fossil record of the Enteropneusta and Pterobranchia (Hemichordata) (adapted from Maletz, 2019a, fig. 3).

later identified as possible Carboniferous plant material (S<small>TRACHAN</small> in A<small>DIE</small>, 1957, p. 22) but the misleading name of the island still exists and is present today on Google Earth. The geological map of the South Orkney Islands shows a Carboniferous to Triassic age for the Greywacke Shale Formation, but paleontological data are poor. The dating is based on Triassic radiolarians from the Weddell Islands to the northwest (F<small>LOW-</small> <small>ERDEW</small>, R<small>ILEY</small>, & H<small>ASELWIMMER</small>, 2011). This example demonstrates how important precise identification of fossil material is.

Currently used graptolite biozones are quite different from those first developed during the late nineteenth and early twentieth centuries. Scientists most commonly use the concept of the First Appearance Datum (FAD) to define the base of a fossil biozone, which in general is a local level and may not represent the worldwide first appearance of a taxon. This is especially noticable in the definitions of chronostratigraphic units based on graptolites. There are now 13 out of 16 stage boundary levels from the base of the Ordovician System to the base of the Devonian System that are defined

by the level of the FAD of a particular graptolite species in a certain section (O<small>GG</small>, O<small>GG</small>, & G<small>RADSTEIN</small>, 2016). Absolute dates for the following charts (Fig. 75–80) are generally taken from G<small>RADSTEIN</small> and others, 2020, which represent the latest available information. Dates have changed considerably over the years as a result of new information. Details are available from the website of the International Commission on Stratigraphy (stratigraphy.org). The website also includes uncertainty intervals of radiometric dates.

Numerous biostratigraphic range charts have been published over the years, many of them providing local biozones, but general overviews are rare. E<small>LLES</small> and W<small>OOD</small> (1914) tabulated the biostratigraphic ranges of all graptolites known at the time from Britain into 36 graptolite zones, preceded only by the succession of L<small>APWORTH</small> (1880f), which counted 20 zones. This initially local (British) E<small>LLES</small> and W<small>OOD</small> biozonation became a worldwide standard and was used unchanged for more than 60 years until R<small>ICKARDS</small> (1976) and later Z<small>ALASIEWICZ</small> and others (2009) revised the British standard biozonation and counted 60 biozones and

subzones leading up to the middle Ludlow. Younger graptolite zones were not recognized in Britain. Bulman (1955, fig. 5) provided a chart in *Treatise,* Part V showing the stratigraphic distribution of the main groups of graptolites and later added graptolite biozonal schemes for Britain and Australia as a guideline to the graptolite biostratigraphy in the second edition of *Treatise,* Part V (Bulman, 1970). Unified international biostratigraphies are difficult to construct due to the biogeographic differentiation of many faunas (e.g., Goldman & others, 2013), but a generalized graptolite zonal sequence for the Silurian was proposed by Jaeger (1991) and Koren' and others (1995, 1996). A standard graptolite biozonation may also be used for the Lower Devonian, as the faunas of this time interval are fairly monotonous (Jaeger, 1978b, 1988; Lenz, 2013).

A number system was introduced in Germany by Eisel (1899), based on the succession of Lapworth (1880f, table 11–12), but slightly different index species were employed (Eisel, 1903). This scheme was still used by Münch (1952) in his overview on Silurian graptolites of Germany, but Jaeger (1991) used and adjusted the succession of Elles and Wood (1914) for the German Silurian and indicated a number of intervals not covered in their scheme. Maletz (2001a) suggested abandoning the number system in Germany, following Rickards (1995a, p. 133) and advocated using only index species for the biozonation.

The graptolite biozonation presented here is largely based on the excellent compilation of Loydell (2012), including additional references in his figure captions. New information needing to be incorporated is reflected herein.

ORDOVICIAN

According to Goldman, Sadler, and Leslie (2020), the Ordovician System (Lapworth, 1879a) is approximately 43.78 Ma in duration (486.85–443.07 Ma), including three series, the Lower Ordovician (15.59 Ma),

the Middle Ordovician (13.08 Ma), and the Upper Ordovician (15.11 Ma), of which the middle one is somewhat shorter. The three series include seven stages, highly uneven in length. The Darriwilian Stage (458.18–469.42 Ma) is the longest stage at approximately 11.24 Ma, and the Hirnantian (443.07–445.21 Ma) is the shortest at only about 2.14 Ma, including two graptolite zones (note, the precise radiometric ages may differ considerably based on the source used). Gradstein and others (2012, 2020) is used for all units discussed herein, but numbers may change in the future (compare with Cooper & Sadler; 2012; Ogg, Ogg, & Gradstein, 2016).

The (informal) Ordovician stage slices of Bergström and others (2009) are not correlated herein. They were introduced as defined chronostratigraphical units, based on biostratigraphical data and explained to have "potential for precise correlations in both carbonate and shale facies" (Bergström & others, 2009, p. 97). They were used to correlate the $\delta^{13}C_{org}$ curve to the chronostratigraphy. These stage slices should not be confused with the time slices in Webby and others (2004), a term created to provide a precise key to correlate biostratigraphic intervals based on various fossil groups. The individual intervals were estimated to be between 1.6 and 2.5 Ma in duration.

THE LOWER ORDOVICIAN

The Lower Ordovician includes the Tremadocian and Floian stages (Fig. 75). The base of the Ordovician System and the Tremadocian Stage is defined at the level of the FAD of the conodont *Iapetognathus fluctivagus* Nicoll & others, 1999 (Cooper, Nowlan, & Williams, 2001; Terfelt, Bagnoli, & Stouge, 2012; X.-F. Wang & others, 2019, 2021). The occurrence of *Rhabdinopora* Eichwald, 1855 is typically more easily recognized in dark shale in basal Ordovician strata (Henningsmoen, 1973; Bassett & Dean, 1982; Norford, 1982, 1988), although the FAD of *Rhabdinopora* occurs at a level slightly higher than the Global

Stratotype Section and Point (GSSP) level. The biozones in the Australasian succession are named by index species, but only their widely known and commonly used zonal notations are shown herein (Fig. 75–77). See VandenBerg and Cooper (1992) and Percival, Quinn, and Glen (2011) for details and full biozonal names.

The base of the Floian Stage is defined at the level of the FAD of *Paratetragraptus approximatus* (Nicholson, 1873) in the Diabasbrottet section, Västergötland, Sweden (Bergström, Löfgren, & Maletz, 2004; Bergström & others, 2006). This level is equivalent to the level of the FAD of the common Scandinavian graptolite *Tetragraptus phyllograptoides* Strandmark, 1902. The name *Tetragraptus phyllograptoides* Biozone is usually used to identify the interval in Scandinavia (Baltica) and South America (Egenhoff, Maletz, & Erdtmann, 2004; Toro & others, 2015).

Maletz, Egenhoff, and Alonso (2010) and Maletz and Ahlberg (2018) published the latest biozonation for the Tremadocian to early Darriwilian of Baltica, representing one of the most complete successions known (Fig. 75). Maletz, Egenhoff, and Alonso (2010), following Maletz and Egenhoff (2001), identified a local *Kiaerograptus stoermeri* Biozone beneath the *Kiaerograptus supremus* Biozone of Lindholm (1991), which is not indicated in the chart (Fig. 75), because it has been identified in only a single section. Zalasiewicz and others (2009) discussed the graptolite biostratigraphy of Britain and listed the known faunas of the Lower Ordovician. Maletz and Ahlberg (2011a, fig. 8) provided a correlation of the British succession to the Scandinavian succession, showing that the British graptolite succession is fairly incomplete, and some intervals are not documented by fossil faunas (Fig. 75). Zhang and others (2019) provided the latest overview on the Ordovician graptolite biostratigraphy of China as a combination of the North China platform and the Yangtze Region. The North China succession starts with the *Rhabdinopora*

proparabola interval (Fig. 75) but is not known with certainty from other regions of China (Maletz, Wang, & Wang, 2022).

The basal Ordovician (early Tremadocian) and the Floian intervals of the North American succession are best known from western Newfoundland (Williams & Stevens, 1988; Cooper, Nowlan, & Williams, 2001), but the late Tremadocian to early Floian succession of Yukon Territory, Canada (Jackson & Lenz, 2003, 2006) is a more detailed succession of *Paradelograptus* Erdtmann, Maletz, & Gutiérrez Marco, 1987 species used to subdivide the latest Tremadocian strata. Williams and Stevens (1991) recognized only the *Aorograptus victoriae* Biozone in the late Tremadocian of western Newfoundland, which is probably correlatable with the *Kiaerograptus kiaeri* interval of Baltica (Maletz, 1999b).

Lower Ordovician successions are widely distributed in South America and have been described in some detail from Bolivia and Argentina (Maletz & Egenhoff, 2003; Egenhoff, Maletz, & Erdtmann, 2004; Toro & others, 2015). They have been correlated with the Scandinavian successions by Maletz and Ahlberg (2011a). Albanesi and Ortega (2016) discussed the Ordovician successions of Argentina and provided the latest information on the graptolite biostratigraphy (Fig. 75–77), which revealed distinct differences between the Argentinian Precordillera and the Gondwanan part of South America. In the eastern Cordillera of Argentina, a differentiation of the *Paratetragraptus akzharensis* Biozone into two subzones, *Cymatograptus protobalticus* and *Baltograptus vacillans* biozones, may even be possible (Vento & Toro, 2011; Vento, Toro, & Maletz, 2012).

The Australasian succession appears to be quite incomplete, at least in the Lower Ordovician (Fig. 75). VandenBerg and Cooper (1992) provided index species for the biostratigraphic intervals, and Percival, Quinn, and Glen (2011) updated the succession in New South Wales. Maletz and Ahlberg (2011a) discussed the correlation of the Australasian

Series & Stages	Baltica	Avalonia/Britain	China	North America	South America/Argentina	Austral-asia
FLOIAN (471.26)	Isograptus spjeldnaesi	Isogr. victoriae	Azygograptus suecicus	Isograptus lunatus	Didymograptellus bifidus	Ca 1
	Baltograptus minutus	Expansograptus simulans	Baltograptus deflexus	Didymograptellus bifidus		Ch 2
			Didymograptellus eobifidus			Ch 1
	Baltograptus jacksoni	Baltograptus jacksoni	Tshallograptus fruticosus/ Acrograptus filiforms	Tshallograptus fruticosus	Baltograptus 'deflexus'	Be 4
						Be 3
	Baltograptus vacillans				Paratetragr. akzharensis / Baltogr. vacillans	Be 2
	Cymatograptus protobalticus	Tetragraptus phyllograptoides			Cymatogr. proto-balticus	Be 1
	Tetragraptus phyllograptoides		Paratetragraptus approximatus	Paratetragraptus akzharensis	Tetragraptus phyllograptoides	La 3
(477.08)				Paratetragraptus approximatus		
TREMADOCIAN	Hunnegraptus copiosus		Hunnegraptus copiosus	P. kinnegraptoides / Hunnegr. copiosus	Hunnegr. copiosus	La 2
	Sagenograptus murrayi	Sagenograptus murrayi		Paradelograptus pritchardi	Sagenograptus murrayi	
	Kiaerograptus supremus		Aorograptus victoriae	Paradelograptus antiquus	Aorograptus victoriae	
	Kiaerograptus kiaeri		Psigraptus jacksoni	Psigraptus jacksoni	Bryograptus kjerulfi	La 1.5
	Bryograptus ramosus					
	Adelograptus tenellus	Adelograptus tenellus		Adelograptus tenellus	Adelograptus	
	Rhabdinopora anglica		Rhabdinopora anglica	Rhabdinopora anglica	Rhabdinopora anglica	
	Anisograptus matanensis	Rhabdinopora flabelliformis	Anisograptus matanensis	Anisograptus matanensis	Aniso. matanensis	
	Rhabdinopora campanulatum		Rhabdinopora campanulatum	Rhabdinopora campanulatum	Rhabdinopora campanulatum	La 1
(486.85)			Rhabdinopora proparabola			

FIG. 75. Correlation of Lower Ordovician graptolite biozones. Shaded intervals indicate possible gaps (not recognized faunal intervals) in the successions.

succession and noted this incompleteness of the Tremadocian, in which only a few graptolitic horizons were recognized, leading to a number of biostratigraphic gaps (Fig. 75). VANDENBERG (2017) revised the early Floian succession, but new data on the Middle and Upper Ordovician are not available.

THE MIDDLE ORDOVICIAN

The Middle Ordovician includes the Dapingian and Darriwilian stages (Fig. 76). The base of the Dapingian is set at the stratigraphic level of the FAD of the conodont *Baltoniodus triangularis* (LINDSTRÖM, 1955) in the Huanghuachang section of China (WANG & others, 2009). This level is within the local *Azygograptus suecicus* graptolite Biozone, but the graptolite record is poor in the type section. WANG and others (2013) described the graptolite fauna of the GSSP section and provided a detailed international correlation of the graptolite faunas. The base of the Dapingian is approximately correlatable with the base of the *Isograptus victoriae* Biozone in other regions (MALETZ, 2011a). The Dapingian is characterized by

a succession of isograptid species (*Isograptus* Moberg, 1892, *Oncograptus* T. S. Hall, 1914, *Cardiograptus* Harris & Keble in Harris, 1916) as important index taxa (Cooper, 1973; VandenBerg & Cooper, 1992; Maletz, 2011a). Recently, Herrera-Sánchez, Toro, & LoValvo (2019) and Toro and others (2020) discussed the correlation of the Floian and Dapingian succession of Argentina and correlated the regional *Azygograptus lapworthi* Biozone with the early Dapingian (Fig. 76), followed by the *Isograptus victoriae* Biozone of the Central Andean Basin of Argentina and Bolivia.

The base of the Darriwilian is defined at the level of the FAD of *Levisograptus austrodentatus* (Harris & Keble, 1932) in the Huangnitang section, Zhejiang Province, China, and two subzones are differentiated (Mitchell & others, 1997). Maletz and Ahlberg (2020) and Maletz, Ahlberg, and Lundberg (2020) discussed the international correlation of the Darriwilian in some detail. The authors also included the complex succession of Bohemo-Iberia (Gutiérrez-Marco & others, 2017), in which the chronostratigraphical differentiation includes the regional Arenigian, Oretanian, and Dobrotivian Stages (not shown in Fig. 76). In the past, the correlation of the Darriwilian had been difficult due to the presence of latitudinally restricted taxa, especially the pendent didymograptids (see Goldman & other, 2013), but Maletz (1997a) and Maletz and others (2011) used pandemic faunal elements to introduce a biostratigraphical succession of the late Darriwilian (the Llanvirn of the British regional chronostratigraphy) as an international standard. Maletz (1997b) revised the Darriwilian succession of Quebec, Canada, and differentiated the *Levisograptus austrodentatus* and *Levisograptus dentatus* biozones into two subzones each (Fig. 76). Maletz, Ahlberg, and Lundberg (2020) discussed the Darriwilian interval of South America, showing a fairly complete succession from the *Levisograptus austrodentatus* Biozone to the *Pterograptus elegans* Biozone. This succes-

sion was pieced together from numerous localities. The *Pseudamplexograptus distichus* Biozone from the Puna region of Argentina (Brussa, Toro, & Vaccari, 2008) was not used in their compilation. Kaufmann (2019) described the Darriwilian to basal Katian succession of the Sierra de Villicum in the Argentinian Precordillera.

THE UPPER ORDOVICIAN

The Upper Ordovician is differentiated into three stages, the Sandbian, Katian, and Hirnatian (Fig. 77), each stage being defined at the level of the FAD of a graptolite species.

The base of the Sandbian Stage is taken at the level of the FAD of the distinctive *Nemagraptus gracilis* (Hall, 1847) in the Fågelsång section, Scania, Sweden (Bergström & others, 2000), a species that is known to have a worldwide distribution (Brussa & others, 2007). The precise level of the FAD of this species in southern Scandinavia has recently been questioned (Maletz & Ahlberg, 2020). Chitinozoan records may also indicate problems with the GSSP section at Fågelsång (Vandenbroucke, 2004; Hennissen & others, 2010). A detailed correlation of the Sandbian graptolite succession, including the *Nemagraptus gracilis* Biozone and the overlying *Climacograptus bicornis* Biozone, is difficult to make (Williams & others, 2004).

The base of the Katian is defined at the level of the FAD of *Diplacanthograptus caudatus* (Lapworth, 1876a) in the Black Knob Ridge section, Oklahoma, USA (Goldman & others, 2007) and is followed by a rapid succession of first appearances of other graptolite species useful for a wider correlation of the level. Katian graptolite faunas are widely distributed, but the correlation is invariably difficult due to the presence of endemic faunal elements. A separate biozonation was established in the Appalachian Basin of eastern North America (Ruedemann, 1912, 1925a; Riva, 1974b; Goldman, Mitchell, & Joy, 1999; Achab & others, 2011) and is shown here (Fig. 77). It includes a number of endemic faunal

Series & Stages		Baltica	Avalonia/Britain	China	North America		South America/Argentina		Austral-asia
458.18 / 459	DARRIWILIAN	*Jiangxigraptus vagus*	*Hustedograptus teretiusculus*	*Jiangxigraptus vagus*	*Hustedograptus teretiusculus*		*Hustedograptus teretiusculus*		Da 4b
460		*Pseudamplexogr. distichus*	*Didymograptus murchisoni*	*Pseudamplexogr. distichus*			*Pseudamplexogr. distichus*		Da 4a
461 / 462		*Pterograptus elegans*		*Pterograptus elegans*	*Pterograptus elegans*		*Pterograptus elegans*		Da 4a
463		*Nicholsonograptus fasciculatus*	*Didymograptus artus*	*Nicholsonograptus fasciculatus*	*Nicholsonogr. fasciculatus*		*Nicholsonogr. fasciculatus*		Da 3
464		*Holmograptus lentus*	*Didymograptus artus*	*Acrograptus ellesae / Didymograptus artus*	*Holmogr. spinosus* / *Holmogr. lentus*		*Holmogr. spinosus* / *Holmogr. lentus*		Da 3
465 / 466		*Eoglyptograptus cumbrensis*	*Aulograptus cucullus*		*Levisograptus dentatus*	*Arienigr. angulatus* / *Levisogr. dentatus*	*Levisograptus dentatus*	*Arienigr. angulatus* / *Levisogr. dentatus*	Da 2
467.3 / 468 / 469		*Levisograptus austrodentatus* — *Levisograptus sinicus* / *Arienigraptus zhejiangensis*		*Levisograptus austrodentatus* — *Levisogr. sinicus* / *Arienigr. zhejiangensis*	*Levisograptus austrodentatus*	*Levisogr. sinicus* / *Arienigr. zhejiangensis*	*Levisograptus austrodentatus*	*Levisogr. sinicus* / *Arienigr. zhejiangensis*	Da 1
469.42	DAPINGIAN	*A. dumosus* / *P. manubriatus*	*Isograptus gibberulus*	*Exigraptus clavus*	*Oncograptus*		*Cardiograptus* / *Oncograptus*		Ya 1-2
470		*Isogr. mobergi* / *M. schmalenseei*	*Isograptus gibberulus*	*Expansogr. hirundo* / *Isogr. imitatus*	*Isogr. maximus*		*Isogr. maximus*		Ca 3-4
471 / 471.26		*Isograptus rigidus*	*Isogr. v. victoriae*	*Azygograptus suecius*	*Isogr. victoriae*		*Isograptus victoriae* / *Azygogr. lapworthi*		Ca 2

FIG. 76. Correlation of Middle Ordovician graptolite biozones. Shaded intervals indicate possible gaps.

elements of the genera *Geniculograptus* MITCHELL, 1987 and *Paraorthograptus* MU & others, 1974 that occur only in this basin (GOLDMAN & others, 2013). They represent the best example of a restriction of Upper Ordovician graptolite faunas to a certain biogeographic area.

The Katian includes a *Geniculograptus pygmaeus* Biozone in China (CHEN & others, 1995; ZHANG & others, 2019), but the taxon is not discussed or illustrated in MU and others (2002). Thus, because *Geniculograptus* is considered to be an endemic taxon of eastern North America, its presence in China may be questioned (GOLDMAN & others, 2013). *Alulagraptus uncinatus* (KEBLE & HARRIS, 1934) is used in Australia to determine the Australasian Bolindian 1 (Bo 1), the *Alulagraptus uncinatus* Biozone, in the middle Katian. The species was recently found in the *Anticostia macgregorae* beds in

East Qilianshan, northwestern China (CHEN & others, 2019), a region in which a highly local biostratigraphy was described for the Katian interval (not shown in Fig. 77). It is also common in the Bolindian 1 of Idaho, USA (CARTER, 1972; MITCHELL & others, 2003). A *Diceratograptus mirus* Subzone of the *Paraorthograptus pacificus* Biozone may be differentiated locally on the Yangtze Platform of China and in Nevada, USA (CHEN & others, 2006a; ŠTORCH & others, 2011).

The base of the Hirnantian is defined in the Wangjiawan North section, near Wangjiawan Village, Hubei Province, China, at the level of the FAD of *Metabolograptus extraordinarius* (SOBOLEVSKAYA, 1974) (CHEN, FAN, & others, 2005, Chen & others, 2006a). The whole Hirnantian is less than 80 cm thick in the type section. It includes the *Metabolograptus extraordinarius* Biozone, overlain by the *Metabolograptus persculptus*

Series & Stages	Baltica	Avalonia/Britain	China	North America		South America Argentina	Austral-asia
HIRNANT. Metabolograptus persculptus	Metabolograptus persculptus	Metabolograptus persculptus	Metabolograptus persculptus	Metabolograptus persculptus		Metabolograptus persculptus	Bo 5
	graptolite faunas unknown	Metabolograptus extraordinarius	Metabolograptus extraordinarius	Metabolograptus extraordinarius		Metabolograptus extraordinarius	Bo 4
KATIAN		Dicellograptus anceps	Diceratograptus mirus / Paraorthograptus pacificus	Paraorthograptus pacificus		possible gap	Bo 3
			Dicellograptus complexus	Dicellogr. ornatus	Paraorthogr. prominens	Dicellograptus ornatus	Bo 2
	Dicellograptus complanatus	Dicellograptus complanatus	Dicellograptus complanatus	Dicello-graptus complanatus	Dicello-graptus complanatus	Dicellograptus complanatus	Bo 1
	Pleurograptus linearis	Pleurograptus linearis	Dicellogr. elegans O. quadrimucronat.	Styraco-graptus tubuliferus	Paraorthogr. manitoulinensis	Styracograptus tubuliferus	Ea 4
			Geniculograptus pygmaeus ?		Geniculogr. pygmaeus		Ea 3
	Dicranograptus clingani	Dicranogr. clingani / Dicellogr. morrisi	Diplacanthogr. spiniferus	Diplacanthogr. spiniferus	Diplacanthogr. spiniferus	Diplacantho-graptus caudatus	Ea 2
		Diplacanthogr. caudatus	Diplacanthograptus caudatus	Diplacanthogr. caudatus	O. ruedemanni / C. americanus		Ea 1
SANDBIAN	Mesograptus foliaceus	Mesograptus foliaceus	Climacograptus bicornis	Climaco-graptus bicornis	Diplogr. foliaceus	Climacograptus bicornis	Gi 2
	Nemagraptus gracilis	Nemagraptus gracilis	Nemagraptus gracilis	Nemagraptus gracilis		Nemagraptus gracilis	Gi 1

FIG. 77. Correlation of Upper Ordovician graptolite biozones. Local biozonation of Appalachian Basin (*gray*).

Biozone. A thin limestone with the Hirnantian brachiopod fauna (the Kuanyinchiao bed) separates the graptolite biozones. CHEN and others (2006b) discussed the worldwide correlation of the Hirnantian Stage in some detail.

The British Upper Ordovician succession of ZALASIEWICZ and others (2009) combined elements of the biozonations used in Baltica and Scotland. A detailed biostratigraphic zonation for the Upper Ordovician of South America does not presently exist because few faunas have been described from this interval. ALBANESI and ORTEGA (2016) indicated a possible gap between the *Dicellograptus ornatus* Biozone (Katian) and the *Metabolograptus extraordinarius* Biozone (Hirnantian).

SILURIAN

After the introduction of the Silurian System by MURCHISON (1839), numerous changes were made before the modern concept emerged and series and stages were established. DAVIES and others (2011) provided the latest overview on its development in Britain, along with information to understand the individual chronostratigraphic intervals. According to MELCHIN, SADLER, and CRAMER (2020), the Silurian System is approximately 24.07 Ma long (443.07–419.0 Ma) and is quite unevenly differentiated into four series, the Llandovery (10.14 Ma), Wenlock (6.19 Ma), Ludlow (4.01 Ma), and Pridoli (3.73 Ma). Interestingly, the GSSPs were initially

defined biostratigraphically with reference to standard graptolite zones, although the index taxa for these zones are not present in some of the GSSP localities (MELCHIN, SADLER, & CRAMER, 2012, p. 526). Some of the stages are currently under revision and details may change accordingly (see MELCHIN, SADLER, & CRAMER, 2020). The main information on the Silurian graptolite biostratigraphy (Fig. 78–80) is based on LOYDELL (2012) with revisions as indicated herein.

THE LLANDOVERY SERIES

The Llandovery Series (Fig. 78) is differentiated into three stages: the Rhuddanian, Aeronian, and Telychian (BASSETT, 1985; HOLLAND, 1985; MELCHIN, COOPER, & SADLER, 2004). The base of the Rhuddanian is defined at Dob's Linn, Scotland, UK, at 1.6 m above the base of the Birkhill Shale at the level of the FAD of *Akidograptus ascensus* (COCKS, 1985). Originally, the base of the Rhuddanian was defined at the level of the FAD of *Parakidograptus acuminatus* (NICHOLSON, 1867a) in the same section, but due to a revison of the graptolite fauna, the definition was revised (MELCHIN & WILLIAMS, 2000; RONG & others, 2008).

The base of the Aeronian has been defined at a level "just below the level of occurrence of *Monograptus austerus sequens,* which indicates the *Demirastrites triangulatus* Zone" (MELCHIN, SADLER, & CRAMER, 2012, p. 526). ŠTORCH (2015) and ŠTORCH and MELCHIN (2019) discussed the graptolites from the Rhuddanian-Aeronian boundary interval of the Czech Republic. The authors redescribed the zonal index for the base of the Aeronian, *Demirastrites triangulatus* (HARKNESS, 1851), and the anagenetic changes in the *Demirastrites triangulatus* lineage. The GSSP level has recently been re-investigated at Rheidol Gorge, Wales, UK, since the original location was insufficient for further correlations (see MELCHIN & others, 2018). The gap in the late Aeronian of the Yangtze Platform of China indicated by LOYDELL (2012) can be closed, at least in part, by the record of *Stimulograptus sedgwickii* (PORTLOCK, 1843)

(MALETZ & others, 2021). MALETZ, WANG, and WANG (2021) recognized a considerably extended *Lituigraptus convolutus* Biozone in the Yichang region, Hubei Province, China, and subdivided it into the *Metaclimacograptus sculptus* and *Paramonoclimacis sidjachenkoi* subzones based on the common occurrence of the index species.

The base of the Telychian is defined between the LAD of the brachiopod *Eocoelia curtisi* ZIEGLER, 1966 and the FAD of *Eocoelia intermedia* (HALL, 1860), a level correlated to the base of the *Spirograptus turriculatus* Biozone by HOLLAND (1985). According to a revision of the genus *Spirograptus* GÜRICH, 1908*,* this level now equals the base of the *Spirograptus guerichi* Biozone (LOYDELL, ŠTORCH, & MELCHIN, 1993; MELCHIN, SADLER, & CRAMER, 2012). The detailed biostratigraphy of the *Spirograptus guerichi* and *Spirograptus turriculatus* biozones (seven subzones) in Wales, UK (LOYDELL, 1992) has not been used outside this region and is not discussed herein. MELCHIN, LENZ, and KOZŁOWSKA (2017) revised the Llandovery succession of Arctic Canada and subdivided the *Campograptus curtus* Biozone into two subzones, a lower *Demirastrites triangulatus/Demirastrites pectinatus* Subzone and a *Rastrites orbitus* Subzone.

THE WENLOCK SERIES

The base of the Wenlock Series and the Sheinwoodian Stage (Fig. 79) is defined in the Hughley Brook section, Shropshire, UK, at the base of bed G of the Buildwas Formation (BASSETT & others, 1975; HOLLAND, 1980; MARTINSSON, BASSETT, & HOLLAND, 1981). This level was supposed to correlate with the base of the *Cyrtograptus centrifugus* Biozone, but no graptolites were found in the section. The inference was, in fact, based on other localities. MULLINS and ALDRIDGE (2004) indicated that the GSSP level correlates with a level in the upper *Cyrtograptus centrifugus* Biozone or the lower *Cyrtograptus murchisoni* Biozone. MELCHIN, SADLER, and CRAMER (2012) considered the GSSP level to be in the lower part of the *Cyrtograptus murchisoni* Biozone. The

Series & Stages	Britain Avalonia/Baltica	Peri-Gondwana	China	Laurentia Arctic Canada	Gondwana North Africa
432.93	Cyrtograptus murchisoni	Cyrtograptus murchisoni	not recognized	Cyrtogr. murchisoni	not recognized
	Cyrtograptus centrifugus	Cyrtograptus centrifugus		Cyrtograptus centrifugus	
434	Cyrtograptus insectus	Cyrtograptus insectus		Cyrtograptus insectus	
	Cyrtograptus lapworthi	Cyrtograptus lapworthi	C. sakmaricus / C. lapworthi	Cyrtograptus sakmaricus	
435	Oktavites spiralis	Oktavites spiralis	Monoclimacis geinitzi / Oktavites spiralis	Oktavites spiralis	
	Monoclimacis crenulata	Torquigraptus tullbergi	Torquigraptus tullbergi	Monoclimacis crenulata/ Monoclimacis griestoniensis	Metaclimacograptus flamandi + Parapetalolithus meridionalis
436	Monoclimacis griestoniensis	Monoclimacis griestoniensis	'Monoclimacis griestoniensis'		
	Streptograptus sartorius	Streptograptus crispus			
437	Streptograptus crispus		Streptograptus crispus	Streptograptus crispus	
438	Spirograptus turriculatus	Spirograptus turriculatus	Spirograptus turriculatus	Spirograptus turriculatus	Spirograptus turriculatus + Spirograptus guerichi
438.59	Spirograptus guerichi	Spirograptus guerichi	Spirograptus guerichi	Spirograptus guerichi	
	Stimulograptus halli	Stimulograptus sedgwickii	Stimulograptus sedgwickii	Stimulograptus sedgwickii	Stimulograptus sedgwickii
439	Stimulograptus sedgwickii				
	Lituigraptus convolutus	Lituigraptus convolutus	Lituigr. convol. / P. sidjachenkoi / M. sculptus	Lituigraptus convolutus	Lituigraptus convolutus
440	Pribylograptus leptotheca	Pribylograptus leptotheca	Pribylograptus leptotheca	Campograptus curtus	Pribylograptus leptotheca
	Neodiplograptus magnus	Demirastrites simulans	Coronograptus gregarius	Rastrites orbitus	Coronograptus gregarius/ Paraclimacograptus lybicus
	Demirastrites triangulatus	Demir. pectinatus / D. triangulatus		D. pectinatus / D. triangulatus	
440.49	Coronograptus cyphus	Coronograptus cyphus	Coronograptus cyphus	Coronograptus cyphus	Neodiplograptus fezzanensis
	Lagarograptus acinaces	Cystograptus vesiculosus	Cystograptus vesiculosus	Lagarograptus acinaces	Neodiplograptus africanus
442	Atavograptus atavus			Atavograptus atavus	
	P. acuminatus / A. ascensus	P. acuminatus	P. acuminatus	P. acuminatus	Neodiplograptus imperfectus / Neodiplograptus incommodus / Parclimacograptus kiliani / Normalograptus tilokensis
443.07		A. ascensus	A. ascensus	A. ascensus	

FIG. 78. Correlation of Llandovery (Rhuddanian to Telychian) graptolite biozones.

Sheinwoodian is largely zoned by species of the genus *Cyrtograptus* CARRUTHERS in MURCHISON, 1867a, which are the most conspicuous faunal elements. LOYDELL and LARGE (2019) revised the British biozonation of the Sheinwoodian slightly and eliminated the *Cyrtograptus perneri/Cyrtograptus ramosus* Biozone (see LOYDELL, 2012, fig. 5) in the uppermost Sheinwoodian. LENZ and others (2012) revised the succession of Arctic Canada. ZALASIEWICZ and others (2009) listed *Cyrtograptus perneri* BOUČEK, 1933 from the British *Cyrtograptus lundgreni* Biozone of basal Homerian age and questionably from the *Cyrtograptus rigidus* Biozone of the latest Sheinwoodian age.

The base of the Homerian is defined at the level of the FAD of *Cyrtograptus lundgreni*

Tullberg, 1883 at Sheinton Brook, Homer, UK (Holland, 1980; Martinsson, Bassett, & Holland, 1981). The Homerian time interval includes one of the largest extinction events in graptoloid history, the *Lundgreni* Extinction Event (Koren', 1987; Jaeger, 1991), during which most graptoloid taxa disappeared at the top of the *Cyrtograptus lundgreni* Biozone (e.g., Jaeger, 1991). Porěbska, Kozłowska-Dawidziuk, and Masiak (2004) discussed three separate events from the local biostratigraphic scheme of the Bartoszyce section of Poland (Fig. 79), partly supported by an investigation by Manda and others (2019) from the Czech Republic. Both suggested additional graptolite biozone intervals above the *Cyrtograptus lundgreni* Biozone and below the *Pristiograptus parvus* interval. However, these biozone intervals are not recognized worldwide.

Barca and Jaeger (1990) refined the Wenlock graptolite biostratigraphy supported by the detailed work of Koren' (1992, 1994) from Central Asia. The Wenlock is poorly represented in China, and very few graptolites have been described from this region. Chen (1984) provided information on the Silurian graptolite biozonation, including the Wenlock succession of southern Shaanxi, China as the most complete succession of this interval, listing a number of biozones defined by *Cyrtograptus* species. Lenz, Chen, and Ni (1996) discussed Wenlock to Pridoli graptolites from Guangxi, China and recognized a few levels with late Homerian (late Wenlock) and Gorstian to early Ludfordian (Ludlow) graptolites. They also reported a single taxon from the Pridoli, *Monograptus* cf. *rectiformis* Přibyl, 1981. Ni (1997) described a fauna of late Homerian graptolites from western Yunnan, China, indicating the presence of the *Colonograptus praedeubeli/Colonograptus deubeli* Biozone.

THE LUDLOW SERIES

The Ludlow Series and Gorstian Stage (Fig. 79) have their stratotype at Pitch Coppice, Shropshire, England, UK, at the base of the Lower Elton Formation, based on the level of the FAD of *Neodiversograptus nilssoni* (Barrande, 1850) (Holland, 1980; Holland & Bassett, 1989). However, the fossil record of the GSSP section is extremely poor and unreliable; only two poorly preserved specimens identified as *Neodiversograptus nilssoni* and *Saetograptus varians* (Wood, 1900) have been discovered (White, 1981). Štorch and others (2016) discussed the graptolite fauna of the Wenlock-Ludlow boundary interval of the Czech Republic. These authors stated that *Saetograptus varians* first appeared in the biostratigraphically higher *Lobograptus progenitor* Biozone. Biostratigraphically important successions are present in Arctic Canada (Lenz & Kozłowska-Dawidziuk, 2004), Kyrgyzstan (Koren' & Sujarkova, 2004) and the East European Platform (Urbanek & Teller, 1997).)

Many of the late Wenlock (*Cyrtograptus lundgreni* Biozone) to Ludlow (*Saetograptus leintwardinensis* Biozone) graptolites are known from chemically isolated specimens collected from glacial boulders of northern Germany and Poland (e.g., Urbanek, 1958; Radzevičius & others, 2010; Maletz & Schöning, 2017). This material has its origin in the Silurian foreland basin succession of the Colonus Trough of Scania, southern Sweden (Beier, Maletz, & Böhnke, 2000; Eriksson, 2012), which is poorly exposed. These graptolites have been investigated mainly in drill core material from Poland (e.g., Urbanek, 1963, 1966, 1970).

THE PRIDOLI SERIES

Kříž and others (1986) discussed and defined the Přídolí (now Pridoli) Series (Fig. 80) in great detail, based on the GSSP section in the Prague Basin. The level of the FAD of *Skalograptus parultimus* (Jaeger, 1975) defines the base of the Pridoli. Their work also provided a detailed graptolite biostratigraphy of the whole interval. Teller (1997a, 1997b) and Urbanek (1997a) provided the latest overview on the Pridoli graptolite biostratigraphy and taxonomy of the East European Platform. Ni, Lenz, and Chen (1998) discussed the record of Pridoli graptolites in China and recognized only a single biozone, based on collections

Series & Stages	Baltica/ E. European Platform	Peri-Gondwana (Europe)	Britain	Laurentia Arctic Canada
422.73 / 423 — LUDLOW / LUDFORDIAN	Uncinatograptus spineus	Formosograptus formosus	No later zones recorded in Britain	Formosograptus formosus
	Uncinatogr. protospineus			
	Uncinatograptus acer			
424	Ps. latilobus/S. balticus	Ps. latilobus/S. balticus		Bohemograptus tenuis + Bohemograptus praecornutus
	Neocucullogr. kozlowskii	Neocucull. kozlowskii		
	Neocucull. inexpectatus	Neocucull. inexpectatus		
	Neolobogr. auriculatus	Bohemograptus tenuis	Bohemograptus	
	Bohemograptus cornutus			
	Bohemogr. praecornutus		Saetograptus leintwardinensis	
425.01	C. aversus/S. leintwardinensis	Saetogr. linearis		'M.' ceratus-S. linearis
LUDLOW / GORSTIAN	Cucullogr. hemiaversus	Lobograptus scanicus/ Saetograptus chimaera	Saetograptus incipiens	Lobograptus scanicus
	Lobograptus invertus			
426	Lobogr. parascanicus		Lobograptus scanicus	
	Lobograptus progenitor	Lobograptus progenitor	Neodiversograptus nilssoni	Lobograptus progenitor
426.74	Neodiversogr. nilssoni	Neodiversogr. nilssoni		
427 — WENLOCK / HOMERIAN	Colonograptus ludensis	Colonograptus ludensis	Colonograptus ludensis	Colonograptus ludensis
428	Colonograptus deubeli + Colonogr. praedeubeli	Colonograptus deubeli+ Colonogr. praedeubeli		Colonograptus deubeli+ Colonograptus praedeubeli
429	Gothograptus nassa	Gothograptus nassa	Gothograptus nassa	Pristiograptus dubius+ Gothograptus nassa
	Pristiograptus dubius / M. flemingii/P. dubius / Testograptus testis (Poland)	Pristiograptus parvus		
430 / 430.62	Cyrtograptus lundgreni	Cyrtograptus lundgreni	Cyrtograptus lundgreni	Cyrtograptus lundgreni
431 — WENLOCK / SHEINWOODIAN	Cyrtograptus perneri	Cyrtograptus perneri/ Cyrtograptus ramosus	Cyrtograptus rigidus	Cyrtograptus perneri
	Cyrtograptus rigidus	Cyrtograptus rigidus+ Monogr. belophorus		Monograptus opimus
432	Pristiograptus dubius	Pristiograptus dubius	Pristiograptus dubius	Monoclimacis flumendosae
	Monogr. riccartonensis	Monograptus riccartonensis	Monograptus riccartonensis	Monograptus instrenuus Cyrtograptus colobus
433	Monograptus firmus	Cyrtograptus murchisoni	Monograptus firmus	Cyrtograptus murchisoni
432.93	Cyrtograptus murchisoni		Cyrtograptus murchisoni	

FIG. 79. Correlation of Wenlock-Ludlow (Silurian) graptolite biozones.

from northern Xinjiang, northwest China. The fauna is similar to that described by KOREN' (1983, 1989) from Kazakhstan and KOREN' and SUJARKOVA (1997) from southern Tian Shan, Kyrgyzstan. LENZ and KOZŁOWSKA-DAWIDZIUK (2004) introduced the *Uncinatograptus birchensis* Biozone in the Arctic Islands, Canada, and suggested

it to be largely of basal Devonian age. They suggested a possible latest Silurian age for the base of the interval, but LENZ (2013) included it entirely in the Pridoli.

DEVONIAN

It is well established that planktic graptolites range biostratigraphically into the Lower Devonian (Fig. 80), but the exact level of their disappearance is still in discussion. The base of the Devonian System is defined at the level of the FAD of *Uncinatograptus uniformis* (PŘIBYL, 1940a) in the Klonk section, Czech Republic (CHLUPÁČ & KUKAL, 1977; CHLUPÁČ & VASEK, 2003). The absolute ages of the Devonian graptolite zone FADs are based on BECKER, GRADSTEIN, and HAMMER (2012) and indicate a much longer duration of Early Devonian graptolite biozones in comparison with the Silurian time intervals (Fig. 80). The base of the Pragian Stage (Lower Devonian) is based on the level of the FAD of the conodont *Eognathodus sulcatus sulcatus* PHILIP, 1965 in the Velká Chuchle Quarry, Czech Republic. This level is considered to be above the *Uncinatograptus hercynicus* graptolite zone (CHLUPÁČ & OLIVER, 1989). The base of the Emsian is defined at the level of the FAD of the conodont *Polygnathus kitabicus* YOLKIN & OTHERS, 1994 in Uzbekistan (YOLKIN & others, 1997), but a discussion for revision has begun (CARLS, SLAVÍK, & VALENZUELA-RÍOS, 2008). JAEGER (1978b) suggested an early Emsian age for the youngest monograptids and later supported this view in his discussion of the correlation with the conodont record (JAEGER, 1988). JAEGER (1970, 1978b, 1988) described the Devonian graptolite biostratigraphy in some detail using all data available to him at the time. JAEGER (1970) suggested *Uncinatograptus pacificus* JAEGER in CHURKIN, JAEGER, and EBERLEIN, 1970 as the youngest Devonian monograptid and established the *Uncinatograptus pacificus* Biozone as the latest graptolite zone, but it is now known that the interval can be correlated with the *Uncinatograptus yukonensis* Biozone (LENZ, 2013).

KOREN' (1974, 1975, 1978) discussed the Early Devonian graptolite faunas of central Asia. LENZ (2013) provided the most recent overview on the Early Devonian graptolite faunas of the Arctic Islands, Canada, which has a fairly high number of these faunas interpreted as cosmopolitan. PORĚBSKA (1984) described the Early Devonian graptolites from the Bardo Mountains and established a very detailed biostratigraphy for the region. The author discussed a 30 cm thick linograptid interregnum (PORĚBSKA, 1984) at the top of the Pridoli *Skalograptus transgrediens* Biozone that LENZ (2013) correlated with the *Uncinatograptus birchensis* Biozone of Arctic Canada.

LENZ (1988) recognized *Uncinatograptus yukonensis* (JACKSON & LENZ, 1963) as the youngest Devonian monograptid in the Yukon region of Canada. LENZ (2013) rejected the *Uncinatograptus pacificus* Biozone of JAEGER (1970) due to new records in Arctic Canada and considered the *Uncinatograptus yukonensis* Biozone as the youngest Devonian graptolite biozone (Fig. 80). CHEN and others (2015) revised the Devonian graptolite faunas of China (Fig. 80) and differentiated four biozones, stating that the succession has only moderate diversity and that certain intervals are not recognizable by their index species. However, this general succession compares well with the worldwide standard.

THE DURATION OF GRAPTOLITE BIOZONES

The duration of graptolite biozones has always been considered quite variable, and the duration of Silurian intervals was regarded as shorter than the Ordovican or Devonian intervals (RICKARDS, 1976; HUGHES, 1995; ZALASIEWICZ & others, 2009). The advent of radiometric dating finally provided better information on the precise duration of biostratigraphic intervals, but there are few reliable radiometric dates from the early Paleozoic. LOYDELL (2012) used the timescale of OGG, OGG, and GRADSTEIN (2008) to estimate the duration of graptolite

Series & Stages			Baltica/ East European Platform	Laurentia Arctic Canada	China
406		EMSIAN	EXTINCTION OF PLANKTIC GRAPTOLITES		
407	LOWER DEVONIAN		faunas not reported	*Uncinatograptus yukonensis*	*Uncinatograptus yukonensis*
408		PRAGIAN			
409			*Uncinatograptus craigensis*		
410			*Uncinatograptus thomasi*		
411			*Neomonograptus fanicus*	*Neomonograptus falcarius*	*Neomonograptus falcarius*
		LOCHKOVIAN	*Neomonograptus falcarius*		
412			*Uncinatograptus hercynicus*	*Uncinatograptus hercynicus*	*Uncinatograptus praehercynicus*
413					
414			*Uncinatograptus praehercynicus*	*Uncinatograptus uniformis*	
415					
416			*Uncinatograptus uniformis*		*Uncinatograptus uniformis*
417					
418					
419				*Uncinatograptus birchensis*	
	SILURIAN	PRIDOLI	*Skalograptus transgrediens*	*Skalograptus transgrediens*	faunas not reported
420			*Skalograptus perneri*	*Skalograptus bouceki*	*Skalograptus bouceki*
			Skalograptus bouceki		
421			*Skalograptus samsonowiczi*	*Skalograptus branikensis*	faunas not reported
			Skalograptus chelmiensis		
422			*Skalograptus lochkovensis*		
			Skalograptus ultimus	*Skalograptus ultimus*	
422.73			*Skalograptus parultimus*	*Skalograptus parultimus*	

FIG. 80. Correlation of Pridoli (Silurian) and early Devonian graptolite biozones.

zones. General estimates for the Early and Middle Ordovician based on GRADSTEIN and others (2020) indicate a duration of ~1 Ma for a graptolite biozone and a duration of ~1.5 Ma for a graptolite biozone in the Late Ordovician. The estimates are between 400,000 and 600,000 years for the Silurian and ~2 Ma for the Lochkovian. The estimation for the Pragian, the youngest interval for a graptolite biozone, is ~1.5 Ma. Only a few intervals may be zoned more precisely, as the differentiation of

the *Spirograptus guerichi* and *Spirograptus turriculatus* biozones demonstrates. LOYDELL (1992, fig. 7) indicated a combined seven subzones for this interval, which lasted ~1 Ma.

Because graptolites are most common in dark and black shales, in which other fossils are rare or lacking, a precise correlation of the graptolite biostratigraphy with the succession of other fossil groups may be difficult. More information on other groups exists in biostratigraphic literature and especially in the discussion of chronostratig-

raphy (see GRADSTEIN & others, 2012; OGG, OGG, & GRADSTEIN, 2016). Biostratigraphic relevant acritarchs and chitinozoans are most commonly associated with graptolites; but because they are microfossils, different methods have to be used for their extraction from the sediments. Graptolites are associated in limestones with numerous other fossils, including conodonts, radiolarians, ostracods, and other small organisms; and these cases can be used for direct biostratigraphic integration (e.g., BERGSTRÖM, 1986; NOBLE & MALETZ, 2000).

Graphic correlation and quantitative biostratigraphy is very useful—and in some cases, absolutely key—to determining biostratigraphic successions and gaining insight into the correlation of various fossil groups as well as to integrating sedimento-logical data and event horizons with paleontological data (SADLER, 2004, 2012; SADLER, COOPER, & MELCHIN, 2009, 2011; SADLER, COOPER & CRAMPTON, 2014; GOLDMAN, NÕLVAK, & MALETZ 2015). Efforts to produce a more precise chronostratigraphic time scale for the Paleozoic have been undertaken by integration of various means (CRAMER & others, 2010).

Automated stratigraphic correlation (see SADLER, 2004, 2012) integrates biostratigraphic and chemostratigraphic data with radiometric dates, producing a single composite of stratigraphic data. This method has increasingly been used to develop the Ordovician and Silurian time scales. It has also enabled analysis of the changing global graptolite biodiversity and its relationship with environmental change.

PALEOGEOGRAPHY OF THE HEMICHORDATA

JÖRG MALETZ

INTRODUCTION

Nearly all organisms exhibit at least some biogeographic restriction in their distribution, and this aspect has commonly been used to interpret paleogeographic issues in geology, e.g., plate tectonic configuration, oceanic development, latitudinal differentiation. Plate tectonics is one of the major aspects, initially relying largely on paleontological data and dating back to WEGENER (1915), even though the concepts of continental drift and modern plate tectonics appear to describe somewhat different things. Still, they are based on various geological and paleontological investigations, and modern plate tectonics and paleobiogeography are closely connected (see HARPER & SERVAIS, 2013; TORSVIK & COCKS, 2013).

The Graptolithina, one of the major fossil groups of all marine environments in the early Paleozoic, are not an exception when we, as paleontologists, think of Paleozoic paleobiogeography. However, little is known on the biogeographic distribution of their sister group, the Enteropneusta. Extinct taxa are known only from a few specimens, and extant taxa have not been in the focus of biologists either. Thus, their biogeographical distribution is very incompletely documented. Even the precise biogeographic distribution of the extant Pterobranchia is largely unknown, as the recent description of the first *Rhabdopleura* ALLMAN in NORMAN, 1869a species in the Mediterranean demonstrates (BELI & others, 2018). Equally, not a single species of the non-colonial Cephalodiscida has been discovered in the Mediterranean to date, but a new *Cephalodiscus* M'INTOSH, 1882 species from Sagami Bay, Japan, was recently introduced by MIYAMOTO, NISHIKAWA, and NAMIKAWA (2020). Therefore, the remark, that "rhabdopleurids can only be found close to marine research stations" (MALETZ, 2017a, p. 12), is not just an oversimplification, but clearly shows that scientific interest often limits our knowledge and that more new records of Pterobranchia may be expected in the future.

EXTANT HEMICHORDATA

The two extant groups of the Hemichordata have not attracted much scientific interest by biologists in a long time, and even knowledge of their living taxa is relatively poor, while the fossil Graptolithina, as an exception, has gained considerable interest by paleontologists and geologists in the past due to their application in biostratigraphic interpretations and the dating of marine sedimentary sequences.

Extant enteropneusts are widely distributed and occur in marine environments from shallow water shelf regions to the deep waters of the abyssal regions of the oceans and can also be found attached to rocks close to hydrothermal vents at the mid-ocean ridges (WOODWICK & SENSENBAUGH, 1985). Four families can be differentiated, all exclusively in marine regions, usually burrowing into the sediment and rarely living as epibenthos (CAMERON, 2018). The epibenthic torquaratorids have been discovered only quite recently. Thus, their record is still extremely spotty; and, due to their dwelling in deeper oceanic regions, it is difficult to ascertain their possibility for a worldwide biogeographic distribution (JABR, 2017; JABR, ARCHAMBAULT, & CAMERON, 2018). Valuable zoogeographical conclusions are also unavailable for the other enteropneust families, because most species have been reported from a single locality only or are known from relatively small geographical regions (CAMERON, DELAND, & BULLOCK, 2010). Only a few species have been described from larger regions or are
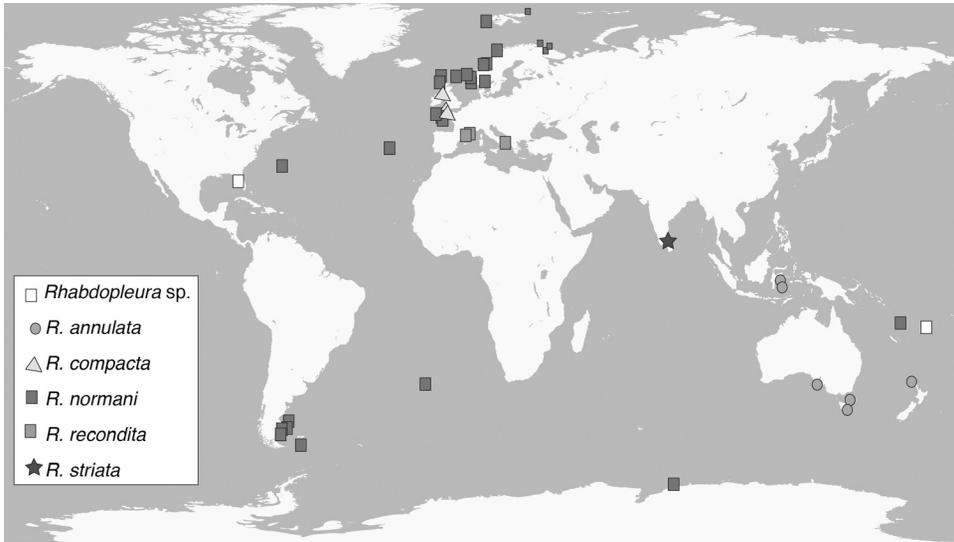
Fig. 81. Global distribution of *Rhabdopleura* Allman in Norman, 1869a species (adapted from Beli & others, 2018, fig. 4).

reported to have a wider but often patchy and discontinuous distribution. The documented distribution of extant enteropneusts may be interpreted in different ways as relict populations, either of once more widely distributed taxa or as the result of too little systematic search. Cameron, Deland, and Bullock (2010) suggested that the enteropneusts represent an ancient and declining group, which may be supported by their spotty fossil record and their possibly early Cambrian origin (Maletz, 2019a).

Beli and others (2018) discussed the biogeographical distribution of extant rhabdopleurids and differentiated five species of which *Rhabdopleura normani* Allman in Norman, 1869a appears to be the taxon with the widest geographical distribution. It is present in the northern and southern Atlantic Ocean but has also been collected in the Antarctic Ocean (Fig. 81). Rhabdopleurids occur from the deeper waters of the polar regions to the shallow tropical regions close to the equator and, thus, do not have extensive ecological restrictions.

The relatively uneven geographical distribution of the few known taxa (Fig. 81) may be based on lack of scientific interest and the difficulty of collecting these small and inconspicuous organisms.

FOSSIL HEMICHORDATA

Fossil hemichordates are largely known from the tubaria of the Graptolithina, whereas the fossil Enteropneusta are too rare to provide sufficient information for a paleobiogeographic interpretation. Cameron (2018) discussed the fossil material of the Enteropneusta, of which the most specimen-rich material comes from the Burgess Shale of British Columbia, Canada and includes specimens of *Spartobranchus tenuis* (Walcott, 1911) and *Oesia disjuncta* Walcott, 1911, also representing the oldest known enteropneusts. None of the fossil taxa are known from more than one locality and most taxa are described from single specimens, except for the Carboniferous *Mazoglossus ramsdelli* Bardack, 1997 from the Mazon Creek fauna of Illinois, USA, which is a moderately common species (Maletz, 2014a; Cameron, 2016).

Large data sets on fossil graptolite faunas have been collected in the past and provide a good insight into the ecology and paleobiogeography of the Graptolithina (see
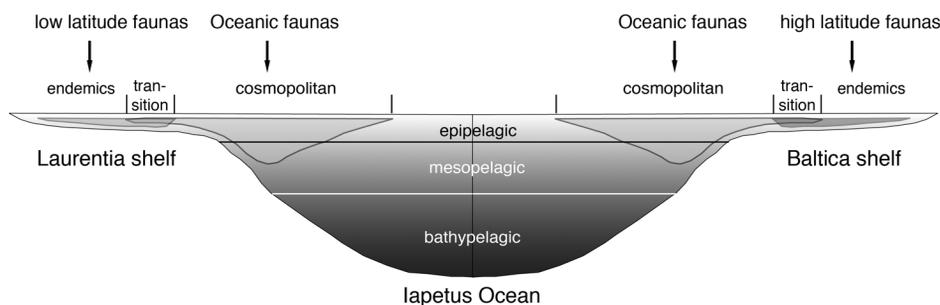
FIG. 82. Biogeographical and paleoecological distribution of the Graptolithina across the Lower Paleozoic Iapetus Ocean, showing endemic and cosmopolitan oceanic graptolite faunas, as well as shallow to deeper water distributions (adapted from Maletz & others, 2011, fig. 9).

COOPER & others, 2004, 2017; GOLDMAN & others, 2013). The problems of precise biostratigraphic correlation between continents during the Lower to Middle Ordovician initiated the research into the paleobiogeography of graptolite faunas. A number of factors were suggested to be responsible for faunal differentiations (e.g., BERRY, 1960, 1962a, 1979; BOUČEK, 1972; ROSS, 1961; BERRY & BOUCOT, 1972; CISNE & CHANDLEE, 1982; BULMAN, 1964, 1971a), leading to two main competing models to explain the ecological controls on graptolite species distribution. SKEVINGTON (1973, 1974) discussed the cool-temperate Atlantic Province and the paleo-tropical Pacific Province and considered latitudinal variation in surface water temperature as the main control for graptolite provincialism. CISNE and CHANDLEE (1982) suggested a depth stratification model to explain graptolite distribution patterns during the Late Ordovician Utica Shale of the Taconic foreland basin of the northeastern Appalachians (USA); FINNEY (1986) explained the same pattern by lateral differentiation of water mass specificity and not depth stratification. COOPER, FORTEY, and LINDHOLM, 1991 and COOPER and others (2012, 2017) recognized a shallow epipelagic biotope with cosmopolitan species, combining two models: 1) a deeper mesopelagic biotope, the isograptid biofacies; and 2) an inshore biotope that included largely endemic species, the didymograptid biofacies. MALETZ and others

(2011) discussed the faunal differentiation on a transect across the Iapetus Ocean from the moderate to higher latitudes of Baltica to the low latitudes of Laurentia (Fig. 82) during the Darriwilian (Middle Ordovician) and recognized endemic and pandemic faunal elements due to their presence and absence. GOLDMAN and others (2013) stated that both depth and surface temperature played an important role in the biogeographic differentiation of graptolite faunas. The authors also suggested discussing graptolite distributions in terms of low, medium, and high latitudes and abandoning the Atlantic and Pacific Provinces of SKEVINGTON (1973, 1974), which are based on modern geographical concepts and not applicable to plate tectonic configurations in the Paleozoic. The main differentiation of Paleozoic planktic graptolite faunas is clearly based on paleo-latitude, but certain graptolite taxa may be restricted to a certain paleocontinent or restricted depositional basin (GOLDMAN & other, 2013). Thus, a latitudinal gradation from low latitude to high latitude faunas is combined with true endemicity based on other factors in the Paleozoic oceans.

BIOGEOGRAPHY

GOLDMAN and others (2013) provided a current overview on the knowledge of biogeographical differentiation of planktic graptolite faunas through time and is useful to consult for details. Paleogeographic interpretations are based on plate tectonic

reconstructions of which the Scotese maps (McKerrow & Scotese, 1990; www.Scotese.com) are the best known. Early Paleozoic paleogeography has generated considerable interest in recent years (Harper & Servais, 2013) and sedimentological and paleontological data still form a considerable part of the interpretations (Torsvik & Cocks, 2013) to which data on the distribution of individual graptolite taxa may be added (Fig. 83). Biogeographic differentiation of graptolite faunas is best known from the Ordovician, a time period that numerous papers have identified as having a high endemicity of graptolite faunas (Goldman & others, 2013).

Unfortunately, there is no information available for the paleogeographical distribution of the dendroid (benthic) graptolites. They are usually described from small fragments of their colonies, and complete, undistorted specimens are comparatively rare. It is likely that their distribution is restricted by temperature barriers, as is the distribution of some planktic taxa. Otherwise, a restriction of individual species or even genera to certain paleocontinental plates may be supposed but cannot be verified.

THE ORDOVICIAN

The base of the Tremadocian experienced a rapid dispersal of early planktic graptolites and any biogeographic differentiation is lacking, as can be surmised from the worldwide correlation of graptolite zones (see Cooper & others, 1998; Cooper, 1999; Loydell, 2012). The middle Tremadocian genus *Bryograptus* Lapworth, 1880a demonstrates the start of some faunal differentiation, as it appears to be restricted to the cooler water regions of higher latitudes (Maletz, Egenhoff, & Alonso, 2010), possibly indicating the start of a general biogeographic faunal differentiation. In the upper Tremadocian, *Kiaerograptus supremus* Lindholm, 1991 represents another taxon restricted to high latitude regions (Lindholm, 1991; Maletz & Egenhoff, 2001). The best-known and investigated interval to

document Ordovician graptolite biogeography appears to be the Floian to Darriwilian time interval (Cooper, Fortey, & Lindholm, 1991; Goldman & others, 2013). During this time interval, the planktic graptolite faunas attained a diversity and faunal differentiation not known in this extreme in younger time intervals.

The problems of the differentiation of pendent didymograptids (Berry, 1960, 1967; Skevington, 1963b; Cooper & Fortey, 1982; Maletz, Goldman, & Cone, 2005), commonly used for biostratigraphic purposes, led to the detailed investigation of their proximal end construction and a revision of taxonomy and biostratigraphy of the Floian to Darriwilian graptolite faunas (Cooper & Fortey, 1982; Gutiérrez Marco, 1986; Maletz, 1994b, 2010a; VandenBerg, 2018a). Thus, a number of graptoloid genera occurring in high latitudes (*Aulograptus* Skevington, 1965; *Azygograptus* Nicholson & Lapworth in Nicholson, 1875; *Baltograptus* Maletz, 1994b; *Didymograptus* M'Coy in Sedgwick & M'Coy, 1851–1854; *Jenkinsograptus* Gutiérrez-Marco, 1986) and low latitudes (*Didymograptellus* Cooper & Fortey, 1982; *Paraglossograptus* Mu in Mu & others, 1962; *Yutagraptus* Riva, 1994) were differentiated and are useful as biostratigraphical markers in the individual regions (Beckly & Maletz, 1991; Maletz, 1994b; Toro 1996; Toro & Maletz, 2007). Due to the co-occurrence with other pandemic faunal elements in mixed assemblages, these endemics can generally be correlated indirectly with coeval shallow-water endemic faunas from other continental regions. During the Dapingian, the isograptids formed the main stock of pandemic faunal elements and were used extensively for long distance biostratigraphic correlations (Harris, 1933; Cooper, 1973; Williams & Stevens, 1988; Maletz, 2011a). They were very useful to correlate many largely endemic faunas of this time interval. Fortey and Cocks (1986) even successfully used the presence of isograptids, the isograptid biofacies, to infer the presence

of oceanic basins and the rims of ancient continents.

The base of the Darriwilian had a major rearrangement of graptolite faunas with the evolution of the Axonophora, and faunal differentiation became more difficult due to the apparent similarities of flattened biserial graptolites in shales. However, axonophorans can also be demonstrated to have a considerable provincialism in the Middle and Late Ordovician, and a number of endemic taxa have been described (MALETZ & others, 2007; GOLDMAN & others, 2013). In eastern and southeastern North America, the endemic genus *Geniculograptus* MITCHELL, 1987 evolved during the Late Ordovician but is absent even in western Laurentia, leading to considerable problems in the intra-continental correlation of Laurentia as well as correlation to other continents (RIVA, 1969, 1974b; BERRY 1977; BERGSTRÖM 1978; GOLDMAN, BERGSTÖM, & MITCHELL, 1995). Some of the apparent faunal endemism of the South China platform faunas has been revised by the discovery of species previously considered to be endemic in other regions (e.g., *Tangyagraptus* MU, 1963a; CHEN, MELCHIN, & others, 2005; GOLDMAN & others, 2007).

Provinciality increased throughout the later Ordovician (Katian) due to the onset of climate change leading to the Hirnantian glaciation. Faunal differences made it increasingly difficult to correlate between low latitude and high latitude faunal localities during this time interval (e.g., WILLIAMS & others, 2003; ZALASIEWICZ, RUSHTON, & OWEN, 1995).

A major reorganization of graptolite faunas occurred due to the Hirnantian glaciation in the latest Ordovician. The Dicranograptidae-Diplograptidae-Orthograptidae (or DDO) faunas of MELCHIN and MITCHELL (1991) were rapidly replaced by species of *Normalograptus* LEGRAND, 1987 (their Monograptidae fauna; now the Neograptina) that invaded from the southern high latitudes (GOLDMAN & others, 2011). During the *Metabolograptus extraordinarius* to *Metabolograptus persculptus* biozones, neograptine

FIG. 83. Floian, Lower Ordovician paleobiogeography showing the distribution of *Baltograptus* species in *dark gray* (high latitude faunas). Low latitude faunal regions in *light gray*. Cross-section line shows approximate position of section in Fig. 82 (adapted from Egenhoff & Maletz, 2007, fig. 2).

elements dominated the graptolite faunas and the diplograptines were forced into extinction. The neograptines originated during the early Darriwilian and experienced a dramatic radiation that formed the base from which all clades of the Silurian and Early Devonian graptoloids (e.g., ŠTORCH & others, 2011; MALETZ, 2019b) originated.

THE SILURIAN

Graptolite provincialism during the Silurian has only more recently been explored and commonly has been considered as of lesser degree than graptolite provincialism in the Ordovician, especially as a standard biozonation was easily applied in the Silurian (e.g., RICKARDS, 1976; KOREN' & others, 1995, 1996; LOYDELL, 2012). ŠTORCH (1998b) and LEGRAND (2009) discussed the endemic graptolite faunas of the northwest African part of Gondwana, interpreted as a distinct cool water paleobiogeographic region during the Llandovery and Wenlock, with the strongest endemicity present during the late Hirnantian to Rhuddanian. MELCHIN (1989) demonstrated that a number of taxonomic groups were

restricted to the paleotropical regions of Laurentia, Baltica, Siberia, Kazakhstan, and China and considered these as a circum-equatorial faunal province, supported by the interpretation of RICKARDS, RIGBY, and HARRIS (1990). ŠTORCH (1998b) noted that the lower paleolatitude regions of Avalonia and southern Baltica represent transitional faunas between the cooler-water faunas of the peri-Gondwanan and circum-equatorial regions. Little is known about biogeographic differences in the Ludlow to Pridoli interval (e.g. KOREN', 1979; BERRY & WILDE, 1990). However, according to GOLDMAN and others (2013), considerable differences in the faunal composition between Kazhakstan, northern Laurentia, and Bohemia (see KOREN', 1989; LENZ, 1988, 1990; PŘIBYL, 1983) may indicate the presence of faunal provinces in the late Silurian.

THE DEVONIAN

The graptolite faunas of the Devonian have low diversity and no apparent biogeographic provinciality. JAEGER (1978b, 1988) discussed a worldwide distribution of Lower Devonian graptolite faunas, but it is clear from new paleogeographic interpretations that these faunas appear to be restricted to equatorial regions (BERRY & WILDE, 1990). Lower Devonian graptolites of southwestern Europe were usually restricted to outer shelf regions and are not found in inner shelf areas (LENZ & others, 1996), suggesting that the expanses of the Paleozoic oceans may have been the last refuge of the planktic graptoloids in order to escape from competition with other planktonic organisms. KOREN' (1979) suggested that this restriction of Devonian planktic graptolites may have been a significant factor in their final extinction. LENZ (2013) demonstrated the distribution of Early Devonian graptoloids was not limited to tropical, equatorial regions. He indicated a presence also in cold-water sites and suggested a probably universally moderate climate for the Early Devonian but regarded the reasons for the graptoloid extinction as not understood.

HISTORICAL BIOGEOGRAPHY

The paleogeographical origin of certain graptolite taxa or clades, or historical paleobiogeography, has rarely been considered in the interpretation of graptolite faunas. ERDTMANN (1982b) and COOPER (1999, p. 9) discussed the possible origin of the first planktic graptolites of the genera *Rhabdinopora* and *Staurograptus* EMMONS, 1855 in a deep-water biotope on the continental slope and a subsequent expansion into the shallow-water shelf regions. As benthic graptolites appear to be largely limited to the shallow water regions of the oceans, the idea of a deeper water origin of planktic graptoloids might be difficult to explain and needs further investigation. ZHANG and CHEN (2007, 2008) suggested a deep-water origin and shallow-water dispersal model in graptolite evolution, based on the distribution of early Darriwilian pseudisograptids and early axonophorans in China. The authors suggested that the Axonophora evolved in the deep-water regions in which their ancestors, the isograptids and pseudisograptids, lived. Thus, they favored a model of evolution of certain planktic graptoloid clades from equally planktic ancestors in oceanic regions, in which the planktic graptoloid taxa were supposedly living, but they did not discuss the origin of planktic graptolites per se.

GOLDMAN and others (2013) discussed historical biogeography in order to explain the patterns of changes of graptolite faunas through time and to recognize regions of evolutionary innovations and origins of faunal dispersal. The authors used published cladistics trees to pinpoint the evolutionary origin of certain clades to particular regions, based on a parsimony-based analysis, mapping geographical states to ancestral nodes. They noted a possible origin of early axonophorans in South China but also recognized a considerable diversification center in high- to mid-latitudinal regions, leading to a number of new clades. These

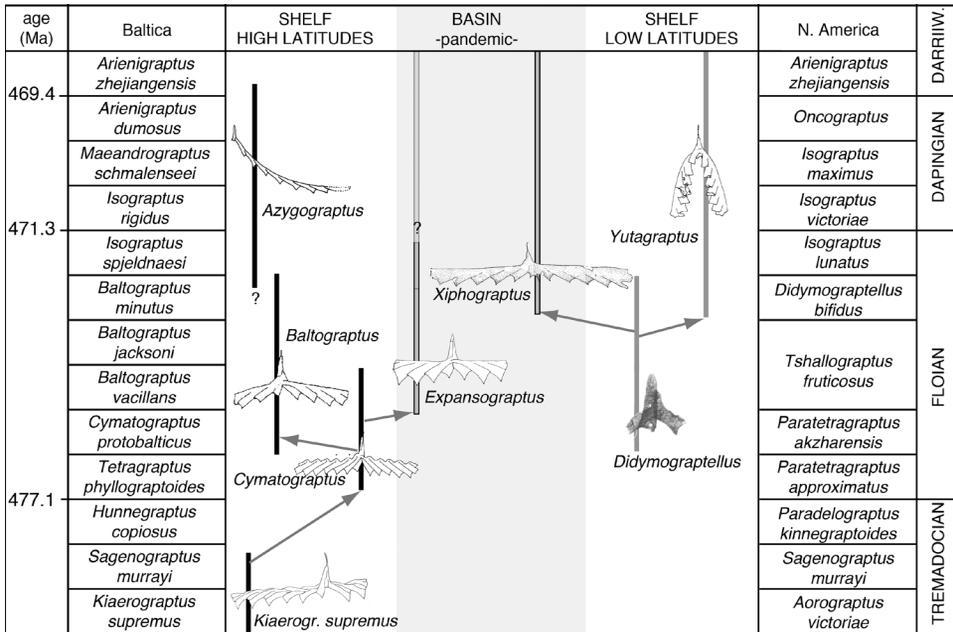| age (Ma)	Baltica	SHELF HIGH LATITUDES	BASIN -pandemic-	SHELF LOW LATITUDES	N. America	
469.4	*Arienigraptus zhejiangensis*				*Arienigraptus zhejiangensis*	DARRIIW.
	Arienigraptus dumosus				*Oncograptus*	DAPINGIAN
	Maeandrograptus schmalenseei	*Azygograptus*			*Isograptus maximus*	
	Isograptus rigidus		?	*Yutagraptus*	*Isograptus victoriae*	
471.3	*Isograptus spjeldnaesi*		*Xiphograptus*		*Isograptus lunatus*	
	Baltograptus minutus	?			*Didymograptellus bifidus*	FLOIAN
	Baltograptus jacksoni	*Baltograptus*			*Tshallograptus fruticosus*	
	Baltograptus vacillans		*Expansograptus*			
	Cymatograptus protobalticus				*Paratetragraptus akzharensis*	
	Tetragraptus phyllograptoides	*Cymatograptus*		*Didymograptellus*	*Paratetragraptus approximatus*	
477.1	*Hunnegraptus copiosus*				*Paradelograptus kinnegraptoides*	TREMADOCIAN
	Sagenograptus murrayi				*Sagenograptus murrayi*	
	Kiaerograptus supremus	*Kiaerogr. supremus*			*Aorograptus victoriae*	

Fig. 84. Historical paleobiogeography of the late Tremadocian to early Darriwilian time interval, showing the introduction of the genera *Expansograptus* Bouček & Přibyl, 1952a and *Xiphograptus* Cooper & Fortey, 1982 into the pandemic graptolite faunas of the marine basins from the respective low latitude and high latitude shelf regions (new; radiometric ages (MA) from Cooper & Sadler, 2012) .

interpretations, however, are regarded as preliminary by the authors, as they consider the available data sets as incomplete.

Goldman and others (2013) provided a number of examples to document historical biogeography of graptolite clades. Thus, the origin of the expansograptids (e.g., *Expansograptus* Bouček & Přibyl, 1952a; *Didymograptus; Baltograptus*) was considered to be in the shallow-water regions of the high latitudes, preceded by the two-stiped *Kiaerograptus supremus* Lindholm, 1991 (Fig. 84). The genus *Cymatograptus* Jaanusson, 1965 suddenly appeared during the middle of the *Tetragraptus phyllograptoides* Biozone, considerably before the origination of the cosmopolitan genus *Expansograptus* (Egenhoff & Maletz, 2007). *Cymatograptus* is present in most high latitude regions, but only a single record has been established in lower latitude regions—in the Cow Head Group of western Newfoundland (Toro & Maletz, 2008, p. 981). The *Expansograptus*

holmi-Expansograptus suecicus group in the upper part of the *Cymatograptus protobalticus* Biozone (Egenhoff & Maletz, 2007, fig. 3) made the expansograptids successful on a global scale after several million years of evolution as high latitude faunal elements (Fig. 84) with a probable origin in the middle Tremadocian. The evolution of xiphograptids in the low latitude regions demonstrates another example of a biogeographically determined origin of clades in graptoloid evolution. The genus *Didymograptellus* in the *Paratetragraptus akzharensis* Biozone, as discovered in western Newfoundland, represents the oldest xiphograptid in the fossil record as an endemic of the low latitude fauna (Maletz, 2010a). Global dispersal and invasion of the derived genera *Xiphograptus* Cooper & Fortey, 1982 and *Pterograptus* Holm, 1881a into the cosmopolitan oceanic biofacies happened during the Dapingian to Darriwilian, where these taxa enjoyed long-time success until the demise of the

group in the upper Darriwilian. The genus *Didymograptellus,* mainly represented by the short-lived *Didymograptellus bifidus* (Hall, 1865), was only moderately successful in the late Floian in the low latitude fauna. *Yutagraptus* had greater species longevity, originating in the late Floian and lasting until the early Darriwilian, but was also restricted to the low latitudes or perhaps even endemic to Laurentia (Maletz, 2010a).

The radiation of the Neograptina, and especially of the genus *Normalograptus,* represents an excellent example of the biogeographic component of macroevolutionary processes. *Normalograptus* species were uncommon during the Darriwilian to Sandbian and were widely distributed in high latitudes, but during the early Hirnantian, species of *Normalograptus* invaded the paleotropics and rapidly replaced DDO species during the Late Ordovician extinction event (Melchin & Mitchell, 1991; Chen, Melchin, & others, 2005). Eventually, only species of *Normalograptus* survived the extinction and re-populated the early Silurian oceans before a new diversification occurred during the Rhuddanian (early Silurian), initially based on biserial Neograptina but followed by the origin and radiation of the Silurian Monograptidae.

The genus *Cyrtograptus* Carruthers in Murchison, 1867a may in the future provide another useful example to understand the evolutionary history of graptoloids through the late Llandovery and Wenlock (mid-Silurian). The genus *Cyrtograptus* has significant provincial differences in distribution during the late Telychian, and Melchin (1989) used the distribution of *Cyrtograptus sakmaricus* Koren', 1968 and related forms as indicators of the circum-tropical faunal province. *Cyrtograptus* disappeared completely from the southern paleolatitudes in the middle Sheinwoodian but is well documented during this interval in the Canadian Arctic (Lenz & Melchin, 1991). In the late Sheinwoodian *Cyrtograptus rigidus* Biozone, *Cyrtograptus* reappears in Avalonia, Baltica, and Bohemia. The reason for this pattern is unclear, especially as the origin and early evolution of the genus *Cyrtograptus* has not been verified. A number of authors discussed a polyphyletic origin of the genus *Cyrtograptus* (e.g., Rickards, Hutt & Berry, 1977; Fu, 1985; Williams & Zalasiewicz, 2004; Lenz & others, 2012). Because this question is not resolved, a suitable phylogenetic analysis and paleobiogeographic interpretation is impossible to provide.

GEOLOGICAL APPLICATIONS

Jörg Maletz and Alfons H. M. VandenBerg

INTRODUCTION

Graptolites are probably best known for their role in biostratigraphic dating of rock sequences and by paleontologists for the fascinating complexity of their colonies. However, they have much more to offer, and a look back into the history of graptolite research shows their importance for a variety of geological applications. The distribution of Middle Ordovician isograptids, for instance, has been used to infer the presence of oceanic basins and to outline the rims of ancient continents (Fortey & Cocks, 1986). Plus, the paleogeographical information graptolites provide make them valuable for tracing natural resources such as petrochemicals and mineral deposits, thus adding an economic dimension to the study and usefulness of this fossil group.

The early understanding of the distribution of graptolites was not without controversies, as illustrated by the debate between Joachim Barrande and Charles Lapworth. Barrande's concept of graptolite colonies place him as a staunch supporter of Cuvier's theory of catastrophism, which interprets faunas from tectonic blocks as originating through a number of extinctions and creations (Barrande, 1859, 1861, 1862, 1865, 1870, 1881). Barrande's views stood in direct contradiction with Lapworth's understanding of graptolite faunas as successions of species through time. At the end, the interpretation of Lapworth (1878) was proven correct, and his graptolite research provided the nucleus of modern graptolite biostratigraphy and the basis for many modern applications of graptolite research.

DATING OF ROCK SEQUENCES

The study of Earth history was initially concerned with dating sedimentary sequences; and very early on, graptolites were used for just that purpose. As early as 1850, James Hall (1850) realized the importance of graptolites for dating certain geological periods, thus laying the groundwork for the biostratigraphic application of graptolite faunas. Henry Alleyne Nicholson (1868b) provided the first workable chart showing the distribution of graptolite species through time. These scientists made the first steps toward the wider application of graptolites in the geological sciences.

Modern stratigraphy is unthinkable without the use of paleontology, even though this was not always acknowledged after radiometric dating became one of the key methods of chronostratigraphic dating. Our modern understanding of deep time employs numerous additional methods (e.g., Gradstein & others, 2020), including the use of fossils and the recognition of a precise and highly reliable succession of fossil faunas that have developed during the last two centuries. For graptolites, this means that internationally recognized chronostratigraphic units in the early Paleozoic, GSSPs (Global Stratotype Sections and Points) are largely defined by the First Appearance Datum (FAD) of graptolite species (Fig. 85). Thus, graptolites are one of the exemplary groups of fossils for dating rock sequences and correlating them across the planet (Maletz, 2017a). As a group of macrofossils, they are also easily used in the field and do not require extensive work in the laboratory, as is typical for the investigation of microfossils (e.g., acritarchs, chitinozoans, conodonts, spores, foraminifera).

STRUCTURAL GEOLOGY AND BASIN RECONSTRUCTION

Lapworth (1878), in his important paper on the Moffat Series of the UK, established graptolite biostratigraphy as an important geological mapping tool for unraveling

complexly folded and faulted lithological sequences based on the distribution of graptolite faunas. However, he had already indicated earlier (LAPWORTH, 1872) that he used graptolites for biostratigraphic purposes (HAMILTON, 2001). Because it used graptolites for the first time to solve a geological problem, LAPWORTH's (1878) work on the Moffat Series was a milestone in graptolite research. It is noteworthy that LAPWORTH's graptolite biostratigraphy for the region is still valid and useful with little revision after nearly 150 years (FORTEY, 1993).

The Lachlan Orogen of eastern Australia is another prime example of the use of graptolite faunas and dating to understand the geological history of the region. The geological structure of the area is complex, but age control on the turbidite-dominated Ordovician rocks is possible using the presence of rich graptolite faunas (VANDENBERG, 1989; VANDENBERG & COOPER, 1992). The work began with publication of a pioneering study of the Castlemaine goldfield by Thomas Sergeant HALL (1895). HALL developed this work during the next 25 years, and additional work by William John HARRIS and David Evan THOMAS in the 1930s achieved the subdivision of the Early and Middle Ordovician rocks into 21 graptolite zones (HARRIS & THOMAS, 1938a). This work made it possible to subdivide the monotonous turbidite–black shale sequence of the Castlemaine Group, which extends over the westernmost Lachlan Orogen, and unravel its structure, which consisted of tight, closely spaced concertina-like folds interrupted by numerous faults that follow strike. This made it possible to map the Bendigo goldfield, with more than 3,000 graptolite localities, at 1:10,000 scale (WILKINSON, WILLMAN, & GARRATT, 1988; WILLMAN, 1992, 1994).

Problems in solving the structural complexity of the eastern Lachlan Orogen, however, could not be tackled until a workable zonation of the Late Ordovician was achieved in the 1980s (VANDENBERG, 1981, 1989; VANDENBERG & COOPER, 1992). With

an extent of more than ten million km^2—much of it in mountainous terrain with granites making up about half of the region—the Ordovician rocks seemingly consisted of turbidites with rare intervals of black shale. Mappable lithological units seemed to be absent and, fossils were few over the widely scattered localities. This picture changed when the region was mapped, initially at a regional scale and subsequently in more detail. This demonstrated the Ordovician sequence could be subdivided into two main units, the Adaminaby Group and the overlying Bendoc Group (VANDENBERG & STEWART, 1992). The Adaminaby Group consists of turbidites with rare cherts containing conodonts and very rare graptolites that represented an age ranging from at least the early Floian (Be1) *Paratetragraptus approximatus* plus *Tshallograptus fruticosus* biozones to the late Darriwilian (Da3) *Archiclimacograptus decoratus* Biozone (VANDENBERG & STEWART, 1992). The overlying black shale-dominated Bendoc Group contains an almost complete Late Ordovician graptolite sequence ranging from the early Sandbian *Nemagraptus gracilis* Biozone to the late Katian *Paraorthograptus pacificus* Biozone. Careful mapping demonstrated that the peculiar ribbon-like outcrop pattern of the Bendoc Group was due to thin-skinned deformation, with the slippery black shale providing a preferred horizon for sliding of multiple stacked thrust sheets (GLEN & VANDENBERG, 1987; GLEN, STEWART, & VANDENBERG, 1990; FERGUSSON & VANDENBERG, 1990; VANDENBERG & others, 1990; VANDENBERG, NOTT, & GLEN, 1992).

The importance of graptolites to understanding basin evolution can also be demonstrated through the investigation of the Ordovician graywackes of the southern Baltic Sea. A number of drill cores made during the 1960s demonstrated the presence of a thick succession of early Paleozoic strata in the subsurface of the German island of Rügen (JAEGER, 1967). MALETZ (1997c) discussed the succession of the G-14 drill core north of Rügen and demonstrated a
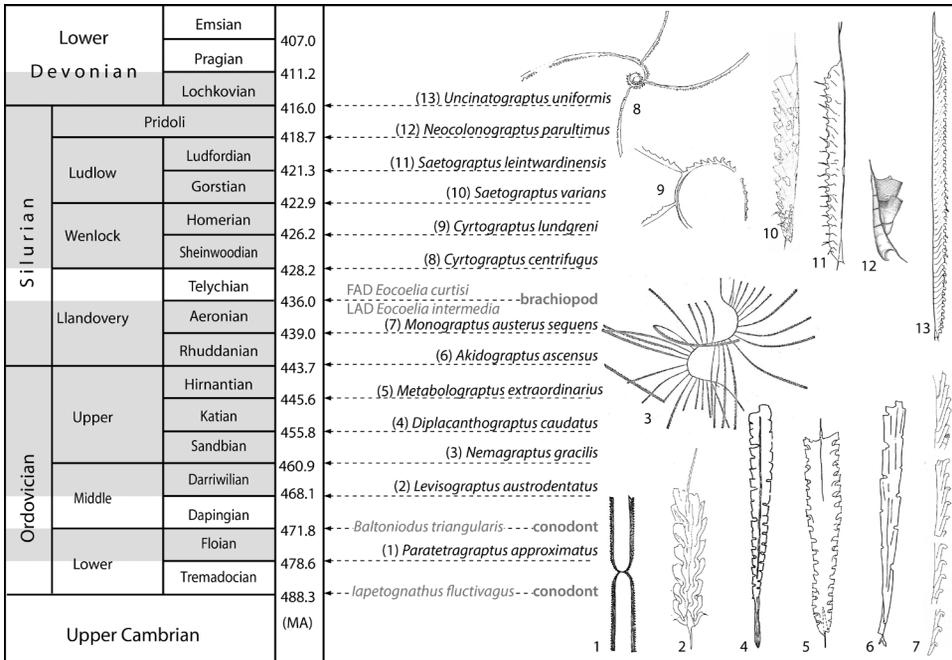
FIG. 85. Index species of graptolites for Global Stratotype Sections and Points (GSSP) in the Paleozoic. Stratigraphic intervals defined by graptolite FADs (First Appearance Datum), highlighted in *gray*. Non-graptolitic fossils defining intervals in *gray* print (adapted from Maletz, 2017c, fig. 8).

close litho- and biostratigraphical connection to the platform succession of Baltica. Whereas the Middle Ordovician Tøyen Shale Formation is strongly condensed, a thick Telychian (Llandovery, Silurian) graptolite succession was documented, similar to that on the Danish island of Bornholm (BJERRESKOV, 1975) and of Scania, southern Sweden (TULLBERG, 1882a). On the island of Rügen, off the southern coast of the Baltic Sea, a number of deep drill cores encountered Middle to Late Ordovician (Darriwilian to Sandbian) graptolite successions with tectonic repetition (MALETZ, 1998a, 2001b). MALETZ and others (1998) and BEIER, MALETZ, and BÖHNKE (2000) interpreted the strata as the remains of a peripheral foreland basin, formed when the microplate East Avalonia collided with Baltica during the Middle Ordovician to late Silurian. The authors interpreted the stacked succession of Ordovician shales, graywackes, and sandstones (Wittow Group;

see BEIER & others, 2001) through the effect of thrusting northward onto the shelf region of Baltica. The whole succession was investigated during the unsuccessful exploration for oil and gas in northeastern Germany—a great success, however, for the scientific community because no surface exposures exist of these strata (FRANKE & others, 1994; HOFFMANN & others, 1998).

The Ordovician succession of southern Bolivia provides another example of the use of graptolite faunas for interpreting the basin evolution of an extremely thick monotonous lithological succession (MÜLLER, KLEY, & JACOBSHAGEN, 2002; EGENHOFF, MALETZ, & ERDTMANN, 2004). The Eastern Cordillera of Argentina includes an extremely thick succession of early Paleozoic sediments that only fairly recently have been investigated in more detail. MALETZ and EGENHOFF (2001, 2003) described the diverse Early to Middle Ordovician graptolite faunas of southern Bolivia and recognized a fairly

complete biostratigraphic succession from the Tremadocian to the late Floian that EGENHOFF (2000) used to interpret the basin evolution of the region.

Graptolites have also proven useful in other geological applications, based on the style of their occurrence on shale surfaces. SCHLEIGER (1968) and others have demonstrated that graptolite tubaria may be aligned, to a variable degree and depending on their shape, with paleocurrent directions in the turbidites in which they occur, as described by Maletz (see p. 84–85) and Cooper and others (see p. 97) (Fig. 86). From this, paleoslope directions can be determined, and these can be used in basin reconstruction.

In deformed rocks, graptolites with symmetrical tubaria can be used as strain markers (JENKINS, 1987; MALETZ, 2020a). COOPER (1990) offered a mathematical method of restoring symmetrical fossils from which strain ellipses could be calculated, thus giving the amount and direction of maximum compression of the host rock. Some 27 years later, VANDENBERG (2017, fig. 27–28) demonstrated an easier method that gave similar results using modern image processing software.

ECONOMIC GEOLOGY

The value of graptolites for exploration of economic resources cannot be underestimated. Apart from the modern use of graptolite biostratigraphy in the exploration of oil and gas resources worldwide, a number of further important aspects are worth noting here. These have shaped and even initiated the scientific paleontological research of graptolite faunas in many regions of the world.

URANIUM EXPLORATION

VESKI and PALU (2003) discussed the Cambrian–Ordovician Alum Shale Formation, including the early Tremadocian former *Dictyonema* oil shale and the Middle Ordovician kukersite deposits of Estonia that were the focus of intensive exploration (see also BAUERT & KATTAI, 1997; DYNI, 2005;

SOESOO, VIND, & HADE, 2020). In Estonia, kukersite beds can reach an organic content of 40–45 wt% (BAUERT, 1994). The exploration for uranium in the *Dictyonema* Shales of Estonia after World War II was of the highest priority (ALTHAUSEN, 1992). Uranium prospecting also took place in the graptolitic Silurian successions of Thuringia, Germany by SAG/SDAG Wismut, producing ~220,000 tons of uranium ore between 1947 and 1990. The uranium ore was concentrated in lower Paleozoic lithological units, especially in the Unterer Graptolithenschiefer (e.g., GATZWEILER & others, 1997; WISMUT, 2010) but also in other units of the succession like the Ockerkalk and the Devonian and Carboniferous intrusions. At the time, the then German Democratic Republic (DDR) in eastern Germany was one of the largest producers of uranium in the world (KÄMPF & others, 1995; CZEGA & others, 2006), and the Ronneburg mining area was the largest uranium mine in Europe, covering an area of 60 km^2 and extending to a depth of 940 m (PAUL & others, 2002). Graptolite specialists are familiar with the invaluable monograph on the Silurian graptolite fauna of Thuringia by SCHAUER (1971), based in part on graptolites collected from sections of the Unterer Graptolithenschiefer (Lower Graptolite Shale) in the Ronneburg area. Most of the paleontological data attained by the uranium industry in central Europe were not officially available for several decades (see DUFKA, KŘÍŽ, & ŠTORCH, 1995). All information on the uranium production from the Silurian strata by Wismut in eastern Germany (DDR) was under strict confidentiality (WISMUT, 2010), indicating the strategic importance of the uranium industry. Thus, very little has been published about the results.

MATURITY STUDIES AND PETROLEUM GEOLOGY

Graptolite shales can be important for the exploration of oil and gas source rocks. KONYUKHOV and AGAPITOV (2014) provided a recent overview of the distribution of
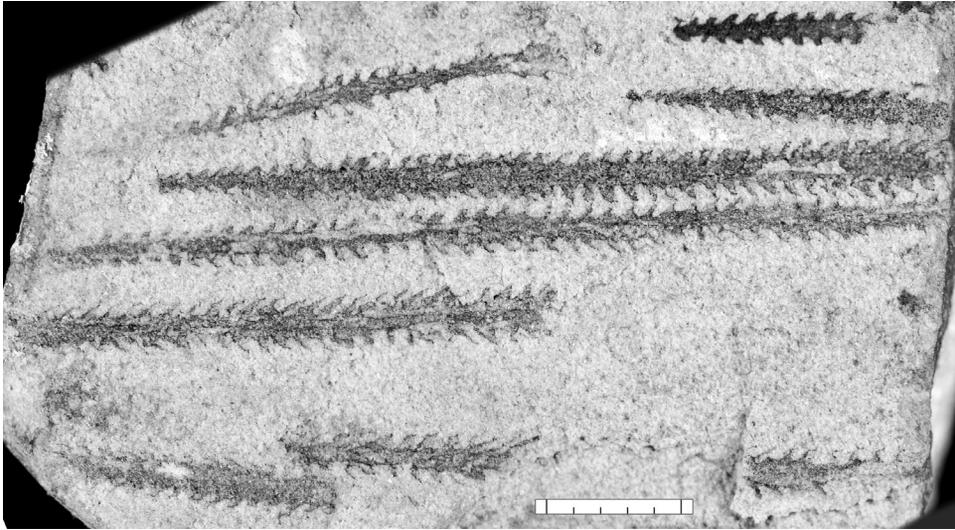
Fig. 86. Current-aligned biserial graptolites from Tb (planar laminated) portion of a turbidite bed from Late Ordovician Sunbury Group, central Victoria, Australia, scale bar, 5 mm (new; A.H.M. VandenBerg). Color version available in *Treatise Online* 155.

Paleozoic graptolite shales around the world and their potential as hydrocarbon resources. They noted that Silurian graptolite shales may have been the source of 80–90% of the hydrocarbons stored in the giant oil fields of North Africa and also may have played the main role in the formation of the gas field of the Persian Gulf, the largest natural gas field in the world. Graptolites are made from organic material and thus provide a useful tool for identifying unconventional hydrocarbon deposits, including shale gas, without the need of complicated and expensive analytical studies. Graptolites are equally important for estimating the TOC (Total Organic Carbon) contents. There are many examples of investigations of hydrocarbon potential in graptolite-bearing Paleozoic successions around the world (e.g., Fello & others, 2006; Grundman & others, 2012; Podhalańska, 2013; Colțoi, Nicolas, & Safa, 2016; Șen, 2017; Luo & others, 2016, 2018, 2020; Borjigin & others, 2017; Ye Wang & others, 2019; Gong & others, 2020).

Numerous authors have used the reflectance of the graptolite fusellum to determine the organic maturity of lower Paleozoic sediments (Fig. 87), because its behavior is similar to that of other organic materials like plants, chitinozoans, and scolecodonts (Teichmüller, 1978; Bertrand & Héroux, 1978; Bertrand, 1990; Goodarzi, 1990; Petersen, Schovsbo, & Nielsen, 2013; Hartkopf-Fröder & others, 2015; Zheng & others, 2021). Graptolite reflectance can be compared with the vitrinite reflectance of fossil plant material (Goodarzi & Norford, 1985, 1989). Graptolite reflectance data are compared to the CAI (color alteration index) in conodonts and may provide information on the maximum overburden of sedimentary successions through the known depth temperature gradient (Bergström, 1980). Therefore, the graptolite fusellum provides important information on the burial history of sedimentary basins through changes in the optical properties of the organic material. Through paleo-temperature evaluation and thermal alteration, the metamorphism and overburden of the sedimentary succession can be evaluated. Important information for basin evolution and tectonics can be gained through the investigation of the thermal history as shown by the example of the central Andean Basin in
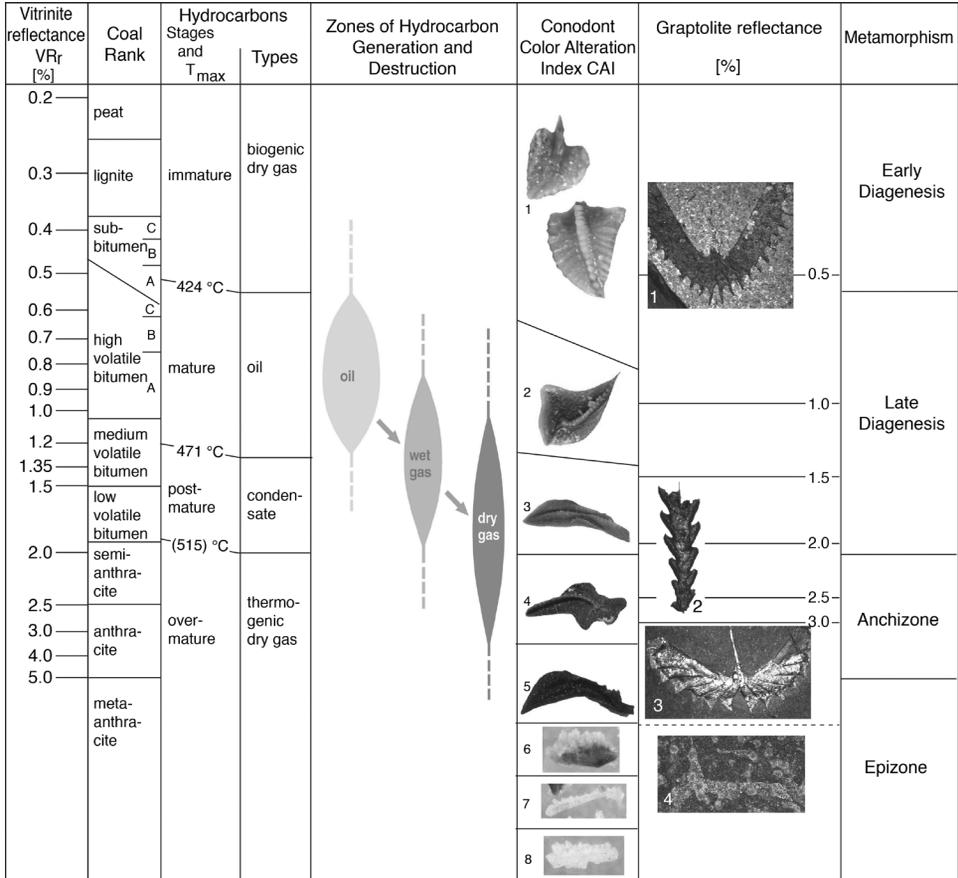
FIG. 87. A comparison of hydrocarbon generation and graptolite reflectance. Conodont specimens from HARTKOPF-FRÖDER and others (2015) to demonstrate CAI values. Graptolites: *1*, *Parisograptus imitatus* (HARRIS, 1933) , GSC 139246, Cow Head Group, western Newfoundland; *2*, *Orthograptus apiculatus* ELLES & WOOD, 1907, PMU 35732, Gullhögen Quarry, Billingen, Västergötland, Sweden; *3*, *Isograptus rigidus* MALETZ, 2011a, PMO 234.063, Slemmestad, Oslo Region, Norway; *4*, *Baltograptus geometricus* (TÖRNQUIST, 1901), LO 1585T, lectotype, Diabasbrottet, Hunneberg, Sweden. Specimens not to scale (adapted from Maletz, 2020a, fig. 6).

Argentina (see HERRERA SÁNCHEZ & others, 2021). The color change of the graptolite tubaria through a temperature gradient is easy to recognize, from dark brown to black (unchanged) to a silvery hue (highly mature) resulting from deep burial or contact and regional metamorphism of the sediments (MALETZ, 2020a). With increasing grade or depth, the original organic material of the graptolite disappears completely.

SCHOVSBO, NIELSEN, and GAUTIER (2014) explored the potential of the Scandinavian Alum Shale Formation as an unconventional gas play in Denmark and provided a geological model that underlies this assessment. They predicted the prospective areas for gas in the Norwegian-Danish Basin. The research is complimented by a discussion by KOSAKOWSKI and others (2017) of the Alum Shale Formation in the Baltic Basin and the Podlasie Depression as important petroleum source rocks.

Hydrocarbon exploration has also been the driving force behind the investigation of Silurian Hot Shales in northern Africa and Arabia in recent years (LÜNING & others, 2000, 2005; LOYDELL, BUTCHER, & AL-JUBOURY, 2013; LOYDELL, BUTCHER, & FRÝDA, 2013).

In these regions, early Silurian (Rhuddanian) successions have been identified as important hydrocarbon source rocks. They represent 80–90% of the Paleozoic hydrocarbons in Arabia and North Africa.

Discontinuous basins filled with organic-rich shales developed on the northern rim of Gondwana, where their thickness was controlled by an early Silurian paleorelief related to the Late Ordovician glaciation event. Extensional and compressional regional tectonics also influenced the distribution of these graptolitic shales. Detailed biostratigraphical correlation of the successions is important for understanding the source potential of these deposits for economic exploration in the regions (LÜNING & others, 2000, 2005).

The most important recent development in the exploration for oil and gas comes from the South China Platform. The investigation has concentrated on the Longmaxi Formation (latest Ordovician to basal Silurian) in the Sichuan Basin and also outside this region on the Yangtze Platform. Numerous gas and oil fields have been developed (HU, HE, & CHEN, 2012; CHEN, LU, & DING, 2014; CHEN & others, 2014; GUO & others, 2014; JIANG & others, 2015; SHAN & others, 2015; TANG & others, 2015; ZOU & others, 2015; MA, 2017; SUN & others, 2020).

BIOSEQUENCE STRATIGRAPHY

Evolutionary studies on graptolites have often included origination and extinction events and their effects on the diversity of the faunas (see p. 138–140), but the connection with sedimentological research has usually been neglected even though it is urgently needed (see HOLLAND & ALLEN, 2008). It is well known that graptolites are preserved more commonly and much better in certain sediment types, especially in black, anoxic shales (MALETZ, 2020a). This knowledge clearly indicates the need for closely connected sedimentological and paleontological research. Sedimentological research can indicate the effects of sea-level changes in fossiliferous successions, and the faunas provide a deeper insight into the amount of paleontological change and also allow an interpretation of the reasons behind this change. The effect of sea-level changes on the preservation of graptolite faunas, and especially their effect on the preservation of shallow-water and deep-water faunal elements in the successions, can help us understand graptolite distribution through time. EGENHOFF and MALETZ (2007) investigated the use of graptolites as indicators for maximum flooding surfaces in monotonous deep-water shelf successions in the Diabasbrottet section in Västergötland, Sweden. The authors noted the migration of shallow-water endemics and pandemics landward and the increasing frequency of deep-water pandemics in the succession. At the peak of the transgression, the deep-water pandemics dominated the faunas but were in turn replaced by endemic faunas when the sea level fell. EGENHOFF and MALETZ (2007) thus recognized four levels of deep-water faunas as maximum flooding surfaces in the Diabasbrottet section, combining a sequence stratigraphic approach with graptolite biostratigraphy and diversity studies.